

## Fungal Systematics and Evolution: FUSE 5

Jie Song<sup>1</sup>, Jun-Feng Liang<sup>1,\*</sup>, Mehdi Mehrabi-Koushki<sup>2,3</sup>, Irmgard Krisai-Greilhuber<sup>4,\*</sup>, Barkat Ali<sup>5,6</sup>, Vinod Kumar Bhatt<sup>7</sup>, Agustín Cerna-Mendoza<sup>8</sup>, Bin Chen<sup>1</sup>, Zai-Xiong Chen<sup>9</sup>, Hong-Long Chu<sup>10</sup>, Mike Anderson Corazon-Guivin<sup>8</sup>, Gladstone Alves da Silva<sup>11</sup>, André De Kesel<sup>12</sup>, Bálint Dima<sup>13</sup>, Francesco Dovana<sup>14</sup>, Reza Farokhinejad<sup>2</sup>, Guliano Ferisin<sup>15</sup>, Juan Carlos Guerrero-Abad<sup>8,16</sup>, Ting Guo<sup>17</sup>, Li-Hong Han<sup>10</sup>, Sobia Ilyas<sup>18</sup>, Alfredo Justo<sup>19</sup>, Abdul Nasir Khalid<sup>20</sup>, Sadigheh Khodadadi-Pourarpanahi<sup>2</sup>, Tai-Hui Li<sup>21</sup>, Chao Liu<sup>10</sup>, Marilinda Lorenzini<sup>22</sup>, Jun-Kun Lu<sup>1</sup>, Abdul Samad Mumtaz<sup>5</sup>, Fritz Oehl<sup>23</sup>, Xue-Yu Pan<sup>1</sup>, Viktor Papp<sup>24</sup>, Wu Qian<sup>25</sup>, Abdul Razaq<sup>26</sup>, Kamal C. Semwal<sup>27</sup>, Li-Zhou Tang<sup>10</sup>, Xue-Lian Tian<sup>10</sup>, Adela Vallejos-Tapullima<sup>8</sup>, Nicolaas A. van der Merwe<sup>6</sup>, Sheng-Kun Wang<sup>1</sup>, Chao-Qun Wang<sup>21</sup>, Rui-Heng Yang<sup>17</sup>, Fei Yu<sup>1</sup>, Giacomo Zapparoli<sup>22</sup>, Ming Zhang<sup>21</sup>, Vladimir Antonín<sup>28</sup>, André Aptroot<sup>29</sup>, Ali Aslan<sup>30</sup>, Arghya Banerjee<sup>31</sup>, Subrata Chatterjee<sup>32</sup>, Alden C. Dirks<sup>33</sup>, Leila Ebrahimi<sup>34</sup>, Khalil-Berdi Fotouhifar<sup>35</sup>, Youbert Ghosta<sup>36</sup>, Lyudmila B. Kalinina<sup>37</sup>, Dilara Karahan<sup>38</sup>, Jingyu Liu<sup>39</sup>, Mrinal Kumar Maiti<sup>40</sup>, Abhirup Mookherjee<sup>40</sup>, Partha Sarathi Nath<sup>31</sup>, Birendranath Panja<sup>31</sup>, Jayanta Saha<sup>31</sup>, Hana Ševčíková<sup>28</sup>, Hermann Voglmayr<sup>4,41</sup>, Kenan Yazıcı<sup>38</sup> & Danny Haelewaters<sup>39,42,43,44</sup>

<sup>1</sup> Key Laboratory of State Forestry Administration on Tropical Forestry Research, Research Institute of Tropical Forestry, Chinese Academy of Forestry, Guangzhou 510520, P.R. China

<sup>2</sup> Department of Plant Protection, Faculty of Agriculture, Shahid Chamran University of Ahvaz, Ahvaz, Iran

<sup>3</sup> Biotechnology and Bioscience Research Center, Shahid Chamran University of Ahvaz, Ahvaz, Iran

<sup>4</sup> Department of Botany and Biodiversity Research, Universität Wien, Rennweg 14, 1030 Wien, Austria

<sup>5</sup> Department of Plant Sciences, Faculty of Biological Sciences, Quaid-i-Azam University, Islamabad, 45320, Pakistan

<sup>6</sup> Department of Biochemistry, Genetics and Microbiology, Division of Genetics, Forestry and Agricultural Biotechnology Institute (FABI), University of Pretoria, Private Bag X20, Pretoria 0028, South Africa

<sup>7</sup> Navdanya, 105, Rajpur Road, Dehradun, Uttarakhand, India

<sup>8</sup> Laboratorio de Biología y Genética Molecular, Universidad Nacional de San Martín, Jr. Amador 315, Morales, Peru

<sup>9</sup> Management Bureau of Danxiashan National Nature Reserve of Guangdong, Shaoguan 512300, China

<sup>10</sup> College of Biological Resource and Food Engineering, Center for Yunnan Plateau Biological Resources Protection and Utilization, Qujing Normal University, Qujing, Yunnan 655011, China

<sup>11</sup> Departamento de Micologia, CB, Universidade Federal de Pernambuco, Av. da engenharia s/n, Cidade Universitária, 50740-600, Recife, PE, Brazil

<sup>12</sup> Meise Botanic Garden, Nieuwelaan 38, 1860 Meise, Belgium

<sup>13</sup> Department of Plant Anatomy, Institute of Biology, Eötvös Loránd University, H-1117 Budapest, Hungary

<sup>14</sup> Department of Life Sciences and Systems Biology, University of Torino, Viale P.A. Mattioli 25, I-10125 Torino, Italy

<sup>15</sup> Via A. Vespucci 7, 33052 Cervignano del Friuli (UD), Italy

<sup>16</sup> Instituto Nacional de Innovación Agraria (INIA). Dirección General de Recursos Genéticos y Biotecnología. Av. La Molina 1981, La Molina - Lima, Peru

<sup>17</sup> Key Laboratory of Edible Fungal Resources and Utilization (South), National Engineering Research Center of Edible Fungi, Key Laboratory of Agricultural Genetics and Breeding of Shanghai, Institute of Edible Fungi, Shanghai Academy of Agricultural Sciences, Shanghai 201106, China

<sup>18</sup> Department of Botany, Lahore College for Women University, Lahore, Pakistan

<sup>19</sup> New Brunswick Museum, 277 Douglas Ave., Saint John, New Brunswick, E2K 1E5, Canada

<sup>20</sup> Department of Botany, University of the Punjab, Lahore, Pakistan

<sup>21</sup> State Key Laboratory of Applied Microbiology Southern China, Guangdong Provincial Key Laboratory of Microbial Culture Collection and Application & Guangdong Open Laboratory of Applied Microbiology, Guangdong Institute of Microbiology, Guangzhou 510070, China

<sup>22</sup> Università degli Studi di Verona, Dipartimento di Biotecnologie, Italy

<sup>23</sup> Agroscope, Competence Division for Plants and Plant Products, Ecotoxicology, Müller-Thurgau-Strasse 29, CH-8820 Wädenswil, Switzerland

<sup>24</sup> Department of Botany, Szent István University, H-1518 Budapest, Hungary

<sup>25</sup> Bureau of Parks and Woods of Mt. Huangshan Administrative Committee, Huangshan, Anhui 245000, China

<sup>26</sup> Discipline of Botany, Faculty of Fisheries and Wildlife, University of Veterinary and Animal Sciences (UVAS), Ravi Campus, Pattoki, Pakistan

<sup>27</sup> Department of Biology, College of Sciences, Eritrea Institute of Technology, Mai Nafhi, Asmara, Eritrea

<sup>28</sup> Department of Botany, Moravian Museum, Zelný trh 6, CZ-659 37 Brno, Czech Republic

<sup>29</sup> ABL Herbarium G.v.d.Veenstraat, 107 NL-3762, XK Soest, The Netherlands

- <sup>30</sup> Yüzüncü Yıl University, Faculty of Pharmacy, 65080 Campus, Van, Turkey;  
 Kyrgyz-Turkish Manas University, Faculty of Arts and Science, Dept. of Biology, Bishkek, Kyrgyzstan  
<sup>31</sup> Department of Plant Pathology, Bidhan Chandra Krishi Viswavidyalaya, Nadia-741252, West Bengal, India  
<sup>32</sup> Department of Agricultural Entomology, Bidhan Chandra Krishi Viswavidyalaya, Nadia-741252, West Bengal, India  
<sup>33</sup> Department of Ecology and Evolutionary Biology, University of Michigan, 1105 North University Avenue,  
 4050 Biological Sciences Building, Ann Arbor, MI 48109, USA  
<sup>34</sup> Department of Entomology and Plant Pathology, Aburairhan Campus, University of Tehran, Tehran, 33916-53755, Iran  
<sup>35</sup> Department of Plant Protection, Faculty of Agricultural Sciences and Engineering, College of Agriculture and Natural  
 Resources, University of Tehran, Karaj, 31587-77871, Iran  
<sup>36</sup> Department of Plant Protection, Faculty of Agriculture, Urmia University, Urmia, P. O. Box 165, Iran  
<sup>37</sup> Russian Academy of Sciences, Komarov Botanical Institute, Prof. Popov Str. 2, St. Petersburg RU-197376, Russia  
<sup>38</sup> Department of Biology, Faculty of Science, Karadeniz Technical University, 61080, Trabzon, Turkey  
<sup>39</sup> Department of Botany and Plant Pathology, Purdue University, 915 W. State Street, West Lafayette, IN 47907, USA  
<sup>40</sup> Department of Biotechnology, Indian Institute of Technology Kharagpur, 721302, West Bengal, India  
<sup>41</sup> Institute of Forest Entomology, Forest Pathology and Forest Protection, BOKU-University of Natural Resources and  
 Life Sciences, Peter-Jordan-Straße 82/I, 1190 Wien, Austria  
<sup>42</sup> Harvard University Herbaria, 22 Divinity Avenue, Cambridge, MA 02138, USA  
<sup>43</sup> Herbario UCH, Universidad Autónoma de Chiriquí, Apartado Postal 0427, David, Panama  
<sup>44</sup> Smithsonian Tropical Research Institute, Apartado Postal 0843-03092, Balboa, Panama

\* e-mails: jfliang2000@163.com; irmgard.greilhuber@univie.ac.at

Song J., Liang J.-F., Mehrabi-Koushki M., Krisai-Greilhuber I., Ali B., Bhatt V.K., Cerna-Mendoza A., Chen B., Chen Z.-X., Chu H.-L., Corazon-Guivin M.A., da Silva G.A., De Kesel A., Dima B., Dovana F., Farokhinejad R., Ferisin G., Guerrero-Abad J.C., Guo T., Han L.-H., Ilyas S., Justo A., Khalid A.N., Khodadadi-Pourarpanahi S., Li T.-H., Liu C., Lorenzini M., Lu J.-K., Mumtaz A.S., Oehl F., Pan X.-Y., Papp V., Qian W., Razaq A., Semwal K.C., Tang L.-Z., Tian X.-L., Vallejos-Tapullima A., van der Merwe N.A., Wang S.-K., Wang C.-Q., Yang R.-H., Yu F., Zapparoli G., Zhang M., Antonín V., Aptroot A., Aslan A., Banerjee A., Chatterjee S., Dirks A.C., Ebrahimi L., Fotouhifar K.-B., Ghosta Y., Kalinina L.B., Karahan D., Maiti M., Mookherjee A., Nath P.S., Panja B., Saha, J., Ševčíková H., Voglmayr H., Yazıcı K. & Haelewaters D. (2019): Fungal Systematics and Evolution 5. – *Sydowia* 71: 141–245.

Thirteen new species are formally described: *Cortinarius brunneocarpus* from Pakistan, *C. lilacinoarmillatus* from India, *Curvularia khuzestanica* on *Atriplex lentiformis* from Iran, *Gloeocantharellus neoechinosporus* from China, *Laboulbenia bernaliana* on species of *Apenes*, *Apristus*, and *Philophuga* (Coleoptera, Carabidae) from Nicaragua and Panama, *L. oioveliicola* on *Oiovelia machadoi* (Hemiptera, Veliidae) from Brazil, *L. termiticola* on *Macrotermes subhyalinus* (Blattodea, Termitidae) from the DR Congo, *Pluteus cutefractus* from Slovenia, *Rhizoglosum variabile* from Peru, *Russula phloginea* from China, *Stagonosporopsis flaccidivarum* on *Vitis vinifera* from Italy, *Strobilomyces huangshanensis* from China, *Uromyces klotzschianus* on *Rumex dentatus* subsp. *klotzschianus* from Pakistan. The following new records are reported: *Alternaria calendulae* on *Calendula officinalis* from India; *A. tenuissima* on apple and quince fruits from Iran; *Candelariella oleaginescens* from Turkey; *Didymella americana* and *D. calidophila* on *Vitis vinifera* from Italy; *Lasiodiplodia theobromae* causing tip blight of *Dianella tasmanica* 'variegata' from India; *Marasmiellus subpruinus* from Madeira, Portugal, new for Macaronesia and Africa; *Mycena albidolilacea*, *M. tenuispinosa*, and *M. xantholeuca* from Russia; *Neonectria neomacrospora* on *Madhuca longifolia* from India; *Nothophoma quercina* on *Vitis vinifera* from Italy; *Plagiosphaera immersa* on *Urtica dioica* from Austria; *Rinodina sicula* from Turkey; *Sphaerosporium lignatile* from Wisconsin, USA; and *Verrucaria murina* from Turkey. Multi-locus analysis of ITS, LSU, *rpb1*, *tef1* sequences revealed that *P. immersa*, commonly classified within Gnomoniaceae (Diaporthales) or as Sordariomycetes *incertae sedis*, belongs to Magnaporthaceae (Magnaporthales). Analysis of a six-locus Ascomycota-wide dataset including SSU and LSU sequences of *S. lignatile* revealed that this species, currently in Ascomycota *incertae sedis*, belongs to Pyronemataceae (Pezizomycetes, Pezizales).

Keywords: 13 new species, 16 new records, Agaricomycetes, Dothideomycetes, Glomeromycota, integrative taxonomy, Laboulbeniomycetes, Magnaporthaceae, Pezizomycetes, Pucciniomycetes, Pyronemataceae, Sordariomycetes.

The present paper is the fifth contribution in the FUSE series published by *Sydowia* (Crous et al. 2015, Hernández-Restrepo et al. 2016, Krisai-Greilhuber et al. 2017, Liu et al. 2018). Again, new species and new records are presented. For two taxa (*Plagiosphaera immersa*, *Sphaerosporium lignatile*), molecular phylogenetic data were employed to resolve their familial placement. The FUSE series addresses the “fusion” between phenotypic data and molecular genetic data. Contributions are wide in scope – including interesting observations of known species, newly introduced sexual–asexual connections and taxonomic consequences following the

One Fungus One Name (1F1N) principle (Hawsworth et al. 2011, Wingfield et al. 2012), epitypification of previously described species, and the use of phylogenetic data to resolve the placement of known taxa. Authors who wish to contribute to the next part in this series, FUSE 6, can e-mail submissions to Danny Haelewaters (danny.haelewaters@gmail.com) or Irmgard Krisai-Greilhuber (irmgard.greilhuber@univie.ac.at).

For FUSE 6, we urge authors to incorporate data from morphology, molecular phylogeny, ecology, host specificity, mating behaviour, and/or geography. As we are uncovering more and more cryptic

diversity, it becomes difficult to accept taxonomic conclusions based on morphology alone. We have seen this “integrative taxonomy” approach being increasingly used in different groups of fungi – e.g., *Aspergillus* (Eurotiales, Eurotiomycetes; Pringle et al. 2005), *Helvella*, *Octospora* (Pezizales, Pezizomycetes; Skrede et al. 2017, Sochorová et al. 2019), *Hesperomyces* (Laboulbeniales, Laboulbeniomycetes; Haelewaters et al. 2018), *Ophiocordyceps* (Hypocreales, Sordariomycetes; Araújo et al. 2015), *Phialocephala* (Helotiales, Leotiomycetes; Grünig et al. 2008), *Protoparmelia* (Lecanorales, Lecanoromycetes; Singh et al. 2015), *Cortinarius* (Agaricales, Agaricomycetes; Stefani et al. 2014), *Crepidotus* (Inocybaceae, Agaricomycetes; Aime 2004), *Geastrum*, *Myriostoma* (Geastrales, Agaricomycetes; Sousa et al. 2017, Accioly et al. 2019), *Hericium* (Russulales, Agaricomycetes; Jumbam et al. 2019), *Tranzscheliella* (Ustilaginales, Ustilaginomycetes; Li et al. 2017), and several entries in the present paper. Descriptions of new species based on single isolates will only be accepted by the discretion of the Editorial Board. Authors must refer to the International Code of Nomenclature for algae, fungi, and plants (Turland et al. 2018) before describing taxa, and author(s) of introduced taxa (author names or their abbreviations) must be according to the International Plant Names Index (IPNI 2019). A diagnosis of a newly proposed taxon may be presented, highlighting the differences to the most similar known species. When citing GenBank accession numbers, we highly encourage authors to cite those papers in which the sequences were first published. Specific *Author's Guidelines* for future FUSE submissions will be uploaded to the website of Sydowia (<http://www.sydowia.at/>) in the first half of 2020.

### Materials and methods

#### Sample collection, isolation, and specimen examination

Basidiomata of *Cortinarius* were collected from different localities in northwestern Himalayan forests in India and Pakistan. Collections were tagged, packed after noting macro-morphological characters, and air-dried. For microscopic study, thin sections were prepared and stained in 5 % KOH and Melzer's reagent. Dimension ranges were measured for 25 basidiospores, 20 basidia, and 20 marginal cells for each collection. The following abbreviations were used in the descriptions: av. = mean spore size, Q = quotient of L/W ratios, Qav. = mean of Q values. Line drawings of spores were prepared us-

ing a camera lucida. Herbarium specimens are deposited at LAH (Department of Botany, University of the Punjab, Lahore, Pakistan) and CAL (Central National Herbarium, Botanical Survey of India, Howrah, West Bengal, India).

During June 2016, five asymptomatic samples of *Atriplex lentiformis* (Fig. 6a), a salt-tolerant plant, were collected from saline deserts and dry salt-marshes around Abadan and Ahvaz (Kozeria), Khuzestan province, southwestern Iran. Small pieces (0.3–0.5 cm) of the roots were surface-sterilized by sodium hypochlorite and plated on potato dextrose agar (PDA, Difco, MI) supplemented with streptomycin (50 mg/l). After 10 days incubation at 28 °C, two *Curvularia* isolates were obtained and subjected to further characterization. The isolates were purified by single spore method (Babaahmadi et al. 2018). The holotype specimen (dried culture) was deposited at IRAN (Herbarium Ministerii Iranici Agriculturae, Iranian Research Institute of Plant Protection, Tehran, Iran) (IRAN 16941F). In addition, living cultures were deposited at IRAN, CBS (Westerdijk Fungal Biodiversity Centre, Utrecht, Netherlands), and SCUA (Collection of Fungal Cultures, Department of Plant Protection, Shahid Chamran University of Ahvaz, Iran).

Growth experiments were performed on PDA at 28 °C with 12 h fluorescent light and 12 h darkness for 5–15 days. Fungal structures were mounted in lactophenol and lactophenol-cotton blue using the method of Riddle (Riddle & Briggs 1950). Color codes follow Kornerup & Wanscher (1967). Morphological characters including morphometry were observed using a Leitz Wetzlar (SM-LUX) Basic Biological Light Microscope; 100 measurements for each structure were recorded and analyzed using SPSS software (SPSS, Chicago, IL). Dimensions are given as a maximum and minimum range followed by 95 % confidence intervals and mean  $\pm$  standard deviation. Photomicrographs were captured with an Olympus BX51 microscope (Olympus, Melville, NY) connected to an Olympus DP12 digital camera.

*Gloeocantharellus* specimens were photographed and annotated in the field and then dried in an electric dryer. Macroscopic descriptions were gained from original field notes and photographs. Color codes follow Kornerup & Wanscher (1967). Micro-morphological features were observed from dried material after sectioning and mounting in 5 % KOH, 1 % Congo Red, or Melzer's reagent. In the description of *Gloeocantharellus*, notation of basidiospores (n/m/p) indicates that measurements were made on n basidiospores from m basidiomata of p collections. The notation (a)b–c(d) was used to

describe basidiospores dimension, with 'b-c' representing  $\geq 90$  % of the measured values and 'a' and 'd' being the extreme values. Q refers to the length/width ratio ranges of an individual basidiospore and  $Q_m$  = the average Q of all basidiospores  $\pm$  sample standard deviation. Sections were studied at a magnification of up to 1000 $\times$  using an Olympus BX51 microscope. All line-drawings of microstructures were drawn from rehydrated material by free hand. Studied specimens are deposited at GDGM (Macrofungi Herbarium, Guangdong Institute of Microbiology, Guangzhou, China).

Thalli of *Laboulbenia* were removed from host specimens at the foot and mounted on microscope slides in Amann's solution (Benjamin 1971), with the help of Minuten Pins (BioQuip #1208SA) inserted manually onto wooden rods. The micropin was first submerged in Hoyer's medium to make the thalli stick to the pin and prevent them from getting lost or flying away. Thalli or groups of thalli were placed in a droplet of Hoyer's on a microscope slide, aligned and oriented vertically, and allowed to settle briefly. We placed a drop of Amann's solution on a coverslip and dropped it sideways onto the thalli in the Hoyer's medium. Finally, the coverslip was ringed with nail varnish. Mounted specimens were studied microscopically at 400–1000 $\times$  magnification. Slides are deposited at BCB (Universitat Autònoma de Barcelona, Spain), BR (Meise Botanic Garden, Belgium), FH (Farlow Herbarium, Harvard University, USA), INPA (Instituto Nacional de Pesquisas da Amazônia, Brazil), and MIUP (Museo de Invertebrados G.B. Fairchild, Universidad de Panamá, Panama).

The macroscopic descriptions of *Pluteus cutedractus* sp. nov. are based on observations of fresh material, photographs were taken with a Canon EOS 80D camera. Terminology follows Vellinga (1990). The micro-morphological characters are based on the study of fresh and dried material. Dry specimens were rehydrated in distilled water before observation and mounted in aqueous Congo Red. The notation [n/m/p] indicates that measurements were made on "n" randomly selected basidiospores from "m" basidiomata of "p" collections. Q indicates the quotient of length and width of the spores in sideview. Basidiospore dimensions are presented as (a) b-c-d (e), with (a) = minimum value, b = (average - standard deviation), c = average, d = (average + standard deviation), and (e) = maximum value. Q represents the range of the length/width ratio for all measured spores. For other microscopic structures 20 elements were measured. Voucher specimens are deposited at

MCVE (New Herbarium, Museo di Storia Naturale di Venezia, Venice, Italy).

For the *Rhizoglosum* study, soil samples (0–30 cm depth) were taken in agricultural field sites with Inca nut (*Plukenetia volubilis* L.) in Palmiche (06°20'02.40"S, 076°36'00.00"W, 858 m a.s.l.) in the Peruvian Amazonia lowlands and adjacent Andean low mountain ranges in the Department San Martín of the province Lamas. This area is a traditional agroforestry site, in which the Inca nut is grown in mixed cultures with maize, beans, and other field crops without addition of chemical fertilizers and pesticides. Mean annual temperatures are about 25–27 °C, with variation between 18 and 32 °C throughout the year. Mean annual precipitation is approximately 1300 mm. Bait cultures were established in the greenhouse under ambient temperature conditions, in several cylindrical 1 l pots with 1 kg of substrate as described in Corazon-Guivin et al. (2019a). The substrate consisted of a 1:1 mixture of field-collected soil samples and coarse river sand. The substrate mixtures were autoclaved at 121 °C for 60 min, three weeks before establishment of the bait cultures. At inoculation and bait culture establishment, the pots were first filled to 75 % with the autoclaved substrate. Thereafter, 50–60 spores were added to the substrate surface and five seeds of each of the four plant species *Sorghum vulgare* L., alfalfa (*Medicago sativa* L.), *Brachiaria* sp., and Inca nut (*Plukenetia volubilis*) were seeded in order to establish the mycorrhizal association and reproduce spores of the new fungal species. The seeds were surface sterilized before seeding, using sodium hypochlorite (0.5 %). Finally, the seeds were covered with the remaining 25 % of the autoclaved substrate. The cultures were maintained in the greenhouse of the Facultad de Ciencias Agrarias, Universidad Nacional de San Martín-Tarapoto for ten months, with 21.4 °C, 29 °C, and 38.2 °C as minimum, mean, and maximum temperature, respectively. The relative humidity was from 45 % to 75 % between March and December 2018. The pots were irrigated every other day and fertilized with a Long Anston nutrient solution (Hewitt 1966) every two weeks, with reduced P contents (60 % reduction). Spores of *Rhizoglosum variable* sp. nov. were separated from the bait cultures and single species substrates by a wet sieving process (Sieverding 1991). The description of the morphological spore characteristics and their subcellular structures are based on observations of specimens mounted in polyvinyl alcohol-lactic acid-glycerol (PVLG; Koske & Tessier 1983), Melzer's reagent, a mixture of PVLG and Melzer's reagent (Brundrett et al. 1994), a mixture

of lactic acid to water at 1:1, and water (Spain 1990). Terminology of the spore structure follows Blaszowski (2012) and Oehl et al. (2015) for species with glomoid spore formation. Photographs were taken with a digital camera (Leica DFC 295) on a compound microscope (Leitz Laborlux S), using Leica Application Suite version 4.1 software (Leica Microsystems, GmbH, Bochum, Germany). Specimens mounted in PVLG and a (1:1) mixture of PVLG and Melzer's reagent were deposited at Z (Institut für Systematische Botanik, Universität Zürich, Switzerland) and ZT (Herbarium, Eidgenössische Technische Hochschule Zürich, Switzerland). Staining of the mycorrhizal root structures was carried out according to Vierheilig et al. (1998).

Collections of *Russula* were obtained from Yunnan, China in 2017. Notes and photographs were taken on macro-morphological features based on fresh mature basidiomata, and specimens were then dried in an oven at 50 °C until completely desiccated. Studied specimens were deposited at LI (personal herbarium of Haijiao Li) and RITF (herbarium at the Research Institute of Tropical Forestry, Chinese Academy of Forestry, Beijing, China). Terminology for descriptive terms follows Vellinga (1988). Color names and codes follow the HTML Color Code (<http://www.htmlcolorcode.org/>). Microscopic examinations are according to Song et al. (2018). Tissues of specimens were firstly immersed in 5 % KOH, then stained with 1 % aqueous Congo red solution for microscopic observation with an Olympus BX41 microscope under a 100× oil immersion objective lens. Observations and measurements of the basidiospores and ornamentation were made in Melzer's reagent. A 10 % FeSO<sub>4</sub> solution was used to test for chemical reactions on fresh specimens. Sulphovanillin (SV) solution was used to test for reactions of cystidia. Cresyl blue was used for performing metachromatic reactions (Buyck 1989). Scanning electron microscope (SEM) photos were captured with a JEOL JSM-6510 microscope (Tokyo, Japan). The abbreviation [n/m/p] indicates 'n' basidiospores measured from 'm' basiodata of 'p' collections. In the basidiospore dimension notation, (a)b–c(d), b–c is the range including 90 % or more of the measured values, with a and d being the extreme values. Q = variation in the L/W ratios between the specimens studied.

Two *Didymellaceae* strains (S3 and CG7) were recovered from a survey performed on withered grapes on 2017 vintage and another three strains (UC23, UC30, UC56) from a previous survey (Lorenzini et al. 2016). The five isolates were deposited

at CBS (Westerdijk Fungal Biodiversity Institute, Utrecht, Netherlands) under the following accessions: UC30 = CBS 145105, CG7 = CBS 145107, UC56 = CBS 145106, S3 = CBS 145109, UC23 = CBS 145113). Berries of Corvina and Garganega grape variety were collected in fruit-drying rooms located in Valpolicella and Gambellara winemaking areas (Italy). The berries were directly plated on potato dextrose agar (PDA, Difco Laboratories, Detroit, MI) for 5 d at 25 °C, after which colonies were isolated, purified, and maintained on the same medium. To observe cultural characteristics and micro-morphology, all isolates were incubated on PDA, MEA (2 % w/v malt extract, 0.1 % w/v peptone, 2 % w/v dextrose, 1.5 % w/v agar) and OA (5 % w/v oatmeal and 2 % w/v agar) at 25 °C in alternating cycles for 7 d of 12 h fluorescent light and 12 h darkness conditions. The growth rate (diam. in mm) was measured daily for 7 d (three replicate plates for each isolate) and the experiments were performed twice. The micro-morphology of each strain was examined on PDA, MEA, OA and, also on pine needle on water agar (WA, 15 g/l agar) after 7, 14, 30, and 60 d. The strains were analyzed using stereomicroscopy (Leica EZ4D, Leica Microsystems, Wetzlar, Germany) and light microscopy (Leica DM750) with camera attached. Length and width of 20 pycnidia, 20 chlamydospores, and 50 conidia from each isolate were measured. The isolates were tested for pathogenicity on young and old leaves, canes, and berries of grapevine. Healthy leaves, berries, and canes were excised from the test plants and surface sterilized by immersion for 5 min in 0.5 % NaOCl, rinsed twice with sterile distilled water, and placed in plastic trays appropriately spaced. Fungal isolates were transferred onto MEA and grown for 5 d at 25 °C in 12 h light/12 h dark. Five mm plugs of each isolate were placed mycelium-side down onto surface sterilized plant tissues. Negative control trials were performed placing non-inoculated plugs of MEA. Positive control trials were performed placing *Botrytis cinerea* ITEM 17200 plugs on berries and leaves and *Neofusicoccum parvum* ITEM 17213 plugs on canes. The experiment was performed two times with ten replicates at least. Isolations from infected plant tissues were performed to confirm fungal colonization (Koch's postulate).

*Strobilomyces* samples were collected from Huangshan, a mountain range in eastern China. The locality is occupied by a forest dominated by Fagaceae, Pinaceae, and Theaceae. Macroscopic descriptions and ecological information were recorded based on field notes and digital images. Color codes in the description follow Kornerup & Wan-

scher (1981). Microscopic characters were observed using a light compound microscope (Leica DM2500). Sections of dried specimens were mounted in 5 % KOH. Basidiospores were examined with a scanning electron microscope (Zeiss EVO18, Thornwood, New York, NY), and the method follows Wu et al. (2014). The abbreviation n/m/p means 'n' basidiospores from 'm' basidiomata of 'p' collections. The notation (a)b–c(d) indicates the size of basidiospores, in which 'b–c' contains a minimum of 90 % of the measured values, and 'a' and 'd' are the extreme values. Spore length/width ratios are recorded as Q.  $Q_m$  refers to the mean values of  $Q \pm$  sample standard deviation. Specimens observed in this study are deposited at HKAS (Herbarium of Cryptogams, Kunming Institute of Botany, Chinese Academy of Sciences, Kunming).

*Uromyces*-infected leaves of *Rumex dentatus* were collected during a rust fungi survey in Pakistan in 2015. Using a sterile blade, the spores were isolated from infected leaves and mounted on a glass slide in distilled water for temporary observations. These preparations were fixed in glycerin jelly as semi-permanent slides for light microscopy. At least 30 spores, including the smallest and largest spores, were measured for each stage and photographed using a compound microscope (HM LU Leitz) equipped with digital camera (Ali et al. 2016a). *Uromyces* samples examined for this study are deposited at ISL (Herbarium of Pakistan, Department of Plant Sciences, Quaid-i-Azam University, Islamabad, Pakistan).

In summer 2015, quinces (*Cydonia oblonga*) and apples (*Malus domestica*) with symptoms of *Alternaria* black and brown rot, respectively, (Fig. 35) were collected from gardens in Nour city, Mazandaran Province, Iran. The fruits were surface sterilized in 0.5 % (v/v) sodium hypochlorite solution and rinsed with ddH<sub>2</sub>O. Pieces of fruit tissue from boundaries of healthy and diseased areas were placed on 2 % water agar (WA). Pure fungal cultures of grown fungi were obtained by transferring hyphal tips to potato dextrose agar (PDA). Isolates were stored on PDA slant culture medium at 4 °C. Identification to species level was done using morphological characteristics of the fungal isolate on potato carrot agar (PCA) at 25 °C in the dark and under fluorescent light source (8 h light/16 h darkness). After 5–7 d, three-dimensional sporulation patterns were observed. After 7 d, microscopic slide mounts were prepared in lactophenol solution using the sellotape technique (*sensu* Schubert et al. 2007). Measurements (50× for each characteristic) and microphotographs were taken from slides using

an Olympus BH2 light microscope (Olympus, Tokyo, Japan). After the isolation step, two pure isolates were recovered, one from the diseased part of apple fruit and one from quince fruit. Both fungal isolates were similar based on the morphological features, and only one representative isolate (from quince) was selected for molecular investigation. A PDA culture of this isolate was deposited at IRAN (Herbarium Ministerii Iranici Agriculturae, Department of Botany, Iranian Research Institute of Plant Protection, Tehran, Iran). We also performed a pathogenicity assay. Apple (Golden delicious) and quince fruits were washed with 70 % EtOH for 30 s, followed by dipping in 0.1 % sodium hypochlorite solution and rinsing with ddH<sub>2</sub>O. The disinfected fruits were wounded by nail at three sites about 2.5 mm in diam. and three mm in depth (Etebarian et al. 2005). A total of 30 µl of  $1 \times 10^6$  conidia/ml suspension of the recovered isolate was inoculated to each of the wounds. Control treatments were inoculated with ddH<sub>2</sub>O. After inoculation, fruits were placed in enclosed plastic trays to maintain high relative humidity (above 90 %) and then incubated at 25 °C for 14 d. Treatments were set up in four replicates.

A lichenological survey was conducted in eastern Turkey from June to August 2018. Hand-made sections were observed with a Zeiss Stemi 2000-c stereomicroscope and a Zeiss Axio Imager.A2 light microscope. Macrophotographs and microphotographs were taken with a Zeiss AxioCam ERc5s digital camera. Species concepts follow Giralt & Llimona (1997), Khodosovtsev (2004), Smith et al. (2009), and Sheard et al. (2017). Voucher collections are deposited at KTUB (Herbarium, Department of Biology, Karadeniz Technical University, Trabzon, Turkey).

For the *Lasiodiplodia theobromae* study, diseased *Dianella tasmanica* 'variegata' leaves were cut into small pieces, surface sterilized in 1 % sodium hypochlorite for 45–60 sec, 3× rinsed in ddH<sub>2</sub>O, plated on water agar, and then incubated at 28 °C for 5 d. Hyphal tips from the margin of developing colony were picked up and transferred to potato dextrose agar (PDA) slants for pure culture. Material was deposited at HCIO (Herbarium, Division of Mycology and Plant Pathology, Indian Agricultural Research Institute, New Delhi, India) and ITCC (Indian Type Culture Collection, New Delhi, India).

Fruiting bodies of *Marasmiellus* (Agaricales, Omphalotaceae) were collected in two localities during the foray of the XVII Congress of European Mycologists held in Maderia, Portugal in September 2015. Collections were photographed and mac-

roscopic descriptions were based on the fresh basidiomata. Color codes follow Kornerup & Wanscher (1967). Microscopic characters were observed on dried material mounted in water and Congo Red using an Olympus BX-50 light microscope under 400× and 1000×. The microscopic description is based on 30 measurements of basidiospores, and 20 of cheilocystidia and caulocystidia per voucher collection. Morphological terminology follows Antonín & Noordeloos (2010). Abbreviations used: E = quotient of length and width in any one basidiospore, Q = mean of E values. Studied specimens are deposited at BRNM (Herbarium, Botany Department, Moravian Museum, Brno, Czech Republic), PRM (Herbarium, Mycological Department, National Museum, Prague, Czech Republic), IB (Herbarium, Institut für Botanik, Universität Innsbruck, Austria), and L (Naturalis Biodiversity Center, Nationaal Herbarium Nederland, Leiden, The Netherlands).

*Mycena* specimens were collected in 2017 and 2018. The material was studied according to standard methods used in fungal taxonomy (Ivoilov et al. 2017). Macroscopic descriptions are based on fresh material shortly after collecting. Photos of basidiomata were taken in the field with natural light. Microscopic characters were observed in squash preparations of small parts of dried basidiomata mounted in 5 % KOH or 1 % Congo Red in 10 % NH<sub>4</sub>OH. Amyloidity of spores was checked in Melzer's reagent. Microscopic measurements were made with a Zeiss Axio Imager A1 microscope at 1000× using an oil immersion objective and Nomarski interference contrast. Drawings of microcharacters were made using InkScape from microphotographs taken with AxioCam MRc5 and AxioVision Microscopy Software. Basidiospore measurements are based on at least 20 spores (unless otherwise indicated). For measurements of basidia, cystidia, pileipellis, and stipitipellis hyphae and related structures (excrescences, terminal cells, caulocystidia) at least 10 elements were measured. The basidia were measured without sterigmata, and the basidiospores without apiculus. All specimens are deposited at LE (Russian Academy of Sciences, Komarov Botanical Institute of RAS, Saint Petersburg, Russia).

Microscopic observations of *Plagiosphaera immersa* were made in tap water except where noted. Methods of microscopy included stereomicroscopy using a Nikon SMZ 1500 equipped with a Nikon DS-U2 digital camera, and Nomarski differential interference contrast (DIC) using a Zeiss Axio Imager.A1 compound microscope equipped with a Zeiss AxioCam 506 colour digital camera. Images

and data were gathered using the NIS-Elements D version 3.22.15 or Zeiss ZEN Blue Edition software packages. Measurements are reported as maxima and minima in parentheses and the range representing the mean plus and minus the standard deviation of a number of measurements given in parentheses. Studied specimens are deposited at WU (Herbarium, Faculty Center Botany, Faculty of Life Sciences, Universität Wien, Austria). Isolates were prepared from ascospores as described in Jaklitsch (2009) and grown on MEA or on 2 % corn meal agar plus 2 % w/v dextrose (CMD). Growth of liquid culture was performed as reported previously (Voglmayr & Jaklitsch 2011, Jaklitsch et al. 2012).

Fruiting bodies of *Sphaerosporium lignatile* were collected from a ravine in 2017. Macroscopic and microscopic photos were taken from dried material. Microscopic characteristics were observed using squash preparations in deionized water or 5 % KOH stained with phloxine on a Zeiss Axio Imager A2 microscope (Zeiss, White Plains, NY) at 400× magnification. Photographs were made with an AxioCamMR3 camera (Zeiss). Conidia measurements include the cell wall. Measurements are reported as the minimum and maximum in parentheses, the mean plus and minus one standard deviation, and the number of measurements. All measurements were taken in 5 % KOH stained with phloxine. The studied collection is deposited at MICH (Herbarium, University of Michigan, USA).

DNA extraction, PCR amplification, and sequencing

DNA of *Cortinarius* basidiomata was extracted from small pieces of dried specimens using the Extract-N-Amp Plant PCR Kit (Sigma-Aldrich, St. Louis, MO) or the E.Z.N.A. SP Fungal DNA Mini Kit (Omega Bio-Tek, Norcross, GA) following manufacturer's protocols. For amplification of the ITS (ITS1–5.8S–ITS2) rDNA region, 1 µl of extracted DNA was used in a 20 µl PCR reaction using ITS1F and ITS4 primers (White et al. 1990, Gardes & Bruns 1993). PCR products were checked on 1 % agarose gel. Positive PCR products were sent to Macrogen (South Korea) and LGC Genomics (Germany) for direct sequencing in both directions using the same primers.

*Curvularia* mycelial biomass was grown in potato-dextrose-broth (PDB), collected by passing through filter paper, and freeze-dried. DNA was extracted using a phenol- and chloroform-based method as described by Raeder & Broda (1985) with some modifications (Ahmadpour et al. 2017). The

ITS rDNA region and *gpd* were amplified in a 50 µl PCR reaction on a MJ Mini™ Gradient Thermal Cycler (BioRad, Hercules, CA) using the ITS1 and ITS4 (White et al. 1990) and *gpd1* and *gpd2* (Berbee et al. 1999) primers, respectively. PCR mix consisted of 0.1 mM dNTPs, 0.4 µM of each primer, 0.06 U/µl Prime Taq DNA Polymerase, 1× prime Taq Reaction Buffer, 2.5 mM of MgCl<sub>2</sub>, and 5 ng/µl template DNA. Cycler conditions were as follows: initial denaturation at 94 °C for 3 min; followed by 35 cycles of denaturation at 94 °C for 30 s, annealing at 54 °C (ITS) or 56 °C (*gpd*) for 30 s, and extension at 72 °C for 60 s; and a final extension at 55 °C for 30 s. Amplicons of the expected size were excised from gel agarose and purified with the GF-1 AmbiClean Kit (Vivantis, Malaysia). Amplified products were sequenced by Macrogen (South Korea). Consensus sequences were obtained with DNA Baser Sequence Assembler version 4 (Heracle BioSoft, Romania). Generated sequences were deposited in NCBI GenBank (Tab. 1).

Genomic DNA of *Gloeocantharellus* was extracted from silica-gel dried specimens using the Sangon Fungus Genomic DNA Extraction kit (Sangon Biotech, Shanghai, China) following the manufacturer's instructions. The internal transcribed spacer (ITS) and large subunit nuclear ribosomal DNA (LSU) regions were amplified using primer pairs ITS1/ITS4 (White et al. 1990) and LR0R/LR5 (Vilgalys & Hester 1990, Rehner & Samuels 1994), respectively. Amplified products were sequenced by the Beijing Genomic Institute (BGI) using the same primers. Generated sequence reads were assembled by SeqMan version 7.1.0 (DNASar, Madison, WI) and submitted to NCBI GenBank.

DNA was isolated from thalli of *Laboulbenia oioveliicola* sp. nov. using the QIAamp DNA Micro Kit (Qiagen, Stanford, CA) with modifications (Haelewaters et al. 2015). We removed 8 thalli (3 juvenile, 5 mature) from the host and performed the standard procedure until step 3. Then the sample was processed in a FastPrep FP120 Cell Disrupter (5.0 m/sec, 15 sec) and incubated overnight at 56 °C before proceeding with the manufacturer's instructions. Amplification of the large subunit ribosomal DNA region (LSU rDNA) was done using primers LIC24R (5'-GAAACCAACAGGGATTG-3') and LR3 (5'-GGTCCGTGTTTCAAGAC-3') (Vilgalys & Hester 1990, Miadlikowska & Lutzoni 2000). PCR reactions consisted of 13.3 µl of Extract-N-Amp PCR ReadyMix (Sigma-Aldrich, St. Louis, MO), 2.5 µL of each 10 µM primer, 5.7 µl of H<sub>2</sub>O, and 1 µl of template genomic DNA. Amplification reactions were run under the following thermocycler condi-

tions: initial denaturing at 94 °C for 3 min; then 35 cycles of denaturing at 94 °C for 1 min, annealing at 50 °C for 45 sec, extension at 72 °C for 1.5 min; and a final extension step of 72 °C for 10 min. Successful PCR products were cleaned using the QIAquick PCR Purification Kit (Qiagen) and subsequently sequenced by the Harvard University FAS Division of Science Bauer Core Facility. We prepared 10 µl sequencing reactions containing the same primers and 1 µl of purified PCR product. Sequencing reactions were performed using the Big Dye® Terminator v3.1 Cycle Sequencing Kit (Life Technologies, Carlsbad, CA). Generated forward and reverse sequence reads were assembled, trimmed, and edited in Sequencher version 4.10.1 (Gene Codes Corporation, Ann Arbor, MI).

Genomic DNA was extracted from *Pluteus* basidiomata using the CTAB procedure of Doyle & Doyle (1987). The ITS region was amplified with primers ITS1F (Gardes & Bruns 1993) and ITS4 (White et al. 1990). Sequences were assembled and edited in Geneious version 8.1.2 (Kearse et al. 2012) and then submitted to GenBank. Accession numbers are reported in Fig. 16.

Healthy and intact *Rhizogloium* spore clusters were isolated from the single species cultures and superficially cleaned of soil particles by friction on cellulose filter paper (WHATMAN, Grade 50; Corazon-Guivin et al. 2019b). Spores were surface-sterilized (Mosse 1962) using a solution of chloramine T (2 %), streptomycin (0.02 %), and Tween 20 (2–5 drops in 25 ml final volume) for 20 min and rinsing five times in milli-Q H<sub>2</sub>O. Two independent groups of sterile spore clusters, each containing 20–30 spores, connected by a common hypha were selected under a laminar flow hood and individually transferred into Eppendorf PCR tubes as described in Corazon-Guivin et al. (2019b). Crude extract was obtained by crushing the individual spore clusters with a sterile disposable micropestle in 23 µl milli-Q H<sub>2</sub>O (Palenzuela et al. 2013). Direct PCR of these crude extracts was performed in an Eppendorf Mastercycler nexus instrument (Hamburg, Germany) with a Platinum Taq DNA Polymerase High Fidelity (Invitrogen, Carlsbad, CA) with 0.4 µM of each primer. A two-step PCR was conducted to amplify the ribosomal fragment consisting of partial SSU, ITS, and partial LSU rDNA using the primers SSUmaf/LSUmar and SSUmc/LSUmb, consecutively (Krüger et al. 2009). PCR products from the second round of amplifications (~1500 bp) were separated electrophoretically on 1.2 % agarose gels, stained with Diamond™ Nucleic Acid Dye (Promega, Madison, WI) and viewed by UV illumination.



Tab. 1. Details of sequences and isolates included in the molecular analysis for the new species and interesting reports<sup>1</sup>.

Species name	ID (isolate, strain <sup>1</sup> , status <sup>2</sup> , voucher)	Country, isolation source	Accession numbers								Reference	
			ITS	LSU	mtSSU	tefi	rpb1	rpb2	cox3	gpd		
<i>Afroboletus elegans</i>	HKAS 102628	Benin				KX869266	KX869521	KX869592	KX869139			Han et al. (2018a)
<i>Afroboletus luteolus</i>	PC 0723573	Zambia				KX869290	KX869545	KX869416	KX869158			Han et al. (2018a)
<i>Afroboletus multiyugus</i>	PC 0723570	Burundi				KX869298	KX869554	KX869425	KX869167			Han et al. (2018a)
<i>Afroboletus sequestratus</i>	PC 0723575	Zambia				KX869374	KX869631	KX869504	KX869246			Han et al. (2018a)
<i>Alternaria alstroemeriae</i>	CBS 118808	USA, <i>Alstroemeria</i> sp.	KP124296									
<i>Alternaria alternata</i>	CCTU 254	Iran, <i>Helianthus annuus</i>	KC935769									
<i>Alternaria alternata</i>	Pessimon	<i>Diospyros</i> sp.	EF452443									
<i>Alternaria arborescens</i>	BBGD4	Netherlands, <i>Malus domestica</i>	MG744452									
<i>Alternaria arborescens</i>	DPM14	Oman, <i>Phoenix dactylifera</i>	KY484887									
<i>Alternaria destruens</i>	EGS 46-069	USA	AY278836									
<i>Alternaria gossypina</i>	CBS 100.23	<i>Malus domestica</i>	KP124429									
<i>Alternaria limoniasperae</i>	BC2-RLR-1s	USA	JX397904									
<i>Alternaria longipes</i>	CBS 113.35	<i>Nicotiana tabacum</i>	KP124440									
<i>Alternaria tenuissima</i>	15-242	South Korea, <i>Aronia melanocarpa</i>	LC134322									
<i>Alternaria tenuissima</i>	15-243	South Korea, <i>Aronia melanocarpa</i>	LC134323									
<i>Alternaria tenuissima</i>	M06-1553-3b	USA, <i>Sorghum</i> sp.	JN634834									
<i>Alternaria tenuissima</i>	IRAN 2428 C	Iran, <i>Cydonia oblonga</i>	KU323573									
<i>Bambusicularia brunnea</i>	CBS 133559, T	Japan, <i>Sasa</i> sp.	KM484830	KM484948								
<i>Bartramomyces calathiae</i>	CBS 129274	Brazil, <i>Calathea longifolia</i>	KM484831	KM484950								
<i>Bifusisporella sorghi</i>	URM 7442, T	Brazil, <i>Sorghum bicolor</i>	MK060155	MK060153								
<i>Bifusisporella sorghi</i>	URM 7442, T	Brazil, <i>Sorghum bicolor</i> , endophyte from leaves	MK060155	MK060153								
<i>Bipolaris drechsleri</i>	MUS0028	USA, <i>Microstegium vimineum</i>	KF500532									
<i>Boletus reticulocaps</i>	HKAS 55431	China										
<i>Budunggurubania cynodonticola</i>	BRIP 59305, T	Australia; <i>Cynodon dactylon</i>	KP162134	KP162140								
<i>Eurogeneneria spartinae</i>	ATCC 22848	USA; <i>Spartina alterniflora</i> , leaves	JX134666	DQ341492								
<i>Bussabanomyces longisporus</i>	CBS 125232, T	Thailand; <i>Anomum siamense</i> , leaves	KM484832	KM484951								
<i>Cortinarius annae-maritae</i>	F74990 (O)		NR153053									
<i>Cortinarius armillatus</i>	TUB01193		AY669671									
<i>Cortinarius bacioflavivus</i>	JFA13668		NR153055									
<i>Cortinarius bacioflavivus</i>	Beug 03MWB120308		KU041730									
<i>Cortinarius bacioflavivus</i>	Beug 01MWB110910		KU041731									
<i>Cortinarius bacioflavivus</i>	Beug 02MWB043009		KU041732									
<i>Cortinarius bacioflavivus</i>	Beug 01MWB032411		KU041729									
<i>Cortinarius bacioflavivus</i>	Beug 01MWB030809		KU041728									
<i>Cortinarius bacioflavivus</i>	Beug 01MWB021910		KU041726									
<i>Cortinarius biriensis</i>	TEB638-15 (O)		KX831118									
<i>Cortinarius boulderensis</i>	VMS27		F717363									
<i>Cortinarius borinus</i>	JB-8431/14		KU953944									
<i>Cortinarius brunneocarpus</i>	LAH2408.10		XXXXXXX									
<i>Cortinarius brunneus</i>	TN04-929		EU266637									
<i>Cortinarius bulliardii</i>	TUB011899		AY669659									
<i>Cortinarius colymbadinus</i>	IK99-295 (H)		KJ206494									

Species name	ID (isolate, strain <sup>1</sup> , status <sup>2</sup> , voucher)	Country, isolation source	Accession numbers							Reference	
			ITS	LSU	mtSSU	tef1	rpb1	rpb2	cox3		gpd
<i>Cortinarius conicombonatus</i>	KATO-3455b		MF696141								Sesli & Liimatainen (2018)
<i>Cortinarius conicombonatus</i>	KATO-3455		MF696139								Sesli & Liimatainen (2018)
<i>Cortinarius fulvopulidosus</i>	H6033460		NR154888								Liimatainen (2017)
<i>Cortinarius fuscescens</i>	F74962 (O)		KT591596								Brandrud et al. (2015)
<i>Cortinarius helobius</i>	CFF542		DQ102686								Lundström et al. (2008)
<i>Cortinarius helvobius</i>	TUB011905		AY669667								Garnica et al. (2005)
<i>Cortinarius hinnuleoarmillatus</i>	G 00052098		NR 131790								Niskanen et al. (2006)
<i>Cortinarius hinnuleoarmillatus</i>	IK01-021 (H)		DQ499462								Niskanen et al. (2006)
<i>Cortinarius hinnuleoarmillatus</i>	F3953 (S)		DQ499461								Niskanen et al. (2006)
<i>Cortinarius hinnuleoarmillatus</i>	TN03-083 (H)		DQ499460								Niskanen et al. (2006)
<i>Cortinarius hinnuleocerinus</i>	TN12-175 (H)		MG136827								Liimatainen (2017)
<i>Cortinarius hinnuleus</i> (I)	IB19960139		AY083183								Peintner et al. (2003)
<i>Cortinarius hinnuleus</i> (I)	IB19930113		AY083184								Peintner et al. (2003)
<i>Cortinarius hinnuleus</i> (I)	TUB011512		AY669665								Niskanen et al. (2006)
<i>Cortinarius hinnuleus</i> (II)	CFF332		DQ117926								Niskanen et al. (2006)
<i>Cortinarius hinnuleus</i> (III)	TU105466		UDB020294								UNITE
<i>Cortinarius hinnuleus</i> (III)	AT2005074		UDB002196								UNITE
<i>Cortinarius intemptivus</i>	PML1157 (PC)		KX831120								Brandrud et al. (2017)
<i>Cortinarius lilacinoarmillatus</i>	KCS2428		XXXXXXX								Present study
<i>Cortinarius longispitatus</i>	FH00304566		MF872641								Saba et al. (2017)
<i>Cortinarius nausosouraceus</i>	SMIA24		FJ039683								Harrower et al. (2011)
<i>Cortinarius parvanulatus</i>	TUB011909		AY669664								Garnica et al. (2005)
<i>Cortinarius puellaris</i>	TEB 431-14 (O)		KT591581								Brandrud et al. (2015)
<i>Cortinarius safranopes</i>	TAAM128790		UDB016116								UNITE
<i>Cortinarius</i> cf. <i>serripes</i>	MC01-514		AJ889699								Kjoller R., unpubl.
<i>Cortinarius</i> sp.	P36 (EcM isolate)		AJ534713								Tedersoo et al. (2003)
<i>Cortinarius</i> sp.	BD91 (environ. sample)		JQ666714								Zhiguan et al. (2016)
<i>Cortinarius</i> sp.	BD24 (environ. sample)		JQ666647								Zhiguan et al. (2016)
<i>Cortinarius</i> sp.	BD32 (environ. sample)		JQ666655								Zhiguan et al. (2016)
<i>Cortinarius</i> sp.	BD52 (environ. sample)		JQ666675								Zhiguan et al. (2016)
<i>Cortinarius</i> sp.	BL5 (environ. sample)		JQ666324								Zhiguan et al. (2016)
<i>Cortinarius</i> sp.	MT2 (EcM sampl)		KJ610811								Yang N., Polle A. & Pena R., unpubl.
<i>Cortinarius 'subserripes'</i>	OC13		FJ039552								Harrower et al. (2011)
<i>Cortinarius torvus</i>	TUB011515		AY669668								Garnica et al. (2005)
<i>Cortinarius umbrinolens</i>	TUB011918		AY669658								Garnica et al. (2005)
<i>Curvularia aeri</i>	CBS 294.61	Brazil, air	HE861850								HF565450
<i>Curvularia affinis</i>	CBS 154.34	Indonesia	KJ909780								KM230401
<i>Curvularia abazensis</i>	CBS 144673	Iran, <i>Zinnia elegans</i>	KX139029								MG428693
<i>Curvularia akaii</i>	CBS 317.86	Japan, <i>Themada triandra</i>	KJ909782								KM230402
<i>Curvularia akaiensis</i>	BRIP 16080		KJ415539								KJ415407
<i>Curvularia alcornii</i>	MFLUCC 100703	Thailand, <i>Zea</i> sp.	JX256420								JX276433
<i>Curvularia americana</i>	UTHSC 072649	USA, toe tissue	HE861834								HF565486
<i>Curvularia americana</i>	UTHSC 08-3414	USA, <i>Homo sapiens</i>	HE861833								HF565488

Species name	ID (isolate, strain <sup>1</sup> , status <sup>2</sup> , voucher)	Country, isolation source	Accession numbers					Reference		
			ITS	LSU	mtSSU	tef1	rpb1		rpb2	cox3
<i>Curvularia asianensis</i>	MFLUCC 100711	Thailand, <i>Panicum</i> sp.	JX256424							JX276436
<i>Curvularia australiensis</i>	BRIP 12044	Unknown, <i>Oryza sativa</i>	KJ415540							KJ415406
<i>Curvularia australiensis</i>	CBS 172.57	Vietnam, <i>Oryza sativa</i>	JN601026							JN601036
<i>Curvularia australis</i>	BRIP 12247a	Australia, <i>Eragrostis ciliaris</i>	KC424609							KC747759
<i>Curvularia australis</i>	BRIP 12521	<i>Sporobolus caroli</i>	KJ415541							KJ415405
<i>Curvularia bamnoui</i>	BRIP 16732	USA, <i>Jaquemonia tamijolia</i>	KJ415542							KJ415404
<i>Curvularia beasleyi</i>	BRIP 10972	Australia, <i>Chloris gayana</i>	MH414892							MH433638
<i>Curvularia beerburmensis</i>	BRIP 12942	Australia, <i>Eragrostis bahiensis</i>	MH414894							MH433634
<i>Curvularia boeremae</i>	IMI 164633	India, <i>Portulaca oleracea</i>	MH414911							MH433641
<i>Curvularia borrierae</i>	AR5176r	South Africa, <i>Sorghum bicolor</i>	KP400637							KP419986
<i>Curvularia borrierae</i>	MFLUCC11-0422	Thailand, grass	KP400638							KP419987
<i>Curvularia bothriochloae</i>	BRIP 12522	Australia, <i>Bothriochloa</i> sp.	KJ415543							KJ415403
<i>Curvularia brachyspora</i>	CBS 186.50	India, soil	KJ922372							KM061784
<i>Curvularia brachyspora</i>	ZW020185		HM053667							HM053655
<i>Curvularia buchloes</i>	CBS 246.49	USA, <i>Buchloe dactyloides</i>	KJ909765							KM061789
<i>Curvularia carica-papayae</i>	CBS 135941	India, <i>Carica papaya</i>	HG778984							HG779146
<i>Curvularia chlamydospora</i>	UTHSC 072764	USA, toe nail	HG779021							HG779151
<i>Curvularia clara</i>	BRIP-61680	Australia, <i>Oryza</i> sp.	KU552205							KU552167
<i>Curvularia coctiae</i>	BRIP 24261	Australia, <i>Litchi chinensis</i>	MH414897							MH433636
<i>Curvularia coicis</i>	CBS 192.29	Japan, <i>Coix lacryma</i>	JN192373							JN600962
<i>Curvularia colbranni</i>	BRIP 13066	Australia, <i>Cynum zeylanicum</i>	MH414898							MH433642
<i>Curvularia crustacea</i>	BRIP 13524	Indonesia, <i>Sporobolus</i> sp.	KJ415544							KJ415402
<i>Curvularia cymbopogonis</i>	CBS 419.78	Netherlands, <i>Yucca</i> sp.	HG778985							HG779129
<i>Curvularia dactyloctenicola</i>	CPC 28810	Thailand, <i>Dactyloctenium aegyptium</i>	MF490815							MF490837
<i>Curvularia dactyloctenii</i>	BRIP 12846	Australia, <i>Dactyloctenium radulans</i>	KJ415545							KJ415401
<i>Curvularia ellisi</i>	CBS 193.62	Pakistan, air	JN192375							JN600963
<i>Curvularia ellisi</i>	IMI 75862	Pakistan, air	KJ922379							KM061792
<i>Curvularia eragrosticola</i>	BRIP 12538	Australia, <i>Eragrostis pilosa</i>	MH414899							MH433643
<i>Curvularia eragrostidis</i>	CBS 189.48		HG778986							HG779154
<i>Curvularia geniculata</i>	CBS 187.50	Indonesia, seed	KJ909781							KM063609
<i>Curvularia gladioli</i>	CBS 210.79		HG778987							HG779123
<i>Curvularia gladioli</i>	ICMP 6160	New Zealand, <i>Gladiolus</i> sp.	JX256426							JX276438
<i>Curvularia graminicola</i>	BRIP 23186a	Australia	JN192376							JN600964
<i>Curvularia harveji</i>	BRIP 57412	Australia, <i>Triticum aestivum</i>	KJ415546							KJ415400
<i>Curvularia hauaiensis</i>	BRIP 11987	USA, <i>Oryza sativa</i>	KJ415547							KJ415399
<i>Curvularia heteropogoncola</i>	BRIP 14579	India, <i>Heteropogon contortus</i>	KJ415548							KJ415398
<i>Curvularia heteropogonis</i>	CBS 284.91	Australia, <i>Heteropogon contortus</i>	JN192379							JN600969
<i>Curvularia hominis</i>	CBS 136985	USA, <i>Homo sapiens</i>	HG779011							HG779106
<i>Curvularia homomorpha</i>	CBS 156.60		JN192380							JN600970
<i>Curvularia inaequalis</i>	CBS 102.42	France, sand dune soil	KJ922375							KM061787
<i>Curvularia inaequalis</i>	DAOM 20022	Canada, <i>Pisum sativum</i>	KJ922374							KM061786
<i>Curvularia intermedia</i>	CBS 334.64		HG778991							HG779155
<i>Curvularia intermedia</i>	UTHSC 09-3240		HE861855							HF565469
<i>Curvularia ischaeni</i>	CBS 630.82		JX256428							JX276440

Species name	ID (isolate, strain <sup>1</sup> , status <sup>2</sup> , voucher)	Country, isolation source	Accession numbers						Reference	
			ITS	LSU	mtSSU	tef1	rpb1	rpb2		cox3
<i>Curvularia ischaemi</i>	ICMP 6172	New Zealand, <i>Ischaemum indicum</i>	JX256428							JX276440
<i>Curvularia kenpeggi</i>	BRIP 14530	Australia, <i>Triticum aestivum</i>	MH414900							MH433644
<i>Curvularia khuzestanica</i>	CBS 144736	Iran, <i>Atriplex lentiformis</i>	MH688044							MH688043
<i>Curvularia khuzestanica</i>	SCUA-11C-2	Iran, <i>Atriplex lentiformis</i>	MH688046							MH688045
<i>Curvularia kusanoi</i>	CBS 137.29	Japan, <i>Eragrostis major</i>	NR152455							LT715862
<i>Curvularia lamingtonensis</i>	BRIP 12259	Australia, <i>Microlaena stipoides</i>	MH414901							MH433645
<i>Curvularia lunata</i>	CBS 730.96	USA, lung biopsy	JX256429							JX276441
<i>Curvularia malina</i>	CBS 131274	USA, <i>Zoysia</i> sp.	JF812154							KP153179
<i>Curvularia malina</i>	FLS-119	USA, Bermuda grass	KR493070							KR493083
<i>Curvularia meibaldii</i>	BRIP 12900 T	Australia, <i>Cynodon tranaalensis</i>	MH414902							MH433647
<i>Curvularia meibaldii</i>	BRIP 13983	Australia, <i>Cynodon dactylon</i>	MH414903							MH433646
<i>Curvularia microspora</i>	GUCC 6272	China, <i>Hippocrepium striatum</i>	MF139088							MF139097
<i>Curvularia microspora</i>	GUCC 6273	China, <i>H. striatum</i>	MF139089							MF139098
<i>Curvularia miyakei</i>	CBS197.29	Japan, <i>Eragrostis pilosa</i>	KJ909770							KM083611
<i>Curvularia mosadeghii</i>	IRAN 3131C	Iran, <i>Syngonium cumini</i>	MG846737							MH392155
<i>Curvularia mosadeghii</i>	IRAN 3123C	Iran, <i>Vigna unguiculata</i>	MG971270							MG975597
<i>Curvularia muehlenbeckiae</i>	CBS 144.63	USA, <i>Sorghum</i> sp.	KP400647							KP419996
<i>Curvularia neergaardii</i>	BRIP 12919	Ghana, <i>Oryza sativa</i>	KJ415550							KJ415397
<i>Curvularia neonidica</i>	IMI 129790	India, <i>Brassica nigra</i>	MH414910							MH433649
<i>Curvularia nicotinae</i>	BRIP 11983	Algeria, soil	KJ415551							KJ415396
<i>Curvularia nisikadoi</i>	CBS 192.29	Thailand, <i>Digitaria ciliaris</i>	AF081447							AF081410
<i>Curvularia nodosa</i>	CPC 28800	Vietnam, <i>Oryza sativa</i>	MF490816							MF490838
<i>Curvularia nodulosa</i>	CBS 160.58	Thailand, <i>Digitaria ciliaris</i>	JN601033							JN600975
<i>Curvularia oryzae</i>	CBS 169.53	Vietnam, <i>Oryza sativa</i>	KP400650							KP645344
<i>Curvularia ovaricola</i>	CBS 286.91	Australia, <i>Eragrostis interrupta</i>	HG778994							HG779145
<i>Curvularia ovaricola</i>	CBS 470.90	Java, air	JN192384							JN600976
<i>Curvularia pallescens</i>	CBS 156.35	Unknown, <i>Acacia karroo</i>	KJ922380							KM083606
<i>Curvularia papendoffii</i>	BRIP 57608	South Africa, <i>Acacia karroo</i>	KJ415552							KJ415395
<i>Curvularia papendoffii</i>	CBS308.67	Australia (Cape York), <i>Perotis rara</i>	KJ909774							KM083617
<i>Curvularia perotidis</i>	CBS 350.90	Australia, <i>Dactyloctenium aegyptium</i>	JN192385							JN601021
<i>Curvularia petersonii</i>	BRIP14642	Australia, <i>Dactyloctenium aegyptium</i>	MH414905							MH433650
<i>Curvularia pisi</i>	CBS 190.48	Canada, <i>Pisum sativum</i>	KY905678							KY905690
<i>Curvularia platzii</i>	BRIP 27703b	Australia, <i>Cenchrus clandestinum</i>	MH414906							MH433651
<i>Curvularia portulacae</i>	BRIP 14541	USA, <i>Portulaca oleracea</i>	KJ415553							KJ415393
<i>Curvularia portulacae</i>	CBS 239.48	USA, <i>P. oleracea</i>	KJ909775							KM083616
<i>Curvularia prasadii</i>	CBS 143.64	India, <i>Jasminum sambac</i>	KJ922373							KM061785
<i>Curvularia protuberata</i>	5876	<i>Fragaria</i> sp.	KT012665							KT012626
<i>Curvularia protuberata</i>	CBS 376.65	UK, <i>Deschampsia flexuosa</i>	KJ922376							KM083605
<i>Curvularia pseudobrachiyspora</i>	CPC 28808	Thailand, <i>Eileusine indica</i>	MF490819							MF490841
<i>Curvularia pseudolunata</i>	UTHSC 092092	USA, nasal sinus	HE861842							HF565459
<i>Curvularia pseudobubusta</i>	UTHSC 083458	USA, nasal sinus	HE861838							HF565476
<i>Curvularia ravenelii</i>	BRIP 13165	Australia, <i>Sporobolus fertilis</i>	JN192386							JN600978
<i>Curvularia ravenelii</i>	CBS 127709	Australia, air	HG778999							HG779109
<i>Curvularia reesii</i>	BRIP 4358	Australia, air	MH414907							MH433637

Species name	ID (isolate, strain <sup>1</sup> , status <sup>2</sup> , voucher)	Country, isolation source	Accession numbers							Reference		
			ITS	LSU	mtSSU	tef1	rpb1	rpb2	cox3		gpd	
<i>Curvularia richardiae</i>	BRIP 4371	Australia, <i>Richardia brasiliensis</i>	KJ415555								KJ415391	
<i>Curvularia robusta</i>	CBS 624.68	USA, <i>Dichanthium amulatum</i>	KJ909783								KM083613	
<i>Curvularia rouhamii</i>	CBS 144674	Iran, <i>Synagonium velozianum</i>	KX139030								MG428694	
<i>Curvularia rouhamii</i>	CBS 144675	Iran, <i>Eucalyptus</i> sp.	KX139032								MG428696	
<i>Curvularia ryleyi</i>	BRIP 12554	Unknown, <i>Sporobolus creber</i>	KJ415556								KJ415390	
<i>Curvularia ryleyi</i>	CBS 349.90	Australia, <i>Sporobolus creber</i>	KJ909766								KM083612	
<i>Curvularia senegalensis</i>	CBS 149.71	Iran, soil	HG779001								HG779128	
<i>Curvularia shahidchamanensis</i>	IRAN 3139C	Iran, soil	MH550084								MH550083	
<i>Curvularia shahidchamanensis</i>	SCUA-8.1	Iran, soil	MH550087								MH550086	
<i>Curvularia soli</i>	CBS 222.96	Papua New Guinea, soil	KY905679								KY905691	
<i>Curvularia sorghina</i>	BRIP 15900	Australia, <i>Sorghum bicolor</i>	KJ415558								KJ415388	
<i>Curvularia spicifera</i>	CBS 274.52	Spain, soil	JN192387								JN600979	
<i>Curvularia sporobolicola</i>	BRIP 2304.0b	Australia, <i>Sporobolus australasicus</i>	MH414908								MH433652	
<i>Curvularia subpseudorhynchos</i>	CBS 656.74	Egypt, desert soil	KJ909777								KM061791	
<i>Curvularia trifolii</i>	CBS 173.55	USA, <i>Trifolium repens</i>	HG779023								HG779124	
<i>Curvularia tripogonis</i>	BRIP 12375	Australia	JN192388								JN600980	
<i>Curvularia tropicalis</i>	BRIP 14834	India, <i>Coffea arabica</i>	KJ415559								KJ415387	
<i>Curvularia tsudae</i>	ATCC 44764	Japan, <i>Chloris gayana</i>	KC245496								KC747745	
<i>Curvularia tsudae</i>	MAFF 236750	Japan, <i>C. gayana</i>	KP400651								KM061790	
<i>Curvularia tuberculata</i>	CBS 14663	India, <i>Zea mays</i>	JX256433								JX276445	
<i>Curvularia uncinata</i>	CBS 221.52	Vietnam, <i>Oryza sativa</i>	HG779024								HG779134	
<i>Curvularia variabilis</i>	CPC 28813	Thailand, <i>Digitaria ciliaris</i>	MF490820								MF490842	
<i>Curvularia variabilis</i>	CPC 28815	Thailand, <i>Chloris barbata</i>	NR154866								MF490844	
<i>Curvularia variabilis</i>	CBS 537.75	New Zealand, <i>Vanellus miles</i>	HG779026								HG779133	
<i>Curvularia verruciformis</i>	CBS150.63	India, <i>Punica granatum</i>	KP400652								KP645346	
<i>Curvularia verruculosa</i>	MFLUCC 100690	Thailand, <i>Oryza sativa</i>	JX256437								JX276448	
<i>Curvularia verruculosa</i>	BRIP 14817	Australia, <i>Doctyloctenium aegyptium</i>	MH414909								MH433653	
<i>Curvularia sp.</i>	AR5117	USA, <i>Lolium perene</i>	KP400655								KP645349	
<i>Curvularia sp.</i>	MFLUCC 100709	Thailand, <i>Oryza sativa</i>	JX256442								JX276453	
<i>Curvularia sp.</i>	MFLUCC 100739	Thailand, <i>Oryza sativa</i>	JX256443								JX276454	
<i>Curvularia sp.</i>	MFLUCC 120177	Thailand, grass	KP400654								KP645348	
<i>Curvularia sp.</i>	UTHSC 08809	USA, <i>Homo sapiens</i>	HE861826								HF565477	
<i>Didymella americana</i>	UC30, CBS 145.105	Italy, Valle dei Laghi (Trento), grape Nosiola, 2013	KU554584	KU554632							MK02765**	Lorenzini et al. (2016)
<i>Didymella calidophila</i>	CG7, CBS 145.107	Italy, Gambellara (Vicenza), grape Garganega, 2017	MK024766	MK032762							-	Present study
<i>Didymella pomorum</i>	UC56, CBS 145.106	Italy, Valle dei Laghi (Trento), grape Nosiola, 2013	KU554583	KU554631							MK02767**	Lorenzini et al. (2016)
<i>Exserohilum gedarefense</i>	CBS 297.80	Sudan, <i>Sorghum bicolor</i>	NR_155091								LT115895	
<i>Falciophora oryzae</i>	CBS 125863, T	China; <i>Oryza sativa</i> , root, endophytic	EU636699	KJ026705							KJ026706	
<i>Falciophoriella solaniterrestris</i>	CBS 117.83, T	Netherlands; Soil in potato field	KM484842	KM484859							KM485058	
<i>Funneliformis mosseae</i>		UK	FN547475*									
<i>Funneliformis mosseae</i>		UK	FR750028*									
<i>Gaeumannomyces caricis</i>	CBS 388.81, T	UK; <i>Carex rostrata</i>	KM484843	KM484960							KX306674 -	

Species name	ID (isolate, strain <sup>1</sup> , status <sup>2</sup> , voucher)	Country, isolation source	Accession numbers							Reference		
			ITS	LSU	mtSSU	tef1	rpb1	rpb2	cox3		gpd	
<i>Gaeumannomyces anomi</i>	CBS 10935	Thailand; Amomum sp., endophytic in leaves	AY265318	DQ341493		KX306679	-					
<i>Gaeumannomyces arzii</i>	CBS 903.73.T	Australia; Pennisetum clandestinum, (kikuyu grass), stolon	KM484837	KM484953		KX306681	KM485053					
<i>Gaeumannomyces australensis</i>	CBS 141387.T	Australia; Triticum aestivum	KX306480	KX306550		KX306683	KX306619					
<i>Gaeumannomyces avenae</i>	CPC 26258.ET	Ireland; Avena sativa (winter Oats)	KX306486	KX306556		KX306688	KX306622					
<i>Gaeumannomyces californicus</i>	CBS 141377.T	USA; Stenotaphrum secundatum	KX306490	KX306560		KX306691	KX306625					
<i>Gaeumannomyces ellisorum</i>	CBS 387.81.T	UK; Deschampsia caespitosa, dead culm and sheath	KM484835	KM484952		KX306692	KM485051					
<i>Gaeumannomyces floridanus</i>	CBS 141378.T	USA; Stenotaphrum secundatum	KX306491	KX306561		KX306693	KX306626					
<i>Gaeumannomyces fusiformis</i>	CBS 141379.T	USA; Oryza sativa	KX306492	KX306562		KX306694	KX306627					
<i>Gaeumannomyces glycinicola</i>	CPC 26057.T	USA; Glycine max	KX306493	KX306563		KX306695	KX306628					
<i>Gaeumannomyces graminicola</i>	CBS 352.93	Netherlands; Ctenanthe sp., stem base	KM484834	DQ341496		KX306697	KM485050					
<i>Gaeumannomyces graminis</i>	CBS 141384	USA; Cynodon dactylon × C. transvaalensis	KX306498	KX306568		KX306701	KX306633					
<i>Gaeumannomyces hiphopodioides</i>	CBS 350.77.T	UK; Zea mays, root	KX306506	KX306576		KM009204	KM009192					Linhares et al. (2016)
<i>Gaeumannomyces oryzicola</i>	CBS 141390.T	USA; Oryza sativa	KX306516	KX306586		KX306717	KX306646					Linhares et al. (2016)
<i>Gaeumannomyces radicola</i>	CBS 296.53.T	Canada; Zea mays, root	KM484845	KM484962		KM009206	KM485061					Linhares et al. (2016)
<i>Gaeumannomyces setaricola</i>	CBS 141394.T	South Africa; Setaria italica	KX306524	KX306594		KX306725	KX306654					Linhares et al. (2016)
<i>Gaeumannomyces tritici</i>	CBS 249.29	-; Triticum aestivum	KM484840	KM484957		KX306728	KM485056					Linhares et al. (2016)
<i>Gaeumannomyces vaikeri</i>	CBS 141400.T	USA; Stenotaphrum secundatum	KX306543	KX306613		KX306746	KX306670					Present study
<i>Gaeumannomyces wongoonoo</i>	BRIP 60376,	Australia; Buffalo grass	KP162137	KP162146		-	-					Present study
<i>Gloeocantharellus aculeatus</i>	FLOR47977	Brazil	KU884895									Present study
<i>Gloeocantharellus aculeatus</i>	FLOR49692	Brazil	KU884896									Linhares et al. (2016)
<i>Gloeocantharellus aculeatus</i>	FLOE59113	Brazil	KU884897									Linhares et al. (2016)
<i>Gloeocantharellus corneti</i>	FLOR 47978	Brazil	KU884898									Linhares et al. (2016)
<i>Gloeocantharellus echinosporus</i>	CGE 16041	Solomon Islands	KU884899									Present study
<i>Gloeocantharellus neoehinosporus</i>	GDGM75322	China	MK358819	MK358814								Present study
<i>Gloeocantharellus neoehinosporus</i>	GDGM75321	China	MK358820	MK358815								Present study
<i>Gloeocantharellus neoehinosporus</i>	GDGM70585	China	MK358821	MK358816								Linhares et al. (2016)
<i>Gloeocantharellus okapaensis</i>	CGE 16046	Solomon Islands	KU884900									Deng & Li (2008)
<i>Gloeocantharellus persicinus</i>	GDGM21480	China	EU118161									Linhares et al. (2016)
<i>Gloeocantharellus purpurascens</i>	REH 6904	USA	KU884901									Hughes K.W., Petersen R.H. & Lickey E., unpubl.
<i>Gloeocantharellus purpurascens</i>	TENN60063	USA	AY872281									Smith M.E. & Henkel T.W., unpubl.
<i>Gloeocantharellus</i> sp.	TH6525	Guyana	KT339202									Dunham (2007)
<i>Glomus macrocarpum</i>		UK	FR750366*									Mata, Hughes & Petersen (2004)
<i>Glomus macrocarpum</i>		UK	FR750368*									Jang et al. (2016)
<i>Gomphus clavatus</i>	8.2	USA	DQ365637									Wilson et al. (2004)
<i>Gymnopus fusipes</i>	TENN 59217	France	AY256710									
<i>Gymnopus iocaphalus</i>	KUC20140804-02	Republic of Korea	KX513745									
<i>Gymnopus aff. moseri</i>	AWW10	Java	AY263431									

Species name	ID (isolate, strain <sup>1</sup> , status <sup>2</sup> , voucher)	Country, isolation source	Accession numbers							Reference	
			ITS	LSU	mtSSU	tef1	rpb1	rpb2	cox3		gpd
<i>Gymnopus luxurians</i>	BAH05 (TENN)	USA	MF773597								Matheny P.B. & Wolfenbarger A., unpubl.
<i>Gymnopus luxurians</i>	TENN 57910	USA	AY256709								Mata et al. (2007)
<i>Gymnopus luxurians</i>	TENN 50619	Switzerland	KJ416240								Petersen & Hughes (2014)
<i>Gymnopus luxurians</i>	FLAS-F-61276	USA	MH211852								Kaminsky B.S., Smith M.E., Healy R. & Spakes Richter B., unpubl.
<i>Gymnopus luxurians</i>	TENN F-55748	USA	KY026649								Petersen & Hughes (2016)
<i>Gymnopus luxurians</i>	TENN 67854	USA	KJ416241								Petersen & Hughes (2014)
<i>Gymnopus aff. luxurians</i>	TENN 60722	Russia	KJ416237								Petersen & Hughes (2014)
<i>Gymnopus luxurians</i>	KUC20080725-28	Republic of Korea	KM496469								Jang et al. (2016)
<i>Gymnopus luxurians</i>	FLAS-F-61259	USA	MH211839								Kaminsky B.S., Smith M.E., Healy R. & Spakes Richter B., unpubl.
<i>Gymnopus luxurians</i>	M39	Pakistan	KF803760								Saba M. & Khalid A.N., unpubl.
<i>Gymnopus polygrammus</i>	TFB9628	Puerto Rico	DQ450028								Mata et al. (2007)
<i>Gymnopus polygrammus</i>	SFC20120821-64	Republic of Korea	KJ7609162								Lee et al. (2014)
<i>Gymnopus polygrammus</i>	URM 90015	Brazil	KY074640								Coimbra et al. (2015)
<i>Gymnopus polygrammus</i>	CUH.AM082	India	KJ778752								Dutta et al. (2015)
<i>Gymnopus polygrammus</i>	URM 90017	Brazil	KY074642								Coimbra et al. (2015)
<i>Gymnopus polygrammus</i>	URM 90016	Brazil	KY074641								Coimbra et al. (2015)
<i>Gymnopus polygrammus</i>	PR2542TN	Puerto Rico	AY842954								López Ferrer (2004)
<i>Gymnopus polygrammus</i>	TENN 5659	Puerto Rico	AY256701								Mata et al. (2007)
<i>Gymnopus aff. polygrammus</i>	SFSU BAP 668	Puerto Rico	MF100980								Desjardin & Perry (2017)
<i>Gymnopus aff. polygrammus</i>	SFSU DED 8324	Sao Tome	MF100979								Desjardin & Perry (2017)
<i>Gymnopus</i> sp.	URM 90057	Brazil	KY302896								Coimbra et al. (2015)
<i>Gymnopus</i> sp.	Duke c9811	Puerto Rico	DQ480107								Mata et al. (2007)
<i>Gymnopus</i> sp.	Achao 44	Chile	KF638511								Ortiz et al. (2014)
<i>Kohlietropis medullaris</i>	CBS 117849, T	USA; <i>Juncus roemerianus</i>	KM484852	KM484968							
<i>Laboulbenia oiovelicola</i>	D. Haelew. 942b	Brazil; <i>Oiovelia machadoi</i>	MF314142	MF314142							
<i>Macgarriceomyces borealis</i>	CBS 461.65	UK; <i>Juncus effusus</i> , leaf spots	MH858669	DQ341511							
<i>Macgarriceomyces juncticola</i>	CBS 610.82	Netherlands; <i>Juncus effusus</i> , stem base	KM484855	KM484970							
<i>Magnaporthaceae, incertae sedis</i>	CBS 141401	UK; <i>Triticum aestivum</i>	KX306546	KX306616							
<i>Magnaporthaceae, incertae sedis</i>	CBS 141402	UK; <i>Carex acutiformis</i>	KX306547	KX306617							
<i>Magnaporthiopsis incrustans</i>	M35	-	JF414843	JF414892							
<i>Magnaporthiopsis maydis</i>	CBS 662.82A, T	Egypt; <i>Zea mays</i>	KM484836	KM484971							
<i>Magnaporthiopsis poae</i>	M48	USA; <i>Poa pratensis</i>	JF414837	-							
<i>Magnaporthiopsis rhizophila</i>	M23	-; <i>Poa pratensis</i>	JF414834	JF414883							
<i>Magnaporthiopsis</i> sp.	CPC 26038	USA; <i>Cynodon dactylon</i> × C. <i>transvaalensis</i>	KX306545	KX306615							
<i>Marasmiellus subpruinosis</i>	BRNM 781388	Madeira	MK646034								Present study
<i>Marasmiellus subpruinosis</i>	TFB11063	USA	DQ450025								Mata et al. (2007)
<i>Marasmiellus subpruinosis</i>	TFB11066	USA	DQ450027								Mata et al. (2007)

Species name	ID (isolate, strain <sup>1</sup> , status <sup>2</sup> , voucher)	Country, isolation source	Accession numbers										Reference		
			ITS	LSU	mtSSU	tef1	rpb1	rpb2	cox3	gpd					
<i>Mycena tenuispinosa</i>	LE 321754	Russia	MK478466												Present study
<i>Mycena xantholeuca</i>	LE 321753	Russia	MK474930												Present study
<i>Mycena xantholeuca</i>	LE 321752	Russia	MK474933												Present study
<i>Nakataea oryzae</i>	CBS 252.34	Burma; <i>Oryza sativa</i>	KM484862	KM484976											
<i>Neocardana musae</i>	CBS 1393.18, N	Malaysia; <i>Musa</i> sp.	LN713277	LN713290											
<i>Neogaeumammomyces bambusicola</i>	MFLUCC 110390, T	Thailand; Dead culm of bamboo (Bambuseae)	KP744449	KP744492											
<i>Neopyricularia commelinicola</i>	CBS 128308	South Korea; <i>Commelina communis</i> , leaves	FJ850122	KM484985											
<i>Nothophoma quercina</i>	S3, CBS 145109	Italy, Valpolicella (Verona), grape Corvina, 2017	MK024765	MK032761											
<i>Oomnidemptus affinis</i>	ATCC 200212, T	Australia; <i>Panicum effusum</i> var. <i>effusum</i> , grass leaves	JX134674	JX134686											
<i>Ophioceras dolichostomum</i>	CBS 114926	Hong Kong; Wood	JX134677	JX134689											
<i>Ophioceras leptosporum</i>	CBS 894.70, T	UK; Dead stem of dicot plant (probably <i>Urtica dioica</i> )	JX134678	JX134690											
<i>Plagiophaera immersa</i>	D98	Austria; dead stems of <i>Urtica dioica</i>	MN727886	MN727886											
<i>Plagiophaera immersa</i>	D148	Austria; dead stems of <i>Urtica dioica</i>	MN727887	MN727887											
<i>Plagiophaera immersa</i>	D266	Austria; dead stems of <i>Urtica dioica</i>	MN727888	MN727888											
<i>Plagiophaera immersa</i>	D270	Austria; dead stems of <i>Urtica dioica</i>	MN727889	MN727889											
<i>Porphyrellus</i> sp.	HKAS 60479	China													
<i>Proxypyrularia zingiberis</i>	CBS 133594, ET	Japan; <i>Zingiber mioga</i>	AB274434	KM484988											
<i>Pseudophialophora eragrostis</i>	CMI2m9, T	USA; <i>Eragrostis</i> sp.	KF689648	KF689638											
<i>Pseudopyricularia epperi</i>	CBS 133595, T	Japan; <i>Cyperus iria</i>	KM484872	KM484990											
<i>Pseudopyricularia kyliangae</i>	CBS 133597, T	Japan; <i>Kyliang brevifolia</i>	KM484876	KM484992											
<i>Puccinia nepalensis</i>	ISL-26648	Pakistan; <i>Rumex nepalensis</i>	KX225481												
<i>Pyricularia ctenanthicola</i>	ATCC 200218	Greece; <i>Ctenanthe oppenheimiana</i>													
<i>Pyricularia grisea</i>	BR0029	Brazil; <i>Digitaria sanguinalis</i>	KM484880	KM484995											
<i>Pyricularia oryzae</i>	CBS 365.52	Japan; -	KM484890	KM485000											
<i>Pyriculariomyces asari</i>	CBS 141328, T	Malaysia; <i>Asarium</i> sp.	KX228291	KX228342											
<i>Rhizoglyphus arabicum</i>		Oman	KF154764*												
<i>Rhizoglyphus arabicum</i>		Oman	KF154765*												
<i>Rhizoglyphus arabicum</i>		Oman	KF154767*												
<i>Rhizoglyphus clarum</i>		USA	FJ461824												
<i>Rhizoglyphus clarum</i>		Iceland	FM865542*												
<i>Rhizoglyphus clarum</i>		Iceland	FM865544*												
<i>Rhizoglyphus clarum</i>		Greece	KY555054*												
<i>Rhizoglyphus dunense</i>		Greece	KY555055*												
<i>Rhizoglyphus dunense</i>		Greece	KY555056*												
<i>Rhizoglyphus fusciculatum</i>		Not available	FR750071*												
<i>Rhizoglyphus fusciculatum</i>		Not available	FR750072*												
<i>Rhizoglyphus fusciculatum</i>		Not available	FR750073*												
<i>Rhizoglyphus intratruncatus</i>		USA	HE817871*												
<i>Rhizoglyphus intratruncatus</i>		USA	FM865577*												



Species name	ID (isolate, strain <sup>1</sup> , status <sup>2</sup> , voucher)	Country, isolation source	Accession numbers						Reference										
			ITS	LSU	mtSSU	tef1	rpb1	rpb2		cox3	gpd								
<i>Rhizoglyphus intratradices</i>		USA		FR750372*															
<i>Rhizoglyphus invermadium</i>		Ecuador		HG969390*															
<i>Rhizoglyphus invermadium</i>		Ecuador		HG969391*															
<i>Rhizoglyphus invermadium</i>		Ecuador		HG969392*															
<i>Rhizoglyphus irregulare</i>		Australia		FR750186*															
<i>Rhizoglyphus irregulare</i>		Australia		FR750189*															
<i>Rhizoglyphus irregulare</i>		Australia		FR750190*															
<i>Rhizoglyphus manihotis</i>		China		AM158947															
<i>Rhizoglyphus manihotis</i>		China		AM158948															
<i>Rhizoglyphus manihotis</i>		Colombia		FJ461842															
<i>Rhizoglyphus melanum</i>		Norway		HG964396*															
<i>Rhizoglyphus melanum</i>		Norway		HG964397*															
<i>Rhizoglyphus melanum</i>		Norway		HG964398*															
<i>Rhizoglyphus natalense</i>		Brazil		KJ210826															
<i>Rhizoglyphus natalense</i>		Brazil		KJ210827															
<i>Rhizoglyphus natalense</i>		Brazil		KJ210828															
<i>Rhizoglyphus neocaledonicum</i>		France: New Caledonia		KY362436*															
<i>Rhizoglyphus neocaledonicum</i>		France: New Caledonia		KY362437*															
<i>Rhizoglyphus neocaledonicum</i>		France: New Caledonia		KY362438*															
<i>Rhizoglyphus proliferum</i>		France: Guadeloupe		FM982400*															
<i>Rhizoglyphus proliferum</i>		France: Guadeloupe		FM982401*															
<i>Rhizoglyphus proliferum</i>		France: Guadeloupe		FM982402*															
<i>Rhizoglyphus variabile</i>		Peru		MN384870*															present study
<i>Rhizoglyphus variabile</i>		Peru		MN384871															present study
<i>Rhizoglyphus variabile</i>		Peru		MN384872*															present study
<i>Rhizoglyphus variabile</i>		Peru		MN384873*															present study
<i>Rhizoglyphus variabile</i>		Peru		MN384874*															present study
<i>Rhizoglyphus variabile</i>		Peru		MN384875*															present study
<i>Rhizoglyphus variabile</i>		Peru		MN384876*															present study
<i>Rhizoglyphus venetianum</i>		Peru		MN384877*															present study
<i>Rhizoglyphus venetianum</i>		Italy		LS974594*															
<i>Rhizoglyphus venetianum</i>		Italy		LS974595*															
<i>Rhizoglyphus venetianum</i>		Italy		LS974596*															
<i>Rhizoglyphus vesiculiferum</i>		Lithuania		MG836659*															
<i>Rhizoglyphus vesiculiferum</i>		Lithuania		MG836660*															
<i>Rhizoglyphus vesiculiferum</i>		Lithuania		MG836661*															
<i>Russula adusta</i>	223/BB 06.562	Lithuania		KU237476	KU237320														
<i>Russula alboareolata</i>	SUT-1			AY061652															
<i>Russula aquosa</i>	312RUF25			AF345247															
<i>Russula atroaeruginea</i>	53626			AY061657															
<i>Russula cyanocantha</i>	ue92			JX391967	JX391970														
<i>Russula cyanocantha</i>	FH 12-201			AF418608															
<i>Russula dinghuensis</i>	K15052704-3			KR364093	KR364225														
<i>Russula dinghuensis</i>	GDGM45243			KU863581															
<i>Russula dinghuensis</i>				KU863580															

Species name	ID (isolate, strain <sup>1</sup> , status <sup>2</sup> , voucher)	Country, isolation source	Accession numbers							Reference		
			ITS	LSU	mtSSU	tef1	rpb1	rpb2	cox3		gpd	
<i>Russula grisea</i>	449/BB 07.184		KT934006	KU237509	KU237355	KU237939						
<i>Russula heterophylla</i>	UE20.08.2004-2		DQ422006	DQ422006								
<i>Russula ilicis</i>	1174/MF 00.300		AY061682	KU237595	KU237443	KU238021						
<i>Russula indoalba</i>	AG 15-628		KX234820									
<i>Russula lilacea</i>	435/BB 07.213		JN944005	KU237498	KU237343	KU237928						
<i>Russula lotus</i>	LF321		MG214687									
<i>Russula lotus</i>	LF1366		MG214688									
<i>Russula lotus</i>	RITF499		MK860699	MK860706								Present study
<i>Russula lotus</i>	RITF330		MK860698									Present study
<i>Russula nigricans</i>	429/BB 07.342		KX812835	KX812859	KU237539	KU237924						
<i>Russula nigrovirens</i>	HKAS 55222		KP171173									
<i>Russula nigrovirens</i>	HKAS 55042		KP171174									
<i>Russula pallidirosea</i>	UTC00274382		KR831283									
<i>Russula pallidospora</i>	JV02-218		DQ422032	DQ422032								
<i>Russula phloginea</i>	CNX530524068		MK860701	MK860704	MK860708	MK894877						Present study
<i>Russula phloginea</i>	CNX530524304		MK860700	MK860703	MK860707	MK894876						Present study
<i>Russula shingbaensis</i>	KD 11-094		KM386692									
<i>Russula</i> sp.	BPL241		KT933959	KT933818								Present study
<i>Russula subpallidirosea</i>	RITF4083		MK860697	MK860702	MK860705	MK894875						
<i>Russula subpallidirosea</i>	GDGM45242		KU863582									
<i>Russula varriata</i>	JMP0078		EU819436									
<i>Russula vesca</i>	45/BB 06.525		KT933978	KU237465	KU237309	KU237899						
<i>Russula virescens</i>	HJB9989		DQ422014	DQ422014								
<i>Russula werneri</i>	IB1997/0786		DQ422021	DQ422021								
<i>Russula xanthovirens</i>	BI7091630	USA	MG786055									
<i>Sclerocystis sinuosa</i>		USA	AJ437106	FJ461846								
<i>Sclerocystis sinuosa</i>		USA	KM484944	KM485040				KM485158				
<i>Slopeiomyces cylindrosporus</i>	CBS 609.75.T	UK; Grass root, associated with <i>Phialophora graminicola</i>										
<i>Sphaerosporium lignatile</i>	D. Haelew. F-1614a	USA	MN748372	MN749494								Present study
<i>Sphaerosporium lignatile</i>	D. Haelew. F-1614b	USA	MN748373	MN749495								Present study
<i>Stagonosporopsis flacciduarum</i> sp. nov.	UC23, CBS 145113	Italy, Valle dei Laghi (Trento), grape Nosiola, 2013	KU554588	KU554634					MK205423	MK032764**		Lorenzini et al. (2016)
<i>Strobilomyces alpinus</i>	HKAS 77969	China										Han et al. (2018a)
<i>Strobilomyces annulatus</i>	KEP 62753	Malaysia										Sato et al. (2011), Han et al. (2018a)
<i>Strobilomyces atrosquamosus</i>	HKAS 55368	China										Wu et al. (2016), Han et al. (2018a)
<i>Strobilomyces brunneolepidotus</i>	HKAS 80689	China										Han et al. (2018a)
<i>Strobilomyces confusus</i>	WU 17032	USA										Han et al. (2018a)
<i>Strobilomyces echinatus</i>	HKAS 723576	Congo										Han et al. (2018a)
<i>Strobilomyces echinocephalus</i>	HKAS 92153	China										Han et al. (2018a)
<i>Strobilomyces foreatus</i>	FRI 69468	Malaysia										Han et al. (2018a)

Species name	ID (isolate, strain <sup>1</sup> , status <sup>2</sup> , voucher)	Country, isolation source	ITS					Accession numbers					Reference
			LSU	mtSSU	tef1	rpb1	rpb2	cox3	gpd				
<i>Strobilomyces giganteus</i>	MAK s859	Japan			AB589362	AB589418	AB275176						Sato & Murakami (2009), Sato et al. (2011)
<i>Strobilomyces giganteus</i>	HKAS 77026	China			KX869328	KX869384	KX869456	KX869199					Han et al. (2018a)
<i>Strobilomyces giganteus</i>	NY 1393514	Thailand			KX869327	KX869383	KX869455	KX869197					Han et al. (2018a)
<i>Strobilomyces globulius</i>	HKAS 74887	China			KX869278	KX869533	KX869404	KX869146					Han et al. (2018a)
<i>Strobilomyces glabriceps</i>	HKAS 67811	China			KX869283	KX869538	KX869409	KX869151					Han et al. (2018a)
<i>Strobilomyces hongoi</i>	MAK s429	Japan			AB589385	AB589441	AB589375						Sato & Murakami (2009), Sato et al. (2011)
<i>Strobilomyces huangshanensis</i>	HKAS 102612	China			MK329218	MK329216	MK329214						Present study
<i>Strobilomyces huangshanensis</i>	HKAS 102613	China			MK329219	MK329213	MK329217	MK329215					Present study
<i>Strobilomyces latirimosus</i>	HKAS 74865	China			3KF112258	3KF112603	3KF112812	KX869152					Wu et al. (2016), Han et al. (2018a)
<i>Strobilomyces mirandus</i>	HKAS 59408	China			KX869293	KX869548	KX869419	KX869161					Han et al. (2018a)
<i>Strobilomyces mollis</i>	HKAS 59833	China			KX869295	KX869551	KX86942	KX869164					Han et al. (2018a)
<i>Strobilomyces montosus</i>	HKAS 74809	China			KF112254	KF112599	KF112808	KX869165					Wu et al. (2016), Han et al. (2018a)
<i>Strobilomyces rubrobrunnus</i>	HKAS 101906	China			MH485372	MH485366	MH485369	MH485373					Han et al. (2018b)
<i>Strobilomyces parvirimosus</i>	HKAS 74547	China			KX869302	KX869558	KX869429	KX869171					Han et al. (2018a)
<i>Strobilomyces PS1</i>	HKAS 83740	China			KX869329	KX869586	KX869458	KX869201					Han et al. (2018a)
<i>Strobilomyces PS2</i>	HKAS 73175	China			KX869332	KX869589	KX869461	KX869204					Han et al. (2018a)
<i>Strobilomyces PS3</i>	HKAS 74963	China			KX869336	KX869593	KX869465	KX869208					Han et al. (2018a)
<i>Strobilomyces PS4</i>	WU 17062	Mexico			KX869338	KX869595	KX869467	KX869210					Han et al. (2018a)
<i>Strobilomyces PS5</i>	HKAS 74924	China			KX869341	KX869598	KX869470	KX869213					Han et al. (2018a)
<i>Strobilomyces PS5</i>	NY 1393538	Thailand			KX869343	KX869600	KX869472	KX869215					Han et al. (2018a)
<i>Strobilomyces PS6</i>	HKAS 87097	China			KX869345	KX869602	KX869474	KX869217					Han et al. (2018a)
<i>Strobilomyces PS7</i>	NY 1491183	Australia			KX869347	KX869604	KX869476	KX869219					Han et al. (2018a)
<i>Strobilomyces PS8</i>	HKAS 80300	China			KX869350	KX869609	KX869481	KX869222					Han et al. (2018a)
<i>Strobilomyces PS9</i>	HKAS 82354	China			KX869352	KX869609	KX869481	KX869224					Han et al. (2018a)
<i>Strobilomyces PS10</i>	HKAS 87084	China			KX869358	KX869615	KX869487	KX869230					Han et al. (2018a)
<i>Strobilomyces PS11</i>	NY 1193834	Australia			KX869360	KX869617	KX869489	KX869231					Han et al. (2018a)
<i>Strobilomyces PS12</i>	NY 1034410	Australia			KX869324	KX869579	KX869451	KX869193					Han et al. (2018a)
<i>Strobilomyces PS13</i>	HKAS 74893	China			KX869364	KX869621	KX869493	KX869235					Han et al. (2018a)
<i>Strobilomyces PS14</i>	WU 17057	USA			KX869365	KX869622	KX869494	KX869236					Han et al. (2018a)
<i>Strobilomyces PS15</i>	MAK s404	Japan			AB589379	AB589435	AB589443						Sato & Murakami (2009), Sato et al. (2011)
<i>Strobilomyces PS16</i>	HKAS 84055	USA			KX869366	KX869623	KX869495	KX869237					Han et al. (2018a)
<i>Strobilomyces PS17</i>	MAK s563	China			AB589392	AB589448							Sato et al. (2011)
<i>Strobilomyces PS18</i>	KEP 4364	Malaysia			AB589343	AB589399							Sato et al. (2011)
<i>Strobilomyces PS19</i>	NY 1393513	Australia			KX869367	KX869624	KX869496	KX869238					Han et al. (2018a)
<i>Strobilomyces PS20</i>	PC 0723581	Madagascar			KX869368	KX869625	KX869497	KX869239					Han et al. (2018a)
<i>Strobilomyces PS21</i>	HKAS 92326	China			KX869369	KX869626	KX869498	KX869240					Han et al. (2018a)
<i>Strobilomyces PS22</i>	MEL 695356	Australia			KX869370	KX869627	KX869499	KX869241					Han et al. (2018a)
<i>Strobilomyces PS23</i>	NY 1034428	Australia			KX869371	KX869628	KX869500	KX869242					Han et al. (2018a)
<i>Strobilomyces PS24</i>	NY 75253	Costa Rica			KX869371	KX869628	KX869501	KX869243					Han et al. (2018a)

Species name	ID (isolate, strain <sup>1</sup> , status <sup>2</sup> , voucher)	Country, isolation source	ITS					Accession numbers					Reference
			LSU	mtSSU	tef1	rpb1	rpb2	cox3	gpd				
<i>Strobilomyces PS25</i>	NY 75256	Costa Rica			KX869372	KX869629	KX869502	KX869244					Han et al. (2018a)
<i>Strobilomyces PS26</i>	PC 0723567	New Caledonia			KX869373	KX869630	KX869503	KX869245					Han et al. (2018a)
<i>Strobilomyces pteroveticulosporus</i>	HKAS 80350	China			KX869303	KX869559	KX869430	KX869172					Han et al. (2018a)
<i>Strobilomyces seminudus</i>	HKAS 59461	China			KF112260		KF112815	KX869180					Wu et al. (2016), Han et al. (2018a)
<i>Strobilomyces seminudus</i>	NY 1393550	Thailand			KX869310	KX869566	KX869437	KX869179					Han et al. (2018a)
<i>Strobilomyces strobilaceus</i>	MAK s380	Japan			AB589372	AB589428	AB5893787						Sato & Murakami (2009), Sato et al. (2011)
<i>Strobilomyces strobilaceus</i>	HKAS 75466	China			KT990836	KT990986	KT990473	KX869184					Wu et al. (2016), Han et al. (2018a)
<i>Strobilomyces strobilaceus</i>	MAK s224	USA			AB589356	AB589412							Sato et al. (2011)
<i>Strobilomyces strobilaceus</i>	WU 17111	Mexico			KX869316	KX869571	KX869443	KX869185					Han et al. (2018a)
<i>Strobilomyces strobilaceus</i>	HKAS 95079	China			KX869317	KX869572	KX869444	KX869186					Han et al. (2018a)
<i>Strobilomyces subnudus</i>	HKAS 59435	China			KX869318	KF112605	KX869445	KX869187					Han et al. (2018a)
<i>Strobilomyces velutinus</i>	HKAS 84755	China			KX869322	KX869577	KX869449	KX869191					Han et al. (2018a)
<i>Strobilomyces cf. velutipes</i>	NY 1193932	Australia			KX869363	KX869620	KX869492	KX869234					Han et al. (2018a)
<i>Strobilomyces verruculosus</i>	HKAS 77026	China			KX869328	KX869584	KX869456	KX869199					Han et al. (2018a)
<i>Uromyces acetosae</i>	DAOM 159824	Sweden, <i>Rumex acetosa</i>			HQ317587								Liu et al. (2015)
<i>Uromyces appendiculatus</i>	H92832	Japan, <i>Phaseolus vulgaris</i>			AB115740								Chung et al. (2004)
<i>Uromyces appendiculatus</i>	TSH-R1734	Japan, <i>Phaseolus vulgaris</i>			AB115741								Chung et al. (2004)
<i>Uromyces klotzschianus</i>	ISL-45963	Pakistan, <i>Rumex dentatus</i>			MF044015	MF044017							Present study
<i>Uromyces klotzschianus</i>	ISL-45965	Pakistan, <i>Rumex dentatus</i>			MF044016								Present study
<i>Uromyces polygoni-ariculalis</i>	DAOM 181565	Canada, <i>Polygonum aviculare</i>			HQ317558								Liu et al. (2015)
<i>Uromyces rumicis</i>	BP1 910298	USA, <i>Rumex crispus</i>			KY764197								Deners J.E., Romberg M.K. & Castlebury L.A., unpubl.
<i>Uromyces rumicis</i>	DAOM 216123	Hungary, <i>Rumex crispus</i>			HQ317562								Liu et al. (2015)
<i>Uromyces striatus</i>	F457	Switzerland, <i>Trifolium arvense</i>			AF180162								Pfunder et al. (2001)
<i>Uromyces striatus</i>	F456	Switzerland, <i>Trifolium arvense</i>			AF180161								Pfunder et al. (2001)
<i>Urechtiana ciliessia</i>	CBS 128780, T	Netherlands; Phragmites australis, leaves			JF951153	JF951176							Pfunder et al. (2001)
<i>Xenopyricularia zizaniicola</i>	CBS 132356	Japan, <i>Zizania latifolia</i>			KM484946	KM485042							

<sup>1</sup> AFCC: American Type Culture Collection, Virginia, USA; BCC: BIOTEC Culture Collection, National Center for Genetic Engineering and Biotechnology (BIOTEC), Bangkok, Thailand; BRIP: Queensland Plant Pathology Herbarium, Brisbane, Australia; CBS: CBS-KNAW Fungal Biodiversity Centre, Utrecht, The Netherlands; CPC: Culture collection of Pedro Crous, housed at CBS, DAR: Plant Pathology Herbarium, Orange Agricultural Institute, Forest Road, Orange, NSW 2800, Australia; HKUCC: The University of Hong Kong Culture Collection, Hong Kong, China; IMI: International Mycological Institute, CABI-Bioscience, Egham, Basingstoke, United Kingdom; MAFF: Ministry of Agriculture, Forestry and Fisheries, Tsukuba, Ibaraki, Japan; MFLUCC: Mae Fah Luang University Culture Collection, Chiang Rai, Thailand, MUCL: Université Catholique de Louvain, Louvain-la-Neuve, Belgium; URM: Culture collection Prof. Maria Auxiliadora Cavalcanti, Recife, Brazil;

<sup>2</sup> T: ex-type strain; ET: ex-epitype strain; N ex-neotype strain. \* SSU-ITS-LSU. \*\* *Tub2*

The band of the expected size was excised with a scalpel and isolated from the gel with the GFX™ PCR DNA and Gel Band Purification Kit (Sigma-Aldrich, St. Louis, MO) following the manufacturer's protocol, cloned into the pCR2.1 vector (Invitrogen, Carlsbad, CA) and transformed into One Shot® TOP10 chemically competent *Escherichia coli* (Invitrogen). Eight recombinant colonies were selected by blue/white screening and the presence of inserts detected by PCR amplification with KOD DNA Polymerase (Sigma-Aldrich), using universal forward and reverse M13 vector primers. After isolation from transformed cells, plasmids were sequenced on both strands with M13F/M13R primers using the BigDye Terminator kit v3.1 (Applied Biosystems, Foster City, CA). The products were analyzed on an automated DNA sequencer (ABI 3730XL DNA analyzer, Macrogen).

DNA was extracted from dried *Russula* basidiomata with the CTAB protocol (Doyle & Doyle 1987). PCR amplifications were done with primers ITS5 and ITS4 for ITS (White et al. 1990), LR0R and LR7 for LSU (Vilgalys & Hester 1990, Rehner & Samuels 1994), MS1 and MS2 for mtSSU (White et al. 1990), and EF1-F and EF1-R for *tef1* (Morehouse et al. 2003). Amplifications were performed in a 50 µl reaction volume containing 5 µl of 10× PCR reaction buffer, 5 µl of 0.2 mM dNTP mix, 2 µl of each 5 µM primer, and 1.5 U of *Taq* DNA polymerase. The final volume was adjusted to 50 µl with sterile distilled H<sub>2</sub>O (Liang et al. 2009). The DNA sequencing was performed with an ABI 3730 DNA analyzer and an ABI BigDye 3.1 terminator cycle sequencing kit (Shanghai Sangon Biological Engineering Technology & Services Co., Shanghai, China). The basic authenticity and reliability of newly generated sequences were established based on Nilsson et al. (2012). All newly generated sequences were submitted to NCBI GenBank and are listed in Tab. 1.

DNA was extracted from pure cultures of each *Didymellaceae* isolate as previously described (Lorenzini & Zapparoli 2014). ITS, LSU, β-tubulin (*tub2*), and *rpb2* loci were amplified using primer pairs ITS1/ITS4, LR0R/LR5, TUB2Fw/TUB4Rd, and RPB2-5F2/FRPB2-7cR (White et al. 1990, Vilgalys & Hester 1990, Rehner & Samuels 1994, Liu et al. 1999, Sung et al. 2007, Woudenberg et al. 2009). PCR products were purified using the NucleoSpin gel and PCR Clean-up Kit (Macherey-Nagel, Düren, Germany) and sequenced in both directions using the same primers (Eurofins Genomics, Edersberg, Germany). Sequences were submitted to NCBI GenBank (accession numbers in Tab. 1).

Genomic DNA of *Strobilomyces* basidiomata was extracted by using a rapid extraction kit for plant DNA (BIOTEKE Corporation, Jiangsu, China). PCR amplification and sequencing follow Han et al. (2017, 2018a, 2018b). The primer pairs for the amplification of *rpb1*, *rpb2*, *cox3*, and *tef1* were COX3st-F/COX3st-R, RPB1-F/RPB2-R, RPB2-F/RPB2-R, and 983F/1567R (Rehner & Buckley 2005, Sato & Murakami 2009, Han et al. 2018a).

*Uromyces* genomic DNA was extracted from urediniospores (Ali et al. 2016b). PCR amplification was performed with primer pairs Rust2inv/ITS4rust for ITS and LR0R/LR6 for LSU (Ali et al. 2016b). Sequences were generated using the same primers. The host plant was identified with the aid of the Flora of Pakistan (Stewart 1982) and by comparison with specimens held at ISL (Herbarium of Pakistan, Department of Plant Sciences, Quaid-i-Azam University, Islamabad, Pakistan).

For DNA extraction, fungal isolates of *Alternaria* were grown on PDA for 7 d in the dark at 25 °C. Fresh mycelial masses were collected for DNA extraction following the procedure outlined by Cenis (1992). Extracted DNA was diluted in 50 µl distilled water and preserved at -20 °C. Molecular identification was done using ITS rDNA and *gpd* sequences that were amplified using primer pairs ITS1/ITS4 (White et al. 1990) and *gpd1/gpd2* (Beebe et al. 1999). The PCR reaction mixture and cycling conditions for ITS were the same as described by Ebrahimi & Fotouhifar (2016). For amplification of *gpd*, PCR was carried out in a final volume of 25 µl with 11 µl ddH<sub>2</sub>O, 12 µl master mix (Sinagene, Iran), 0.2 pmol of each primer, and 10–30 ng/µl of template DNA. PCR amplification was performed in an Eppendorf Mastercycler eppgradient (Eppendorf, Hamburg, Germany) under the following cycling conditions: initial denaturation at 95 °C for 90 s; followed by 35 cycles of denaturation at 95 °C for 30 s, annealing at 52 °C for 30 s, extension at 72 °C for 30 s; and final extension at 72 °C for 6 min. Direct sequencing in one direction with ITS1 and *gpd1* primers, respectively, was outsourced to Macrogen (South Korea). After sequencing, sequences were manually edited with Chromas 2.4 software (Technelysium, Australia) and submitted to NCBI GenBank.

Genomic DNA of *Lasiodiplodia theobromae* was extracted from pure culture using the CTAB method (Doyle 1991) with minor modifications. PCR amplification of the SSU and ITS rDNA fragments was done using primer pairs NS1/NS2 and ITS1/ITS4, respectively (White et al. 1990). PCR amplicons of 460 bp and 503 bp in length were obtained. Both

amplicons were cloned into a vector pTZ57R/T using the InsTAclone PCR Cloning Kit (ThermoFisher Scientific, Mumbai, India) and subsequently sequenced. Generated sequences were submitted to NCBI GenBank under accession numbers MF803169 (SSU) and MF803168 (ITS).

A collection of *Marasmiellus subpruinus* from Madeira (BRNM 781138) was sequenced by M. Sochor. Total genomic DNA was extracted from <10 mg of herbarium specimen using the CTAB method (Doyle & Doyle 1987). The ITS region was amplified and sequenced using primers ITS1F (Gardes & Bruns 1993) and ITS4 (White et al. 1990). PCR was performed in a 20 µl reaction with Kapa Taq polymerase (Kapa Biosystems, Wilmington, MA) and a touchdown protocol with annealing temperature of 61–56 °C in the first six cycles and 56 °C in the following 34 cycles. PCR products were purified by precipitation with polyethylene glycol (10 % PEG 6000 and 1.25 M NaCl in the precipitation mixture) and sequenced by Macrogen.

*Mycena* DNA was extracted from herbarium material with the Phire™ Plant Direct PCR Kit (ThermoScientific, Pittsburg, PA). The ITS region was amplified using fungal primers ITS1F and ITS4B (Gardes & Bruns 1993). PCR products were checked using electrophoresis on agarose gel and GelRed staining. Purification was performed with the Fermentas Genomic DNA Purification Kit (Thermo Fisher Scientific, Waltham, MA). Purified PCR products were sequenced on an ABI model 3130 Genetic Analyzer (Applied Biosystems, Foster City, CA). The obtained sequences were processed and pairwise distance was calculated in MEGA10 (Kumar et al. 2018). As ITS data on *Mycena* sect. *Filipedes* are insufficient to build a good tree, so we did not include this analysis. Newly generated sequences have been submitted to NCBI GenBank (Tab. 1).

Extraction of genomic DNA from *Plagiosphaera immersa* was done using the DNeasy Plant Mini Kit (Qiagen, Hilden, Germany). The following loci were amplified and sequenced: the complete internal transcribed spacer region (ITS1–5.8S–ITS2) and a ca. 0.9-kb fragment of the large subunit nuclear ribosomal DNA (LSU), amplified as a single fragment with primers V9G (de Hoog & Gerrits van den Ende 1998) and LR5 (Vilgalys & Hester 1990); a ca. 1.2 kb fragment of the RNA polymerase II subunit 1 (*rpb1*) gene with primers RPB1-Af (Stiller & Hall 1997) and RPB1-6R1asc (Hofstetter et al. 2007); and a ca. 1.3–1.5 kb fragment of the translation elongation factor 1-alpha (*tef1*) gene with primers EF1-728F (Carbone & Kohn 1999) and TEF1LLerev (Jaklitsch et al. 2005) or EF1-2218R (Rehner & Buckley 2005).

PCR products were purified using an enzymatic PCR cleanup (Werle et al. 1994) as described in Voglmayr & Jaklitsch (2008). DNA was sequenced using the ABI PRISM Big Dye Terminator Cycle Sequencing Ready Reaction Kit version 3.1 (Applied Biosystems, Warrington, PA) and the same PCR primers; in addition, the following primers were used: ITS–LSU region: ITS4 (White et al. 1990), LR3 (Vilgalys & Hester 1990), and LR2R-A (Voglmayr et al. 2012); *tef1*: TEF1\_INTF (Jaklitsch 2009) and TEFD\_iR1 (Voglmayr & Jaklitsch 2019). Sequencing was performed on an automated DNA sequencer (ABI 3730xl Genetic Analyzer, Applied Biosystems).

*Sphaerosporium* DNA was extracted using the QIAamp DNA Micro Kit (Qiagen, Stanford, CA) as per the manufacturer's instructions. We amplified the internal transcribed spacer region of the ribosomal DNA (ITS) and the nuclear small and large ribosomal subunits (SSU, LSU). Primer combinations used were NS1/NS2 for SSU (White et al. 1990), ITS1f/ITS4 for ITS (White et al. 1990, Gardes & Bruns 1993), and LR0R/LR7 for LSU (Vilgalys & Hester 1990, Rehner & Samuels 1994). PCR amplifications were performed on a pro S Mastercycler (Eppendorf, Hauppauge, NY) with an initial denaturation step at 94 °C for 5 min; followed by 35 cycles of denaturation at 94 °C for 30 s (ITS) / for 45 s (LSU), annealing at 50 °C for 45 s (ITS) / for 1 min (LSU), extension at 72 °C for 45 s; and a final extension step at 72 °C for 7 min. For SSU, cycling conditions included initial denaturation at 95 °C for 5 min; followed by 40 cycles of denaturation at 95 °C for 30 s, annealing at 55 °C for 45 s, extension at 72 °C for 45 s; and a final extension step at 72 °C for 1 min. Purification and sequencing was outsourced to Genewiz (Plainfield, NJ). Generated sequence reads were assembled, trimmed, and edited in Sequencher 5.0 (Gene Codes Corporation, Ann Arbor, MI). Sequences were submitted to NCBI GenBank (accession numbers of ITS and LSU sequences in Tab. 1).

#### Phylogenetic analyses

Initial BLAST of newly generated *Cortinarius* ITS sequences in GenBank (<https://www.ncbi.nlm.nih.gov/genbank/>) and UNITE (<https://unite.ut.ee>) databases was used for comparison with closely related sequences. We downloaded ITS rDNA sequences of species belonging to section *Hinnulei* and other telamonioid lineages (Tab. 1). Multiple sequence alignment was produced with MAFFT version 7 (<http://mafft.cbrc.jp/alignment/server/>)

using the E-INS-I method (Katoh & Standley 2013) under default settings. According to Nagy et al. (2012), the phylogenetically informative indels in the ITS region were coded following the simple indel coding algorithm (Simmons et al. 2001) with FastGap 1.2 (Borchsenius 2009). The dataset of ITS+binary data consisted of 51 sequences and 669 characters. maximum likelihood (ML) analysis was carried out in RAxML (Stamatakis 2014) as implemented in raxmlGUI version 1.5b2 (Silvestro & Michalak 2012). Rapid bootstrap analysis with 1000 replicates was performed. The GTRGAMMA substitution model (for the three nucleotide partitions) and the RAxML default set for binary characters (for the indel partition) were applied. In addition, Bayesian inference (BI) was performed in MrBayes version 3.1.2 (Ronquist & Huelsenbeck 2003). The alignment was divided into four partitions (ITS1, 5.8S, ITS2, and indels). The GTR +  $\Gamma$  substitution model was applied to the nucleotide characters, and the two-parameter Markov model was set for the indels. Two independent runs of four Markov Chain Monte Carlo (MCMC) were performed each over 10 million generations, sampling every 1000 generations, with a burn-in of 30 % (= the first 3000 trees were discarded). Remaining trees were used to compute the 50 % majority rule consensus phylogram. Phylogenetic trees from both ML and BI resulted in largely congruent topologies. The majority rule consensus phylogram was edited in MEGA7 (Kumar et al. 2016) and in Adobe Illustrator CS7.

For the phylogenetic analysis of *Curvularia*, DNA sequences of 129 strains were included. A strain of *Bipolaris drechsleri* (MUS0028) was used as outgroup. DNA sequences of ITS and *gpd* were aligned using BioEdit Sequence Alignment Editor version 7.0.9.0 (Hall 1999) and then concatenated into a composite alignment. Maximum likelihood analysis was performed with all sequences in MEGA6 (Tamura et al. 2013), first with each locus separately, and then with the composite alignment. ML MODEL TEST in MEGA6 was used to select the best model of nucleotide substitution for the phylogenetic analyses. The concatenated ITS-*gpd* alignment used for constructing the phylogenetic tree in Fig. 7 was deposited in TreeBASE (S23087).

ITS sequences of *Gloeocamtherellus* and *Gomphus clavatus* (outgroup) were aligned using MAFFT (Katoh et al. 2005) and manually modified where necessary in BioEdit version 7.0.5.3 (Hall 1999). Substitution models were determined using the Akaike Information Criterion (AIC) implemented in MrModeltest version 2.3 (Posada & Crandall 1998, Nylander 2004). For the maximum likelihood

(ML) analysis in RAxML version 7.2.6 (Stamatakis 2006), all parameters were kept default except for the substitution model, for which we selected GTR-GAMMAI. Nonparametric bootstrap analysis was done using 1000 replicates. Bayesian inference (BI) analysis was run for 2 million generations on MrBayes 3.1.2 (Ronquist & Huelsenbeck 2003) using the selected model GTR+I and the stoprul command with the 'stopval' value set to 0.01; the other parameters were kept default. Resulting trees were summarized and posterior probability support was obtained by using sumt command complemented in MrBayes by discarding the first 25 % trees as burn-in. Branches that received ML bootstrap support (MLBS)  $\geq 50$  and BI posterior probabilities (BIPP)  $\geq 0.9$  were considered as significant.

Based on the BLASTn results, *Pluteus* sequences were downloaded – according to the outcomes of recent molecular phylogenetic studies in *Pluteus* sect. *Celluloderma* (Menolli et al. 2010, 2015; Justo et al. 2011a, 2011b, 2011c, 2012; Pradeep et al. 2012; Malysheva et al. 2016; Ferisin et al. 2019; Crous et al. 2019). The sequences of *P. cervinus* (Schaeff.) P. Kumm. and *P. petasatus* (Fr.) Gillet were used as outgroup following Menolli et al. (2015). Sequences were aligned using MAFFT version 7.017 (Katoh & Toh 2008) with default parameters. Maximum likelihood (ML) were inferred with RAxML version 8 (Stamatakis 2014). The GTR+G model was selected and a total of 1000 bootstrap (BS) replicates were performed.

Newly generated *Rhizoglosum* rDNA sequences (consisting of partial SSU, ITS, and partial LSU) were aligned with other related glomeromycotan sequences from NCBI GenBank in ClustalX (Larkin et al. 2007). *Glomus macrocarpum* Tul. & C. Tul. and *Funneliformis mosseae* (T.H. Nicolson & Gerd.) C. Walker & A. Schüssler were included as outgroup. Prior to phylogenetic analysis, the model of nucleotide substitution was estimated using Topali 2.5 (Milne et al. 2004). Bayesian inference (two runs over  $3 \times 10^6$  generations, sample frequency of 300, burn-in of 25 %) and maximum likelihood analysis (with 1,000 bootstrap replicated) were performed in MrBayes 3.1.2 (Ronquist & Huelsenbeck 2003) and PhyML (Guindon & Gascuel 2003), launched from Topali 2.5, using the GTR + G model.

Sequences of species in *Russula* subsection *Cyanoxanthinae* and related species were downloaded from GenBank (NCBI) based on previous studies (Kropp 2016, Zhang et al. 2017, Li & Deng 2018) and combined with our newly generated sequences to construct a concatenated ITS-LSU-mtSSU-*tef1* dataset. *Russula adusta* (Pers.) Fr. and *R. nigricans*

Fr. were selected as outgroups. *Russula* sequences were aligned in MAFFT version 7 (Katoh & Toh 2008) using the “G-INS-I” strategy, and then manually adjusted in BioEdit (Hall 1999). The sequence alignment was deposited at TreeBase (S24448). The best fit model of nucleotide evolution to the datasets was selected with the Akaike Information Criterion (AIC) using MrModeltest 2.3 (Posada & Crandall 1998, Nylander 2004). Bayesian inference (BI) and maximum likelihood (ML) analyses were performed. Six partitions (ITS1, 5.8S, ITS2, LSU, mtSSU, and *tef1*) were used in the phylogenetic analyses. BI was performed using MrBayes on XSEDE (3.2.6) through the Cipres Science Gateway (Miller et al. 2010) with 2 independent runs, each one beginning from random trees with 4 simultaneous independent chains, performing 2 million generations, sampling every 100 generations. The first 25 % of the sampled trees were discarded as burn-in; the remaining trees were used to reconstruct a majority rule consensus and calculate posterior probabilities (BIPP). ML searches were conducted with RAxML-HPC2 on XSEDE 8.2.10 through Cipres (Miller et al. 2010), under the GTRGAMMA model. Only the maximum likelihood best tree from all 100 searches was kept. A total of 100 rapid bootstrap replicates were run with the GTRCAT model to assess statistical support of nodes. Branches that received MLBS  $\geq 75$  and BIPP  $\geq 0.95$  were considered as significantly supported.

Combined and separate *Stagonosporopsis* trees were generated using ITS, LSU, *tub2*, and *rpb2* sequences of our isolates (UC30, CG7, UC56, S3, and UC23) and reference species belonging to *Didymella*, *Nothophoma*, and *Stagonosporopsis*, which we downloaded from GenBank (Tibpromma et al. 2017, Valenzuela-Lopez et al. 2018). After Clustal W multiple alignment, maximum likelihood (ML) was inferred based on the Tamura-Nei model, and bootstrapping was performed with 1000 replicates. Initial tree(s) for the heuristic search were obtained automatically by applying Neighbour-Joining and BioNJ algorithms to a matrix of pairwise distances estimated using the Maximum Composite Likelihood (MCL) approach, and then selecting the topology with superior log likelihood value. A discrete Gamma distribution was used to model evolutionary rate differences among sites (5 categories; +G, parameter = 0.1270). Phylogenetic analyses were conducted in MEGA7 (Kumar et al. 2016).

Newly generated sequences of *Strobilomyces* and related sequences downloaded from GenBank are listed in Tab. 1. A total of 238 sequences including 7 newly generated in this study formed the

dataset. The sequences of *rpb1*, *rpb2*, *tef1*, and *cox3* were combined by Phyutility (Smith & Dunn 2008), because no significant incongruence was detected among individual genes (Nuhn et al. 2013, BS  $> 70$  %). Alignments were made with MAFFT version 7.130b (Katoh & Standley 2013) and optimized using BioEdit version 7.0.9 (Hall 1999) and Gblocks 0.91b (Castresana 2000). The combined alignment was submitted to TreeBase (S23773). Sequences of *rpb1*, *rpb2*, *tef1*, and *cox3* were divided into 12 blocks based on three codon positions, including *rpb1\_codon1*, *rpb1\_codon2*, *rpb1\_codon3*, *rpb2\_codon1*, *rpb2\_codon2*, *rpb2\_codon3*, *tef1\_codon1*, *tef1\_codon2*, *tef1\_codon3*, *cox3\_codon1*, *cox3\_codon2*, and *cox3\_codon3*. All introns in *rpb1* and *tef1* were treated as a single block, including *rpb1\_intron1*, *rpb1\_intron2*, *tef1\_intron1*, and *tef1\_intron2*. Altogether, there were 13 data blocks predefined for the combined four-locus dataset. The best partitioning schemes and evolution models for each subset were evaluated by PartitionFinder 2.1.1 (Lanfear et al. 2017). Phylogenetic trees were generated from maximum likelihood (ML) and Bayesian inference (BI) analyses based on RAxML version 7.2.6 (Stamatakis 2006) and MrBayes version 3.1.2 (Ronquist et al. 2012). For ML, 1000 replicates were executed based on the rapid bootstrapping algorithm under the GTR+I+G model (Nylander 2004, Stamatakis 2006). For BI, partitioned Bayesian analyses of four simultaneous Markov chains were run for 2 million generations and sampling every 200 trees. Runs were monitored by Tracer version 1.5 (<http://tree.bio.ed.ac.uk/software/tracer/>) to make sure the effective sample sizes (ESS) was higher than 200 and the average standard deviation of split frequencies was below 0.01. A consensus tree was generated after discarding the first 25 % trees as burn-in.

Uredinial ITS sequences were BLAST searched against the reference sequences in GenBank ([www.ncbi.nlm.nih.gov](http://www.ncbi.nlm.nih.gov)). A total of 11 ITS sequences of *Uromyces* species and *Puccinia nepalensis* (outgroup) previously submitted to NCBI GenBank, together with the sequences generated in this study, were used for phylogenetic analysis (Fig. 33). Unfortunately, insufficient sequences of *Rumex*-infecting *Uromyces* species are currently available to conduct a thorough phylogenetic analysis. The sequence data set was aligned using the Muscle E multiple alignment tool within MEGA 7.0 (Kumar et al. 2016). The alignment set was trimmed at terminals to remove the gaps. Phylogenetic analysis of the ITS sequences was performed using maximum likelihood inference with the GTRGAMMA model (Nei & Kumar 2000).



For phylogenetic placement of our *Alternaria* isolate, reference ITS and *gpd* sequences of related species were downloaded from NCBI GenBank (details in Tab. 1). *Exserohilum gedarefense* (El Shafie) Alcorn was used as the outgroup. All sequences were aligned with Clustal W (Thompson et al. 1994). Maximum likelihood (ML) analysis was performed by heuristic search in MEGA6 (Tamura et al. 2013). Bootstrap analysis was performed with 1000 replicates.

Sequence editing of the *Marasmiellus subpruinosis* ITS sequence was done in Bioedit 7.09 (Hall 1999). Other sequences were downloaded from GenBank and aligned with Muscle (Edgar 2004). The best-fit substitution model for the alignment was estimated with the Akaike Information Criterion (AIC) using FindModel web server (<http://www.hiv.lanl.gov/content/sequence/findmodel/findmodel.html>). Phylogenetic reconstructions of the ITS dataset were performed with maximum likelihood (ML) and Bayesian inference (BI). In both ML and BI the best-fit substitution model employed was GTR. ML analysis was run in the PhyML server 3.0 (<http://www.phylogeny.fr>), with 100 rapid bootstrap replicates. BI was performed using MrBayes 3.2.5 (Ronquist et al. 2012).

For *Plagiosphaera immersa*, the newly generated sequences were aligned with selected sequences of Magnaporthales from Hernández-Restrepo et al. (2016) and Silva et al. (2019), with a few recent additions from GenBank; two species of *Ophioceras* (Ophiocercaceae) were added as the outgroup. GenBank accession numbers of sequences used in these analyses are given in Tab 1. Sequence alignments were produced with the server version of MAFFT (<http://mafft.cbrc.jp/alignment/server/>) and checked and refined using BioEdit version 7.2.6 (Hall 1999). The ITS–LSU rDNA, *rpb1*, and *tef1* matrices were combined for subsequent phylogenetic analyses. After exclusion of leading, trailing, and long gaps, the final combined data matrix contained 3341 characters (632 of ITS, 763 of LSU, 1022 of *rpb1*, and 924 of *tef1*). Maximum likelihood (ML) analyses of the ITS–LSU–*rpb1*–*tef1* data matrix were performed with RAxML (Stamatakis 2006) as implemented in raxmlGUI 1.3 (Silvestro & Michalak 2012), using the ML + rapid bootstrap setting and the GTRGAMMA substitution model with 1000 bootstrap replicates. The matrix was partitioned for the different gene regions. Maximum parsimony (MP) analyses of the concatenated matrix were performed with PAUP version 4.0a166 (Swofford 2002), with 1000 bootstrap replicates using five rounds of heuristic search replicates with random addition of

sequences and subsequent TBR branch swapping (MULTREES option in effect, steepest descent option not in effect) during each bootstrap replicate. All molecular characters were unordered and given equal weight; analyses were performed with gaps treated as missing data; the COLLAPSE command was set to minbrlen.

For the placement of *Sphaerosporium lignatile* within a phylogenetically robust tree, we used the six-locus Ascomycota-wide Laboulbeniomycetes dataset from Haelewaters et al. (2019b), an extension of the Schoch et al. (2009) *Ascomycota Tree of Life*. We extracted the SSU and LSU loci from the data matrix and added the respective sequence data of *S. lignatile*. Multiple alignment was run for each locus using MUSCLE v3.8.31 (Edgar 2004) on the Halstead computing cluster at Purdue University. The sequences of both loci were trimmed with trimAl version 1.3 (Capella-Gutiérrez et al. 2009) on the command line with gap threshold (-gt) = 0.6 and minimal coverage (-cons) = 0.5, and then concatenated with the other loci in MEGA7 (Kumar et al. 2016) to form a data matrix of 18,524 characters. Maximum likelihood (ML) analysis of the resulting six-locus data matrix was inferred using RAxML 8.2.9 (Stamatakis 2014) on Halstead with the GTR-CAT model of heterogeneity, 1000 bootstrap (MLBS) replicates, and *Rhizopus oryzae* (Mucoromycota *sensu* Spatafora et al. 2016) as outgroup.

## Taxonomy

### Basidiomycota, Agaricomycetes, Agaricales, Cortinariaceae

*Cortinarius brunneocarpus* Razaq & Khalid, **sp. nov.** – Figs. 1–2

Mycobank no.: MB 830035

**Holotypus.** – PAKISTAN. Khyber Pakhtonkhow Province, Khanspur, 2400–2580 m a.s.l., on the ground of humified soil in *Abies pindrow*–*Pinus wallichiana* vegetation, 24 August 2010, *leg.* A. Razaq, KP-80 (LAH240810; holotype). Sequences ex-holotype: MN738695 (ITS).

**Description.** – Pileus 30–85 mm, campanulate to plano-convex, greyish brown to ochraceous brown with dark brown umbo, lighter towards margin, hygrophorous, surface glabrous, with hygrophorous streaks, margin silky white fibrillose, wavy, recurved. – Lamellae adnexed to emarginate, distant, fairly thick, broad, ochraceous brown, to brown, with concolorous entire edge, lamellulae present. – Stipe 25–60 × 4–10 mm, cylindrical, slightly widening towards base, whitish to light yellowish brown, brownish towards base,



Fig. 1. *Cortinarius brunneocarpus* (holotype). A. Basidiomata, B. Lamellar side of basidiomata. Photos A. Razaq.

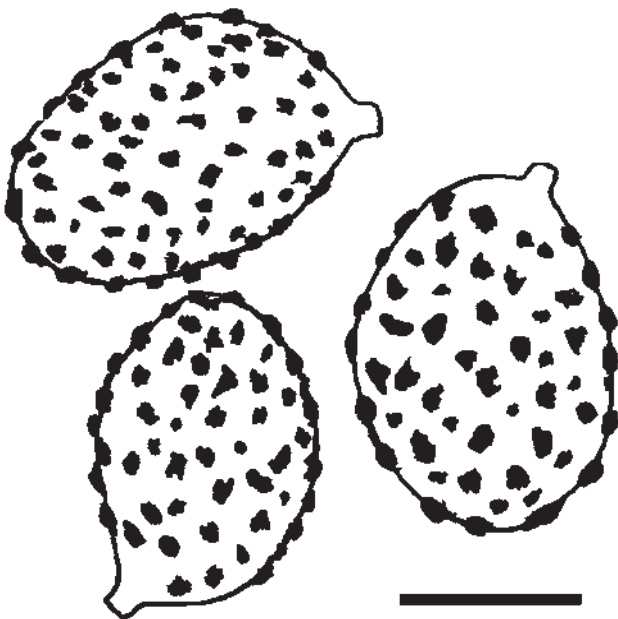
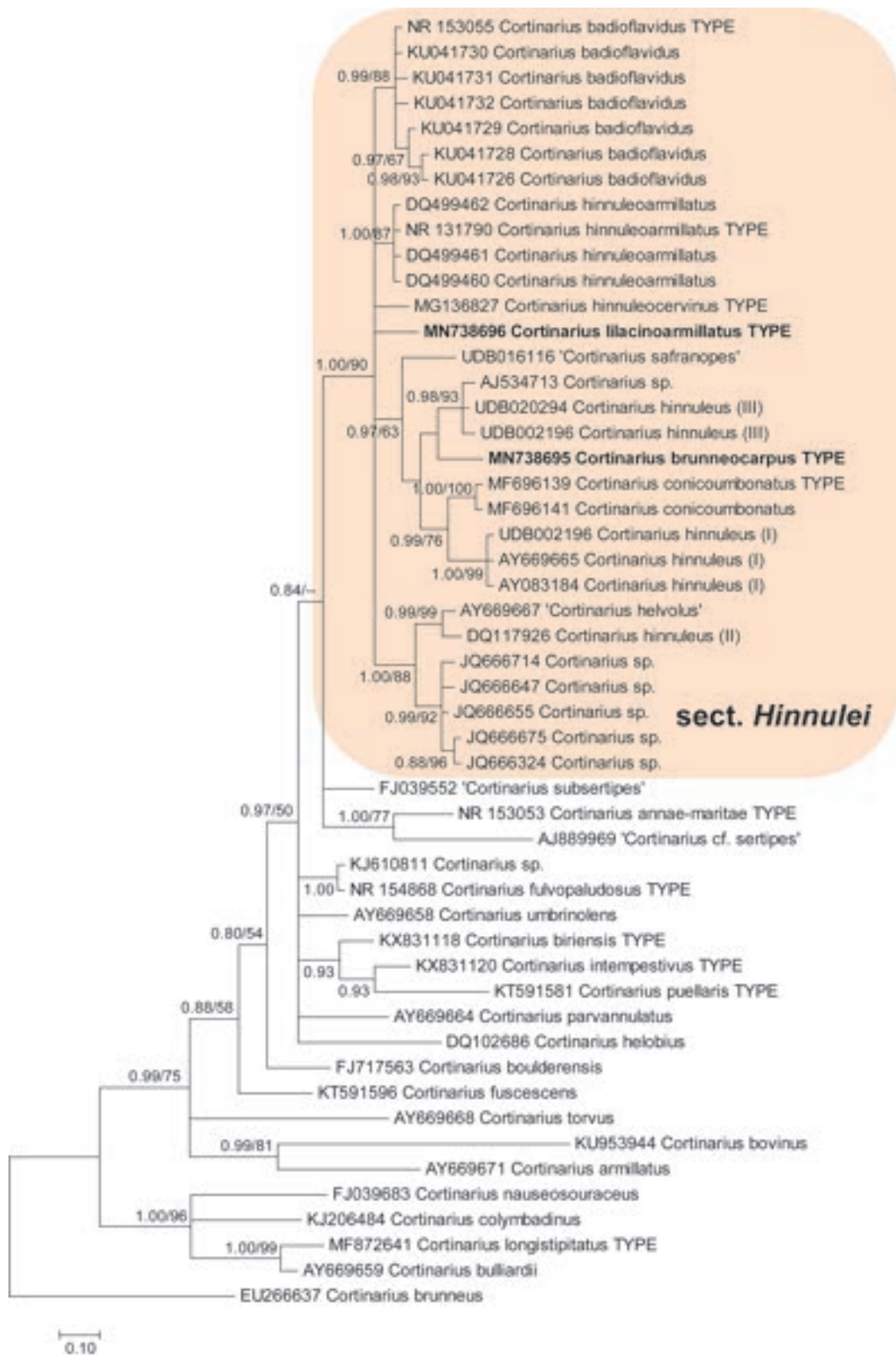


Fig. 2. Spores of *Cortinarius brunneocarpus* (holotype). Scale bar 5 µm, del. H. Bashir.

smooth to fibrillose, universal veil forming a white fibrillose evanescent zone at the half, cortina whitish. – Context whitish to brownish, thin, soft to moderately firm, pale yellowish, brownish in the base, unchanging when bruised or cut. Odour and taste not recorded. – Basidiospores 8.5–11.5 × 6.0–8.5 µm, av.=10.0–7.1 µm, Q=1.35–1.42, Qav.=1.4; subglobose to obovoid, distinctly verrucose, moderately thick-walled, rusty brown to reddish brown in 5% KOH, inamyloid, moderately dextrinoid. – Basidia 30.5–38.0 × 8.0–11.5 µm, 4-spored, sterigmata 3.0–3.5 µm long, hyaline to light pale yellow in 5% KOH, thin-walled, sub-clavate to clavate, transparent. Hymenial trama hyphae, cylindrical, irregular, 11.0–12.0 µm wide. – Marginal cells 19.0–36.5 × 7.5–12.5 µm, cylindrical to broadly clavate, hyaline, thin-walled. – Clamp connections present.

**Etymology.** – Referring to the brown basidioma of the species.

**Habitat and distribution.** – Only known from coniferous forests of western Hima-



**Fig. 3.** ITS phylogeny of sect. *Hinnulei* including the two new species and related taxa inferred from Bayesian inference analysis. New sequences are highlighted in boldface. BIPP  $\geq 0.8$  and MLBS  $\geq 50$  are indicated at the nodes.

laya, Pakistan, from *Abies pindrow*–*Pinus wallichiana* vegetation at ca. 2500 m a.s.l.

**Notes.** – According to the ITS sequence and our phylogenetic analysis (Fig. 3), *C. brunneocarpus* is a distinct species in sect. *Hinnulei*. The most closely related species is *C. hinnuleoarmillatus* from which the new species differs in its ITS sequence by 10 substitution and indel positions (98.1 % sequence similarity).

Morphologically, *C. brunneocarpus* is clearly placed in sect. *Hinnulei* based on the hygrophanous, brownish basidiomata, distant lamellae, whitish universal veil remnants on the stipe, and the ellipsoid coarsely verrucose basidiospores. The spores of *C. hinnuleus* sensu Niskanen & Kytövuori (2012) and the recently described *C. conicoumbonatus* from Turkey (Sesli & Liimatainen 2018) have smaller spores ( $7.0\text{--}9.5 \times 5.4\text{--}6.5 \mu\text{m}$  and  $7.3\text{--}8.6 \times 4.6\text{--}5.8$ , respectively) than those of the Pakistani species ( $8.5\text{--}11.5 \times 6.0\text{--}8.5 \mu\text{m}$ ). *Cortinarius hinnuleoarmillatus* (Niskanen et al. 2006) has almost similar

spores ( $8.8\text{--}10.5 \times 5.4\text{--}6.3 \mu\text{m}$ ) compared to those of *C. brunneocarpus*, but differs by the orange to ochraceous brown pileus, persistent annulus, lamellae with violet tint, and orange red veil.

**Authors:** A. Razaq, S. Ilyas, A.N. Khalid, K.C. Semwal, V.K. Bhatt, V. Papp & B. Dima

**Basidiomycota, Agaricomycetes, Agaricales, Cortinariaceae**

***Cortinarius lilacinoarmillatus* Semwal & Dima, sp. nov.** – Figs. 4–5

Mycobank no.: MB830066

**Holotypus.** – INDIA. Uttarakhand, Pauri Garhwal, Bharsar, 1950 m a.s.l., solitary, among leaf litter, near *Quercus leucotrichophora* and *Corylus jacquemontii*, 2 August 2015, leg. K.C. Semwal, KCS2428 (CAL; holotype). Sequences ex-holotype: MN738696 (ITS).

**Description.** – Pileus 20–40 mm, campanulate to convex with a low umbo at centre, reddish brown to tawny, becoming pale ochraceous



**Fig. 4.** *Cortinarius lilacinoarmillatus* (holotype). **A.** Basidiomata, **B.** Lamellar side of basidiomata. Photos K.C. Semwal.

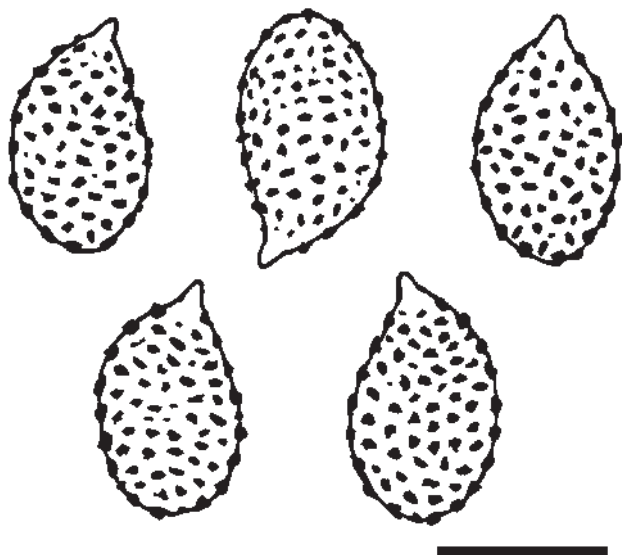


Fig. 5. Spores of *Cortinarius lilacinoarmillatus* (holotype). Scale bar 5  $\mu\text{m}$ , del. V. Papp.

brown when dry, hygrophanous, surface glabrous, margin crenulate. – Lamellae emarginate, distant, broad, violet-lilac when young, becoming brown with age, with concolorous, slightly wavy edge, lamellulae present. – Stipe 50–70  $\times$  6–8 mm, cylindrical, concolorous with the pileus or ochraceous threads towards the base, universal veil forms a whitish-cream evanescent membranous ring at the upper thirds, cortina whitish. – Context cream to brownish, thin, soft to moderately firm, unchanging when bruised or cut. Odour and taste not recorded. – Basidiospores 7.0–8.7  $\times$  (4.5)5.0–6.0  $\mu\text{m}$ , av.=7.9–5.4  $\mu\text{m}$ , Q=1.4–1.6, Qav.=1.5, obovoid to obovoid-subglobose, moderately verrucose, somewhat thick-walled, rusty brown in 5 % KOH, inamyloid, moderately dextrinoid. – Basidia 28.0–35.0  $\times$  7.0–10.5  $\mu\text{m}$ , 4-spored, sterigmata 2.0–3.0  $\mu\text{m}$  long, hyaline, thin-walled, clavate. – Lamellar trama hyphae cylindrical, somewhat irregular, 10.0–13.0  $\mu\text{m}$  wide. – Marginal cells 21.0–32.0  $\times$  6.0–8.7  $\mu\text{m}$ , clavate, hyaline, thin-walled. – Clamp connections present.

**Etymology.** – “*lilacino*” referring to the initially lilac gills, and “*armillatus*” referring to the similarity to *C. hinnuleoarmillatus* as well as to the pronounced *Armillaria*-like membranous partial veil remnants on the stipe.

**Habitat and distribution.** – Known only from type locality. Solitary, occurring among leaf litter, near *Quercus leucotrichophora* (banj oak) and *Corylus jacquemontii* (Turkish hazelnut).

**Notes.** – This specimen was first identified as *C. cf. distans* Peck according to MushroomExpert.com (Kuo 2011) – on the basis of the brownish pileus, the distant lamellae, the ellipsoid, verrucose spores, and the rusty brown spore print (Semwal et al. 2018). However, *C. distans* was described from North America and this species was recombined to *Phaeomarasmius distans* (Peck) Singer (Index Fungorum 2019). The ITS sequence of *C. lilacinoarmillatus* is most closely related to *C. hinnuleoarmillatus* from which it differs by 8 substitution and indel positions (98.5 % sequence similarity).

The purplish lamellae of young basidiomata represent a rare character in sect. *Hinnulei*. *Cortinarius hinnuleoarmillatus* shares this feature with *C. lilacinoarmillatus*, but the former has significantly larger spores (8.8–10.5  $\times$  5.4–6.3  $\mu\text{m}$ ) and an orange reddish veil (Niskanen et al. 2006). The above-described *C. brunneocarpus* from Pakistan lacks the annulus-like veil remnants, its basidiospores are much larger, and it is associated with coniferous trees.

**Authors:** A. Razaq, S. Ilyas, A.N. Khalid, K.C. Semwal, V.K. Bhatt, V. Papp & B. Dima

#### Ascomycota, Dothideomycetes, Pleosporales, Pleosporaceae

***Curvularia khuzestanica*** M. Mehr.-Koushk., Khodadadi & Farokhin., **sp. nov.** – Fig. 6  
Mycobank no.: MB 827195

**Holotype.** – IRAN. Khuzestan Province, Kozeria, on *Atriplex lentiformis*, June 2016, leg. M. Mehrabi-Koushki & S. Khodadadi-Pourarpanahi (IRAN 16941F; holotype). Ex-type cultures: CBS 144736 = IRAN 3135C = SCUA-11C. Sequences ex-holotype: MH688044 (ITS), MH688043 (*gdp*).

**Description.** – Morphology on PDA: Hyphae sub-hyaline to pale-brown, branched, septate, thin and smooth-walled, up to 4.3  $\mu\text{m}$  in width. – Conidiophores singly, simple, septate, approximately equally wide in the basal and medium parts, wider in the upper part, straight or flexuous, geniculate towards the apex, brown, paler in the upper part, cell walls thicker than those of the vegetative hyphae, smooth-walled, (8.6)13–99(108)  $\times$  2.2–5.4(6.8)  $\mu\text{m}$ , 95 % confidence intervals = 46.3–68.1  $\times$  3.4–4.2  $\mu\text{m}$ , ( $\pm$  SD = 57.2  $\pm$  33.1  $\times$  3.8  $\pm$  1.2  $\mu\text{m}$ ). – Conidiogenous cells integrated, mostly with verruculose nodes, terminal or intercalary, with sympodial proliferation, with darkened and thickened scars, brown, sub-cylindrical to slightly swollen. – Conidia ellipsoidal to fusiform, straight or sometimes slightly curved at the first septum from base, smooth-walled, brown, 3–5-dis-

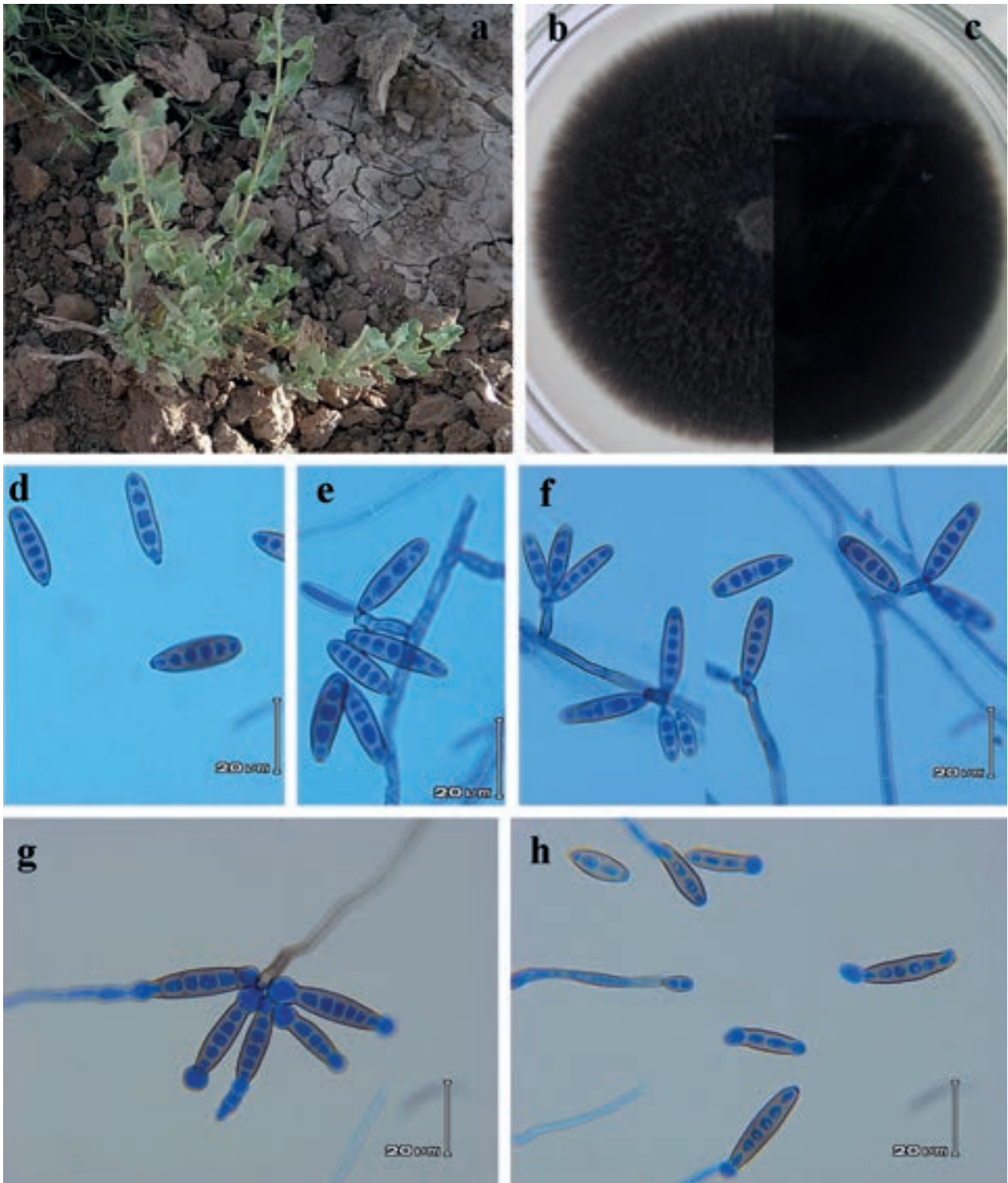


**Fig. 6.** *Curvularia khuzestanica* (CBS 144736). **a.** The host plant, *Atriplex lentiformis*. **b–c.** Colony on PDA (front and reverse). **d–f.** Conidiophores and conidia. **g–h.** Mono- or bipolar germination of conidia.

toseptate, rounded at the apex, with monopolar or bipolar germination,  $(7.5)9\text{--}28(31) \times 4.3\text{--}7.6(8.6) \mu\text{m}$ , 95 % confidence intervals =  $19.1\text{--}22.2 \times 5.8\text{--}6.4 \mu\text{m}$ , ( $\pm \text{SD} = 20.7 \pm 5.8 \times 6.1 \pm 1.1 \mu\text{m}$ ). – Hil a conspicuous and protuberant, thickened and darkened, 1.2–2  $\mu\text{m}$  wide. – Chlamydospores and sexual morph not observed. – Cultural characteristics on PDA: Colonies on PDA attaining 75–80 mm diam. after 6 d at 28 °C, greenish black, floccose, with a fimbriate margin; reverse greyish black.

**E t y m o l o g y.** – Referring to Khuzestan province where the fungus was collected.

**H a b i t a t a n d d i s t r i b u t i o n.** – Thus far only found in Khuzestan province, Iran, as an endophyte of *Atriplex lentiformis*.

**A d d i t i o n a l m a t e r i a l e x a m i n e d.** – IRAN. Khuzestan province, Abadan, on an unidentified plant, June 2016, leg. M. Mehrabi-Koushki & S. Khodadadi-Pourarpanahi (SCUA-11C-2).

**N o t e s.** – The genus *Curvularia* was erected by Boedijn (1933). The type species, *C. lunata* (Wakker) Boedijn, is a phytopathogen causing leaf spots on members of Fabaceae, Cucurbitaceae, Compositae, Solanaceae, Malvaceae, and Graminaceae (Lal et al. 2013). Index Fungorum (2019) currently lists 184 names in *Curvularia*, which are isolated from different sources including air, animals, humans, plants, and soil (Manamgoda et al. 2012a, 2012b, 2014, 2015; Madrid et al. 2014; Tan et al. 2014, 2018; Tomaso-Peterson et al. 2016; Marin-Felix et al. 2017a, 2017b; Dehdari et al. 2018; Heidari et al. 2018; Liang et al. 2018; Mehrabi-Koushki et al. 2018). They are mostly saprobes (Manamgoda et al. 2011, 2012a, 2012b, 2014, 2015; Scott & Carter 2014; Tan et al. 2014, 2018), although a few of them are the causal agents of infectious diseases in animals, humans, and plants (Manamgoda et al. 2011, Madrid et al. 2014). Some species were also found within plants as endophytes (Tadych et al. 2012, Gautam et al. 2013, Jena & Tayung 2013, Heidari et al. 2018).

*Curvularia* species are traditionally distinguished based on morphological features, mainly conidial morphology including size, number of septa, conidial shape, and presence or absence of a protuberant hilum (Nelson 1964, Revankar & Sutton 2010, da Cunha et al. 2013). Presently, they are mainly identified by means of an integrative approach, including morphological characterization and multilocus phylogenetic analyses based on the internal transcribed spacer region (ITS), glyceraldehyde-3-phosphate dehydrogenase (*gpd*), and translation elongation factor 1- $\alpha$  (*tef1*) (Manamgoda et al. 2012a, 2012b, 2014, 2015; Madrid et al.

2014; Tan et al. 2014, 2018; Tomaso-Peterson et al. 2016; Marin-Felix et al. 2017a, 2017b; Dehdari et al. 2018; Heidari et al. 2018; Liang et al. 2018, Mehrabi-Koushki et al. 2018).

Sequence comparison of the newly generated ITS sequences via BLAST showed that the new species of *Curvularia* was most closely related to the type strains of *C. nodosa* and *C. beasleyi* with 99 % similarity (Fig. 7). In the BLAST analysis of the *gpd* sequence, the closest matches were *C. beasleyi* (99 % similarity), *C. dactyloctenii* (98 %), *C. nodosa* (98 %), *C. hawaiiensis* (98 %), and *C. buchloes* (98 %). The composite alignment consisted of 971 sites including gaps (ITS, 468 sites; *gpd*, 503 sites) with 625 conserved (ITS, 333; *gpd*, 292) and 334 variable sites. The best model of evolution for phylogenetic analysis of the composite data set, as calculated by MEGA6, was TN93+G+I). The phylogenetic tree based on the composite alignment clustered both strains of *C. khuzestanica* sp. nov. in a strongly supported clade with (ML bootstrap = 99), distinct from previously described species of *Curvularia* (Fig. 7). The clustering of the ITS- and *gpd*-based phylogenetic trees also supported *C. khuzestanica* as a distinct species of *Curvularia* (not shown). Phylogenetic analyses indicated that the closest relatives of the new species are *C. ahvazensis*, *C. beasleyi*, *C. dactyloctenii*, *C. hawaiiensis*, and *C. nodosa* (Fig. 7). These six species share 97.6 % sequence identity in the ITS region (431 bp) attributed to 5 SNPs (1.2 %) and 5 bp (1.2 %) insertion/deletion, and 96.8 % sequence identity in the *gpd* region (432 bp) attributed to 14 SNPs (3.2 %).

*Curvularia khuzestanica* is placed in a clade containing *C. ahvazensis* Mehr.-Koushki. & Baabaahm (Mehrabi-Koushki et al. 2018), *C. beasleyi* Y.P. Tan & R.G. Shivas (Tan et al. 2018), *C. dactyloctenii* (Alcorn) Y.P. Tan & R.G. Shivas (Alcorn 1982, Tan et al. 2014), *C. hawaiiensis* (Bugnic.) Manamgoda, L. Cai & K.D. Hyde (Manamgoda et al. 2012b), and *C. nodosa* Y. Marín, Cheew. & Crous (Marin-Felix et al. 2017b), which is a subclade within the ‘*spicifera*’ clade *sensu* Madrid et al. (2014). Of those fungi, *C. beasleyi* is most closely related to *C. khuzestanica*. However, the new species can be distinguished from *C. beasleyi* by its less septate and shorter conidia (3–5 distoseptate and 20.7  $\mu\text{m}$  long in *C. khuzestanica* vs. 3–7 distoseptate and 26–29  $\mu\text{m}$  long in *C. beasleyi*). Moreover, *C. khuzestanica* is found on *Atriplex lentiformis*, whereas *C. beasleyi* has been reported from different hosts, including *Chloris gayana* and *Leersia hexandra* (Tan et al. 2018).

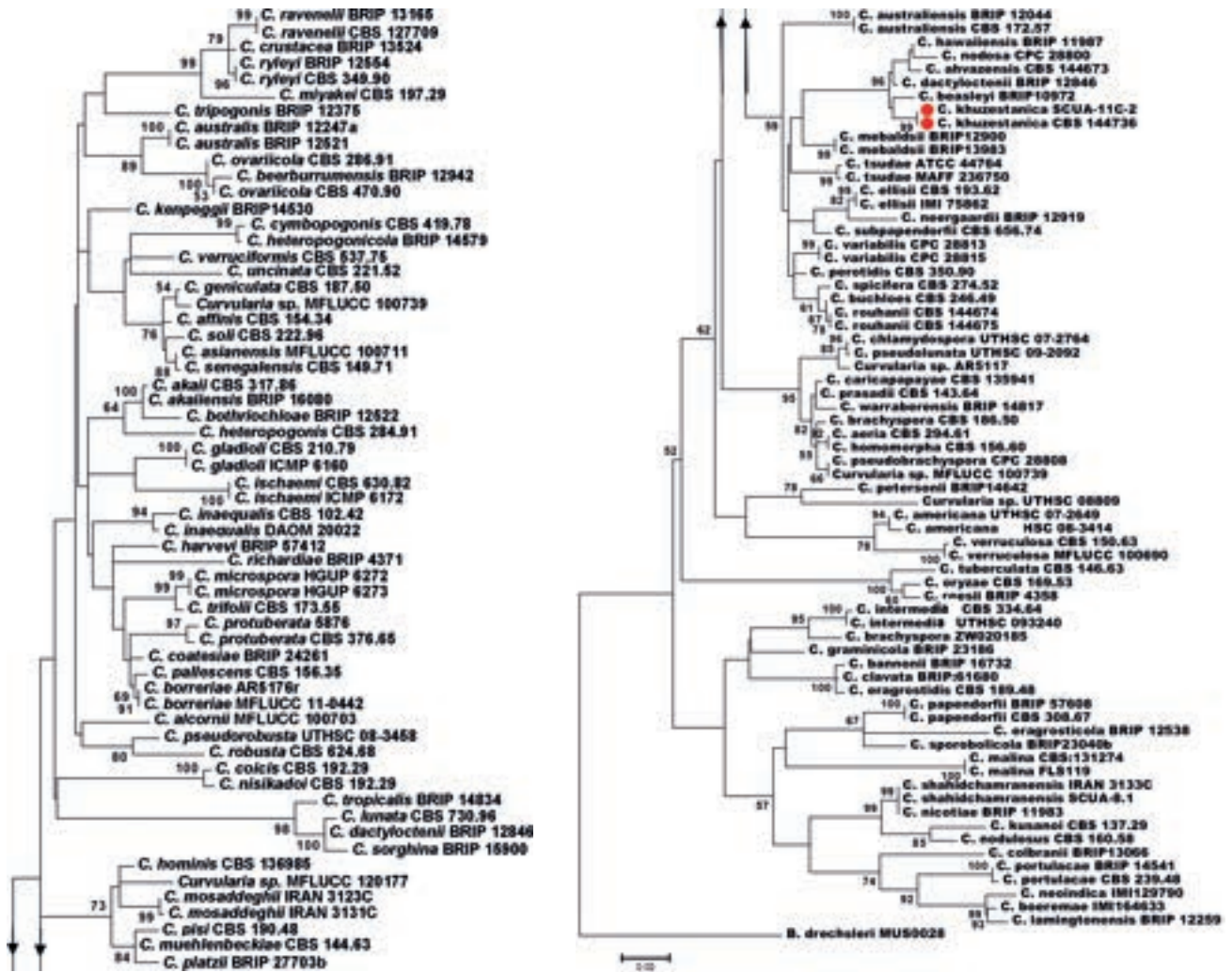


Fig. 7. ML phylogenetic tree reconstructed from a concatenated ITS-gpd dataset of 129 *Curvularia* strains representing previously described species and the her described *C. khuzestanica*. ML bootstrap values > 50 are shown at the nodes.

The ‘spicifera’-clade shows consistent morphological characteristics – mostly straight or slightly curved conidia with conspicuous distosepta. In Madrid et al. (2014), this clade included only six species, but in the present paper it is revealed to include 17 species. The complete spicifera-clade in the tree presented here has an ML bootstrap support of 59. The low support found here is probably due to the use of only two loci. In Madrid et al. (2014), four loci were analyzed. Still, our phylogenetic analysis based on a combined ITS-gpd dataset was able to delimit most species in the genus *Curvularia*.

*Authors:* S. Khodadadi-Pourarpanahi, M. Meh-rabi-Koushki & R. Farokhinejad

## Basidiomycota, Agaricomycetes, Gomphales, Gomphaceae

*Gloeocantharellus neoehinosporus* Ming Zhang & T.H. Li, *sp. nov.* – Figs. 8–9  
Mycobank no.: MB829164

*Diagnosis.* – Different from *G. echinosporus* in having light orange to orange red pileus, close lamellae without furcation or vein at margin and brown to dark brown color changing when bruised, a weak annulus near the stipe apex, and smaller basidia with shorter sterigmata.

*Holotypus.* – CHINA. Guangdong Province, Shaoguan City, Renhua County, Danxiashan National Nature Reserve, 120 m a.s.l., 113°45'E, 25°03'N, 11 September 2018, leg. Ming Zhang (GDGM75321; holotype). Sequences ex-holotype: MK358820 (ITS), MK358815 (LSU).



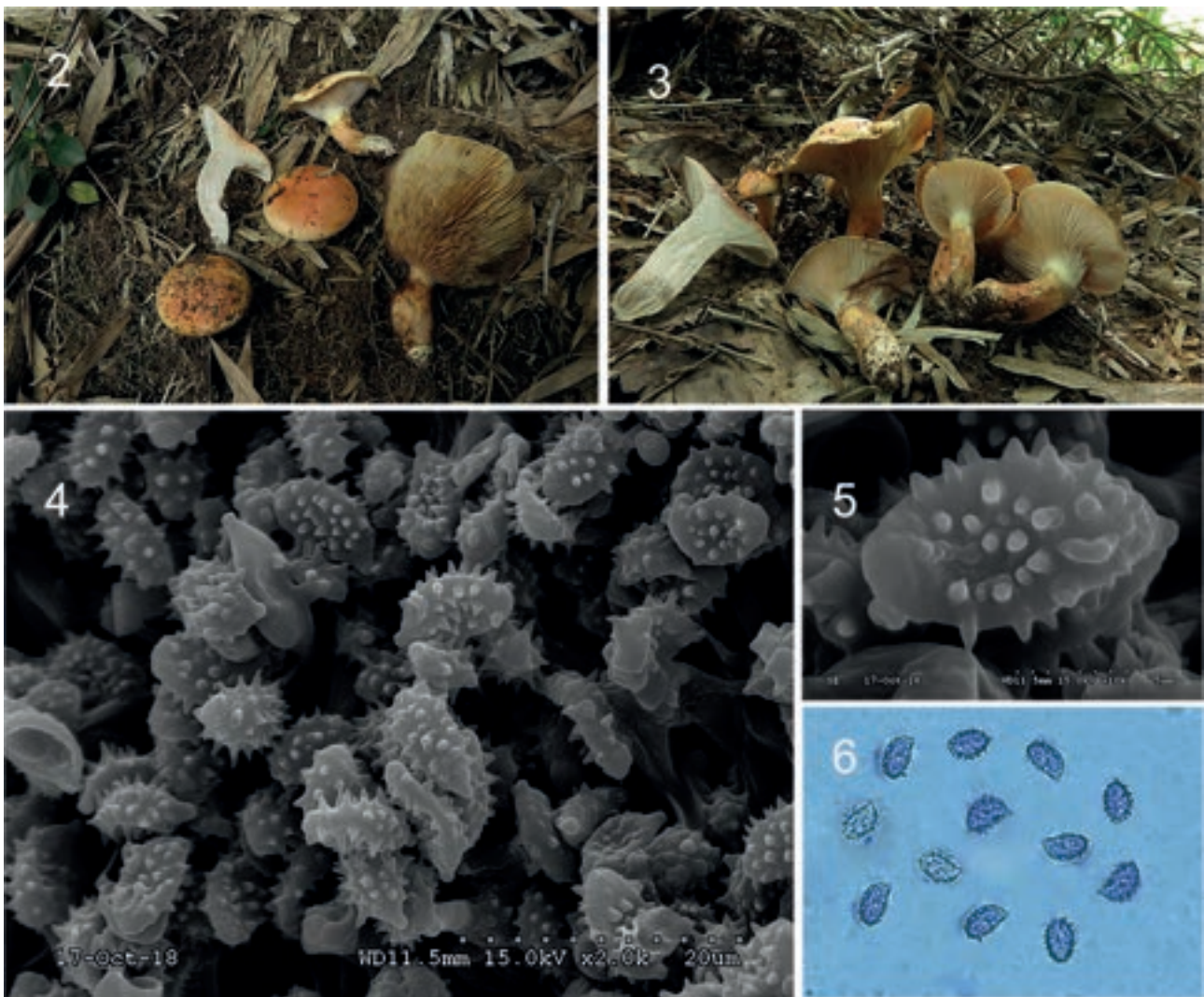


**Fig. 8.** *Gloeocantharellus neoehinosporus*. 2–3. Basidiomata (a: GDGM75322; b: GDGM75321 Holotype!). 4–5. Basidiospores under SEM. 6. Basidiospores in Melzer's reagent. Scale bars 2–3 50 mm, 4–6 5  $\mu$ m.

**Description.** – Pileus 35–100 mm in diam., hemispheric at first, becoming convex to nearly plane with a shallow central depression in age; margin entire, extended to decurved; surface viscous when young or in wet conditions, somewhat dry in age, smooth, velutinous to slightly fibrillose, light orange, orange, deep orange, reddish orange, pastel red to orange red (6A4–6A8, 7A4–7A8, 8A4–8A8) at centre, pale yellow to pale orange (4A3–6A3) towards margin; – Context 8–12 mm thick at stipe, pliable to somewhat firm, white, unchanging or slightly changing to yellowish white to reddish white (4A2–7A2) when cut or exposed, usually with pale red to pastel red (7A3–9A3, 7A4–9A4) tones under the pileipellis. – Lamellae shortly decurrent, up to 5 mm wide, close, even to slightly

fimbriate at edges, white to yellowish white (1A2–4A2) when young, pale yellow, pale orange to greyish orange (4A3–5A3, 4B3–5B3) at maturity, changing to light brown, yellowish brown, brown to dark brown (5D5–7D5, 5E7–7E7, 5F7–7F7) when bruised; – Lamellulae present, 1–7 lamellulae of different lengths between the two complete lamellae, edge entire, concolorous, sometimes forming weak reticulations or longitudinal stripes at apex of stipe. – Stipe 30–70  $\times$  10–17 mm, central, solid, terete to slightly compressed, equal to clavate-bulbous; base obtuse and sometimes tapered downwards and curved bent; surface pulverulent, cracking irregularly and exposing context toward base when mature, usually with weak annulate remnants of inner veil near the stipe apex, white, yellowish white to

pale yellow (1A3–3A3, 1A2–3A2) above the annulus, light yellow, light orange to orange (3A5–7A5) beneath the annulus to the base of stipe, slightly changing to light brown to brown when touched or bruised; stipe context soft, white, unchanging or slightly changing to yellowish white to reddish white (4A2–7A2) when exposed; basal mycelium white. Odour and taste not distinctive. – **B a s i d i -**

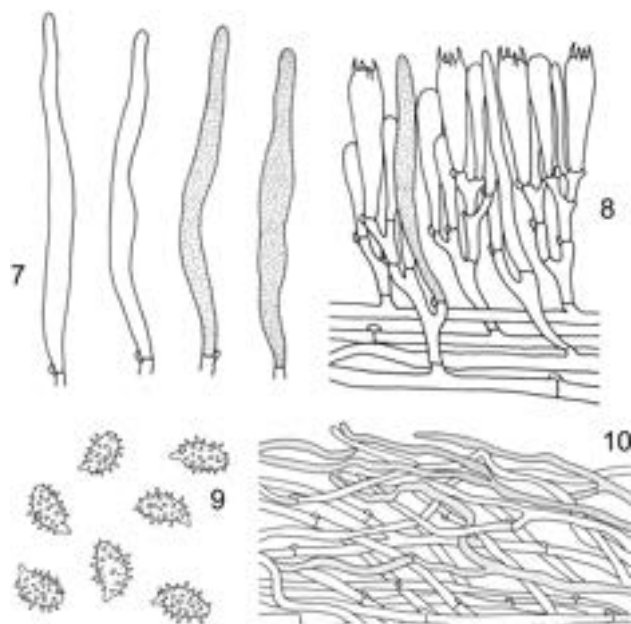


**Fig. 9.** *Gloeocantharellus neoechinosporus*. 7. Gloeocystidia. 8. Basidia and gloeocystidia. 9. Basidiospores. 10. Pileipellis. Scale bars 10  $\mu$ m.

ospores [80/4/4] (8)10–12(12.5)  $\times$  5–7  $\mu$ m, Q = (1.64)1.7–2.09(2.18), Qm = 1.9  $\pm$  0.16, ellipsoid to narrowly ellipsoid, thin-walled, yellowish to light brown, cyanophilic, strongly ornamented with ornamentation up to 1.5  $\mu$ m high, aculeate, ornamentation with apically rounded aculei. – **B a s i d i a** 33–50  $\times$  8–12  $\mu$ m, clavate, deeply tapering towards base, hyaline, 2, 4-spored, thin-walled; sterigmata 3–5  $\mu$ m, clamp connections present. – **B a s i d i o l e s** clavate. – **G l o e o c y s t i d i a** on the sides and margin of the lamellae, 42–94  $\times$  4–8  $\mu$ m, cyanophilic, subventricose, cylindrical to lanceolate with obtuse to subacute apex, deeply tapering and often becoming sinuous towards the base, thin-walled; hyaline and without content when young, then with refringent yellowish brown and densely granular content when old; base inserted in subhymenium or in lamellar trama, rarely protruding above the hymenium. – **H y m e n o p h o r a l t r a m a** parallel to sub-bilateral, somewhat interwoven hyphae 3–10  $\mu$ m

diam., partially to completely gelatinized, gloeoplerous hyphae frequent, flexuous, with yellowish refractive content in KOH, thin-walled. – **P i l e i p e l l i s** an ixocutis, composed of hyphae 3–6  $\mu$ m in diam., loose and frequently slightly interwoven, sinuous, thin-walled, sometimes with granular content. Pileus context with hyphae 6–15  $\mu$ m in diam.; context hyphae interwoven, thin-walled, branched, often inflated, hyaline, intermixed with some gloeoplerous refringent hyphae. – **S t i p i t i p e l l i s** formed of parallel, thin-walled and narrow hyphae 3–6  $\mu$ m in diam., with a trichodermal palisade on the pulverulent portions, without caulocystidia, gloeoplerous elements present as pseudocaulocystidia. – **C l a m p c o n n e c t i o n s** present on almost all septa.

**E t y m o l o g y.** – ‘neo’ = new, ‘echino’ = echinate or echinulate, and ‘spora’ = spore; referring to the presence of echinulate spores similar to *G. echinosporus*.

**H a b i t a t a n d d i s t r i b u t i o n.** – Scattered or in small groups on the ground in broadleaf forests. Tropical to subtropical southern China.

**A d d i t i o n a l m a t e r i a l e x a m i n e d.** – CHINA. Hainan Province, Changjiang County, Bawangling National Nature Reserve, 850 m a.s.l., 7 July 2013, leg. Ming Zhang (GDGM43107); Hainan Province, Ledong County, Jianfengling National Nature Reserve, 1000 m a.s.l., 17 June 2017, leg. Ming Zhang (GDGM70585); Guangdong Province, Shaoguan City, Renhua County, Danxiashan National Nature Reserve, 150 m a.s.l., 113°45'E, 25°03'N, 11 September 2018, leg. Ming Zhang (GDGM75322).

**N o t e s.** – *Gloeocantharellus* Singer (Gomphales, Gomphaceae) is a small genus with *G. purpurascens* (Hesler) Singer as the type species (Singer 1945). The genus is mainly characterized by small and cantharelloid–gomphoid fleshy basidiomata with wrinkled to lamellate hymenium and presence of many gleoplerous hyphae, the presence of verrucose to echinulate basidiospores, and cyanophilous gloeocystidia. The main features used to separate species within *Gloeocantharellus* are the size and ornamentation of the spores, presence or absence of clamp connections or gloeocystidia, habitat, and distribution (Giachini 2004). Morphologically, the cantharelloid basidiomata and usually bifurcate lamellae make *Gloeocantharellus* quite similar to *Cantharellus* Adans. ex Fr. (Cantharellales, Cantharellaceae). However, the latter can be recognized by its interveined hymenophore, smooth basidiospores, and the absence of cyanophilous gloeocystidia. In addition, *Cantharellus* can be easily separated using molecular phylogenetic data. Recent molecular studies show that *Gloeocantharellus* is a monophyletic genus in the Gomphaceae, and close-

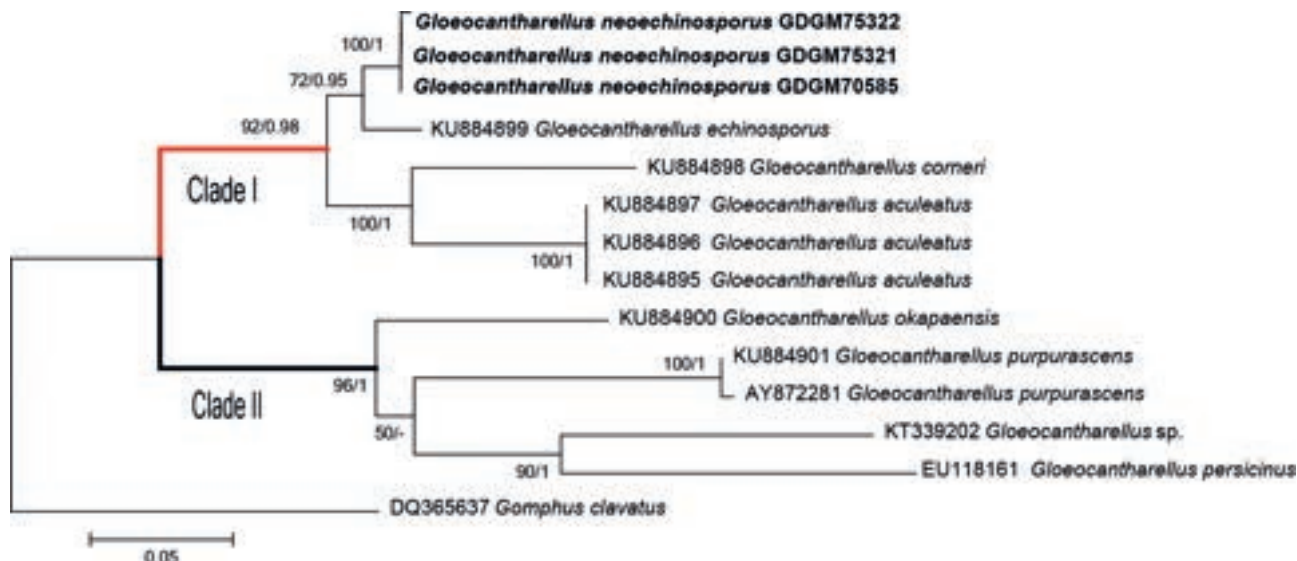


**Fig. 10.** ML phylogenetic tree of *Gloeocantharellus* species reconstructed from ITS sequences. MLBS  $\geq 50$  and BIPP  $\geq 0.9$  are shown above or below the branches.

ly related to *Gomphus* in Phallomycetidae (Giachini 2004, Giachini et al. 2010).

Species of the genus are mainly reported from tropical and subtropical zones of Asia, Australasia, and the Americas; no records are currently known from Europe or Africa (Giachini & Castellano 2011, Linhares et al. 2016). To date, 14 species of *Gloeocantharellus* have been reported worldwide (Giachini 2004, Linhares et al. 2016, Wartchow et al. 2017, Index Fungorum 2019) and only one reliably identified species, *G. persicinus* T.H. Li, Chun Y. Deng & L.M. Wu, has been reported from China (Deng & Li 2008).

Three ITS sequences (MK358819–MK358821) were generated in this study, ten *Gloeocantharellus* were downloaded from NCBI GenBank, and *Gomphus clavatus* (Pers.) Gray was selected as outgroup. The aligned ITS data matrix consisting of 678 nucleotide positions was submitted to Treebase (23924). The phylogenetic trees based on the dataset generated from ML and BI were almost identical, with only minimal differences in support values. The topology from the ML analysis is shown in Fig. 10. This phylogram is similar to the results of Linhares et al. (2016) and displayed that the samples involved in the analysis formed two major clades (clades I and II) but without support. The three collections from southern China formed a monophyletic lineage with high support nested within the well-supported Clade I, and showed close relationships to *G. echinosporus*, *G. corneri* (Singer) Corner, and *G. aculeatus*. Clade II also received high sup-

port and was composed of *G. okapaensis* (Corner) Corner, *G. persicinus*, *G. purpurascens*, and *Gloeocantharellus* sp. (consistent with Linhares et al. 2016). In addition to the ITS sequences, three LSU sequences of the new species generated in this study were deposited to GenBank (MK358814–MK358816).

The annulate remnants of the inner veil on the stipe of the new species are firstly reported in the genus *Gloeocantharellus* and make *G. neoechinosporus* quite distinctive. In addition, the main distinctive features of *G. neoechinosporus* are the pale yellow, orange to orange red pileus, decurrent lamellae without furcation or vein at margin and easily changing to light brown to brown when bruised, the light yellow to orange yellow stipe with a weak annulus at apex, and echinulate basidiospores.

*Gloeocantharellus aculeatus* and *G. echinosporus* are two known species with echinulate basidiospores (Corner 1969, Giachini 2004, Linhares et al. 2016), closely related with *G. neoechinosporus* in morphology and phylogeny. However, *G. aculeatus*, described from Brazil, differs by its dry and orange to salmon pileus, bifurcate and slightly intervenose lamellae and smaller basidiospores (8.5)9–10.5(11)  $\times$  5–6  $\mu\text{m}$  (Linhares et al. 2016). *Gloeocantharellus echinosporus*, described from Singapore, can be separated on account of its orangish to red basidiomata combined with a white, pink to violet hymenium, deeply decurrent and furcated lamellae with slight veins at the edge and unchanging when bruised, a pale white to pale yellow stipe without

annulus, and larger basidia with longer sterigmata up to 10  $\mu\text{m}$  (Corner 1969, Giachini 2004).

Other species in *Gloeocantharellus* with similar pink-orange to red pileus, such as *G. dingleyae* (Segedin) Giachini, *G. novae-zelandiae* (Segedin) Giachini, *G. okapaensis*, and *G. purpurascens*, can be easily distinguished from *G. neoechinosporus* by the verrucose basidiospores.

The only other known species in China, *G. persicinus*, is similar to the new species in some extent. However, it can be distinguished by its light orange to peach pileus, and smaller and verrucose basidiospores 8.5–10  $\times$  4–5.8  $\mu\text{m}$  (Deng & Li 2009). Also, it is positioned within Clade II, whereas *G. neoechinosporus* is placed in Clade I (Fig. 10).

Authors: M. Zhang, Tai-Hui Li, C.Q. Wang & Z.X. Chen

### Ascomycota, Laboulbeniomycetes, Laboulbeniales, Laboulbeniaceae

#### *Laboulbenia bernaliana* Haelew. & Santam, sp. nov.

– Fig. 11

Mycobank no.: MB 832739

Holotypus. – PANAMA. Panamá Province, International Highway 3 km E of Ipell, 3 May 1992, leg. H.P. Stockwell, on *Apenes pallidipes* (Chevrolat, 1835) (Coleoptera, Carabidae, Lebiinae), STOCKWELL STRI-ENT 0 043 489, D. Haelew. 868, deposited at STRI, slide FH00313718 (3 mature thalli from distal third of left elytron; holotype).

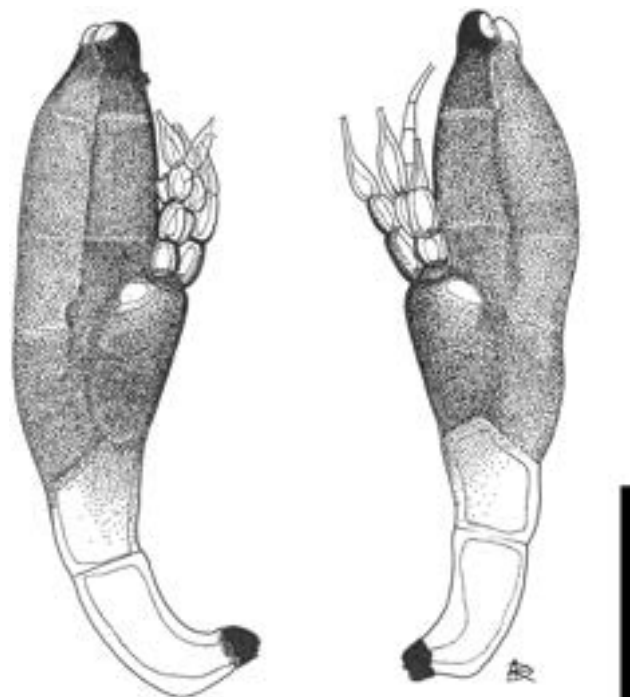


Fig. 11. *Laboulbenia bernaliana*. Two mature thalli from slide FH00313719 (isotype). Scale bar 50  $\mu\text{m}$ , del. A. De Kesel.

Description. – Thallus pale brown, except for the darker foot, perithecial lips, insertion cell, and some parts of the appendage, especially the posterior margins of lower cells of outer appendage. Thallus straight, curved posteriorly at cell I. – Cell I obconical, slightly curved towards posterior at its lower end, 2.6–2.9 $\times$  longer than wide, 37–46  $\times$  13–19  $\mu\text{m}$ . – Cell II stouter, slightly to conspicuously broadening upwards, 23–46  $\times$  17–33  $\mu\text{m}$ ; septum II/VI oblique. – Cells III and IV subequal, 14–23 and 13–20  $\mu\text{m}$  long respectively. – Cell V lens-shaped, in inner-upper corner of cell IV, 7–13  $\times$  4–10  $\mu\text{m}$ . – Insertion cell dark to subopaque, flattened, marking a constriction on the posterior margin of the thallus, situated near the base of the posterior margin of the perithecial wall but separated from it, 3–8  $\times$  10–15  $\mu\text{m}$ . – Inner appendage basal cell 7–9  $\mu\text{m}$  long, rectangular; consisting of several branches divided by successive dichotomies, with lowest cells separated by constricted septa; each branchlet carrying a single flask-shaped and brownish antheridium; antheridia degenerated in older thalli, with supporting branches elongated but not exceeding the perithecial tip, up to 71  $\mu\text{m}$  long. – Outer appendage up to 87  $\mu\text{m}$  long; basal cell 10–14  $\mu\text{m}$  long, unbranched; not exceeding the perithecial tip, with lowest cells rounded distally and separated by black constricted septa. – Cell VI rhomboidal, usually longer than wide, 10–25  $\times$  14–22  $\mu\text{m}$ . – Perithecium asymmetrical, venter inflated, with the posterior margin more convex than the anterior one, 2.4–3.0 $\times$  longer than wide, 67–98  $\times$  67–98  $\mu\text{m}$ , widest around the lower third; perithecial tip slightly asymmetrical, with prominent and rounded posterior lip; preosticular spots blackish, subopaque, the posterior spot occupying most of the respective lips. Total length from foot to perithecial tip 159–212  $\mu\text{m}$ .

Etymology. – In honor of Dr. Juan A. Bernal-Vega (1965–2018), director of Museo de Peces de Agua Dulce e Invertebrados, Universidad Autónoma de Chiriquí—entomologist, collaborator, and friend.

Hosts and distribution. – On species of *Apenes* (Coleoptera, Carabidae, Lebiinae), *Apristus*, and *Philophuga* (Coleoptera, Carabidae, Harpalinae) in Nicaragua and Panama.

Additional material examined. – *Ibid.*, slides D. Haelew. 868b (9 mature thalli from pronotum; isotype at MIUP) and FH00313719 (4 mature thalli from right elytron; isotype); Chiriquí Province, 1 km N of Santa Clara, 1200 m a.s.l., UV light, 24. September 1992, leg. A.R. Gillogly, on *Apenes* sp. 5, STOCKWELL STRI-ENT 0 043 538, D. Haelew. 869, deposited at STRI, slide FH00313720 (1 submature and 2 mature thalli from distal third of elytra; paratype); Veraguas

Province, Alto de Piedra, above Santa Fe, 830 m a.s.l., 28. January 1996, *leg.* H.P. Stockwell, on *Philophuga caerulea* Casey, 1913 [labeled as *Calleida viridis* Chevrolat, 1836] (Coleoptera, Carabidae, Harpalinae), STOCKWELL STRI-ENT 0 043 616, D. Haelew. 874, deposited at STRI, slide FH00313721 (2 mature thalli from left elytron; paratype). NICARAGUA. Estelí Department, Mesas de Moropotente Natural Reserve, 13° 09' 51.7" N, 85° 02' 9" W, 1242 m a.s.l., in pitfall traps, 23–30. August 2007, *leg.* P. Andrés, on *Apristus* sp. (Coleoptera, Carabidae, Harpalinae), slides BCB-SS-E469a, b, c, d (24 juvenile, 2 submature, and 30 mature thalli from elytra, pronotum, legs, antennae, and mouth parts; paratypes).

**Notes.** – *Laboulbenia* species from European Lebiini have had a turbulent taxonomic history, until they were synonymized under the name *L. notiophilii* in Rossi & Santamaría (2006). The same authors preserved the closely related *L. casnoniae* Thaxt. for thalli found on *Colliuris* (Carabidae, Lebiinae) in North America. The most descriptive character to separate both species from each other is the inner appendage. In *L. casnoniae*, its basal cell carries two unbranched appendages that always exceed the perithecial tip in length and each carry a single antheridium at the second cell (Rossi & Santamaría 2006).

For *L. notiophilii*, Rossi & Santamaría (2006) mention the following constant characters: (1) thallus dark pigmented except for cells I and V; (2) cell V located in the upper-inner corner of cell IV; (3) septum IV–V obliquely positioned and straight; (4) outer appendage simple and darker in the lower cells and in their outer margins. In our Panamanian collections of *L. bernaliana*, the thallus is (light-) brown pigmented except for cells I–II and (mostly) V. Cell V is positioned in the upper-inner corner of cell IV and separated from it by an oblique and straight septum. The appendages are short, often with darkened, constricted septa between the cells. The outer appendage is simple, with the basal cell being much larger and bulging at the posterior margin. The inner appendage consists of two dichotomously dividing branches supported by the basal cell, which do not reach the perithecial tip; sometimes a tuft of branchlets is formed. The posterior preostiolar spot occupies most of the respective lips in Panamanian thalli, but this is not the case in the Nicaraguan material.

*Laboulbenia notiophilii* has a broad host spectrum including two distantly related tribes: Notiophilini (subfamily Nebrinae) and Lebiini (subfamily Lebiinae). Within the Lebiini tribe, it is known from 5 subtribes: Cymindiina (*Cymindis*), Demetriadina (*Demetrias*), Dromiusina (*Calodromius*, *Metadromius*, *Paradromius*, *Philorhizus*), Lionychina (*Syntomus*), and Pseudotrechina (*Pseudotrechus*). *Laboulbenia bernaliana* has hosts in 3 differ-

ent subtribes within Lebiini: Apenina (*Apenes*), Calleidina (*Philophuga*), and Dromiusina (*Apristus*). To be complete, the North American *L. casnoniae* is a parasite of *Colliuris* spp., which belong to the tribe Odacanthini of the same subfamily (Lebiinae).

*Authors:* D. Haelewaters & A. De Kesel

### Ascomycota, Laboulbeniomyces, Laboulbeniales, Laboulbeniaceae

*Laboulbenia oioveliicola* Haelew. & Gorczak, **sp. nov.** – Fig. 12

MycoBank no.: MB 821697

**Holotypus.** – BRAZIL. São Paulo State, Biritiba Mirim, Parque Estadual da Serra do Mar, Cachoeira da Pedra Furada, 23°42'16.4"S, 46°02'42.8"W, 725 m a.s.l., on foam masses, 23 August 2014, *leg.* H. Rodrigues, on *Oiovelia machadoi* Rodrigues & Moreira, 2016 (Hemiptera, Veliidae, Veliinae), D. Haelew. 913, deposited at MZUSP, slide D. Haelew. 913d (2 juvenile and 6 mature thalli from right antenna; holotype at INPA).

**Description.** – Cell I and perithecial tip hyaline, the rest of the thallus olivaceous, darkest at cell V and the perithecial venter, which are sub-

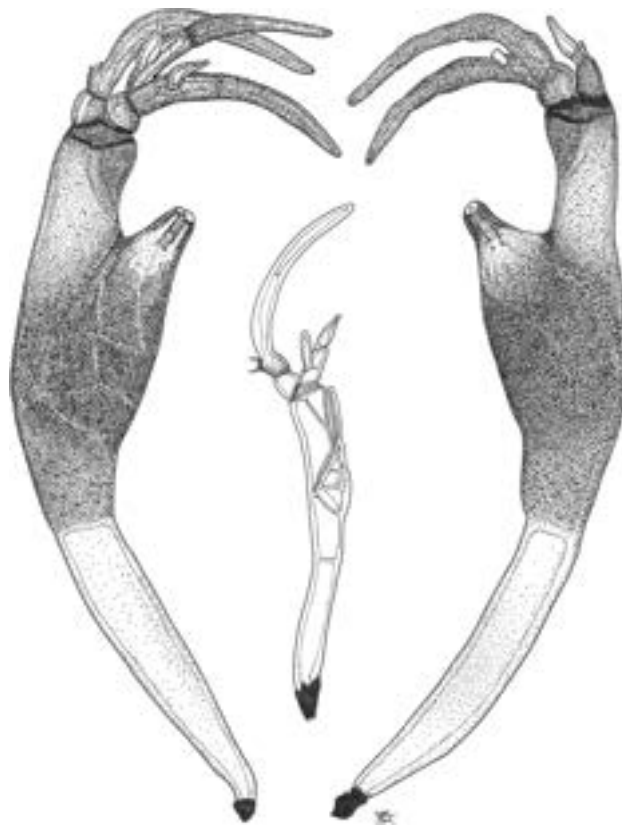


**Fig. 12.** *Laboulbenia oioveliicola*. Two mature thalli from slide FH00313717 (isotype), and juvenile thallus from slide D. Haelew. 913d (holotype). Scale bar 100  $\mu$ m, *del.* A. De Kesel.

paque. Thallus conspicuously curved anteriorly. Outer wall covered with fine, darkened punctures. – Cell I elongated, 39–54 × 25–33 µm. – Cell II stout, broadening upwards, 39–54 × 25–33 µm; septum II/VI very oblique. – Cell III+IV elongated, 81–107 × 21–27 µm, extending above perithecial apex, often sigmoid, its lower half connected to posterior perithecial wall, posterior margin straight or concave. – Cell V triangular and bent anteriorly, 20–26 × 11–18 µm, in the inner-upper corner of cell IV. – Inner appendage up to 67–107 µm long; basal cell hyaline to brown, broadly isodiametric, rounded, bearing two branches bending anteriorly, each consisting of two darkened elongated cells, the first of which carries a single antheridium at the posterior side. – Antheridia pale brown, flask shaped, 14–19 × 4–5 µm. – Outer appendage two-celled, 60–106 µm long, basal cell similar to but less bloated than basal cell of inner appendage, bearing a single, elongated branchlet, similar to the two-celled branches of inner appendage, also bending anteriorly, and carrying externally at the base another cell, which was always broken off, even in developing thalli. – Cell VI very small, inconspicuous, lens-shaped, only visible in young thalli. – Perithecium asymmetrical, with the anterior margin straight or slightly convex and the posterior margin strongly convex, 2.5× longer than wide, 78–90 × 28–36 µm, widest below the middle; outer wall cells unequal, twisted spirally upwards; preostiole spots reduced to conspicuous striae at the septa between the wall cells of the upper tier; perithecial tip symmetrical, rounded, often bearing a minute hyaline tooth. Total length from foot to perithecial tip 262–307 µm.

**Etymology.** – Referring to the host genus, *Oiovelia*, on which the fungus was found.

**Hosts and distribution.** – Only known from *Oiovelia machadoi* in the state of São Paulo, Brazil.

**Additional material examined.** – *Ibid.*, slides FH00313716 (2 mature thalli from right antenna; isotype), FH00313717 (2 mature thalli from right antenna; ISOTYPE), and D. Haelew. 913c (1 mature thallus from right eye; isotype at INPA); *Ibid.*, on *O. machadoi*, D. Haelew. 942, deposited at MZUSP, slide D. Haelew. 942a (1 submature thallus from left antenna; paratype at INPA). Ex-paratype sequences: MF314142 (LSU, isolate D. Haelew. 942b, 3 juvenile and 5 mature thalli from antennae).

**Notes.** – True bugs are parasitized by species belonging to different genera of Laboulbeniales depending on their lifestyle (Santamaría 2008). Twenty-two species of *Coreomyces* Thaxt. are found on aquatic bugs; on terrestrial bugs four monotypic genera are known to occur: *Corethromyces* Thaxt.,

*Cupulomyces* R.K. Benj., *Majewskia* Y.B. Lee & K. Sugiy., and *Polyandromyces* Thaxt. There are many Laboulbeniales on semiaquatic bugs; these have been studied in depth by the late Dr. Richard K. Benjamin. The following genera are known to occur on semiaquatic bugs: *Autophagomyces* Thaxt. (1 species), *Laboulbenia* (11 species), *Monandromyces* R.K. Benj. (11 species), *Prolixandromyces* R.K. Benj. (6 species), *Rhizopodomomyces* Thaxt. (7 species), *Tavaresiella* T. Majewski (4 species) and *Triceromyces* T. Majewski (11 species).

There are 633 species in the genus *Laboulbenia*, of which 40 have been described since 2010 alone (Haelewaters et al. 2017, Rossi & Leonardi 2018, Rossi et al. 2019, present paper). Thus far, 11 *Laboulbenia* species have been found on semiaquatic Hemiptera, suborder Heteroptera (Thaxter 1912, Poisson 1954, Benjamin 1967). These are: *L. drakei* R.K. Benj. from *Rhagovelina* (Veliidae) in Panama, *L. hemipteralis* Thaxt. from *Velia* (Veliidae) in Argentina, *L. leechii* R.K. Benj. from *Microvelia* (Veliidae) in Mexico and the USA, *L. macroveliae* R.K. Benj. from *Macrovelia* (Macroveliidae) in the USA, *L. microveliae* R.K. Benj. from *Microvelia* (Veliidae) in Mexico and the USA, *L. rhagoveliae* R.K. Benj. from *Rhagovelina* (Veliidae) in Mexico and Panama, *L. titschackii* Poisson, nom. inval., from *Velia* (Veliidae) in Peru, *L. truxalii* R.K. Benj. from *Rhagovelina* (Veliidae) in Mexico, *L. uhleri* R.K. Benj. from *Macrovelia* (Macroveliidae) in the USA, *L. usingeri* R.K. Benj. from *Rhagovelina* (Veliidae) in Panama, and *L. veliae* Thaxt. from *Velia* (Veliidae) in Argentina.

With this new species, the number of *Laboulbenia* species on Hemiptera is raised to 12. *Laboulbenia oioveliicola* differs from the other species by the enlarged cells III+IV. Because of this enlargement, cell V, the insertion cell, and the appendages are positioned above the perithecial apex. The insertion cell of all 11 *Laboulbenia* species is disconnected from the perithecium. In *L. hemipteralis*, the androstichum (cells III, IV, and V) looks “normal,” with cell III carrying both cells IV and V, which are equally high. In the other species, the distal part of cell V grows in between the insertion cell and the posterior side of the perithecium, apparently pushing the perithecium anteriorly. In some species (e.g., *L. microveliae*, *L. truxalii*) this feature is more pronounced than in others (*L. veliae*). Also in *L. oioveliicola*, the perithecium is directed anteriorly, because of the unusual development of cell IV. Of the *Laboulbenia* species occurring on semiaquatic Hemiptera, also *L. hemipteralis*, *L. microveliae*, *L. uhleri*, and *L. veliae* have spiraled perithecial cell walls. Only in *L. microveliae*, cells III and IV are

replaced by a single cell, as is the case in *L. oioveliicola*. However, *L. microveliae* is different in other aspects: the habitus is much more compact, cell III+IV is not unusually high, its perithecium is strongly ovoid with an asymmetrical tip, and the appendages are differently structured.

Most species in the genus *Laboulbenia* have a typically 5-celled receptacle (I-V), but some species have undivided cells III+IV or III+IV+V (especially species associated with Chrysomelidae and Curculionidae; Rossi et al. 2015, 2016). In Tab. 2, we listed all known *Laboulbenia* species with an undivided cell III+IV like in *L. oioveliicola*. Their hosts belong to three orders and seven families: Coleoptera (Cleridae, Chrysomelidae); Diptera (Chloropidae, Diopsidae, Lauxaniidae, Richardiidae); and Heteroptera (Veliidae). Within the Chrysomelidae, representatives of multiple tribes are known to host species of *Laboulbenia* with a cell III+IV: Alticini, Luperini, Metacyclini (subfamily Galerucinae), and Eumolpini (subfamily Eumolpinae). This diversity in host usage leads us to hypothesize that the development of an undivided cell III+IV has happened

independently on multiple occasions. This implies that this character is not probably suitable to define groups or sections of *Laboulbenia*. It also hints at developmental plasticity in the genus.

We generated a 468-bp LSU sequence from isolate D. Haelew. 942b. Using the BLASTn tool we found *L. stilicicola* Speg. (isolate D. Haelew. 1467a, GenBank accession number MN394856) to be the closest match with 86.08 % similarity, followed by *L. flagellata* Peyr. (D. Haelew. 1457a, MN394851) with 85.63 % similarity (Haelewaters et al. 2019a). All matches with *Laboulbenia* isolates were between 82 and 86 % similarity. With this evolutionary divergence, one might argue that *L. oioveliicola* is a representative of another, undescribed genus. However, more *Laboulbenia* species with undivided cells III+IV and III+IV+V should be sequenced and compared against *L. oioveliicola* before making such a taxonomic decision.

All studied thalli were positioned on the antennae, except one that was located on the right eye (slide D. Haelew. 913c). The morphology of this specimen differs from the other thalli. Because only

**Tab. 2.** Overview of *Laboulbenia* species with undivided cells III+IV, along with their hosts (genus level) and host classification.

<i>Laboulbenia</i> species	Host(s)	Host classification
<i>L. apotropinae</i> W. Rossi & Ponziani 2008	<i>Apotropina</i>	Diptera, Chloropidae
<i>L. arietina</i> Thaxt. 1914	<i>Disonycha</i>	Chrysomelidae, Galerucinae, Alticini
<i>L. calcarata</i> W. Rossi et al. 2016	Metacyclini undet.	Chrysomelidae, Galerucinae, Metacyclini
<i>L. diabroticae</i> Thaxt. 1914	<i>Diabrotica</i>	Chrysomelidae, Galerucinae, Luperini
<i>L. crispata</i> Thaxt. 1917	<i>Hippelates</i>	Diptera, Chloropidae
<i>L. cristatella</i> Thaxt. 1914	<i>Altica</i> , <i>Asphaera</i> , <i>Lactica</i>	Chrysomelidae, Galerucinae, Alticini
<i>L. drakei</i> R.K. Benj. 1967	<i>Rhagovelia</i>	Heteroptera, Veliidae, Rhagoveliinae
<i>L. flabelliformis</i> K. Sugiy. & T. Majewski 1987	Alticini sp. indet., <i>Asphaera</i> <sup>a</sup>	Chrysomelidae, Galerucinae, Alticini
<i>L. funebris</i> Thaxt. 1914	<i>Altica</i>	Chrysomelidae, Galerucinae, Alticini
<i>L. gratiellae</i> W. Rossi 1987	<i>Teleopsis</i>	Diptera, Diopsidae
<i>L. lacticae</i> Thaxt. 1912 <sup>b</sup>	<i>Lactica</i>	Chrysomelidae, Galerucinae, Alticini
<i>L. maecolaspidis</i> W. Rossi & Cesari 1979	<i>Colaspis</i>	Chrysomelidae, Eumolpinae, Eumolpini
<i>L. muscaria</i> Thaxt. 1917	<i>Sapromyza</i>	Diptera, Lauxaniidae
<i>L. oioveliicola</i> sp. nov.	<i>Oiovelia</i>	Heteroptera, Veliidae, Veliinae
<i>L. opima</i> W. Rossi 2011	<i>Chrysodinopsis</i>	Chrysomelidae, Eumolpinae, Eumolpini
<i>L. parasyphraeae</i> W. Rossi & Bergonzo 2008	<i>Parasyphraea</i>	Chrysomelidae, Galerucinae, Alticini
<i>L. percolaspis</i> A. Weir & W. Rossi 2001	<i>Percolaspis</i>	Chrysomelidae, Eumolpinae, Eumolpini
<i>L. richardiana</i> W. Rossi & Kotrba 2004	<i>Richardia</i>	Diptera, Richardiidae
<i>L. sapromyzae</i> Thaxt. 1917	<i>Sapromyza</i>	Diptera, Lauxaniidae
<i>L. sima</i> W. Rossi et al. 2016	<i>Phyllotrupes</i>	Chrysomelidae, Galerucinae, Alticini
<i>L. tapiae</i> W. Rossi 2011	<i>Priocera</i>	Cleridae, Clerinae
<i>L. truxalii</i> R.K. Benj. 1967	<i>Rhagovelia</i>	Heteroptera, Veliidae, Rhagoveliinae
<i>L. yasuniensis</i> W. Rossi et al. 2016	Percolaspis	Chrysomelidae, Eumolpinae, Eumolpini

<sup>a</sup> *Asphaera* is the host genus as identified in Haelewaters et al. (2017): *Asphaera transversofasciata* in Panama, *A. nobilitata* in Trinidad.

<sup>b</sup> This was a single report from El Salvador, presented by Weir and Beakes (1996). However, the fungus was probably incorrectly identified, because *L. lacticae*, following the original description in Thaxter (1912), has discrete cells III and IV.

one morphologically distinct thallus was available for study, we could not isolate DNA from it. Considering that several species exhibit position-induced morphological plasticity (Santamaría & Faille 2009, Goldmann et al. 2013, Haelewaters & Pfister 2019), it is possible that *L. oioveliicola* is polymorphic. When more material can be collected for study, this variation might be added to the molecular data. What follows is the description of the single thallus removed from the right eye.

**Description of D. Haelew. 913c.** – Cells I and II hyaline, except from brown region around septum I/II, appendages hyaline, the rest of the thallus brown, cell VI and the perithecial venter (sub-)opaque. Cells I and II forming a slender, posteriorly curved stalked. – Cell I elongated,  $80 \times 18 \mu\text{m}$ . – Cell II similar to cell I, making a strong constriction at its distal end,  $82 \times 16 \mu\text{m}$ ; septum II/VI very oblique. – Cell III higher than broad,  $18 \times 15 \mu\text{m}$ . – Cell IV pentagonal, broader than high,  $16 \times 20 \mu\text{m}$ . – Cell V subtrapezoidal, positioned on top of cell IV, its distal margin free in between the posterior margin of the perithecium and the insertion cell,  $19 \times 14 \mu\text{m}$ . – Insertion cell narrow, opaque, placed very obliquely. – Inner appendage consisting of a basal cell, higher than broad, widening downwards, carrying a single elongated antheridium. – Outer appendage consisting of a single branchlet,  $110 \mu\text{m}$  in length; basal cell rectangular, higher than broad; the next two cells gradually smaller; the last cell elongated and curved towards anterior; septa between all cells of the outer appendage darkened. – Cell VI broader than long, very oblique. – Perithecium asymmetrical, the anterior margin marked with clear indentations between different tiers,  $89 \times 26 \mu\text{m}$ ; strongly tapering to the clearly delimited apex, with its parallel walls; perithecial tip asymmetrical, higher at the posterior side, bearing a minute hyaline tooth. Total length from foot to perithecial tip  $239 \mu\text{m}$ .

**Notes.** – The structure of the androstichum in this thallus is similar to the arrangement in *Laboulbenia leechii*, *L. macroveliae*, *L. rhagoveliae*, *L. uhlerii*, and *L. usingerii*. In these species, cells III, IV, and V are also placed on top of each other. Only *L. usingerii* has a slender habitus with elongated cells I and II, like the thallus in slide D. Haelew. 913c. This species, however, is different in its appendage structure and in its perithecial apex, which is blackish at the posterior side (Benjamin 1967). Interestingly, the thallus in slide D. Haelew. 913c and *L. usingerii* were both found on the eyes of their hosts. *Laboulbenia usingerii* occurs on *Rhagovelia* sp. On

one of the host specimens, two other species were removed (Benjamin 1967): *L. drakei* from the posterior legs and *L. rhagoveliae* from the antennae, anterior legs, and sternites. It could be that these represent three morphotypes of the same phylogenetic species.

**Authors:** D. Haelewaters & A. De Kesel

### Ascomycota, Laboulbeniomyces, Laboulbeniales, Laboulbeniaceae

***Laboulbenia termiticola* De Kesel & Haelew., sp. nov.** – Fig. 13

MycoBank no.: MB 832740

**Holotypus.** – DEMOCRATIC REPUBLIC OF THE CONGO. Katanga Province, near Kisangwe, Mikembo sanctuary,  $11^{\circ}28'24.3''\text{S}$ ,  $27^{\circ}39'51.8''\text{E}$ , 1082 m a.s.l., in *Julbernardia-Brachystegia* miombo forest, in rotten tree trunks, 26 January 2018, leg. A. De Kesel, on *Macrotermes subhyalinus* (Rambur 1842) (Blattodea, Termitidae, Macrotermitinae), ADK 6319, deposited at BR, slide BR5020195003490V (1 juvenile and 6 mature thalli from cephalon and legs; holotype).

**Description.** – Lower third of cell I, perithecial apex, and appendages hyaline, the rest of the thallus brown; darkening with age, darkest at cell II and the perithecium. – Cell I elongated, straight or curved near the foot,  $106\text{--}149 \times 19\text{--}28 \mu\text{m}$ ; sometimes conspicuously wider at its apex. – Cell II usually in line with cell I, cylindrical, with parallel margins,  $108\text{--}170 \times 15\text{--}26 \mu\text{m}$ , up to  $10\times$  longer than wide. – Cells III and VI side by side, of similar size and shape, rectangular,  $27\text{--}42 \times 8\text{--}15 \mu\text{m}$ . – Cell IV similar to cell III but shorter,  $19\text{--}27 \times 7\text{--}14 \mu\text{m}$ . – Cell V rounded, in inner-upper corner of cell IV,  $6\text{--}8 \times 5\text{--}8 \mu\text{m}$ . – Insertion cell opaque, flattened, sometimes but not always marking a constriction on the posterior margin of the thallus; attached to the lower third of the posterior margin of the perithecial wall,  $12\text{--}16 \mu\text{m}$  wide. – Inner appendage basal cell  $7\text{--}13 \mu\text{m}$  long; composed of 8 similar branches resulting from successive dichotomies starting at the basal cell; cells gradually longer and narrower towards the distal end, branches exceeding perithecial tip,  $81\text{--}138 \mu\text{m}$  long. – Antheridia short, flask-shaped; arising laterally from suprabasal or third cells. – Outer appendage  $82\text{--}133 \mu\text{m}$  long; similar to inner appendage but basal cell  $9\text{--}15 \mu\text{m}$  long and lowermost 2–3 tiers of cells tinged with yellowish-brown. – Perithecium slightly asymmetrical, ellipsoid, anterior and posterior margins equally convex or the anterior margin more convex than the posterior one,  $2.5\text{--}3.1\times$  longer than wide,  $55\text{--}91 \times 20\text{--}34 \mu\text{m}$ , widest in the middle to its upper third; perithecial



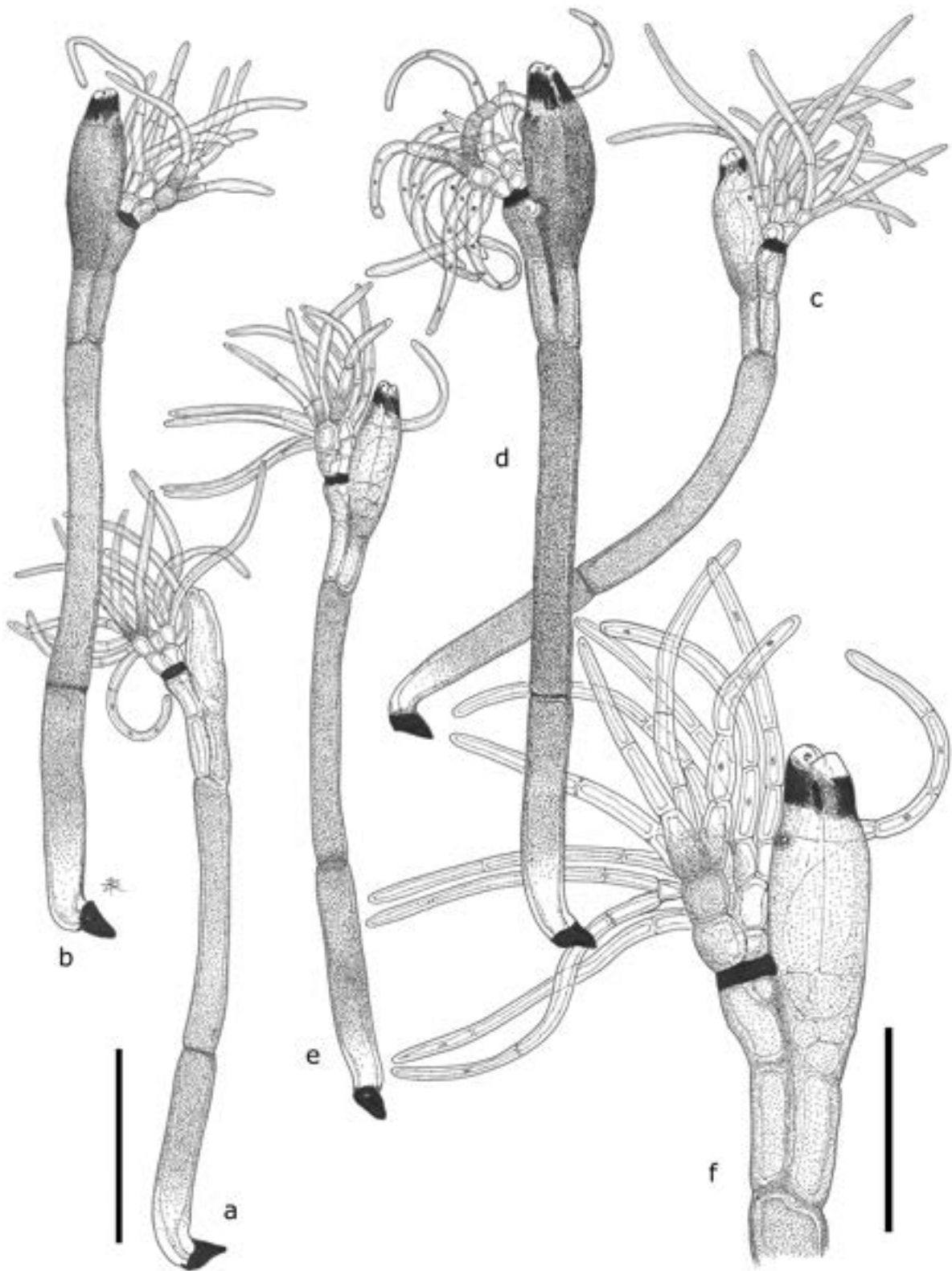


**Fig. 13.** *Laboulbenia termicola*. **a–d.** Mature thalli from legs. **e–f.** Mature thallus from cephalon, with detail of perithecium and branching pattern of appendages. All thalli from slide BR5020195003490V (holotype). Scale bars a–e 100 µm, f 50 µm, *del.* A. De Kesel.

tip asymmetrical, with prominent and rounded posterior lip; preostiole spots black, opaque, the posterior spot occupying most of the respective lips, both merging into a preapical ring in older individuals. Total length from foot to perithecial tip 323–446  $\mu\text{m}$ . – Ascospores two-celled, hyaline, 45–55(62)  $\mu\text{m}$  long.

**Etymology.** – From Latin, referring to the host, a species of termite.

**Hosts and distribution.** – On *Macrotermes subhyalinus* in the DR Congo.

**Additional material examined.** – DEMOCRATIC REPUBLIC OF THE CONGO. Katanga Province, near Kisangwe, Mikembo sanctuary, 11°29'10.2"S, 27°39'11.7"E, in *Julbernardia-Brachystegia* miombo forest, 18 January 2015, leg. A. De Kesel, on *M. subhyalinus*, ADK 6246, deposited at BR, slides BR5020195001434V (2 mature thalli from cephalon; paratype) and BR5020195000406V (1 mature thallus from cephalon; paratype); *Ibid.*, on *M. subhyalinus*, ADK 6486, deposited at BR, slide BR5020195002462V (1 juvenile and 4 mature thalli from cephalon; paratype).

**Notes.** – Soldier and worker termites were collected from rotting logs, not from the nests and only during the rainy season. Thalli of *L. termiticola* occur either pairwise or isolated, always in few numbers per host. We found *L. termiticola* mostly on soldier's cephalon and abdomen; workers seem very rarely infected. The morphology of thalli from soldiers is relatively stable, and independent from the growth position on the host. Old thalli are very darkened towards entirely black and tend to break off above septum I/II, leaving behind only blackish pin-like remains on the host's integument.

Thus far, seven species of *Laboulbenia* are described from termites: *Laboulbenia antemnalis* W. Rossi & M. Leonard from *Macrotermes bellicosus* in Sierra Leone, *L. brignolii* W. Rossi & M. Blackw. on *Macrotermes herus* in Ethiopia, *L. buccalis* from *Amitermes evuncifer* in Sierra Leone, *L. feliciscaprae* W. Rossi on *Anacanthotermes ochraceus* in Libya, *L. geminata* Buchli ex W. Rossi & M. Blackw. on *Odontotermes* spp. in Ethiopia and Kenya, *L. ghanaensis* W. Rossi & M. Blackw. on *A. evuncifer* in Ghana, and *L. hagenii* Thaxt. on *Macrotermes michaelseni* [as *Termes bellicosus* var. *mossambicus*] in Mozambique (Thaxter 1895, 1896; Buchli 1966; Rossi 1974; Rossi & Blackwell 1986; Rossi & Leonardi 2018). Those species are all recognized by their small size. For example, *L. ghanaensis* is among the smallest species in the order – measuring ~70  $\mu\text{m}$  from foot to perithecial tip. In contrast, the habitus of the new species is filiform; thalli are several 100s of  $\mu\text{m}$  in length and look like blackish filiform structures on the integument.

**Authors:** D. Haelewaters & A. De Kesel

## Basidiomycota, Agaricomycetes, Agaricales, Pluteaceae

***Pluteus cutefractus*** Ferisin, Dovana & Justo, sp. nov. – Figs. 14–15

Mycobank no.: MB 823569

**Diagnosis.** – Basidiomata with a markedly cracked pileipellis, globose to broadly ellipsoid basidiospores, predominantly ovoid to broadly clavate cheilocystidia and pleurocystidia, trichohyphenoid pileipellis consisting of broadly utriform and fusiform elements.

**Holotypus.** – SLOVENIA. Nova Gorica, Panovec Park, on buried twigs of broadleaved trees, in wet shady places, 8 July 2017, leg. G. Ferisin & L. Pelizzari (MCVE 30110; holotype). Sequences ex-holotype: MN264751 (ITS).



**Fig. 14.** Basidiomata of *Pluteus cutefractus*, MCVE 30110 (holotype).

**Description.** – Pileus 20–25 mm in diam., plano-concave to concave, straight margin sometimes reflexed, not hygrophanous, very dark brown in center, pallescent towards margin to light brown, in center venulose or smooth, cuticle cracked, markedly so in older specimens, showing whitish flesh underneath. – Lamellae free, moderately crowded, slightly ventricose, up to 4 mm broad, first whitish later pink with flocculose edge. – Stipe 35–50  $\times$  4–5 mm, cylindrical, not bulbous, pubescent, white all over. – Smell and taste not distinctive. – Context white. – Basidiospores [70, 4, 2], (4.9)4.9–6.0–7.1(7.2)  $\times$  (4.2)5.0–5.4–5.8(6.3)  $\mu\text{m}$  Q= (1.00)1.04–1.12–1.20(1.33); globose to broadly ellipsoid, thick-walled, non-amyloid, cyanophilous. – Basidia 21–26  $\times$  8–10  $\mu\text{m}$ , clavate, 4-spored. – Pleurocystidia 40–55  $\times$  20–25  $\mu\text{m}$ , scattered, thin-walled; shape variable from ovoid to broadly clavate, hyaline. – Cheilocystidia 26–76  $\times$  12–26  $\mu\text{m}$ , abundant, hyaline; variable in shape from

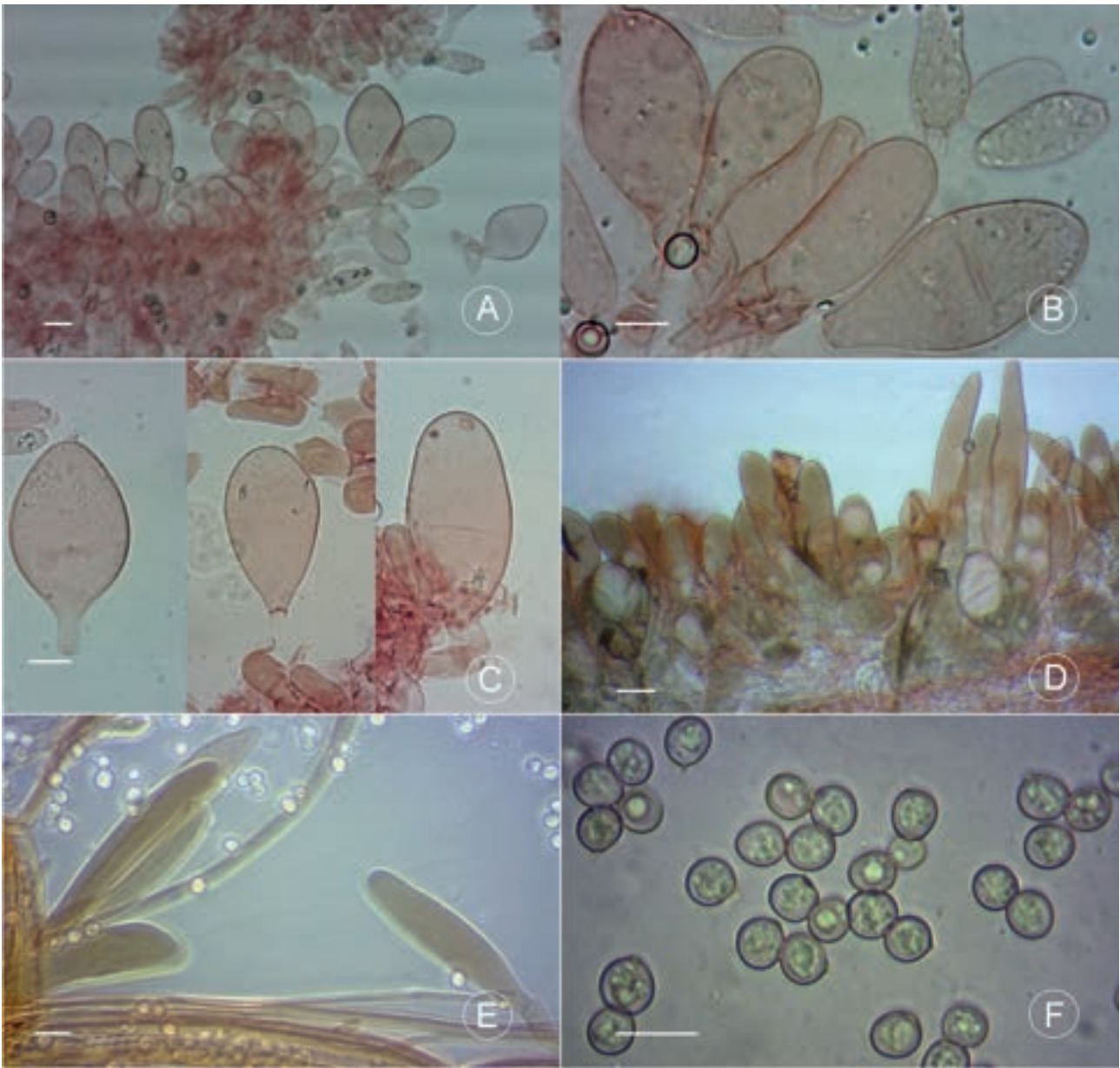


**Fig. 15.** *Pluteus cutefractus*, MCVE 30110 (holotype). **A, B.** Cheilocystidia. **C.** Pleurocystidia. **D.** Pileipellis. **E.** Caulocystidia. **F.** Basidiospores. Scale bars 10  $\mu$ m.

ovoid, clavate to broadly clavate, so numerous as to make the lamellar edge sterile. – Pileipellis a trichohymeniderm made up of broadly utriform ( $45\text{--}60 \times 20\text{--}30 \mu\text{m}$ ) and fusiform ( $100\text{--}135 \times 11\text{--}15 \mu\text{m}$ ) elements, pigment intracellular, vacuolar, light brown or brown. – Stipitipellis a cutis of light brown hyphae,  $4\text{--}10 \mu\text{m}$  wide. – Caulocystidia present, descending to about 1/3 of length of stipe,  $40\text{--}60 \times 12\text{--}18 \mu\text{m}$ , variable in shape from clavate to fusiform, sometimes filled with evenly

dissolved brownish intracellular pigment. – Clamp connections absent in all tissues.

**Etymology.** – From Latin, ‘cutis’ = skin and ‘fractus’ = broken.

**Habit and distribution.** – In groups, on underground twigs of broadleaved trees, during summer. Thus far only known from Slovenia.

**Additional material examined.** – SLOVENIA. Nova Gorica, Panovec Park, on buried twigs of broadleaved trees, 8 July 2017, leg. G. Ferisin (MCVE 30111).

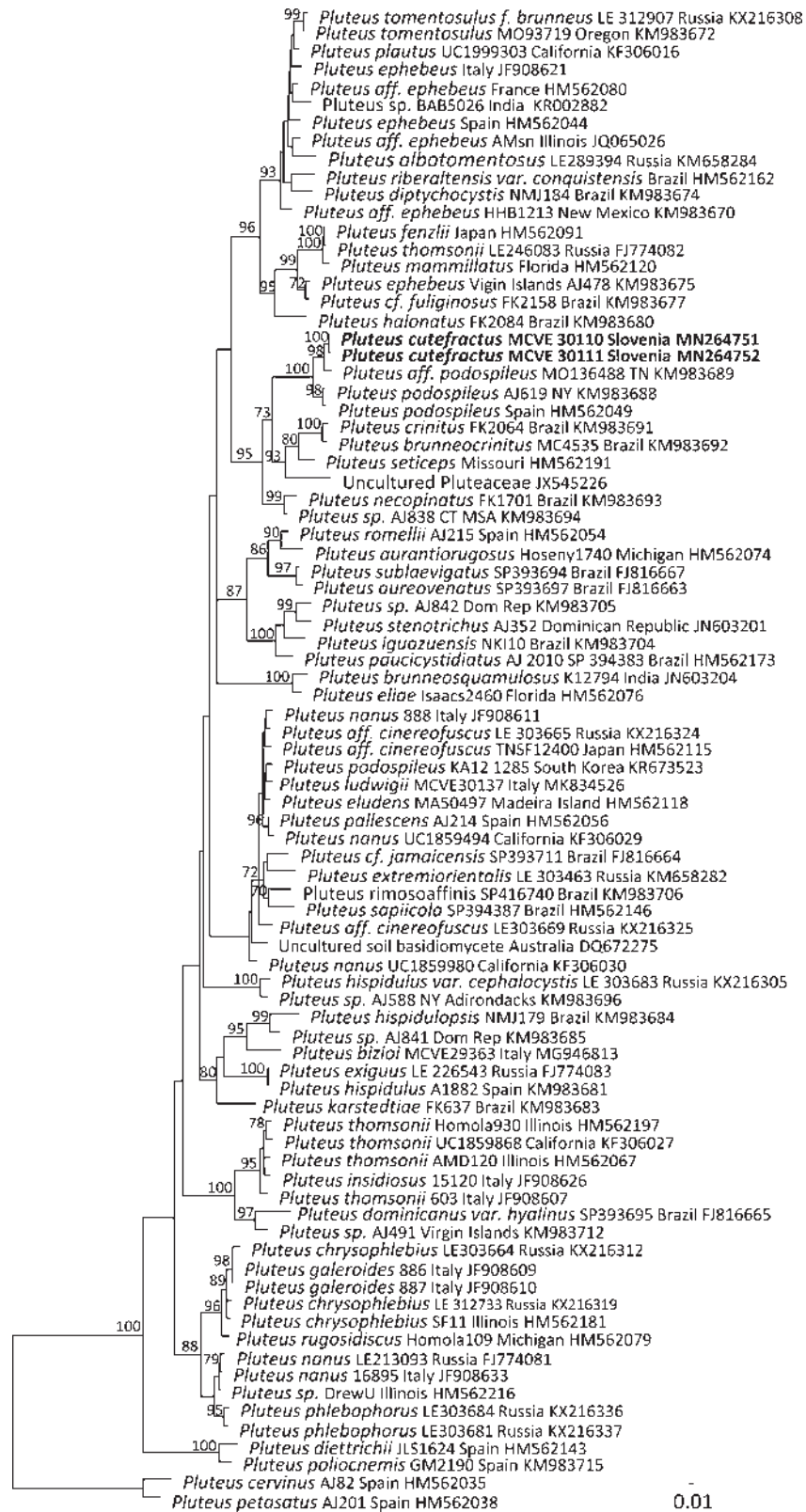


**Fig. 16.** Maximum likelihood tree obtained from an ITS dataset of *Pluteus* sect. *Celluloderma*. MLBS  $\geq 70$  are presented above clade branches. Newly sequenced collections are highlighted in boldface.

Notes. – *Pluteus cutefractus* appears in our phylogenetic reconstruction (Fig. 16) within the *podospileus* clade in *Pluteus* sect. *Celluloderma*, together with *P. brunneocrinitus* Menolli, Justo & Capelari, *P. crinitus* Menolli, Justo & Capelari, *P. necopinatus* Menolli, Justo & Capelari, *P. podospileus* Sacc. & Cub, *P. seticeps* (G.F. Atk.) Singer, and several unnamed and/or undescribed taxa. *Pluteus brunneocrinitus* differs in its darker colors of the pileus; less cracked pileipellis; absence of pleurocystidia; and pigmented cheilocystidia, which are narrowly clavate (Menolli et al. 2015). *Pluteus crinitus* and *P. necopinatus* both have similar pileus color to *P. cutefractus*, and a markedly cracked pileipellis, but both of them differ from the new species in the absence of pleurocystidia (Menolli et al. 2015). Additionally, *P. crinitus* has a heterogeneous lamellar edge, with cheilocystidia intermixed with basidia, and *P. necopinatus* has broadly lageniform or narrowly utriform cheilocystidia (Menolli et al. 2015). All three species are only known from Brazil. *Pluteus seticeps*, a North American species, has a smooth to minutely granulose pileus surface and lacks pleurocystidia (Minnis & Sundberg 2010). *Pluteus podospileus* has a smoother pileus surface, not so markedly cracked, and pleuro- and cheilocystidia that are mostly narrowly utriform, broadly fusiform or narrowly clavate (Vellinga 1990, Takehashi & Kasuya 2009).

Authors: G. Ferisin, F. Dovana & A. Justo

### Glomeromycota, Glomeromycetes, Glomerales, Glomeraceae

***Rhizoglo-mus variabile*** Corazon-Guivin, Oehl & G.A. Silva, sp. nov. – Fig. 17  
MycoBank no.: MB 832472

Diagnosis. – Different from *Rhizoglo-mus antarcticum* by more variable spore sizes and thinner spore wall, especially of the structural laminated wall layer.

Holotypus. – PERU. San Martín State, Lamas Province, Palmiche, 06°20'02.40"S, 76°36'00.00"W, 462 m a.s.l., 25 August 2016, leg. M. Anderson Corazon-Guivin, (ZT Myc 60391; holotype). Derived from a single species culture established on hosts plants *Sorghum vulgare*, alfalfa, *Brachiaria* sp. and the Inca nut in the greenhouse of the Molecular Biology and Genetics Laboratory, Faculty of Agricultural Sciences, National University of San Martín-Tarapoto, Perú. Original soil, from the rhizosphere of the Inca nut.

Description. – Spores formed terminally on subtending hyphae (SH) either singly or, preferably, in small spore clusters, with 2–50 and possibly also more spores per cluster; golden yellow-brown to yellow brown, globose to subglobose to rarely oblong or irregular, (30)70–185 × (30)65–160 µm. –

Spore wall three layered. Outer layer (SWL1) hyaline, evanescent, 0.8–1.5 µm thick. Second layer (SWL2) structural, persistent, laminate, golden-yellow to bright yellow brown, 1.6–2.6(3.2) µm thick. Innermost layer (SWL3) flexible, light-yellow to bright yellow, 1.1–2.0 µm thick, usually tightly adherent to SWL3, sometimes separating or showing a few folds in crushed spores. In Melzer's reagent, SWL2 staining pinkish purple to purple. – Subtending hyphae (SH) of spores cylindrical to slightly funnel-shaped, sometimes recurved, (6)9.0–15.5(18) µm broad and 12–200 µm long, and without introverted wall thickening toward the spore base. Base generally not closed by a septum, but open. Such septa observable in 8–25 µm distance from the spore bases, these being 8–15 µm thick, golden yellow to bright yellow brown. SH layers continuous with the SW layers and in total 2.5–3.6 µm thick usually tapering to 0.5–1.5 µm towards the mycelia hyphae. Mycelia hyphae hyaline, 7–14 µm thick and with 1–2 hyphal wall layers. Mycelial hyphae staining pinkish to purple in Melzer's reagent. – Vesicular-arbuscular mycorrhiza formation with *Sorghum* sp., *Brachiaria* sp. and Inca nut as plant hosts in pot cultures. Mycorrhizal structures consisting of arbuscules, vesicles, and intra- and extraradical hyphae and staining dark blue in 0.05 % trypan blue or with ink (Vierheilig et al. 1998).

Etymology. – Referring to the extremely variable spore sizes, which had not been recognized before in such dimensions within the genus *Rhizoglo-mus*.

Habitat and distribution. – Only known from its type location in Lamas, San Martín State in Peru, from an Inca nut plantation in Palmiche, where Inca nut is cultured in agroforestry systems together with *Zea mays* and *Phaseolus vulgaris*.

Additional material examined. – PERU. San Martín State, Lamas Province, Palmiche, 06°20'02.40" S, 76°36'00.00" W, 462 m a.s.l., 25 August 2016, leg. M. Anderson Corazon-Guivin, (ZT Myc 60392, isotype).

Notes. – The new AM fungus *Rhizoglo-mus variabile* can be distinguished from all other *Rhizoglo-mus* spp. by the combination of spore size, color, and spore wall structure, but most importantly especially by the highly variable spore sizes, which in such an extent is only known from *Funneliformis mosseae* and *Glomus mertonii* (Gerdemann & Trappe 1974, Bentivenga & Hetrick 1991). It forms a triple-layered spore wall including an innermost flexible layer, such as known for *Rhizoglo-mus antarcticum*, *R. clarum*, *R. fasciculatum*, and *R. manihotis*, which

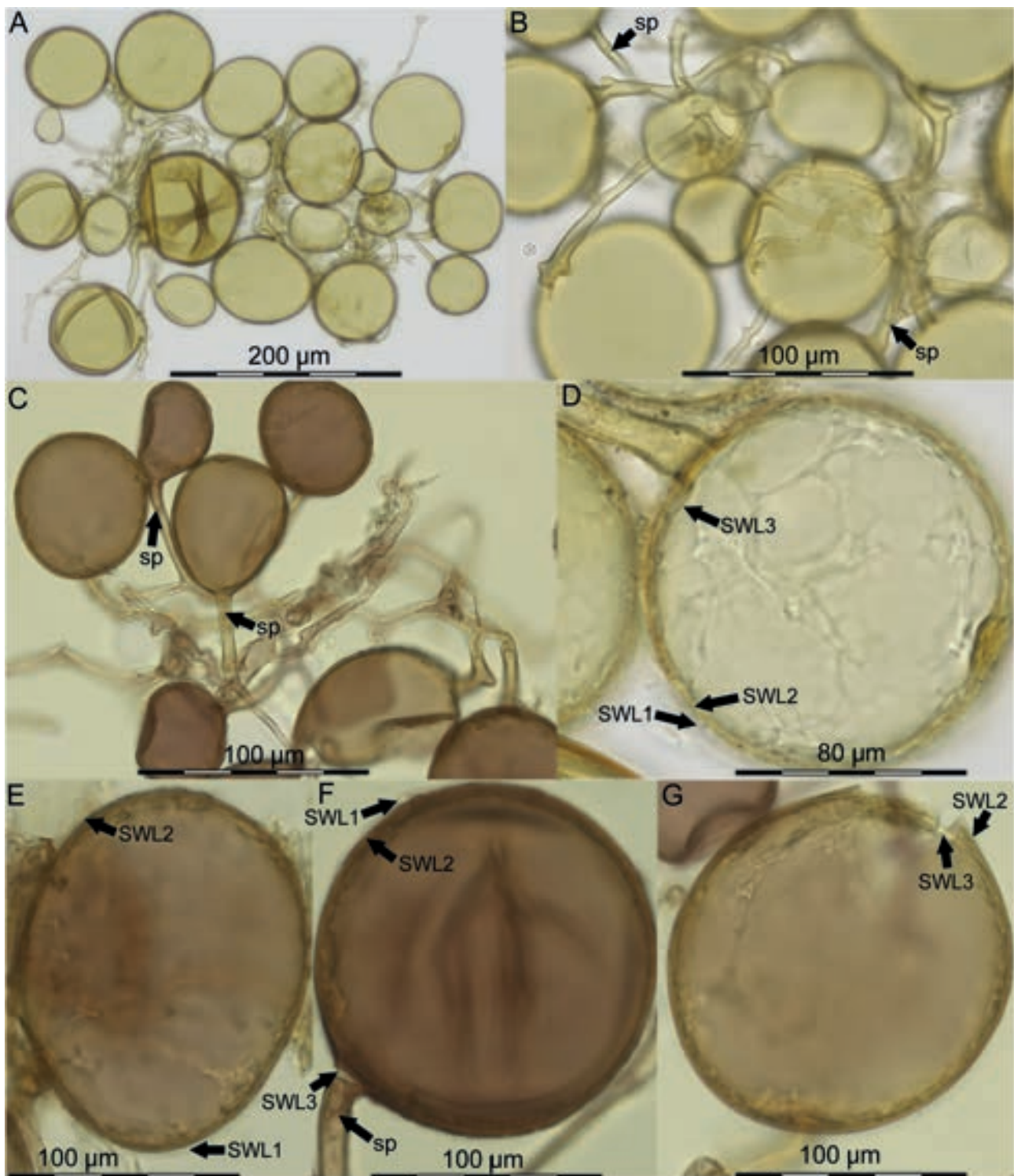


**Fig. 17.** *Rhizoglosum variabile*. **A–B.** Spore clusters in PVLG with spores of very variable sizes. **C.** Spore cluster fragment in PVLG & Melzer's reagent. Pigmented spores and subtending hyphae as well as the hyaline mycelia hyphae stain pinkish purple to purple. **D.** Spore in PVLG with three layers (SWL1, 2, 3) and a slightly funnel-shaped subtending hypha. **E–G.** Spores in PVLG & Melzer's reagent. Hyaline outer and inner layers SWL1 and SWL3 do not stain in Melzer's, while pigmented, structural layer SWL2 stains pinkish purple to purple. Subtending hypha typically cylindrical. Sometimes a septum can be recognized in some distance to the spore base, while the pore at the base regularly is open.

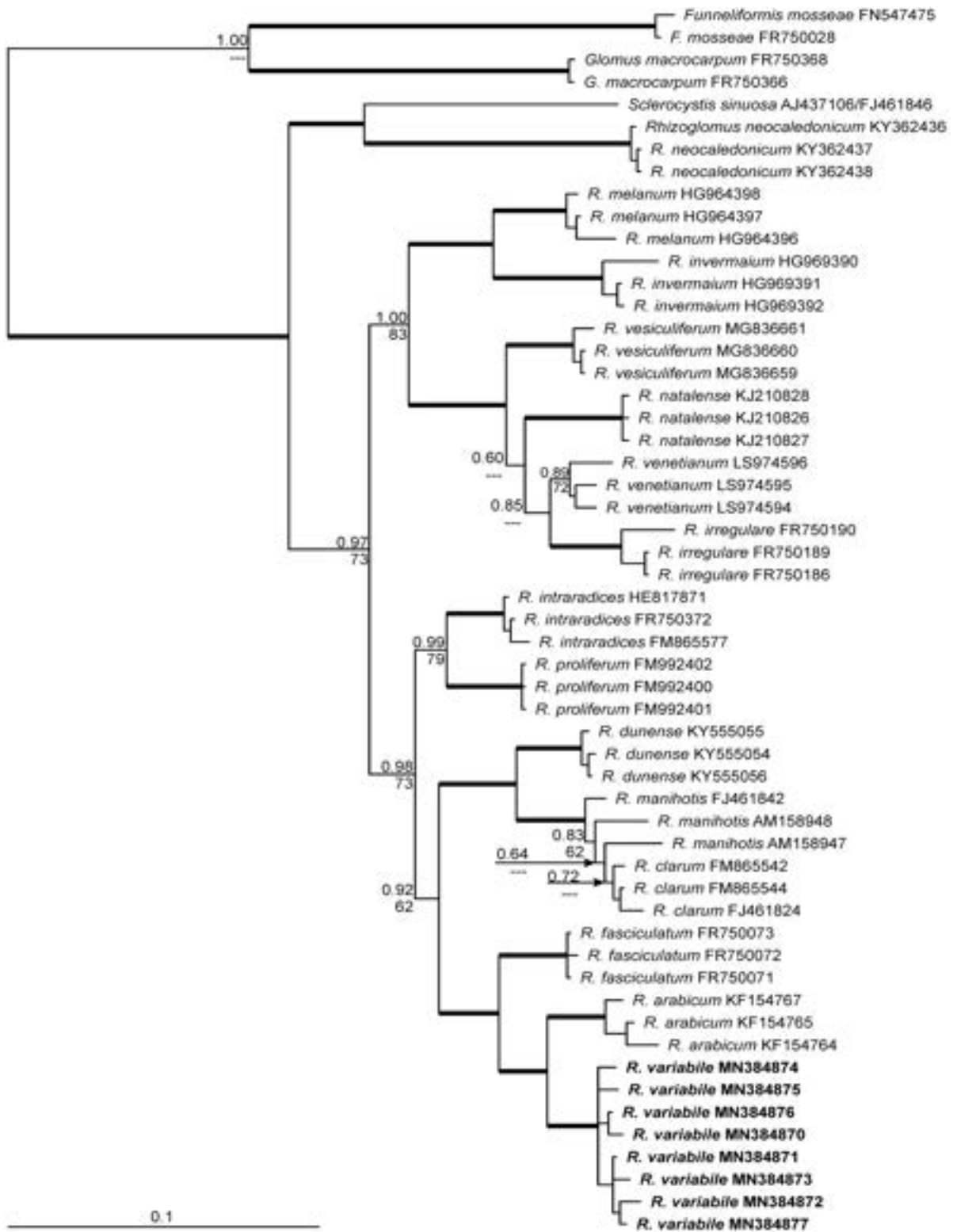


**Fig. 18.** Phylogenetic tree obtained by analysis of partial SSU, ITS, and partial LSU rDNA sequences of different *Rhizoglyphus* spp. Sequences labeled with GenBank accession numbers. Sequences obtained in this study shown in boldface. BI posterior probabilities  $\geq 0.6$  and ML bootstrap support  $\geq 60$  shown above and below branches, respectively. Thick branches represent clades  $\geq 0.9/90$  support.

form either larger spores (*R. clarum* and *R. manihotis*), a broader spore wall (*R. antarcticum*), or creamy and generally smaller spores (*R. fasciculatum*). *Rhizoglosum dunense*, *R. intraradices*, and *R. irregulare* have also triple-layer spores, but their innermost layer is not flexible, hyaline and thin, but laminate, yellow brown, and persistent (Błaszowski et al. 2018, Turrini et al. 2018). Finally, *R. aggregatum* has a bi-layered spore wall and spores that are also less variable in size than those of *R. variabile* (Schenck & Smith 1982, Koske 1985).

Phylogenetic analysis of the newly generated rDNA sequences placed *R. variabile* in the genus *Rhizoglosum* Sieverd., G.A. Silva & Oehl, typified by *R. intraradices* (N.C. Schenck & G.S. Sm.) Sieverd., G.A. Silva & Oehl (Sieverding et al. 2014). Sequences of the new species formed a maximum supported clade with *Rhizoglosum arabicum* (Fig. 18). BLASTn searches showed 94–95 % similarity with *R. arabicum* type sequences, considering the entire Kruger's fragment (Symanczik et al. 2014; accession numbers KF154764, KF154765, KF154766, KF154767). *Rhizoglosum arabicum* can be easily distinguished morphologically from the new species, as it has four layered and generally smaller spores (30–85 × 50–125 µm).

Environmental sequences deposited in public databases indicate that *R. variabile* might have a global distribution, from humid to arid climates. BLASTn analysis of the entire DNA fragment sequenced from *R. variabile* revealed that an environmental sequence obtained from maize roots (KJ701452) from China (Zeng et al. 2015) had 97 % similarity with our new species. Environmental LSU rDNA sequences related to *R. variabile* with ≥ 97 % similarity were obtained from roots of *Trifolium pratense* in Japan (AB935523), in China plant roots (GQ149199), spores from maize fields in the USA (JN937261, JN937262, JN937265, JN937266, JN937273, JN937275, JN937276, JN937278, JN937280, JN937282, JN937284, JN937286, JN937479, JN937482), and from roots of *Acacia gerrardii* in Kuwait (MK247225, MK247236, MK247237) (Li et al. 2010, Moebius-Clune et al. 2013, Suleiman et al. 2019).

*Rhizoglosum variabile* is the third species of *Rhizoglosum* to be described originally from South America. The other two species are *R. manihotis* (Schenck et al. 1984) and *R. natalense* (Błaszowski et al. 2014). Marinho et al. (2018) reported in total 11 *Rhizoglosum* species from tropical forests worldwide, whereas Jobim et al. (2018) listed 10 *Rhizoglosum* species only from the Atlantic rainforest in Brazil, a humid forest biome, separated from the

Amazon rainforest by the Cerrado savanna and the semi-arid Caatinga biome.

*Authors:* M. Anderson Corazon-Guivin, A. Cerna-Mendoza, J.C. Guerrero-Abad, A. Vallejos-Tapullima, G.A. da Silva & F. Oehl

### Basidiomycota, Agaricomycetes, Russulales, Russulaceae

*Russula phloginea* J. Song & J.F. Liang, *sp. nov.* – Figs. 19–20

Mycobank no.: MB 830876

*Holotypus.* – CHINA. Yunnan province, Baoshan, Changning County, Goujie Town, Goujiecun, Make Mountains, on the ground in coniferous and broad-leaved mixed forest, 1924 m a.s.l., 25°03'52.31"N, 99°81'34.27"E, 12 August 2017, leg. H.J. Li, CNX530524068 (LI 8811, holotype; RITF4193).

*Description.* – Basidiomata (Figs. 19A–C) medium-sized. – *Pileus* 4–10 cm in diam., first hemispherical to plano-concave with a depressed centre, becoming sub-infundibuliform when mature, surface pink (#C7A7AC) to amethyst (#9966CC) with localized blanching-almond (#FFEBCD) or dark brown (#423336) zone towards the centre when fresh; pileipellis unpolished with some tiny white scabs or saddle brown (#8B4513) flakes, slightly viscid when moist, peelable; margin decurved when juvenile, acute, becoming straight, smooth, none to slightly striate, slightly cracked with age. – *Context* up to 3.5 mm thick at the centre, white, negative in FeSO<sub>4</sub>. – *Lamellae* adnexed with scattered lamellulae, dense, flexible, frequently forked near the stipe, 3–7 mm broad, regular, white, smooth, unchanging when bruising, edge entire. – *Stipe* 3.5–7.5 cm, cylindrical, glabrous or longitudinally ridged, spongy inside, fleshy, dry, white. – *Odour* distinct. – *Taste* mild. – *Spore print* white. – *Basidiospores* (Figs. 19G–I) (6)6.4–7.8 × 5.2–6.5 µm, Q = 1.21–1.28 [60/2/2], subglobose to ellipsoid, ornamented strongly amyloid, composed of blunt, isolated, cylindrical warts, up to 0.5 µm; suprahilar plage distinct, non-amyloid. – *Basidia* (Figs. 19E, 20A) 29–45 × 9–11 µm, 4-spored, clavate, thin-walled, sterigmata up to 5 × 2 µm. – *Pleurocystidia* (Fig. 20B) (48)60–78.6(79.5) × 7.3–9.6(9.9) µm, thin-walled, dispersed, not abundant, embedded or with the tip projecting slightly beyond the hymenium, subfusiform, clavate to lanceolate with obtuse, subacute, or broken apex, with refractive subaceroses contents, grey in SV (Fig. 19F). – *Cheilocystidia* few, similar to but smaller than pleurocystidia. – *Lamellae* trama composed with hyphae 2–6 µm wide, thin-walled, hyaline, scarcely divergent and with sphaerocytes



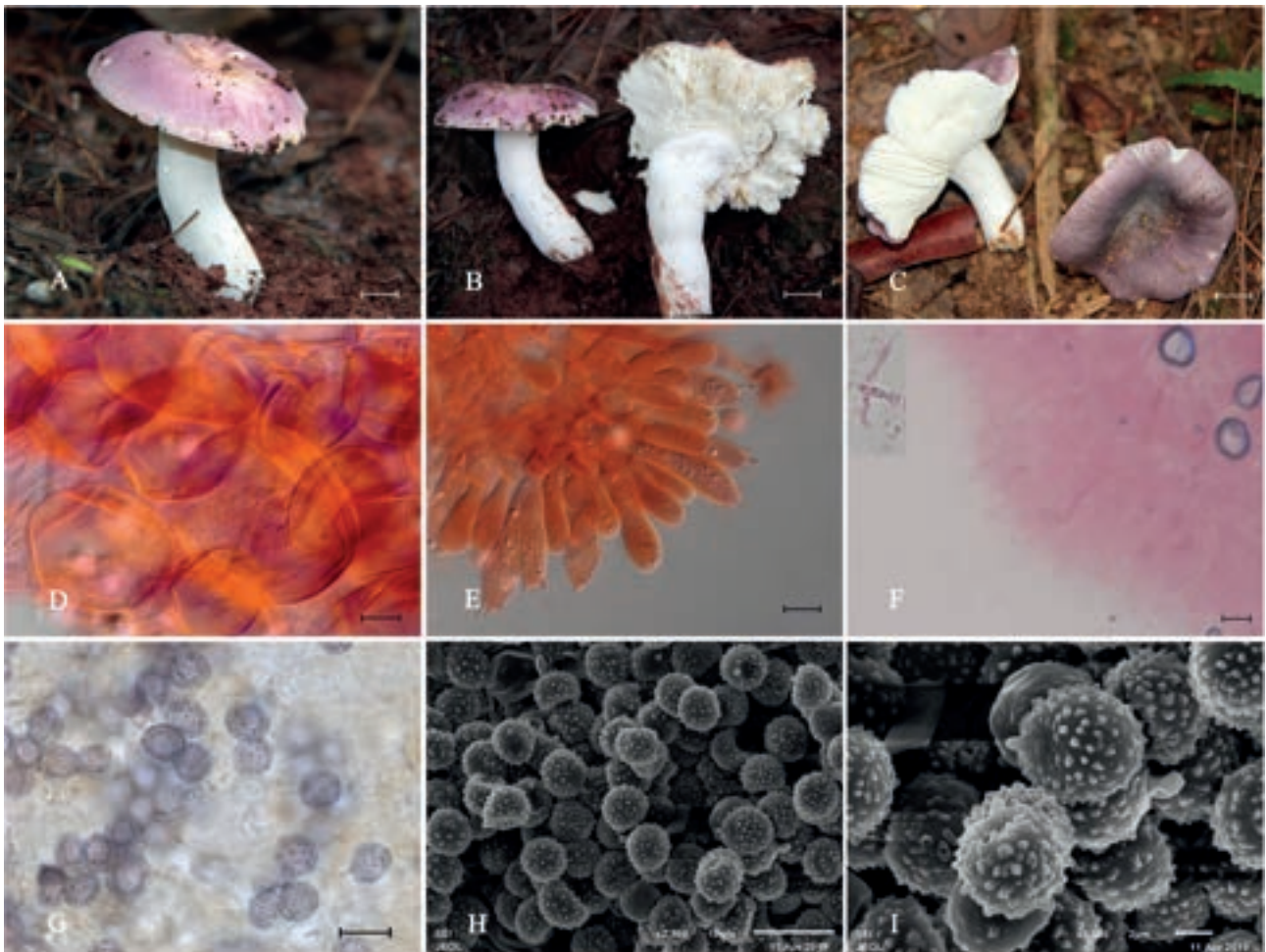


**Fig. 19.** Basidiomata and microscopic structures of *Russula phloginea*. **a–b.** Basidiomata, CNX530524068 (holotype). **c.** Basidiomata, CNX530524304. **d.** Sphaerocytes of lamellae trama in Congo Red reagent. **e.** Hymenium in Congo Red reagent. **f.** Hymenium in SV solution. **g.** Basidiospores in Melzer's reagent. **h–i.** Basidiospores (SEM). Scale bars a, c 1 cm; b 1.5 cm; d–e, g–h 10  $\mu$ m, f 20  $\mu$ m, i 2  $\mu$ m.

(Fig. 19D) 28–55  $\mu$ m in diam., thin-walled, hyaline. – Pileipellis two-layered, slightly gelatinous, metachromatic in Cresyl blue; subpellis ca. 150–240  $\mu$ m thick, composed of hyphae 2–4  $\mu$ m wide, thin-walled, hyaline, rarely septate, branched, sinuous, forming a dense mat close to the underlying trama; suprapellis ca. 40–60  $\mu$ m thick. – Terminal cells (Fig. 20C) near the pileus centre obclavate, measuring 10–40  $\times$  3–5  $\mu$ m, erected arranged; terminal cells (Fig. 20D) near the pileus margin slender, apices obtuse, 23–35  $\times$  1.5–3  $\mu$ m, mostly curving. – Pileocystidia dispersed, clavate to cylindrical in suprapellis (Figs. 20C, E), often with moniliform apex, 23–56  $\times$  3–5  $\mu$ m, one-celled; cylindrical in subpellis (Fig. 20F), with rounded apex, up to 105  $\times$  5  $\mu$ m, thin-walled, grey in SV. – Stipitipellis composed of parallel thin-walled hyphae, 3–5  $\mu$ m

wide in diam. – Caulocystidia abundant (Fig. 20G), fusoid to cylindrical, with rounded or acute apex, up to 108  $\times$  6  $\mu$ m, grey in SV. – Stipe trama composed of connective hyphae and nested sphaerocytes up to 32  $\mu$ m in diam. – Clamp connections absent in all parts of basidioma.

**Etymology.** – From Latin, referring to the amethyst color of the pileal surface similar to the pinkish flower of *Phlox paniculata*.

**Habitat and distribution.** – Known from southwestern China, solitary or scattered, in coniferous and broad-leaved mixed forest at 1927 m a.s.l.

**Additional material examined.** – CHINA. Yunnan province, Baoshan, Changning County, Mengtong Town, Dazhaipo, on the ground in coniferous and broad-leaved mixed forest, 1297 m a.s.l., 24°59'35.23"N, 99°62'36.83"E, 2 August 2017, leg. H.J. Li, CNX530524304 (LI 9026, RITF4194).

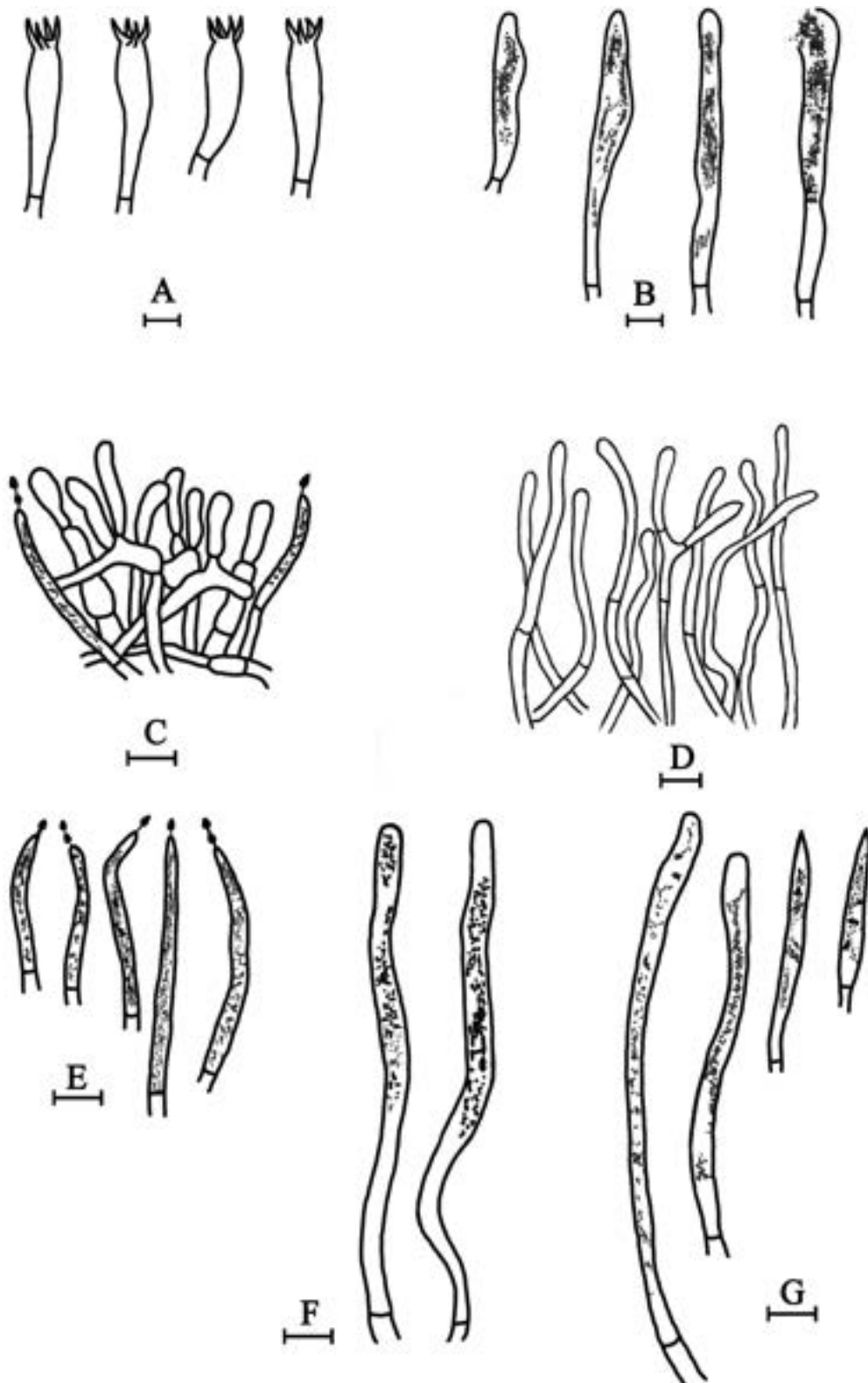


**Fig. 20.** Microscopic structures of *Russula phloginea*, drawn from CNX530524068 (holotype). **a.** Basidia. **b.** Pleurocystidia. **c.** Terminal cell and pleurocystidia in suprapellis. **d.** Pleurocystidia in suprapellis. **e.** Pleurocystidia in subpellis. **f.** Caulocystidia. Scale bars 10  $\mu$ m.

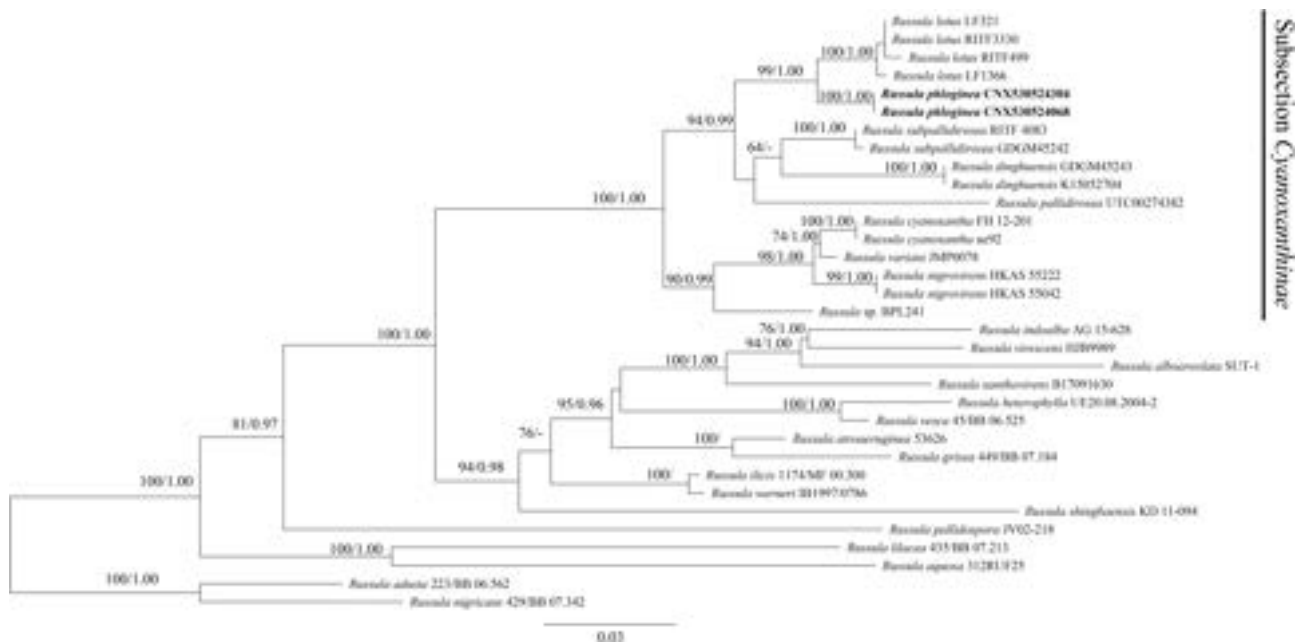


**Fig. 21.** ML phylogenetic tree of *Russula* subsect. *Cyanoxanthinae* reconstructed from the ITS–LSU–mtSSU–*ef1 $\alpha$*  dataset. Branches are labeled with MLBS  $\geq 50$  and BIPP  $\geq 0.95$ . New species shown in boldface.

**Notes.** – Yunnan province is a mountainous area with a generally mild climate located in the Hengduan-Himalayan region of China, which is a global biodiversity hotspot (Myers et al. 2000). Its topographic range combined with tropical moisture sustains extremely high biodiversity and high degrees of endemism. In our survey of *Russula* from Yunnan province, several specimens could not be assigned to any described species. The morphological characters infer that these specimens represent a novel species in subsection *Cyanoxanthinae*, which belongs to *Russula* subg. *Heterophyllidia* Romagnesi based on the latest phylogeny published for the genus (Buyck et al. 2018). *Russula* subsection *Cyanoxanthinae* Sing. is characterized by the complex color of pileipellis, glabrous, sericeous or scurfy cuticle, acute margin of the pileus, flexible and not brittle lamellae with numerous lamellulae or furcations, metachromatic tissues in Cresyl blue, and negative or slightly greyish green context in  $\text{FeSO}_4$  (Singer 1986, Sarnari 1998). Recent studies on *Russula* in China have revealed many new species (Zhao et al 2015, Zhang et al. 2017, Jiang et al. 2018, Li & Deng 2018). Thus far, four species in subsect. *Cyanoxanthinae* have been reported from China: *R. dinghuensis* J.B. Zhang & L.H. Qiu, *R. subpallidirosea* J.B. Zhang & L.H. Qiu, *R. nigrovirens* Q. Zhao, and *R. lotus* Fang Li (Li & Deng 2018).

Our combined ITS–LSU–mtSSU–*tef1* dataset included sequences from 33 isolates representing 25

taxa. The dataset was composed of 2547 characters, of which 1838 were constant and 450 were parsimony-informative. The best model for the combined dataset was GTR with an equal frequency of nucleotides. BI and ML analyses resulted in similar topologies with an average standard deviation of split frequencies = 0.008991 (BI). The resulting ML phylogram ( $-\ln L = 10443.199559$ ) is shown in Fig. 21, revealing that *R. subsect. Cyanoxanthinae* formed a robust monophyletic clade (MLBS = 100, BIPP = 1.0), and relationships of most species in this subsection were well supported. *Russula phloginea* was found to be nested well within subsect. *Cyanoxanthinae* and represented a sister species to *R. lotus* with significant support (MLBS = 99, BIPP = 1.0).

Morphologically, *R. phloginea* can be placed within subsect. *Cyanoxanthinae* based on its not to slightly striate pileus, pink to amethyst pileal surface, acute margin, flexible lamellae, white context negative with  $\text{FeSO}_4$ , glabrous or longitudinally ridged spongy stipe, white spore print, frequently forked lamellae, metachromatic pileipellis in Cresyl blue, grey pleurocystidia in SV, and isolate warts (Singer 1986, Sarnari 1998). Phylogenetically, ML and BI analyses also showed that *R. phloginea* is nested within subsect. *Cyanoxanthinae*. *Russula phloginea* is sister to *R. lotus*, closely related to *R. pallidirosea* Kropp from American Samoa and to two Asian species *R. dinghuensis* and *R. subpallidi-*

*rosea*. *Russula lotus* morphologically resembles *R. phloginea* in the pinkish white to purplish pink pileus, similar size of basidiospores with isolate warts, white spore print, and subfusiform to clavate pleurocystidia. However, *R. phloginea* is different from *R. lotus* by having plentiful clavate to cylindrical pileocystidia with moniliform apex, fusoid to cylindrical caulocystidia, obclavate terminal cell, frequently forked lamellae, cylindrical stipe without tapering base, and by never producing distinct yellowish white pileus centre area (Li & Deng 2018).

*Russula phloginea* can be easily distinguished from *R. dinghuensis*, *R. subpallidirosea*, and *R. pallidirosea* by its macro- and micro-morphological characters. *Russula phloginea* has pink to amethyst pileus, unpolished pileipellis with some tiny white scabs or saddle brown flakes, distinct suprahilar plage, large pleurocystidia ( $60\text{--}80 \times 8\text{--}10 \mu\text{m}$ ), abundant caulocystidia ( $108 \times 6 \mu\text{m}$ ) with rounded or acute apex, clavate to cylindrical pileocystidia with moniliform apex and distinct odour; whereas *R. dinghuensis* produce olive green to dark green pileus mixed with rusty tone, indistinct odour, indistinct suprahilar plage shorter pleurocystidia ( $44\text{--}67 \times 6\text{--}10 \mu\text{m}$ ), shorter caulocystidia ( $43\text{--}76 \times 5\text{--}6.3 \mu\text{m}$ ), cylindrical to clavate pileocystidia without moniliform apex (Zhang et al. 2017); *R. subpallidirosea* has a pale pink to pale grayish-pink pileus, indistinct odour, indistinct suprahilar plage, shorter pleurocystidia ( $35\text{--}50 \times 5\text{--}8 \mu\text{m}$ ) and caulocystidia ( $50\text{--}83 \times 4\text{--}6 \mu\text{m}$ ), and pileocystidia never generating a moniliform apex (Zhang et al. 2017); and *R. pallidirosea* produces pallid to pinkish pileus, indistinct suprahilar plage, shorter pleurocystidia ( $40\text{--}55 \times 5\text{--}7 \mu\text{m}$ ), occasionally forked lamellae with scarce lamellulae, and often tapering pileocystidia (Kropp 2016). A key to the species in *R.* subsect. *Cyanoxanthinae* from China is provided.

For the time being, the taxonomy of the genus *Russula* in China is far from being well studied and many specimens are still unidentified. Our research also indicates that the *Russula* subsect. *Cyanoxanthinae* is largely distributed in Asia. Further studies based on broader sampling and more molecular data are needed to give a deep insight into *Russula* subsect. *Cyanoxanthinae*.

Authors: J. Song, B. Chen, J.F. Liang, J.K. Lu, S.K. Wang, X.Y. Pan & F. Yu

#### Key to species in *Russula* subsect. *Cyanoxanthinae* in China

1. Pileal surface green white, grayish green, olive green to dark green .....2
- 1\*. Pileal surface pale pink to amethyst .....3

2. Occurring at high altitude, higher than 3000 m a.s.l., basidia up to  $75 \times 14 \mu\text{m}$ , terminal cell up to  $46 \times 5 \mu\text{m}$  .....*R. nigrovirens*
- 2\*. Occurring at altitudes less than 1500 m a.s.l., basidia up to  $50 \times 12 \mu\text{m}$ , terminal cell up to  $24 \times 4 \mu\text{m}$  .....*R. dinghuensis*
3. Frequently forked lamellae .....4
- 3\*. Occasionally forked lamellae .....*R. lotus*
4. Pileocystidia with mucronate apex or subterminally constricted, pleurocystidia up to  $50 \times 8 \mu\text{m}$ , caulocystidia up to  $83 \times 6 \mu\text{m}$  .....*R. subpallidirosea*
- 4\*. Pileocystidia with moniliform apex, pleurocystidia up to  $80 \times 10 \mu\text{m}$ , caulocystidia up to  $108 \times 6 \mu\text{m}$  .....*R. phloginea*

#### Ascomycota, Dothideomycetes, Pleosporales, Didymellaceae

*Stagonosporopsis flacciduvarum* M. Lorenzini & Zapparoli, **sp. nov.** – Fig. 22  
Mycobank no.: MB 829182

Holotypus. – ITALY. Provincia Autonoma di Trento, Valle dei Laghi, isolated from withered Nosiola grapes, November 2013, leg. M. Lorenzini and G. Zapparoli, strain UC23 (CBS 145113; holotype specimen and culture, preserved as metabolically inactive culture). Sequences ex-holotype: KU554588 (ITS), KU554634 (LSU), MK032764 (*tub2*), MK205423 (*rpb2*).

Description. – Hyphae hyaline to brown, smooth, septate, 2–5  $\mu\text{m}$  wide. – Conidiomata pycnidial, pale brown to dark brown, solitary, sometimes aggregate, covered by hyphae, subglobose to globose, scarcely detected on PDA [(88)107±20(150) × (73)91±20(135)  $\mu\text{m}$ , n=8] and OA [(62)92±44(170) × (49)78±37(146)  $\mu\text{m}$ , n=6], abundant on pine needles [(49)77±27(146) × (32)63±20(115)  $\mu\text{m}$ , n=20] (Figs. 22D, J). – Pycnidial wall pseudoparenchymatous, composed of oblong to isodiametric cells, melanized, 15–50  $\mu\text{m}$  thick. – Conidiogenous cells enteroblastic/phialidic, hyaline, smooth, ampulliform to doliiform, 5–7.5 × 4–8  $\mu\text{m}$  (n=10) (Fig. 22G). – Chlamydospores not abundant, light brown, multicellular-dictyo/phragmospores arranged in alternarioid chains, intercalary, occasionally terminal, irregular roughened, (25)40±9(50) × (15)20±3(25)  $\mu\text{m}$  on PDA, (10)16±5(25) × (8)15±5(23)  $\mu\text{m}$  on OA (n=10) (Fig. 22F). – Conidia ovoid to ellipsoidal, biguttulate and eguttulate, scarcely produced on PDA [(2.5)3.2±0.4(4) × (1.5)1.7±0.2(2)  $\mu\text{m}$ , n=20], abundant on pine needle [(2.5)3.6±0.5(5.5) × (1.5)2.0±0.2(2.5)  $\mu\text{m}$ , n=51] (Figs. 22H, I). Hyphae coils detected on all media (Fig. 22E).

Culture characteristics. – Colonies on MEA reaching 80 mm diam. after 7 d at 25 °C; my-

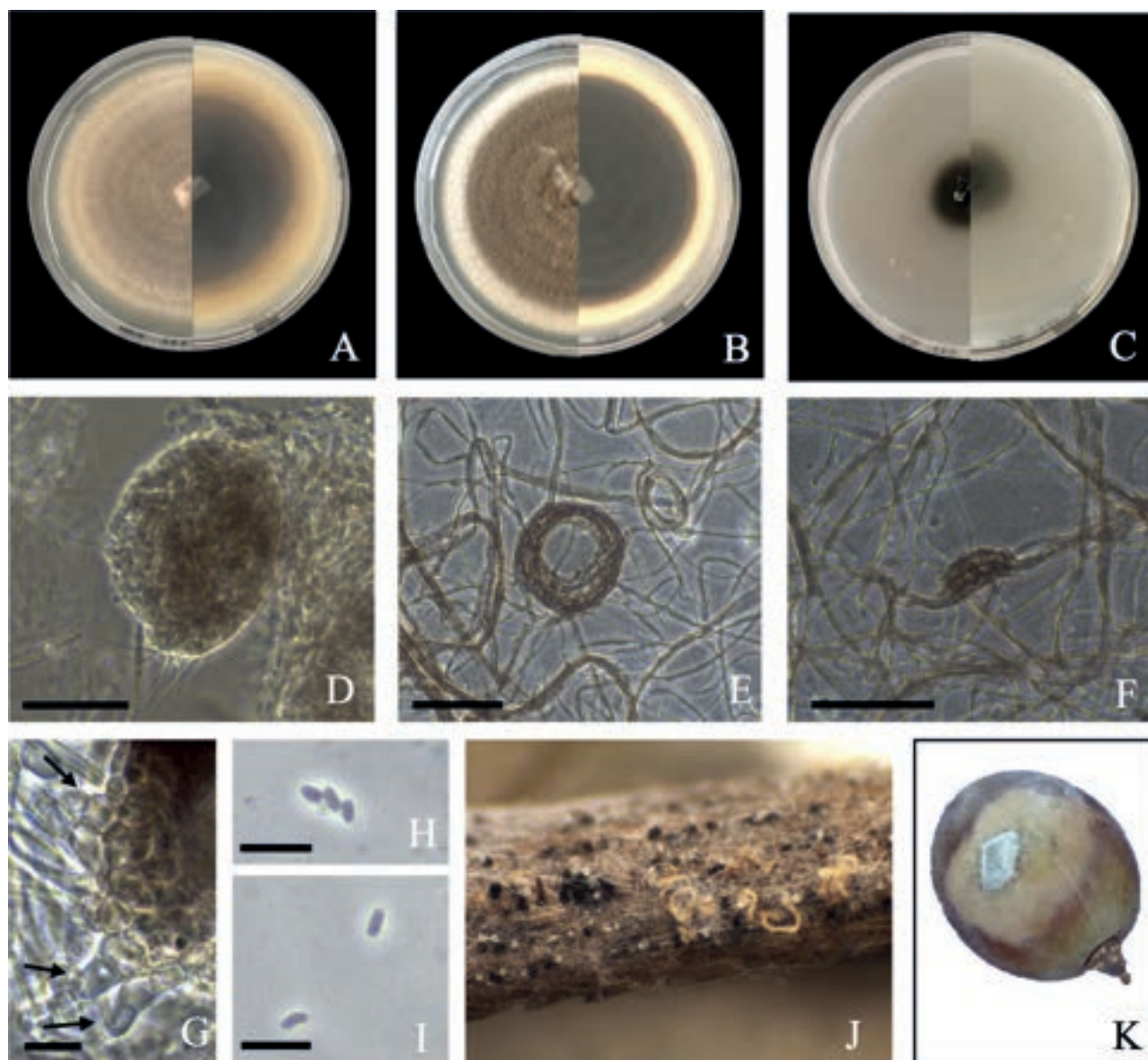


**Fig. 22.** Macro- and micro-morphology of *Stagonosporopsis flaccidivarum*. **A.** Colony morphology of UC23 isolate on MEA. **B.** Colony morphology on PDA. **C.** Colony morphology on OA. **D.** Pycnidia on PDA. **E.** Hyphae coil on PDA. **F.** Chlamydospore on PDA. **G.** Conidiogenous cells indicated by arrows on pine needle. **H–I.** Conidia on pine needle. **J.** Pycnidia on pine needle. **K.** Chlotrotic area produced on berry infected by UC23 isolate. Scale bars D–F 50  $\mu\text{m}$ , G–I 10  $\mu\text{m}$ .

celium plane, dense, cream to light brown, with concentric rings, margin regular; reverse brown to dark brown at center, cream to pale brown at periphery (Fig. 22A). Colonies on PDA reaching 84 mm diam. after 7 d at 25 °C; mycelium felted, cottony, brown, with concentric rings, margin regular, edge whitish; reverse dark at center and whitish at periphery (Fig. 22B). Colonies on OA reaching 76 mm diam. after 7 d at 25 °C; mycelium plane, olivaceous to dark at center, whitish and immersed in the me-

dium at periphery, margin regular; reverse olivaceous at center and whitish at periphery (Fig. 22C). Colonies on all media not growing at 30 °C.

**Etymology.** – From Latin, ‘flaccid’= shriveled and ‘uvarum’ (genitive plural of the noun *uva*) = grape, referring to the withered/shriveled grapes where the strain was isolated.

**Habitat and distribution.** – Saprobe on grape berries of *Vitis vinifera* var. Nosiola stored in fruit-drying room. Only known from northern Italy.

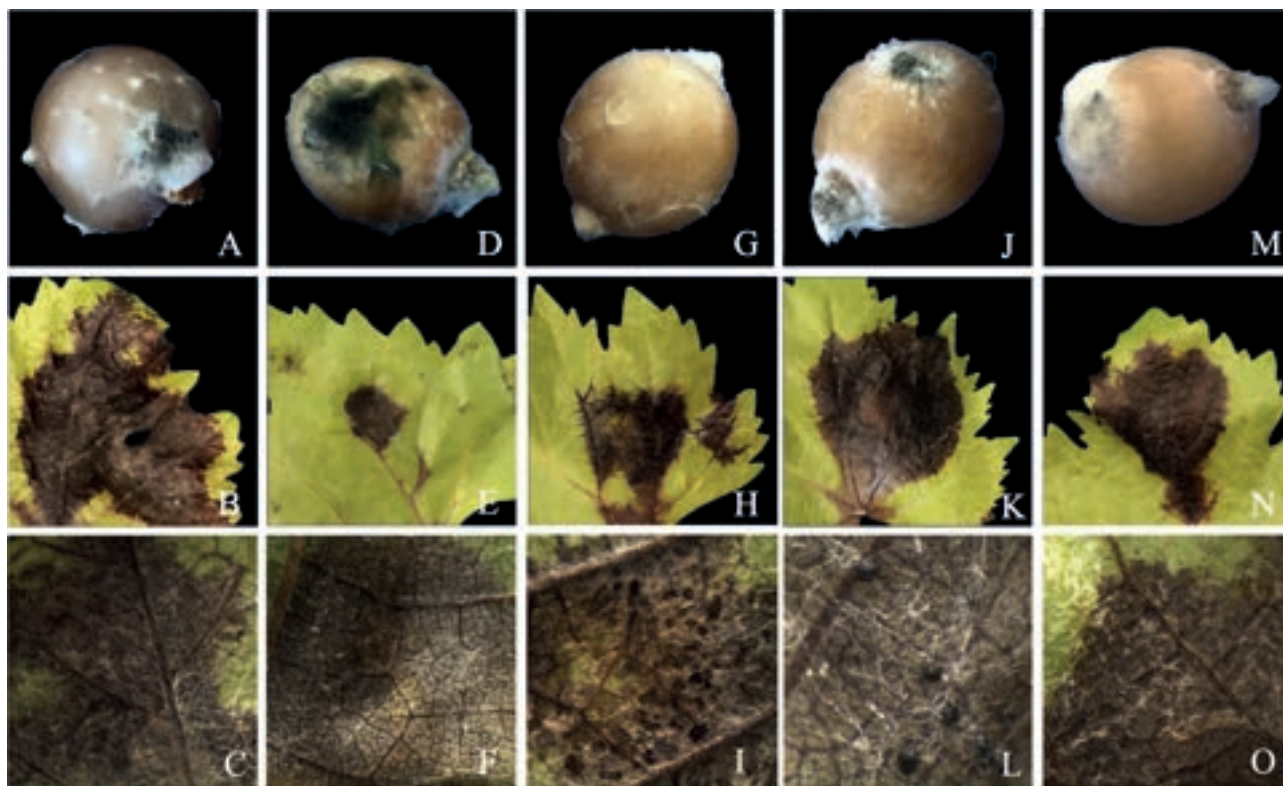


**Fig. 23.** Results of pathogenicity assay in grapevine. Mycelial growth on berry and necrosis on young leaves after inoculum of different isolates at 25 °C after 7 d. **A–C.** *Didymella americana* UC30. **D–F.** *D. calidophila* CG7. **G–I.** *D. pomorum* UC56. **J–L.** *Nothophoma quercina* S3. **M–O.** *Stagonosporopsis flaccidivarum* UC23.

**Pathogenicity assay.** – Our Didymellaceae isolates had a very low capacity to cause disease on *V. vinifera* tissues (Fig. 23). Grape berries inoculated by all strains displayed a localized chlorotic area with mycelium that partially enshrouded the berries. A clear necrotic area was detected only on detached young leaves inoculated by 5 isolates after 7 d. Moreover, only old leaves infected by isolate S3 displayed mycelial growth limited to few millimeters (2–5 mm) beyond the inoculation site. After 12 d, necrotic lesion was observed on canes inoculated by neither of the 5 strains. Mycelial growth around the inoculation site was observed only on cane tissues infected by isolates CG7 and S3.

**Notes.** – The Didymellaceae (Pleosporales) were established by de Gruyter et al. (2009) and represent one of the most speciose families in the fungal kingdom. Recently, this family was taxonomically revised based on multi-locus DNA sequence data, redefining some genera (e.g., *Epicoccum*, *Peyronellaea*, and *Stagonosporopsis*) and adding several new ones (e.g., *Heterophoma*, *Allophoma*, *Paraboeremia*, and *Neoascochyta*) (Aveskamp et al 2010; Chen et al. 2015, 2017; Wijayawardene et

al. 2017). Species of this family are cosmopolitan and inhabit different environments. Most Didymellaceae are plant pathogens of a wide range of hosts; their potential host specificity has not yet been addressed (Chen et al. 2017).

Several species of Didymellaceae have been isolated from *Vitis vinifera*, where they can be either pathogens or saprobes (Hofstetter et al. 2012, Jayawardena et al. 2018). *Phoma*, *Didymella*, and *Epicoccum* are the most representative genera associated with grapevines, whereas others, such as *Ascochyta*, *Boeremia*, *Leptosphaerulina*, and *Stagonosporopsis*, are generally less frequent. Very little is known about their pathogenicity on grapevine and the capacity to cause diseases, such as necrosis, bark crashes, trunk, and cane spot, has been documented only for *D. negriana* and *D. glomerata* (Granata & Refatti 1981, Machowicz-Stefaniak & Król 2007).

Members of Didymellaceae have previously been isolated from withered grapes used for passito wine production (Lorenzini & Zapparoli 2015, Lorenzini et al. 2016). *Epicoccum nigrum* was the most frequent and can cause berry rot. Other isolates belonging to *Didymella* and *Stagonosporopsis* were

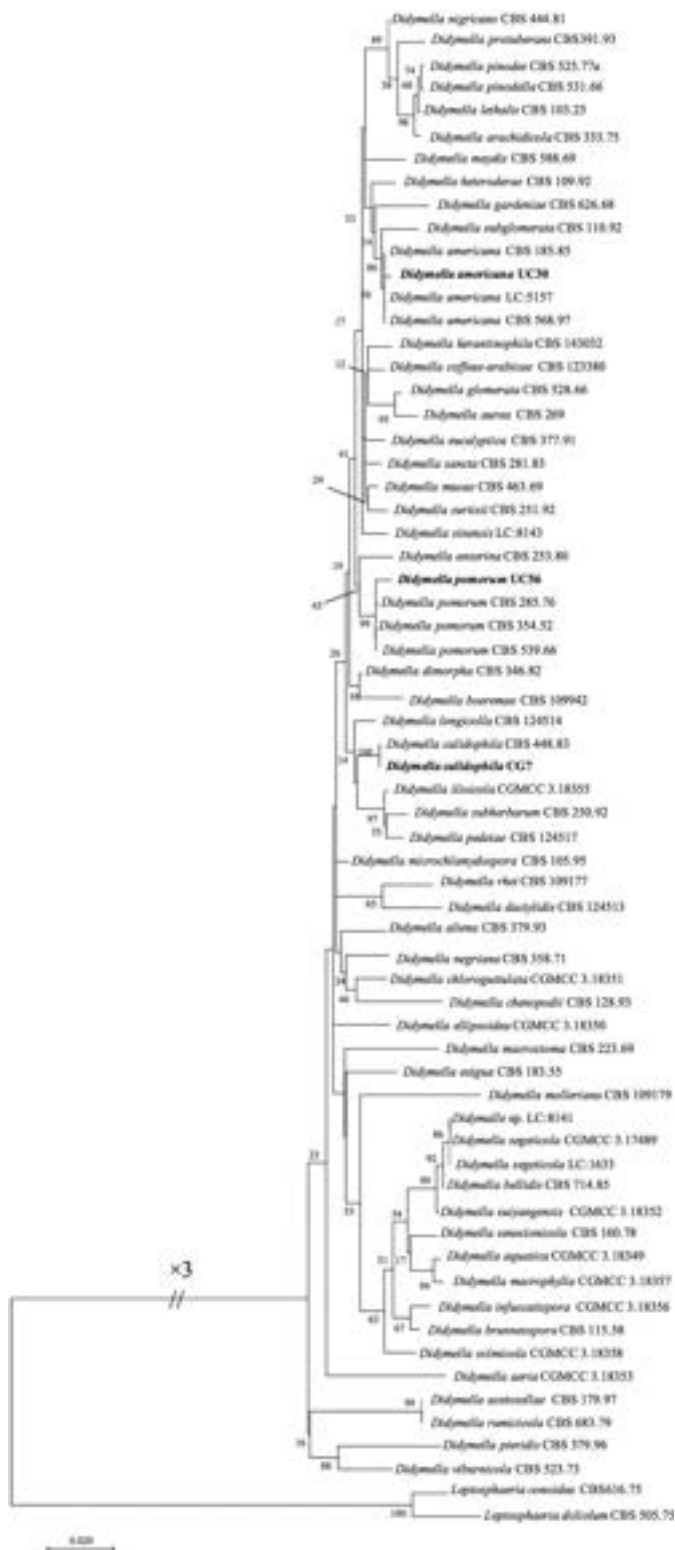


**Fig. 24.** ML phylogenetic tree of *Didymella* species, reconstructed from the combined ITS–LSU–*tub2*–*rpb2* dataset. ML bootstrap support values shown at the nodes. *Leptosphaeria conoidea* and *L. doliolum* served as outgroups.

made, but their identification at species level has not been possible due to their unclear phylogeny using ITS and LSU gene sequences. The recent taxonomic revision of Didymellaceae (Chen et al. 2017), encouraged us to identify Didymellaceae isolates collected from withered grapes during a new survey. The isolates were studied by an integrative approach (multi-locus phylogeny, morphology, pathogenic analysis). Of all isolates studied, one represented a novel *Stagonosporopsis* species described above.

The BLASTn analysis in NCBI GenBank of our newly generated ITS and LSU sequences of UC30, CG7, UC56, and S3 was not informative for species identification. Conversely, *tub2* and *rpb2* gene sequences showed high similarity (99–100 %) to *Didymella americana* (UC30), *D. calidophila* (CG7), *D. pomorum* (UC56), and *Nothophoma quercina* (S3). Considering this information, the phylogenetic position of the three *Didymella* isolates was evaluated using taxa of this genus according to Valenzuela-Lopez et al. (2018). In our concatenated ITS–LSU–*tub2*–*rpb2* phylogenetic tree, isolate UC30 was placed in a cluster of *D. americana* strains (MLBS = 56), isolate CG7 close to *D. calidophila* CBS 448.83 (MLBS = 100), and isolate UC56 in a cluster of *D. pomorum* strains (MLBS = 99) (Fig. 24). Data obtained by phylogenetic analysis of the ITS, *tub2*, and *rpb2* datasets separately were not totally congruent for isolate UC30 with the combined dataset. This isolate was placed in a cluster containing different *Didymella* species comprehending *D. americana* taxa (data not shown). On the other hand, the data obtained by phylogenetic analysis of the ITS, *tub2*, and *rpb2* datasets separately were congruent for isolates CG7 and UC56 with the combined dataset. The phylogenetic analysis of the LSU dataset placed isolates CG7, UC30, and UC56 in a cluster containing different *Didymella* taxa (data not shown).

The colony morphology of isolate UC30 identified as *D. americana*, resembled that described for the holotype (Morgan-Jones & White 1983, Boerema 1993). *Didymella americana* causes diseases on glycines, beans, and gramineae (wheat, sorghum, and corn) worldwide (Boerema et al. 2004, Aveskamp et al. 2010, Gorny et al. 2016, Chen et al. 2017). Isolate CG7 was identified as *D. calidophila*, which is a rare species; only two strains have been recovered more than 35 years ago, ex-neotype CBS 448.83 (neotype CBS H-20168) from desert-soil and PD 84/109 from *Cucumis sativus*. The morphology of strain CG7 was congruent with that of *D. calidophila* (Boerema 1993, Aveskamp et al. 2009). The occurrence of *D.*

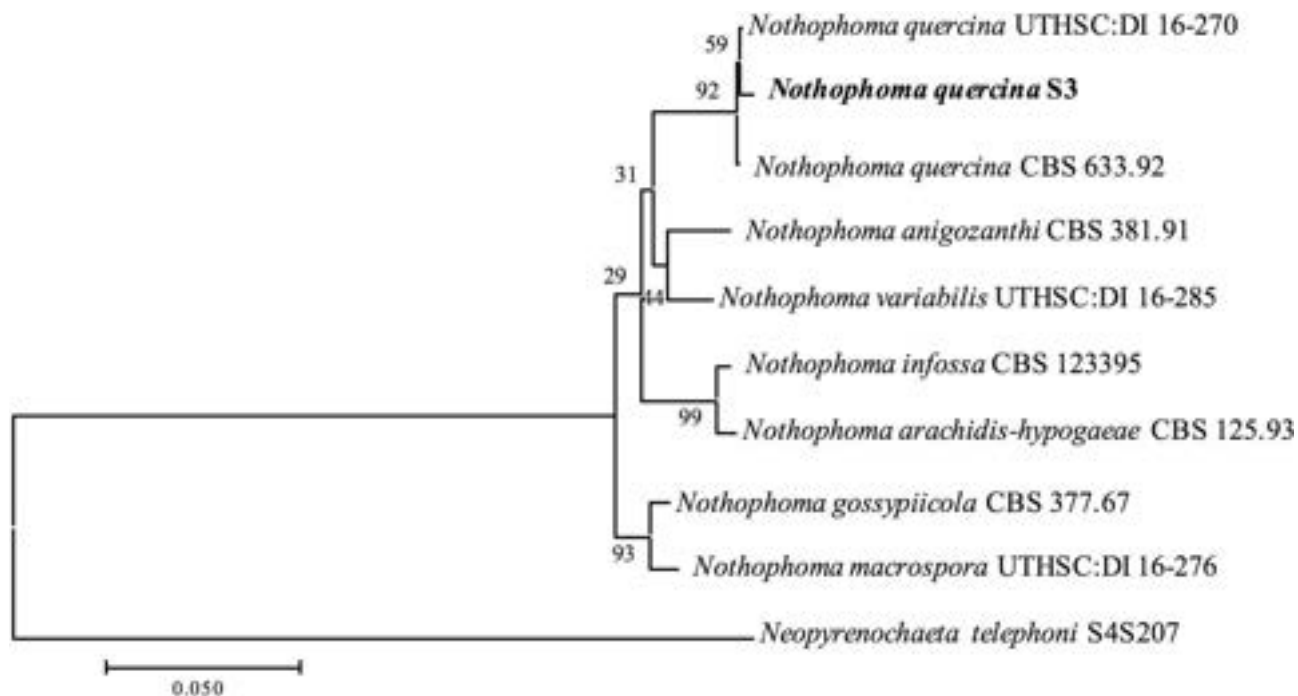


**Fig. 25.** ML phylogenetic tree of *Nothophoma* species, reconstructed from the combined ITS–LSU–*tub2*–*rpb2* dataset. ML bootstrap support values shown at the nodes. *Neopyrenochaeta telephoni* served as outgroup.

*americana* and *D. calidophila* on withered grapes and infectivity on different *V. vinifera* tissues could be indicative of their potential pathogenicity on grapevine. Isolate UC56 was identified as *Didymella pomorum*, a species previously detected on asymptomatic grapevines (Jayawardena et al. 2018). The present study reports for the first time the occurrence and pathogenicity of *D. pomorum* on grape berries.

The phylogenetic position of isolate S3 was evaluated using taxa of the genus *Nothophoma* according to Valenzuela-Lopez et al. (2018). The concatenated phylogenetic tree (ITS–LSU–*tub2*–*rpb2*) placed S3 isolate among strains of *N. quercina* (MLBS = 92) (Fig. 25). Phylogenetic analysis of the *tub2* and *rpb2* datasets separately were congruent with the combined dataset (data not shown). However, based on the ITS dataset, isolate S3 was placed close to *N. variabilis* UTHSC:DI 16-285, whereas based on LSU it was placed in a cluster with strains of *N. quercina* and *N. anigozanthi* (data not shown).

Isolate S3 showed a colony morphology quite different with respect to the holotype of *Nothophoma quercina* (Aveskamp et al. 2010). Macro-morphological differences within this species have previously been described by Moral et al. (2017). This fungus is a worldwide plant pathogen and has been isolated from different diseased plant materials

(e.g., apple, pistachio, oak, and olive trees) in the USA (Arizona), the Mediterranean area, Ukraine, and China (Moral et al. 2017, Liu et al. 2018). The recovery of *N. quercina* from withered grapes and pathogenicity assay suggest that grapevine could be a new host of this fungus.

The ITS, LSU, *tub2*, and *rpb2* sequences of isolate UC23 showed 100 % similarity to *Stagonosporopsis* sp., *S. cucurbitacearum*, *S. dorenboschii*, different strains of *Phoma* sp., and *Pleosporales* sp. for ITS; 99 % similarity to different members of Didymellaceae for LSU; 99 % similarity to *S. ailanthicola* and *S. bomiensis* for *tub2*; and 98 % similarity to *S. bomiensis* and *S. papillata* for *rpb2*. As a result, the phylogenetic position of UC23 isolate was evaluated using taxa of the genus *Stagonosporopsis* according to Chen et al. (2017) and Tibpromma et al. (2017). The combined ML tree (ITS–LSU–*tub2*–*rpb2*) placed isolate UC23 as a sister to a clade with *S. bomiensis* and *S. papillata* (BS = 99) (Fig. 26). Phylogenetic analysis using separate datasets of ITS and LSU placed our isolate UC23 in a cluster comprehending *S. bomiensis*, *S. papillata*, *S. ailanthicola*, and *S. dorenboschii* (data not shown). In the *tub2* tree, isolate UC23 was placed closely related to *S. ailanthicola*, and in the *rpb2* tree it was placed close but separate to *S. bomiensis* and *S. papillata* (data not shown). The *rpb2* sequence is the most in-



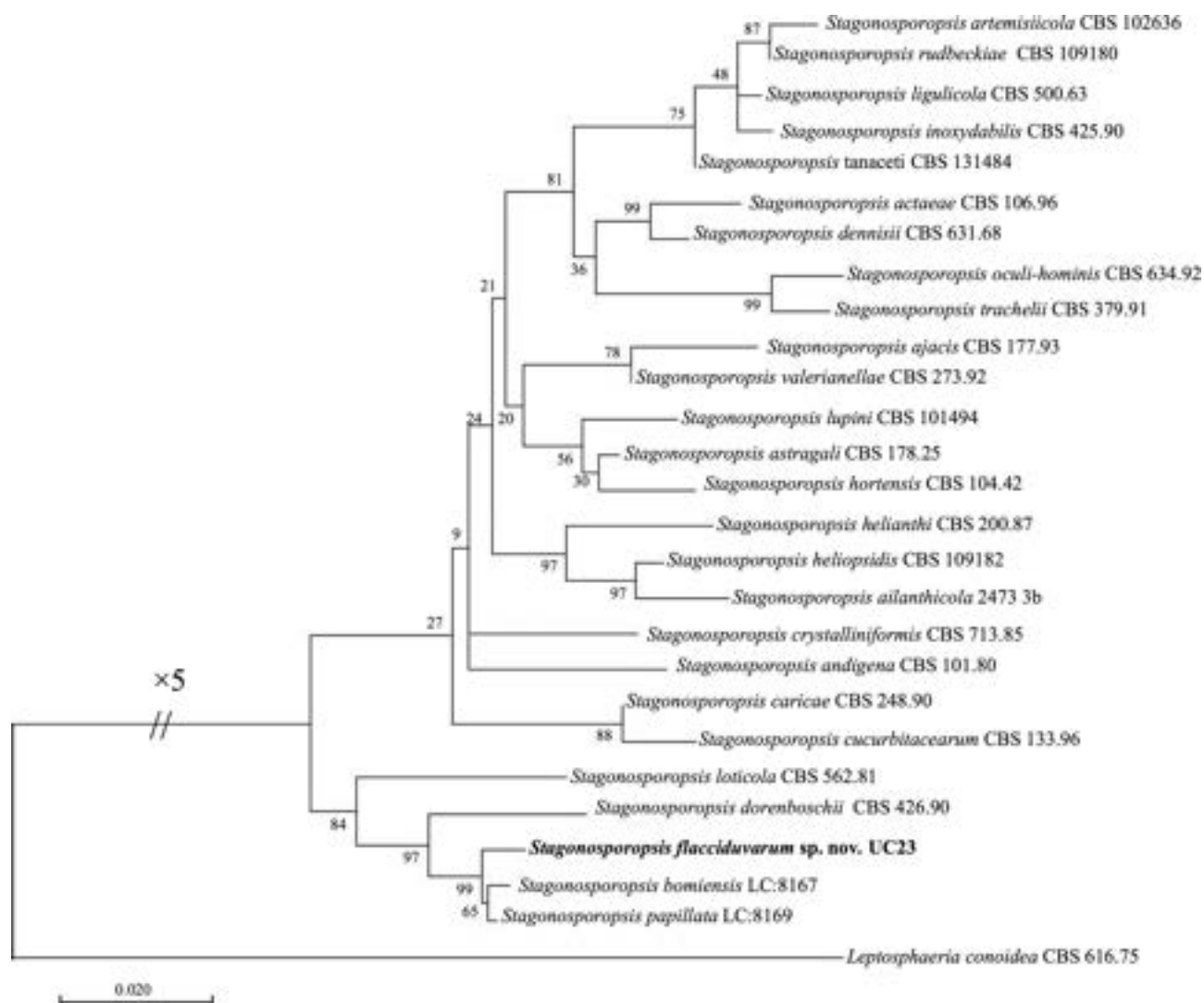


**Fig. 26.** ML phylogenetic tree of *Stagonosporopsis* species, reconstructed from the combined ITS-LSU-*tub2-rpb2* dataset. ML bootstrap support values shown at the nodes. *Leptosphaeria conoidea* served as outgroup.

formative one to differentiate the newly described *S. flacciduvarum* from *S. ailanthicola*, *S. bomiensis*, *S. papillata*, and *S. dorenboschii*.

The taxonomic state of our isolate UC23 was previously unclear (Lorenzini et al. 2016) but is now shown to represent a new species, *S. flacciduvarum*. Phylogenetically, it is related to the recently described species *S. bomiensis* and *S. papillata* (Chen et al. 2017). *Stagonosporopsis flacciduvarum* differs from related species in macro- and micro-morphology. It has a colony texture and color highly different from the holotypes of *S. bomiensis* and *S. papillata* (Chen et al. 2017). Notably, *S. flacciduvarum* does not grow at 30 °C and it has low production of pycnidia and conidia on all tested media. Further, it

differs from *S. bomiensis* and *S. papillata* in its chlamydospores, smaller pycnidia, and slightly smaller conidia (Chen et al. 2017).

Culture and morphological characteristics of *Didymella* and *Nothophoma* isolates. – Growth rate of *D. americana* isolate UC30 on MEA 84–86 mm diam. at 25 °C and 35–41 mm diam. at 30 °C after 7 d; mycelium plane, felted, cream to light brown to; reverse orangish to dark brown. On PDA, growth rate 81–84 mm diam. at 25 °C and 43–46 mm diam. at 30 °C after 7 d; mycelium plane, felted to cottony, light brown; reverse dark. On OA, growth rate 76–84 mm diam. at 25 °C and 31–44 mm diam. at 30 °C after 7 d; mycelium plane, felted, greenish to olivaceous; reverse whitish to greenish. Pycnidia detected only on MEA, subglobose, papillate, melanized. Chlamydospores unicellular, terminally or intercalary, solitary or in chain, smooth, melanized, globose to subglobose, thick-walled. Conidia detected only on MEA, ellipsoidal to ovoid and biguttulate (Tab. 3).

**Tab. 3.** Micro-morphological characteristics of four Didymellaceae strains isolated from withered grapes on different media.

	Media	<i>Didymella americana</i> UC30 (CBS 145105)	<i>Didymella calidophila</i> CG7 (CBS 145107)	<i>Didymella pomorum</i> UC56 (CBS 145106)	<i>Nothophoma quercina</i> S3 (CBS 145109)
Pycnidia (µm)	MEA	(76)89±11(102)×(66)76±8(86)	(65)118±88(330)×(54)93±54(220)	-	(106)135±17(150)×(108)132±19(174)
	PDA	-	(82)192±118(310)×(76)154±78(234)	150-250*	(156)184±29(221)×(112)167±40(200)
	OA	-	(68)172±128(467)×(67)122±67(261)	163-335×151-330*	(127)150±18(178)×(112)147±29(200)
Chlamydospore (µm)	MEA	(16)21±4(26)×(15)20±5(26)	(28)47±12(68)×(17)25±6(33)	20-68×12-25*	-
	PDA	(15)25±8(39)×(18)25±5(33)	(19)24±4(30)×(10)15±2(19)	-	-
	OA	(10)14±3(17)×(8)11±3(15)	(18)33±9(43)×(11)15±3(23)	-	-
Conidia (µm)	MEA	(2.5)3.2±0.4(4)×(1.5)2.2±0.3(3)	(3)4.8±0.7(6.5)×(2)2.9±0.4(3.5)	-	(4)4.8±0.7(7.5)×(2.5)2.9±0.4(4)
	PDA	-	(3.5)4.4±0.4(5.3)×(2)2.7±0.4(3.5)	(2.5)2.7±0.3(3.5)×(1.5)1.5±0.1(2)	(4.5)5.8±0.5(8.5)×(2.5)3.4±0.4(4)
	OA	-	(3)4.3±0.7(6)×(1.5)2.4±0.5(3.5)	-	(3.5)4.8±0.5(5.5)×(2)2.8±0.3(3.5)

\* Measure detected on n<4 of structures.

Growth rate of *D. calidophila* isolate CG7 on MEA 60–62 mm diam. at 25 °C and 22–24 mm diam. at 30 °C after 7 d; mycelium plane, felted, brown; reverse cream to light brown. On PDA, growth rate 62–64 mm diam. at 25 °C and 23–31 mm diam. at 30 °C after 7 d; mycelium and reverse orange to brown. On OA, growth rate 55–59 mm diam. at 25 °C and 20–21 mm diam. at 30 °C after 7 d; mycelium felted, olivaceous to dull black; reverse whitish to olivaceous. Pycnidia subglobose to oblong, papillate and solitary, exuding light brown conidial ooze only on PDA. Chlamydospores abundant and multicellular-dictyo/phragmospores, smooth or irregular roughened, light to dark brown. Conidia oblong, ovoid, biguttulate sometimes eguttulate (Tab. 3).

Growth rate of *D. pomorum* isolate UC56 on MEA 75–77 mm diam. at 25 °C and 31–48 mm diam. at 30 °C after 7 d; mycelium plane, felted, light brown; reverse orangish to brown. On PDA, growth rate 81–84 mm diam. at 25 °C and 26–35 mm diam. at 30 °C after 7 d; mycelium plane, felted, cream to brownish; reverse light brown to brown. On OA, growth rate 73–79 mm diam. at 25 °C and 27–33 mm diam. at 30 °C after 7 d; mycelium plane, light brown to olivaceous; reverse whitish to cream. Pycnidia globose to subglobose. Chlamydospores multicellular-dictyo/phragmospores, tick-walled, irregular roughened, brown, terminal, mostly intercalary. Conidia oblong. Pycnidia, chlamydospores and conidia scarcely detected on all media (Tab. 3). Hyphae coils detected on all media.

Growth rate of *N. quercina* isolate S3 on MEA 41–44 mm diam. at 25 °C and 22–30 mm diam. at 30 °C after 7 d; mycelium plane, felted, cream to brown; reverse cream to brown. On PDA, growth rate 55–57 mm at 25 °C and 24–28 mm at 30 °C after 7 d; mycelium plane, felted, light to dark brown; reverse cream to pale or dark brown. On OA, growth rate 64–66 mm at 25 °C and 26–30 mm at 30 °C after 7 d; mycelium white, abundant black pycnidia scattered over the medium in concentric rings; reverse white. Pycnidia mostly solitary, pale to dark brown, globose to subglobose, peroblate to subperoblate, with single, conspicuous, non-papillate ostiole, exuding light (on MEA) and dark brown conidial ooze (on PDA and OA). Chlamydospores not detected. Conidia subglobose to ovoid, thin walled, smooth and aseptate (Tab. 3).

*Authors:* M. Lorenzini & G. Zapparoli

## Basidiomycota, Agaricomycetales, Boletales, Boletaceae

*Strobilomyces huangshanensis* L.H. Han & T. Guo, **sp. nov.** – Figs. 27–29

Mycobank no.: MB 832764

**Holotypus.** – CHINA. Anhui Province, Huangshan, Tangkou Town, on the ground in a mixed forest of Fagaceae, Pinaceae, and Theaceae, 12 July 2018, *leg.* T. Guo, T. Guo 969 (HKAS 102613; holotype). Sequences ex-holotype: MK329213 (*rpb1*), MK329217 (*rpb2*), MK329219 (*tef1*), MK329215 (*cox3*).

**Description.** – **Pileus** 1.5–4.5 cm in diam., initially convex, then appanate, surface dry, covered with black (5F1), thin, appressed pyramidal scales, 3–5 mm in diam. at base, background dirty white (5A1); margin appendiculate with dirty white (5A1) to grayish (5B1) irregularly fragmented veil remnants; context white (8A1) when young, staining light rusty red (7A2) then black (10E1) when bruised. – **Tubes** up to 3–9 mm long, adnate with decurrent tooth, dirty white (6A1) then fuliginous (9E2) with age; pores angular, 0.5–1 mm in diameter; pores and tubes concolorous, whitish (13A1) then fuliginous (9E2), immediately staining rusty red (6C7) then black (10F3) on exposure or bruising. – **Stipe** 3.0–9.0 cm long, 0.4–1.7 cm in diam., subcylindrical, curved; surface reticulate with shallow and elongate meshes on the upper part, entirely covered with clustered tomentose scales, concolorous with the pileal scales; context white (8A1), changing into light rusty red (6B2) when bruised; annulus absent; basal mycelium dirty white (4B1). – **Basidia** 28–40 × 13–17 µm, clavate, four-spored; sterigmata 4–7 µm long. – **Basidiospores** [80/4/2] 8.5–10(10.5) × 7.5–8.5(9) µm (Q = 1.06–1.25, Qm = 1.17 ± 0.06) excluding ornamentation, subglo-



**Fig. 27.** *Strobilomyces huangshanensis*, HKAS 102613 (holotype). **A.** Basidiomata. **B.** Hymenophore. Photos: T. Guo. Scale bars = 1 cm.

base to broadly ellipsoid, dark brown (6D4) in 5 % KOH solution, reticulate with meshes 1.5–2.5  $\mu\text{m}$  in diameter and 1–2  $\mu\text{m}$  high; apiculus 0.5–1  $\mu\text{m}$  long, with a smooth adaxial patch. – Hymenophoral trama boletoid; hyphae cylindrical, 5–8  $\mu\text{m}$  in diameter. – Cheilocystidia 32–58  $\times$  16–20  $\mu\text{m}$ , numerous, fusiform to narrowly fusiform, hyaline or with brownish (5D6) plasmatic pigment, thin-walled. – Pleurocystidia 32–56  $\times$  15–22  $\mu\text{m}$ , narrowly fusiform to broadly fusiform, thin-walled. – Pileipellis an intricate trichodermium, composed of 8–14  $\mu\text{m}$  wide cylindric hyphae with short

obtuse terminal cells; cell wall dark brown (6E8), slightly thickened (< 1  $\mu\text{m}$ ). – Pileal trama composed of 5–9  $\mu\text{m}$  wide interwoven hyphae. Hyphae of scales on stipe similar to those on pileus. – Stipe trama composed of 5–10  $\mu\text{m}$  wide cylindric hyphae. – Clamp connections absent from all hyphae.

**Etyymology.** – Referring to the type location, Huangshan.

**Habitat and distribution.** – Currently only known from eastern China, in a mixed forest of Fagaceae, Pinaceae, and Theaceae.

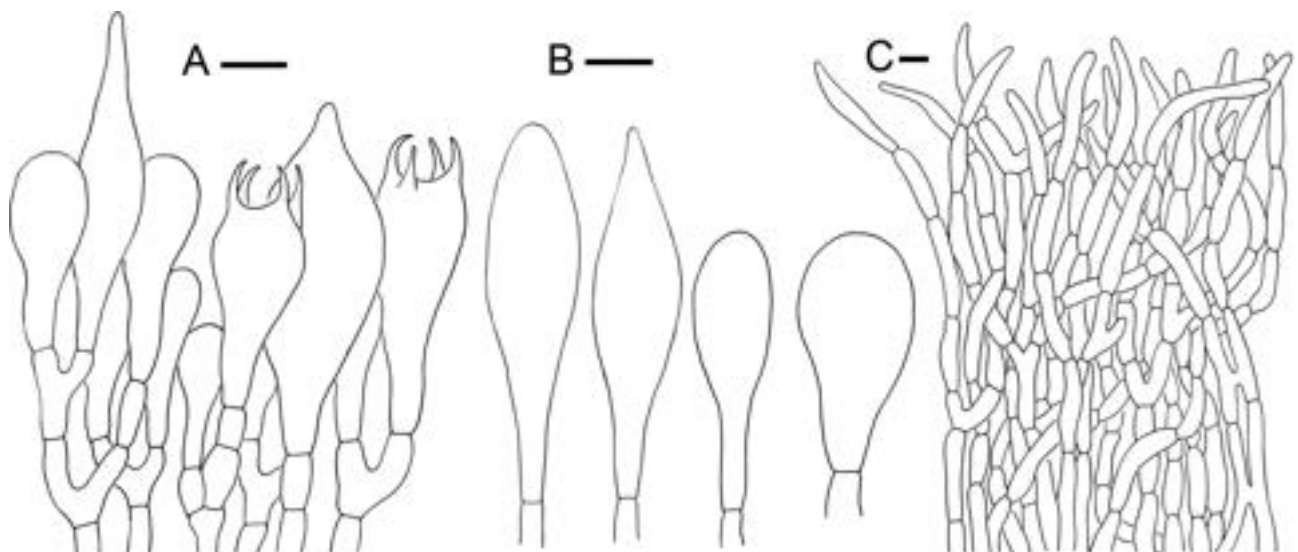


**Fig. 28.** Microscopic characters of *Strobilomyces huangshanensis*, HKAS 102613 (holotype). **A.** Basidia and pleurocystidia. **B.** Cheilocystidia. **C.** Pileipellis. Scale bars 10  $\mu\text{m}$ , del. L.H. Han.

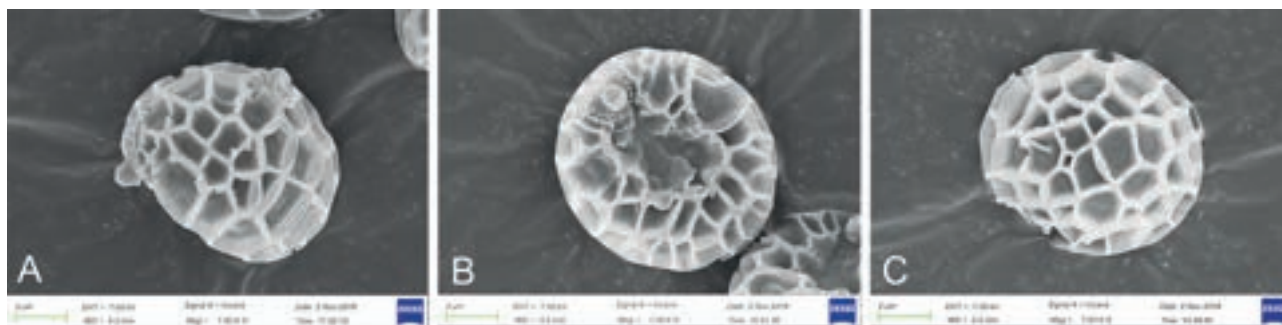


**Fig. 29.** Basidiospores of *Strobilomyces huangshanensis* under scanning electron microscope.

Additional material examined. – *ibid.*, T. Guo 957 (HKAS 102612).

**Notes.** – *Strobilomyces* Berk. is one of the genera of the Boletaceae and appears to have a worldwide distribution (Berkeley 1851, Singer 1986). It is a monophyletic lineage sister to *Afroboletus* (Nuhn et al. 2013, Wu et al. 2014, Han et al. 2018a). *Strobilomyces* is characterized by ornamented basidiospores, blackish to brownish yellow basidiomata, and context turning reddish or blackish when cut (Sato et al. 2007, 2011, 2017; Wu et al. 2014; Han et al. 2017, 2018a, 2018b). East Asia is considered as a center of species diversity of *Strobilomyces* (Han et al. 2018a). Representative species of this genus from East Asia have been published in several studies (Berkeley 1851; Chiu 1948; Corner 1972; Hongo 1982; Ying & Ma 1985; Ying 1986; Wen & Ying 2001; Sato & Murakami 2009; Gelardi et al. 2013; Antonín et al. 2015; Terashima et al. 2016; Han et al. 2018a, 2018b). In China, a thorough investigation on *Strobilomyces* has been carried out recently. So far, at least 18 known species and eight potential new spe-

cies of this genus have been reported (Han et al. 2018a, 2018b).

*Strobilomyces huangshanensis* is characterized by its tiny to small basidiomata (1.5–4.5 cm in diam.); pileus with black, thin, appressed pyramidal scales; stipe with black tomentose scales; small pores (0.5–1 mm in diam.); subglobose to broad ellipsoid spores (8.5–10 × 7.5–8.5 μm) with medium-sized meshes (1.5–2.5 μm in diam.); light rusty red discoloration of the context on exposure; and subtropical distribution in eastern China. Phylogenetically, *S. huangshanensis* occupies a relatively isolated position. Morphologically, *S. huangshanensis* is similar to *S. echinocephalus*, *S. glabriceps*, and *S. parvirimosus*. However, the scales on the pileus of *S. echinocephalus* and *S. parvirimosus* are thicker than those of *S. huangshanensis* (Ying 1986, Gelardi et al. 2013). The basidiomata of *S. glabriceps* possess blackish brown scales (Chiu 1948). The meshes of basidiospores of *S. echinocephalus* and *S. glabriceps* (2–3.5 μm in diameter) are larger than those of *S. huangshanensis* (Chiu 1948, Gelardi et al. 2013).

**Tab. 4.** The best partition schemes and models evaluated by PartitionFinder for the combined four-locus *Strobilomyces* dataset.

Subsets in the best-fit partition scheme	Base positions of each subset	Best-fit Model
<i>rpb1_codon1</i> , <i>tef1_codon1</i>	247–500\3, 532–657\3, 1324–1500\3, 1555–1691\3, 1741–1934\3	TVM+G
<i>rpb1_codon2</i>	248–500\3, 533–657\3	TIMEF+I+G
<i>rpb2_codon1</i>	658–1323\3	TVM+G
<i>rpb2_codon2</i>	659–1323\3	TIM+I
<i>rpb2_codon3</i>	660–1323\3	F81+I
<i>tef1_codon3</i> , <i>cox3_codon3</i>	1326–1500\3, 1557–1691\3, 1743–1934\3, 1937–2512\3	K81UF+I+G
<i>tef1_codon2</i>	1325–1500\3, 1556–1691\3, 1742–1934\3	GTR+G
<i>cox3_codon1</i>	1935–2512\3	HKY+G
<i>cox3_codon2</i>	1936–2512\3	TIM+G
intron	1–246, 501–531, 1501–1554, 1692–1740	K81UF+I+G

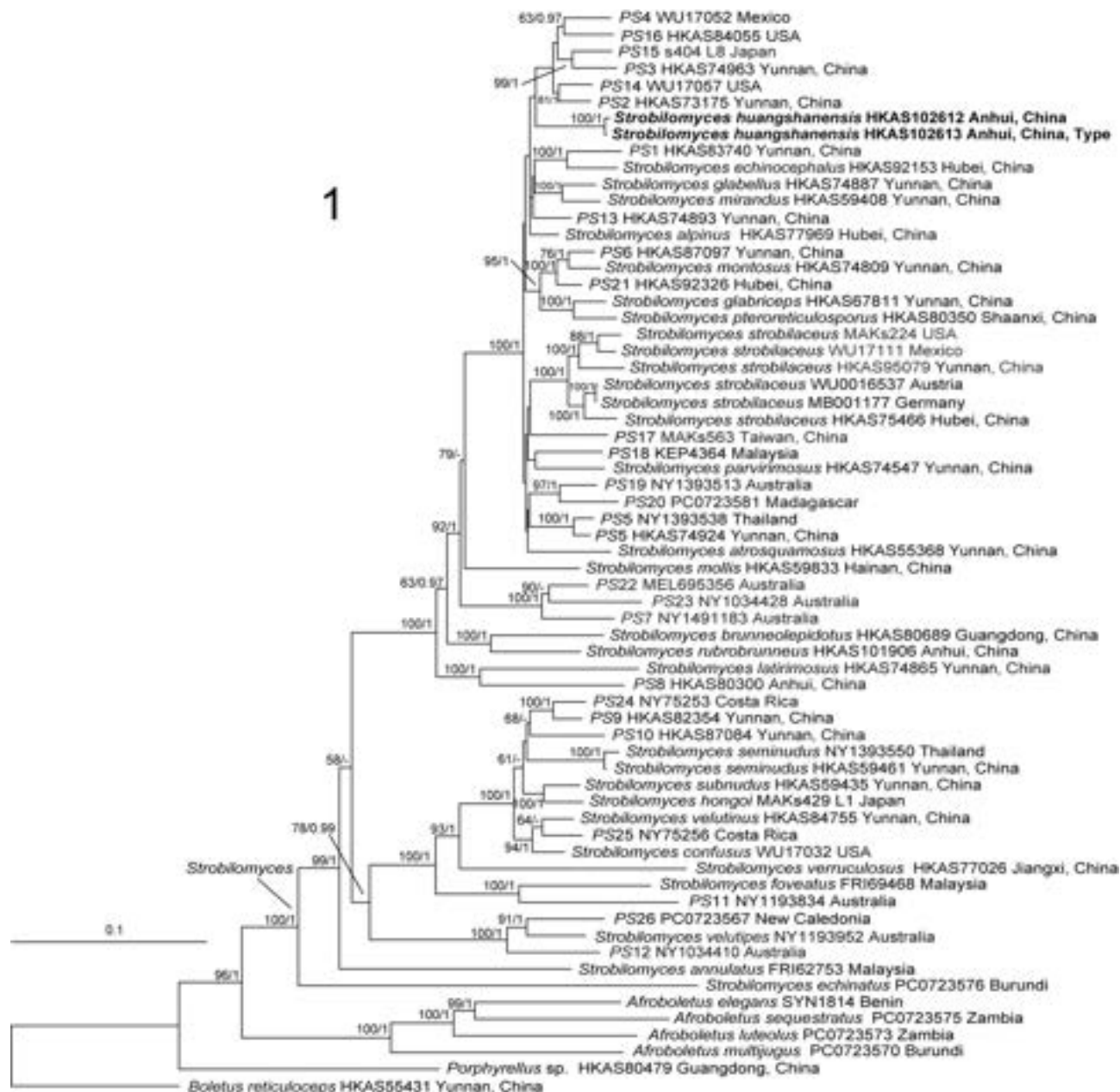


**Fig. 30.** ML phylogenetic tree reconstructed from a four-locus dataset (*rpb1*, *rpb2*, *tef1*, and *cox3*). ML bootstrap support  $\geq 50$  and BI posterior probabilities  $\geq 0.95$  shown at the nodes. *Strobilomyces huangshanensis* sp. nov. shown in boldface.

In our combined *rpb1*–*rpb2*–*cox3*–*tef1* dataset, a total of 2512 bp were included, of which 1030 were conserved, 1076 variable, and 360 parsimony-informative. Eleven subsets were estimated by the best partition schemes and the best-fit models based on PartitionFinder 2.1.1 (Tab. 4). The topology of phylogenetic trees generated from ML and BI analyses are similar, whereas statistical support differs

slightly. Only the phylogram with branch lengths inferred from ML is presented (Fig. 30). The phylogenetic analysis revealed that the samples collected from China represent an independent lineage differing from all other known species with high support, described above as *S. huangshanensis*.

*Authors:* L.H. Han, T. Guo, X.L. Tian, H.L. Chu, R.H. Yang, W. Qian, C. Liu & L.Z. Tang

**Basidiomycota, Pucciniomycetes, Pucciniales, Pucciniaceae**

*Uromyces klotzschianus* Ali, sp. nov. – Figs. 31–32  
MycoBank no.: MB 830188

**Diagnosis.** – Different from other *Uromyces* species by its echinulate urediniospores, lack of papilla, short and thick pedicel, and the host plant (*Rumex dentatus* subsp. *klotzschianus*).

**Holotypus.** – PAKISTAN. Punjab Province, Islamabad, Quaid-i-Azam University, on living leaves of *Rumex dentatus*, 33°28'57.24" N, 74°02'01.95" E, 550 m a.s.l., 10 April 2015, leg. B. Ali, BA91,93 (ISL-45963; holotype). Sequences ex-holotype: MF044015 (ITS), MF044017 (LSU).

**Description.** – Uredinia amphigenous, circular, pulverulent, cinnamon brown, surrounded by pale yellowish rings, scattered in groups with telia, 0.4–2.0 mm in diam. – Urediniospores globose, subglobose, or ovoid, 20–28 × 20–23 µm, light brown to pale yellowish brown, echinulate, germ pores obscured, wall 3–4 µm, cinnamon brown to yellowish brown. – Telia amphigenous, circular, pulverulent, brown, scattered in groups and mixed

with uredinia, 0.5–1.5 mm in diam. – Teliospores single celled, globose to ellipsoidal, chestnut brown, 22–33 × 22–28 µm, apex and base rounded or base slightly narrower than apex, smooth walled, 5 µm thick, no papilla; pedicel cylindrical, sometimes wider at apex, hyaline, 7.5–12.5 µm in length, persistent. Stages II and III of the life cycle occur on same host. – Spermogonia, pycnia, and aecia not observed.

**Etymology.** – Referring to the host plant, *Rumex dentatus* subsp. *klotzschianus*.

**Habitat and distribution.** – Only known from Pakistan (Punjab Province and Azas Jammu and Kashmir Region), on living leaves of *Rumex dentatus* (Polygonaceae).

**Additional material examined.** – PAKISTAN. Azad Jammu and Kashmir Region, District Kotli, on living leaves of *Rumex dentatus*, 33°28'57.24" N, 74°02'01.95" E, 830 m a.s.l., 15 July 2015, leg. B. Ali, BA92 (ISL-45965; paratype).

**Notes.** – Rust fungi (Pucciniales) constitute one of the largest and speciose groups of basidiomycota with over 8,000 species in more than 100

**Tab. 5.** Morphological characters of *Uromyces* species on *Rumex*.

<i>Uromyces</i> species	Host species	Life spore stages	Urediniospores (µm)	Wall (µm)	Teliospores (µm)	Wall (µm)	Pedicel (µm)	Reference
<i>U. acetosae</i>	<i>Rumex</i> spp.	Pycnia, aecia, uredinia, and telia	17–20 × 17–22	Verrucous	23–25 × 19–24	no papilla	Long, deciduous	Saccardo (1888)
<i>U. alpinus</i>	<i>R. alpinus</i> , secondary host <i>Ranunculus</i>	Pycnia, aecia, uredinia and telia	20–26 × 18–22	Light brown, echinulate	28–35 × 11–15	Apex 5 high, very pale brownish, wall dotted or striped	No data	Cohn (1876)
<i>U. borealis</i>	<i>R. alpestris</i>	Pycnia, aecia, uredinia and telia	No data	Verrucous	24–30 × 12–16	With papilla	Very short	Tiedesura (1861), Peck (1881)
<i>U. crassipes</i>	<i>Rumex</i> spp.	Uredinia and telia	25–33 × 18–28	Echinulate	30–40 × 20–30	Yellowish brown, Apex thick (4–8)	Short, about 20, thick	Engler (1904)
<i>U. klotzschianus</i>	<i>Rumex dentatus</i>	Uredinia and telia	20–28 × 20–23	3–4, cinnamon brown to yellowish brown, echinulate	22–33 × 22–28	5, no papilla, chestnut brown	8–13, persistent	Present study
<i>U. polygoni-avicularis</i>	different genera of Polygonaceae including genus <i>Rumex</i>	Aecia, uredinia, and telia	18–24 × 20–29	1.5–3.5, golden brown to cinnamon brown, verrucose	18–24 × 22–31 (–35)2–3	no papilla, apex 4–6, golden brown to chestnut brown	Yellowish or brownish, 8–10 × 90–104, persistent	Afshan et al. (2011), Farr & Rossman (2019)
<i>U. rickerianus</i>	<i>R. geyeri</i>	Aecia, uredinia and telia	17–20 × 17–22	Verrucous	20–25 × 23–35	Apex little thick, no papilla	Very short, deciduous	Saccardo (1905)
<i>U. rumicis</i>	<i>Rumex</i> spp., often <i>R. crispus</i> , secondary host <i>Ranunculus</i>	Pycnia, aecia, uredinia, and telia	20–28 × 18–24	Hyaline to pale yellowish brown, echinulate	24–35 × 18–24	Rather thick, with papilla	Very short, thin, deciduous	Shivas (1987)
<i>U. thellungi</i>	<i>R. vesicarius</i>	Uredinia and telia	24–33 × 21–27	3, light brown, verrucous	22–28 × 20–24	2–3, with papilla, apex thick (up to 7), brown.	Up to 120, persistent	Maire (1917)
<i>U. tingitanus</i>	<i>R. tingitanus</i>	Aecia, uredinia, and telia	17–20 × 17–22	Verrucous	20–38 × 17–22	10, with papilla	180 × 4–5, persistent	Saccardo (1905)

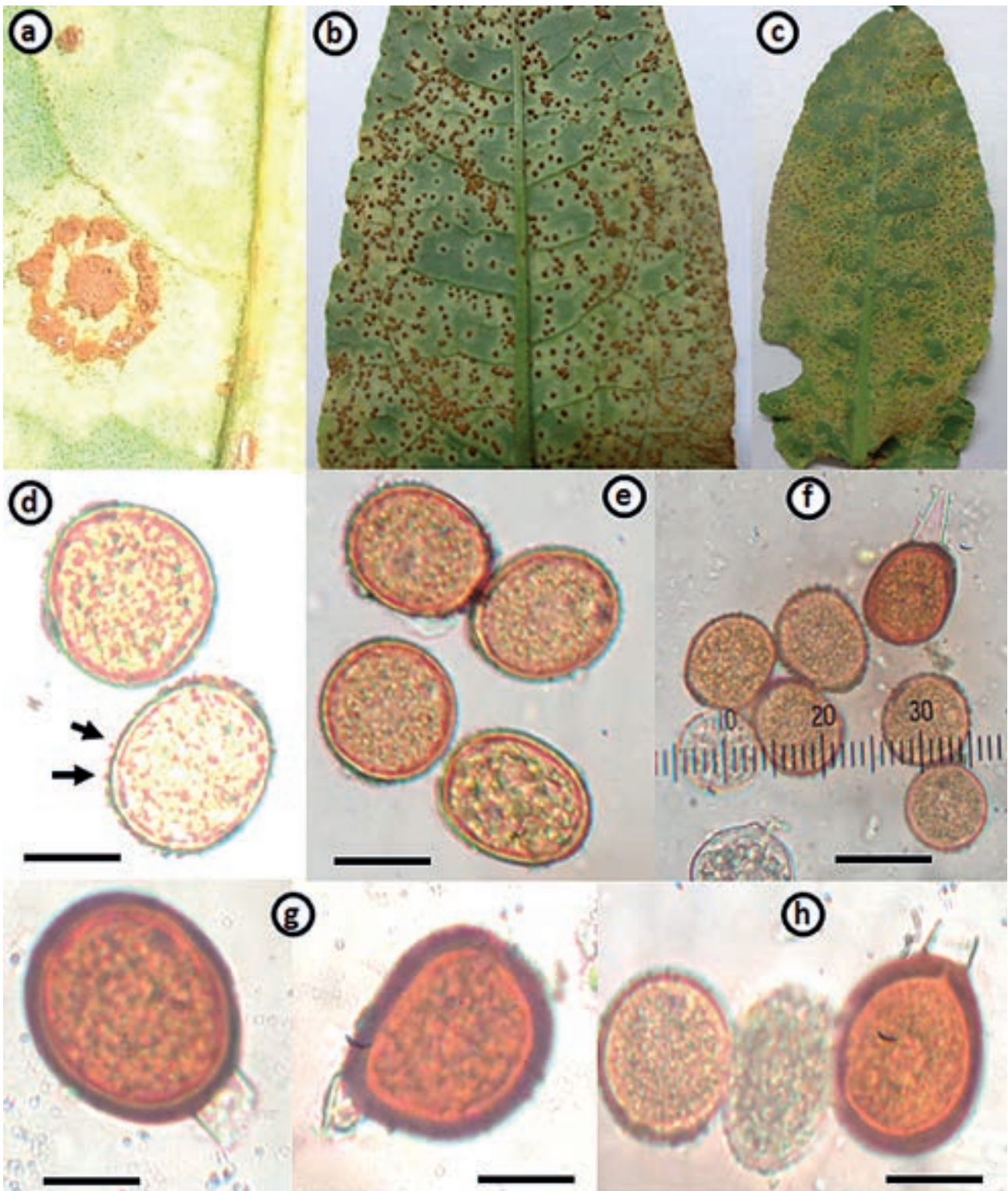


**Fig. 31.** *Uromyces klotzschianus*, ISL-45963 (holotype). **a.** Abaxial view of infected *Rumex dentatus* leaf showing uredinial sorus characterized by two symptomatic rings. **b.** Abaxial view of leaf illustrating mixed uredinial and telial sori. **c.** Adaxial view showing mixed uredinial and telial sori. **d–e.** Urediniospores showing echinulate ornamentation (arrows). **f.** Urediniospores with teliospore indicating that they occur together. **g–h.** Teliospores with chocolate brown epispore and short hyaline pedicel. Scale bars d–f 40  $\mu\text{m}$ , g–h 20  $\mu\text{m}$ .

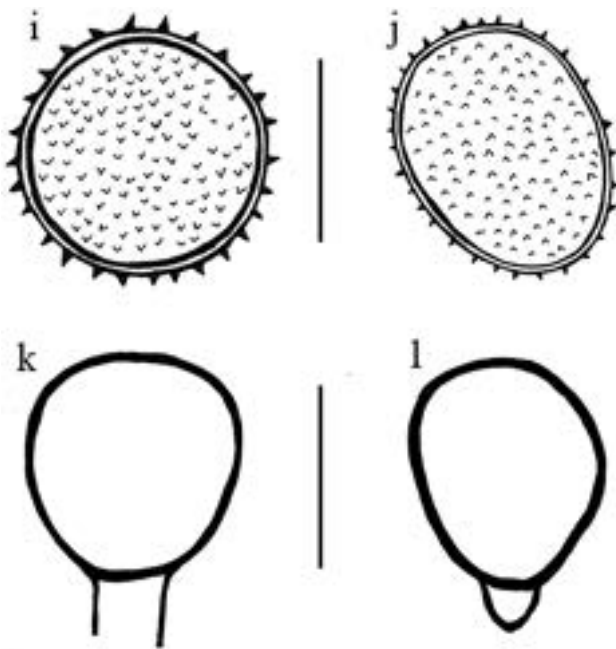


**Fig. 32.** *Uromyces klotzschianus*. i–j. Echinulate urediniospores. k–l. Teliospores with smooth wall and short pedicel. Scale bars 20  $\mu$ m, *del.* B. Ali.

genera (Toome-Heller 2016, Aime et al. 2017, Ali et al. 2017a). The genus *Uromyces* (Link) Unger is the second largest group after *Puccinia* Pers. ex Pers. and contains around 600 species (Cummins & Hiratsuka 2003), with over 64 species reported from Pakistan. *Uromyces* can be distinguished from *Puccinia* by one- or seldom two-celled teliospores (McAlpine 1906, Cummins & Hiratsuka 2003, Van der Merwe et al. 2007). Recent phylogenetic studies clearly separated the genus *Uromyces* from *Puc-*

*cinia* (Aime 2006, Maier et al. 2007, Van der Merwe et al. 2007).

Nine species of *Uromyces* are described from *Rumex* L. and the type species is *Uromyces rumicis* (Schum.) Wint. (Farr & Rossman 2019). Only two *Uromyces* species are reported from Pakistan: *U. rumicis* on *R. chalepensis* Mill. and *U. thellungi* Maire. on *R. vesicarius* L. (Afshan et al. 2015). *Rumex*-infecting *Uromyces* species include both autoecious and heteroecious species, e.g., *U. rumicis* and *U. alpinus* (heteroecious) vs. *U. thellungi* (autoecious). Although autoecious rust species may not occur on a single host, there is also a possibility that the pycnial and aecial stages are overlooked or still undiscovered.

The taxonomy of *Uromyces* rusts infecting *Rumex* spp. is not sufficiently resolved as there are no descriptions and illustrations of some species, while scanty and old literature hampers meaningful taxonomic studies of these species. For instance, *U. appendiculatus* (Pers.) Unger var. *punctiformis* (syn. *U. punctiformis* Syd. & P. Syd.) was only reported from the holotype *Ramarizella strobiliformis* (B. L. Rob.) Rose (syn. *Vigna strobiliphora*), whereas it is reported on *R. hymenosepalus* only in an annotation statement in the USDA fungal database (Farr & Rossman 2019). Similarly, there is no description available for *U. argaeus* (Inman 1970).

*Uromyces polygona-avicularis* (basionym *U. polygona*) has been reported from different genera of Polygonaceae, including *Rumex* (Farr & Rossman 2019). This rust species is distinguished from *U. klotzschianus* by its verrucose urediniospores, yellowish or brownish, and thicker pedicels (90–104  $\mu$ m) (Afshan et al. 2011) as well as its distinct

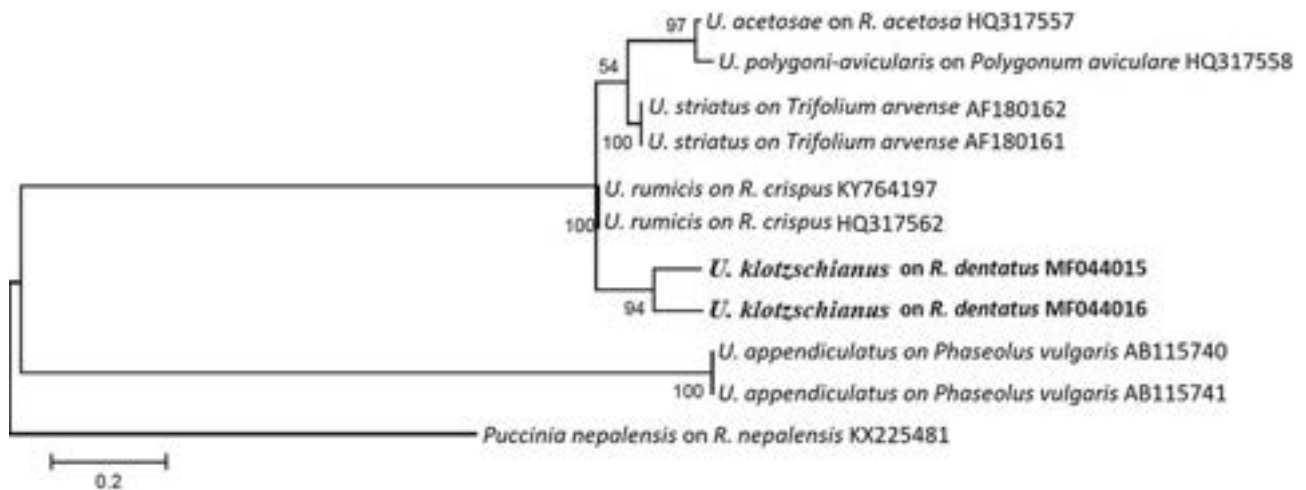


**Fig. 33.** ML phylogenetic reconstruction of the ITS dataset. Bootstrap values for 1000 replicates shown at nodes. New sequences highlighted in boldface.



phylogenetic position (Fig. 33). *Uromyces rumicis* is a heteroecious macrocyclic rust fungus, infecting different species of *Rumex* as primary hosts and *Ranunculus* as secondary host (Inman 1970, Afshan et al. 2015, Farr & Rossman 2019). This species has been reported from many countries including Pakistan (Farr & Rossman 2019). *Uromyces klotzschianus* differs from *U. rumicis* in lacking papilla and by its rather thin urediniospore cell wall and the thick, persistent pedicel (Inman 1970). Moreover, both species formed well-supported clades in the ML analysis (Fig. 33).

*Uromyces thellungi* Maire. on *R. vesicarius* can be distinguished from *U. klotzschianus* by its verrucous urediniospores, teliospores with papilla and thick apex (up to 7 µm), and a longer pedicel (up to 92 µm) (Maire 1917, Afshan et al. 2015). *Uromyces acetosae* Schröt. was described from different species of *Rumex* and is also morphologically different from the new species: it has verrucous urediniospores and a long and deciduous pedicel (Saccardo 1888). *Uromyces acetosae* is also a distinct species based on the ML tree, where it is placed sister to *U. polygoni-avicularis*. This artificial affiliation is probably due to the short ITS sequence of *U. acetosae* in GenBank (207 bp, only ITS2). *Uromyces alpinus* J. Schröt. on *R. alpinus* is delimited from *U. klotzschianus* by its hypophyllous uredinia and telia as well as striped or dotted teliospores (Cohn 1876).

*Uromyces borealis* Liro. was reported only from *R. alpestris* (= *R. arifolius*) and is distinct from *U. klotzschianus* due to the presence of epiphyllous telia, teliospores with papilla, and very short pedicels (Tiedeseura 1861, Peck 1881, Inman 1970). Peck (1881) described *U. borealis* on *Hedysarum boreale* and *H. mackenzii*, but Inman (1970) listed this species on *R. alpestris* who cited Sydow (1902–1924) for the description. *Uromyces crassipies* D. & Neg. infects several *Rumex* species and is characterized by a yellowish brown teliospore wall with a thick apex (4–8 µm) and pedicel (about 20 µm long) (Engler 1904, Farr & Rossman 2019). *Uromyces tingitanus* Henn. on *R. tingitanus* can be distinguished from *U. klotzschianus* due to aecia mixed with uredinia, thick teliospore wall (10 µm) with papilla, and longer pedicels (up to 120 µm). *Uromyces rickerianus* Arth. on *R. geyeri* is different from *U. klotzschianus* by verrucous urediniospores and verrucose teliospores with deciduous pedicel (Saccardo 1905). A comparison of characters is presented in tabular form (Tab. 5).

The host plant of *U. klotzschianus*, *Rumex dentatus* L. (Caryophyllales, Polygonaceae), commonly

known as toothed dock or Aegean dock, is a small annual herb native to some regions in Eurasia and North Africa. In Asia, *R. dentatus* naturally occurs in Afghanistan, China, India, Iran, and Pakistan. In Pakistan, *R. dentatus* is common and mainly occurs in Hazara, Peshawar, Quetta, Ziarat, Waziristan, Parachinar, Kashmir, Rawalpindi, and Islamabad, where it is represented by the subspecies *klotzschianus* (Meisn). Rech. f. (Abbasi et al. 2011).

*Authors:* B. Ali, N.A. van der Merwe & A.S. Mumtaz

### Interesting taxonomical notes, new hosts, and geographical records

#### Ascomycota, Dothideomycetes, Pleosporales, Pleosporaceae

*Alternaria calendulae* Ondřej, Čas. slezsk. Mus. Opavě, Ser. A 23(2): 150 (1974). – Fig. 34

**Material examined.** – Towards the end of February 2018, severe outbreaks of *Alternaria* leaf spot were observed in six different *Calendula officinalis* (Asterales, Asteraceae) gardens on the Bidhan Chandra Krishi Viswavidyalaya university campus, West Bengal, India. The disease began as small sized water-soaked light brown-purple spots, mostly surrounded by yellow halos that gradually enlarged up to 1.5 cm in diam., changing to grey-dark brown, circular to irregular lesions with characteristic concentric rings followed by chlorosis and complete marginal or tip blighting (Fig. 34a). In humid environment, black, dusty conidial masses developed around the spotted regions.

**Culture characteristics.** – One distinct dematiaceous fungus was consistently recovered by single spore isolation technique from surface-sterilized (1 % NaOCl) sections of symptomatic leaf tissue onto 2 % (w/v) water agar containing 0.5 mg/l of chloramphenicol and subsequent sub-culturing on potato dextrose agar (PDA). For conidial production, the fungus was grown on potato carrot agar (PCA) under a 12 h/12 h dark/light photoperiod at 25 °C. Fungal colonies had a dark olive colour on both sides, with loose, cottony mycelium on the surface of cultures. One representative culture was deposited at NFCCI (Agharkar Research Institute, Pune, India).

**Notes.** – On the host, conidiophores were simple or in groups, septate, brown, 50–150 × 5–8 µm; conidia ellipsoid to broadly ellipsoid, with one beak extension, light to tawny brown, 50–120 × 10–20 µm, with 8–12 transverse and 1–4 longitudinal septa,



**Fig. 34.** *Alternaria calendulae* in India. **a.** Necrotic leaf spots followed by leaf tip and marginal blighting of *Calendula officinalis* caused by *Alternaria calendulae*. **b.** Spore morphology of *A. calendulae*. Scale bar = 50  $\mu$ m. **c.** Development of leaf spot symptoms following artificial spray inoculation of *A. calendulae* on *C. officinalis* in greenhouse conditions.

the apical beaks 50–165  $\mu$ m long and taper from base to apex. Average dimension of conidia in PCA were 40–110  $\times$  15–25  $\mu$ m (Fig. 34b). Morphologically, the causal agent was determined as *Alternaria* sp. (Ellis 1971). In addition, DNA was extracted from mycelia of the isolated fungus and the ITS region was amplified using primers ITS1 and ITS2 (White et al. 1990). A representative PCR product of one isolate was sequenced and submitted to GenBank under accession number MN365720. This sequence was 99–100 % similar to existing sequences of *A. calendulae*. As a result, the isolates were identified as *A. calendulae*.

Pathogenicity tests were conducted to confirm Koch's postulates, by spraying healthy leaves of three-month old *C. officinalis* plants with a spore suspension of  $10^6$  conidia/ml. *Alternaria calendulae* spores were suspended in 0.1 % Tween 80 and sprayed onto leaves until run-off. Control plants were sprayed with a sterile 0.1 % Tween 80 mixture until run-off. Plants were covered by polyethylene bags for 3 d to achieve high humidity levels, and incubated in a greenhouse at 25 °C. After seven d, spots similar to those observed in the field appeared on the leaves of inoculated plants (Fig. 34c), whereas control plants remained symptomless. Isolations made from diseased spots consistently yielded *A. calendulae*. Host range studies including *Ageratum*, *Dahlia*, *Helianthus*, *Tagetes*, and *Zinnia* plants (all in the family Asteraceae) revealed that the fungus was pathogenic to *Calendula* but did not infect other genera.

*Alternaria calendulae* is known as a destructive disease and is recorded worldwide. There are previous reports of *A. calendulae* on *Calendula* in Germany (Nirenberg 1977), the Czech Republic (Ondřej 1996), Korea (Yu 2001), and Iran (Taheriyani et al.

2014). To our knowledge, this is the first report of *A. calendulae* on *Calendula officinalis* in India.

*Authors:* A. Banerjee & P. Sarathi

#### Ascomycota, Dothideomycetes, Pleosporales, Pleosporaceae

*Alternaria tenuissima* (Kunze) Wiltshire, Trans. Br. mycol. Soc. 18(2): 157 (1933). – Fig. 35

*Basionym.* – *Helminthosporium tenuissimum* Kunze [as '*Helmsporium*'], in Nees & Nees, Nova Acta Phys.-Med. Acad. Caes. Leop.-Carol. Nat. Cur. 9: 242 (1818).

*Synonyms.* – *Alternaria godetiae* (Neerg.) Neerg., Aarsberetn. J. E. Ohlens Enkes plantepatol. Lab. 1 April 1944–31 Juli 1945: 14 (1945). *Alternaria tenuissima* var. *alluicola* T.Y. Zhang, Mycotaxon 72: 450 (1999). *Alternaria tenuissima* var. *godetiae* Neerg., Trans. Br. mycol. Soc. 18(2): 157 (1933). *Alternaria tenuissima* var. *verruculosa* S. Chowdhury, Proc. natn. Acad. Sci. India, Sect. B, Biol. Sci. 36(3): 301 (1966). *Clasterosporium tenuissimum* (Kunze) Sacc., Syll. fung. (Abellini) 4: 393 (1886). *Macrosporium tenuissimum* (Kunze) Fr., Syst. mycol. (Lundae) 3(2): 374 (1832).

*Material examined.* – IRAN. Mazandaran Province, Nour City, on apple and quince fruits (Fig. 35), 15 September 2015, leg. L. Ebrahimi (IRAN 2428 C).



**Fig. 35.** Fruits with *Alternaria* rot symptoms. **a.** Quince (*Cydonia oblonga*) with black rot disease. **b.** Apple (*Malus domestica*, Golden delicious) with brown rot diseases.

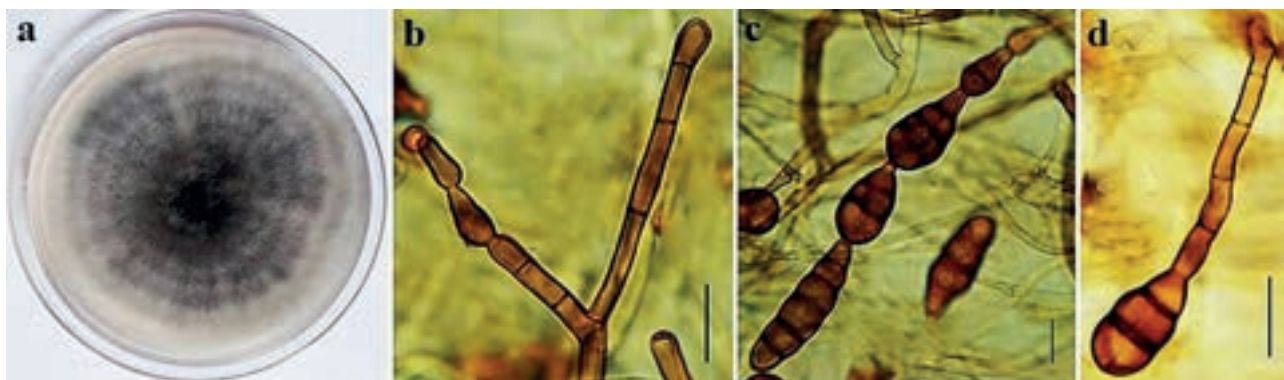


**Fig. 36.** Morphology of *Alternaria tenuissima*. **a.** After 7 d on PCA at 25 °C in 8 h fluorescens light/16 h dark cycle. **b.** Primary conidiophores. **c.** Conidial chain. **d.** Secondary conidiophore. Scale bars 10  $\mu$ m.

**Description.** – Description of colony on PCA – Mycelium superficial, consisting of branched, septate, hyaline and smooth hyphae. – Primary conidiophores brown, simple or branched or with one to several geniculations, (7)13–90  $\times$  4  $\mu$ m [37.12  $\times$  4  $\mu$ m], producing ovoid or ellipsoidal conidia in the branched chain. – Conidia pale to dark brown, smooth or punctuate, arising in short chains (4–8 conidia), (11)17–47(50)  $\times$  8–15  $\mu$ m [28.05  $\times$  10.57  $\mu$ m], with 3–5 transverse septa and 1–2 longitudinal septa. – Secondary conidiophore brown, with 0–10 septa (9)13–98  $\times$  3–4  $\mu$ m [43.56  $\times$  3.27  $\mu$ m], with one or several geniculations (Fig. 36).

**Culture characteristics.** – Colonies on PCA grey, with regular circular margin, and well-defined concentric rings of growth and sporulation, reaching a diam. of 75 mm after 7 d under 8h fluorescent light/16 h dark cycle (Fig. 36a).

**Pathogenicity assay.** – Rot symptoms on apple and quince fruits were observed 7 d and 4–5 d after inoculation, respectively. Brown rot symptom was spread into the fruit tissues and led to black centered spots with grey margins on the surface of quince fruit (surface mold) (Fig. 37b). On apple fruits, brown rot symptom was spread into the fruit tissues without producing the surface mold (Fig. 37a). No symptoms were observed in control inoculations. The fungal disease agent was isolated from the rotten tissues of the inoculated fruits, but not from control treatments, confirming Koch's postulates.

**Notes.** – Morphological features of our isolate from quince were according to the description provided by Simmons (2007) for *A. tenuissima*. Multiple sequence alignment of 14 ITS and *gpd* sequences resulted in 423 and 516 characters, respectively. The concatenated ITS–*gpd* consisted of 962 characters. ML of the combined dataset revealed that *A.*

*tenuissima*, *A. alternata*, *A. alstroemeriae*, *A. destruens*, and *A. arborescens* could not be resolved based on these molecular data in general and these species were grouped in a clade. Our isolate was placed sister to an isolate of *A. tenuissima* from the USA (isolated from *Sorghum* sp.) but with low support (Fig. 38). Based on the available morphological and molecular data, our isolates were identified as *A. tenuissima*.

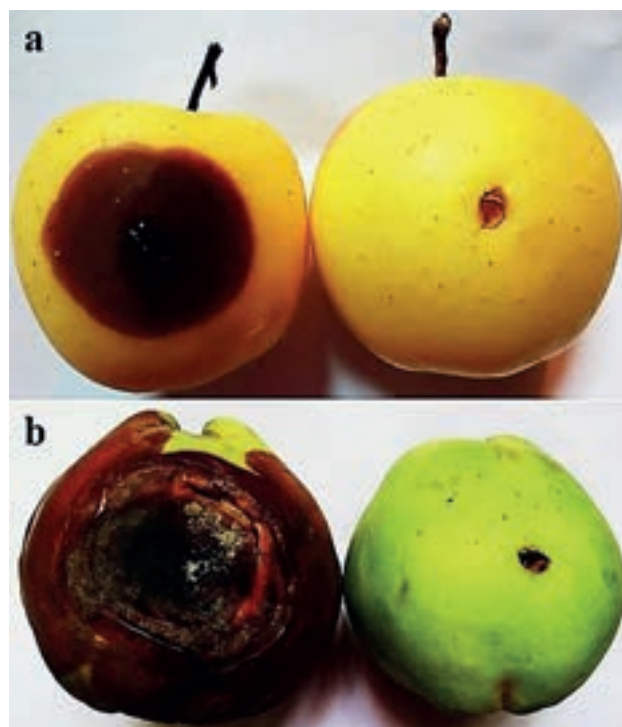


**Fig. 37.** Results of pathogenicity assay. Symptoms of *Alternaria* rot disease caused by inoculation with *A. tenuissima* (left fruits) and control treatments (right fruits) after 14 d at 25 °C with humidity above 90 %. **a.** Symptoms on apple. **b.** Symptoms on quince fruits.

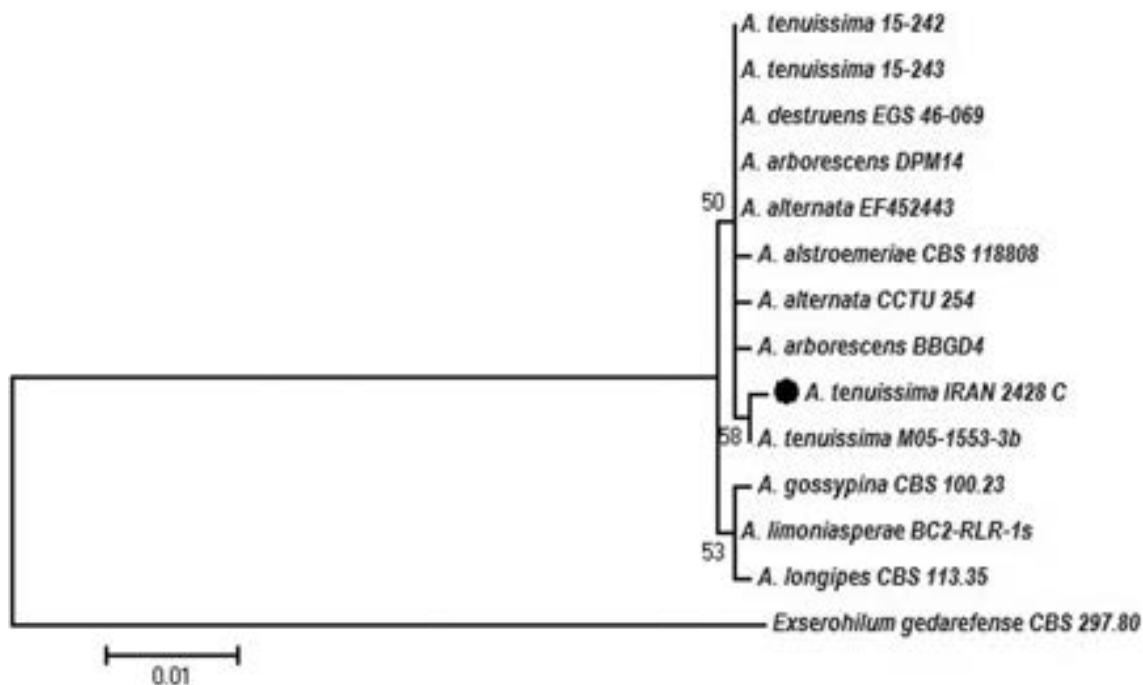


**Fig. 38.** ML phylogenetic tree of *Alternaria* isolates reconstructed from an ITS-*gdp* dataset. Bootstrap support values  $\geq 50$  indicated at the nodes.

*Alternaria* Nees species are often saprophytes commonly found in soil or on decaying plant tissues (Thomma 2003), but some *Alternaria* species are opportunistic plant pathogens reportedly causing a range of diseases of over 380 important host species of cereals, oil crops, ornamentals, fruits, and vegetables (Cota et al. 2008). Different *Alternaria* species have been reported as leaf blotch and fruit rot agents on apple. *Alternaria mali* is the most commonly cited causal agent of *Alternaria* leaf blotch on apple in Iran (Esmailzadeh & Soleimani 2008), Japan (Sawamura 1962), China (Wang et al. 1997), Yugoslavia (Bulajic et al. 1996), and the USA (Filajdic & Sutton 1991). Also, *A. alternata* s.l. has been implicated as causal agent of leaf blotch disease of apple (Kusaba & Tsuge 1994). Zakii & Ershad (1986) introduced *A. alternata* as a storage pathogen of apple fruits in Iran. Hartevelde et al. (2013) surveyed *Alternaria* isolates obtained from apple leaves and fruits in Australia with leaf blotch and fruit spot symptoms. Their results revealed that *A. arborescens*-like isolates were most prevalent (47 %), whereas *A. alternata*/*A. tenuissima* were intermediate in abundance (14 %) and *A. tenuissima*/*A. mali* isolates were least prevalent (6 %). Norin & Rumpunen (2003) found fruit spot on Japanese quince in Sweden and isolated *A. tenuissima*, *Phylctema vagabunda*, *Phoma exigua*, and *P. glomerata*

from affected fruits. These spots were black, gradually becoming greyish in the middle, varied from some mm to cm in diam.

In this study, two *Alternaria* isolates were recovered from apple brown rot and quince black rot symptoms. Both isolates were identified as *A. tenuissima* based on morphological features (Simmons 2007). Molecular species-level delimitation was not conclusive with the available sequence data of the single isolate from quince. To our knowledge, the present study is the first report of *A. tenuissima* causing brown rot disease on apple and black rot disease on quince in Iran and it is the first report of *A. tenuissima* as the causal agent of black rot on quince in the world.

*Authors:* L. Ebrahimi, K.-B. Fotouhifar & Y. Ghosta

#### Ascomycota, Candelariomycetes, Candelariales, Candelariaceae

*Candelariella oleaginescens* Rondon, in Vězda, Lichenes Selecti Exsiccati (Průhonice) 14: 341 (1965). – Fig. 39

Material examined. – TURKEY. Tunceli Province, 2 km to Sütlüce district, roadside, 39°07'19"N, 39°34'12"E, 1095 m a.s.l., on limestone, 17 July 2018, leg. K. Yazıcı & D. Karahan (KTUB-2468); Bingöl Province, Kiğı, Topraklık village, side of Dam, 39°22'35"N, 40°20'15"E, 1465 m a.s.l., on

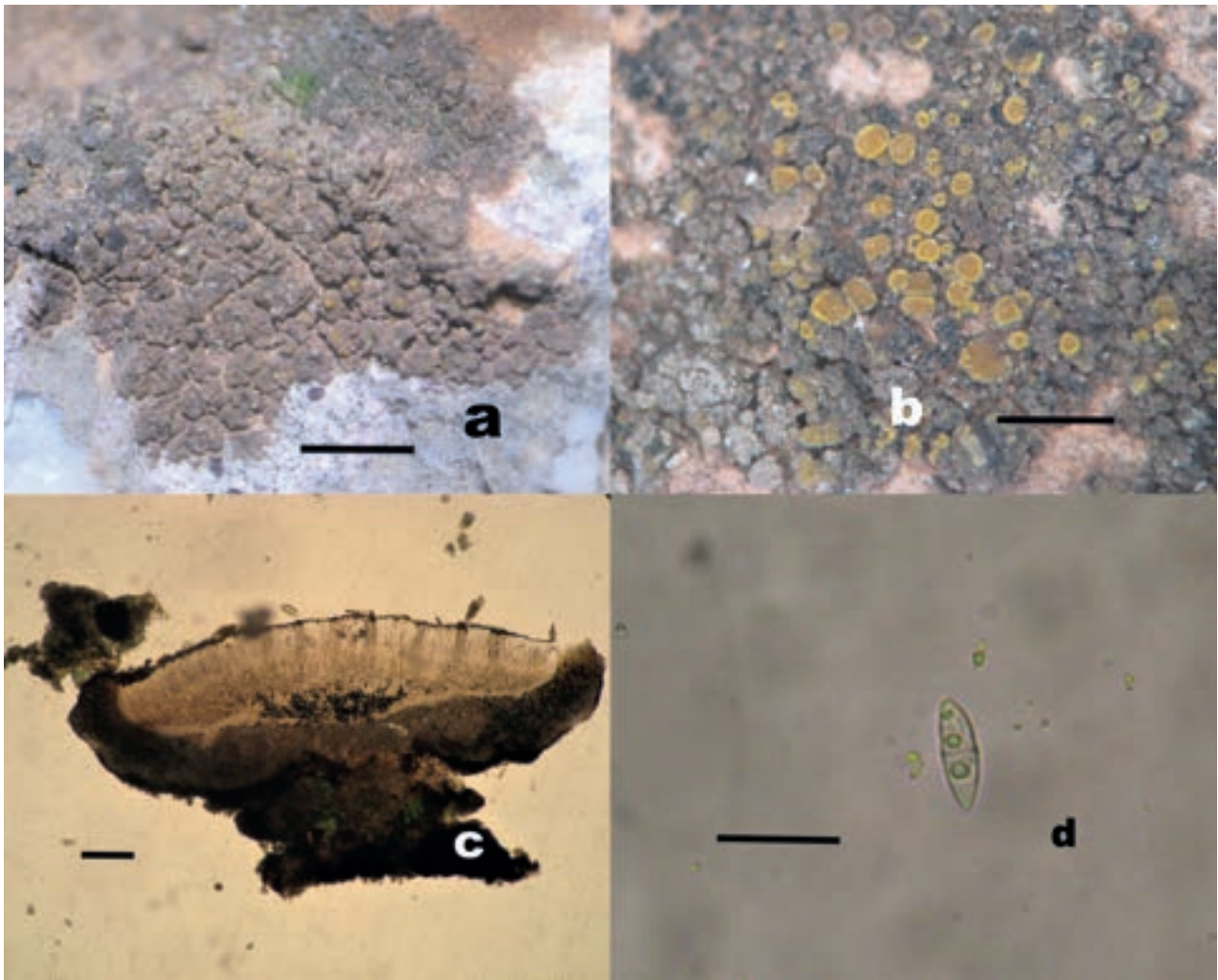


**Fig. 39.** *Candelariella oleaginescens*. **a.** Thallus with young apothecia. **b.** Thallus with apothecia. **c.** Ascoma in water, with epiphytium, hymenium, and hypothecium. **d.** Ascospore in water. Scale bars a 250  $\mu\text{m}$ , b 2 mm, c 100  $\mu\text{m}$ , d 20  $\mu\text{m}$ .

limestone, 02 August 2018, leg. K. Yazıcı & D. Karahan (KTUB-2469). Associated species: *Acarospora cervina*, *Candelariella aurella*, *C. vitellina*, *Lathagrium cristatum*, *Myriolecis crenulata*, *Pyrenodesmia variabilis*.

**Description.** – Thallus crustose, up to ca. 1.5 cm in diam., mostly irregular, areolate, flattened or granular to squamulose, ca. 0.2 mm thick, grey-green, greyish-beige or dark grey; areoles dispersed, to 1 mm in diam. – Apothecia sessile, to 0.8 (1.0) mm in diam., lecanorine; thalline margin yellow to dark yellow; disc smooth, citrine, yellow or slightly yellow brown or dirty yellow when old (Figs. 39a, b). – Hymenium colourless, ca. 80  $\mu\text{m}$  high; epithecium yellow-brown and distinctly granular; hypothecium colourless (Fig. 39c). – Paraphyses mostly simple and sometimes branched and with slightly swollen apices; asci clavate, 60–70

$\times$  7–9  $\mu\text{m}$ , 8-spored, *Candelaria*-type. – Ascospores colourless, simple or 1-septate,  $\pm$  cylindrical or oblong-ellipsoid, slightly curved and rounded ends, 16–19  $\times$  3–4  $\mu\text{m}$  (Fig. 39d). Detailed description in Rondon (1965).

**Habitat and distribution.** – On calcareous rocks and limestones, mostly from the coast. Thus far known from France, Greece, Iran, Israel, Kazakhstan, Morocco, Spain, Turkey, and Ukraine (Thor & Wirth 1990, Galun & Mukhtar 1996, Coppins et al. 2001, Khodosovtsev et al. 2004, Burgaz 2006, Roux 2012, Valadbeigi 2014, present study).

**Notes.** – Although approximately 1,650 lichen species have been previously reported from Turkey (John & Türk 2017), of which only 13 taxa were known from Bingöl and 89 from Tunceli (Mayrhofer

& Poelt 1979, Çobanoğlu & Yavuz 2007, Çobanoğlu & Doğan 2010, Vondrák et al. 2016). Before this paper, 15 taxa of *Candelariella*, 28 of *Verrucaria*, and 57 of *Rinodina* were reported from Turkey (John & Türk 2017). Our records of *Candelariella oleaginescens*, *Rinodina sicula*, and *Verrucaria murina* add to these numbers.

*Candelariella oleaginescens* is similar to *C. plumbea* and *C. boikoi*. It differs from *C. plumbea* in having a thinner areolate to squamulose thallus, smaller apothecia, and longer spores. Smaller apothecia (up to 1 mm), a more flattened thallus, and dispersed areoles in *C. oleaginescens* help to differentiate it from *C. boikoi* (Khodosovtsev et al. 2004).

**Authors:** K. Yazıcı, D. Karahan, A. Aslan & A. Aptroot

#### Ascomycota, Lecanoromycetes, Caliciales, Physciaceae

***Rinodina sicula*** Mayrhofer & Poelt, Bibliotheca Lichenol. 12: 143 (1979). – Fig. 40

**Material examined.** – TURKEY. Tunceli Province, Pertek, Akdemir village, 38°59'10"N, 39°10'24"E, 1205 m a.s.l., 22 June 2018, leg. K. Yazıcı & D. Karahan (KTUB-2474). Associated species: *Acarospora cervina*, *Calogaya decipiens*, *C. saxicola*, *Candelariella vitellina*, *Diplotomma epipolium*, *Lathagrium cristatum*, *Lobothallia radiosa*, *Physcia dubia*, *Pyrenodesmia variabilis*, and *Verrucaria nigrescens*.

**Description.** – Thallus crustose, thin, sometimes partly discontinuous, 1–4 cm in diam., pale to dark grey, partially cracked-areolate, prothallus black; soredia and isidia absent. – Apothecium lecanorine, 0.5–1.0 mm in diam., adnate or mostly sessile, abundant and ± aggregated; thalline margin ± concolorous with the thallus, grey or dark grey, distinctly thick, prominent; disc dark brown to black, plane (Figs. 40a, b); hymenium 100–110 µm high, colourless; epihymenium red brown or dark-brown; hypothecium colourless, 50–60 µm high (Figs. 40c, d). – Ascus *Lecanora*-type, 65.25–85.75(90) × 25–27 µm (Figs. 40d, e). – Ascospores *Physconia*-type, thin wall, 12.25–19.6 × 8–9.8 µm (Figs. 40e, f). – Thallus K–, C–, P–, thalline margin C+ red. Detailed description in Mayrhofer & Poelt (1979).

**Habitat and distribution.** – Early colonizer of compact siliceous rocks, often in nutrient-rich crevices, also gravestones, mainly coastal. It is known from Denmark, England, France, Greece, Ireland, Italy, Japan, Korea, Russia, Sweden, and Turkey (Mayrhofer & Sheard 2007, Sheard et al. 2017, present study).

**Authors:** K. Yazıcı, D. Karahan, A. Aslan & A. Aptroot

#### Ascomycota, Eurotiomycetes, Verrucariales, Verrucariaceae

***Verrucaria murina*** Leight., Brit. Sp. Ang. Lich.: 59 (1851). – Fig. 41

**Material examined.** – TURKEY. Bingöl province, Solhan, Asmakaya village, Tarhan district, 38°47'52"N, 41°04'30"E, 1500 m a.s.l., 31 August 2018, leg. K. Yazıcı & D. Karahan (KTUB-2475). Associated species: *Circinaria contorta*.

**Description.** – Thallus crustose, 1–1.5 cm in diam., superficial or ± immersed, greenish to light brown, generally small flecks and patches with gonocysts. – Isidia, blastidia, and soredia absent. – Perithecia ca. 200–350 (400) µm in diam., moderately dispersed and projecting, slightly domed, sometimes aggregated in 3–4 perithecia, mostly prominent, rarely collapsed (Figs. 41a, b). – Involucrellum present, ± appressed to the exciple basally poorly developed, flat, thin and pale brown (Figs. 41c, d). – Ascus clavate, 49 µm in length, fissitunicate, the ocular chamber inconspicuous, 8-spored. – Ascospores simple, oblong or sometimes broadly ellipsoid, thin and smooth wall, arranged biserially, 18–22 × 8.2–9.3 µm (Figs. 41e, f). Detailed description in Smith et al. (2009).

**Habitat and distribution.** – On siliceous rocks, limestone, chalk, small stones, and dolomite near streams in upland areas. Known from England, Denmark, France, Germany, Greece, Ireland, Italy, Latvia, Maltese Islands, Montenegro, Poland, Spain, Switzerland, Sweden, the Netherlands, Turkey, and Ukraine (Dietrich 2012, Fiorentina 2002, Krzewicka 2009, present study). This species is new to Turkey and Asia.

**Notes.** – *Verrucaria dolosa* resembles *V. murina* but has smaller ascospores and a more conical involucrellum (Smith et al. 2009). Our record of *V. murina* is the first one for the Asian continent.

**Authors:** K. Yazıcı, D. Karahan, A. Aslan & A. Aptroot

#### Ascomycota, Dothideomycetes, Botryosphaeriales, Botryosphaeriaceae

***Lasiodiplodia theobromae*** (Pat.) Griffon & Maubl., Bull. Soc. Mycol. Fr. 25: 57 (1909). – Fig. 42

**Material examined.** – INDIA. West Bengal, Agricultural Society of India, Alipore Road, Kolkata, 22°53'N, 88°33'E, *Dianella tasmanica* 'variegata' necrotic leaf tips (HCIO 52025, ITCC 7906), IARI (National Herbarium of Cultivated Plants, National Bureau of Plant Genetic Resources, Indian Agricultural Research Institute).

**Culture characteristics.** – Mycelium thin, whitish, fluffy from the top but dull to

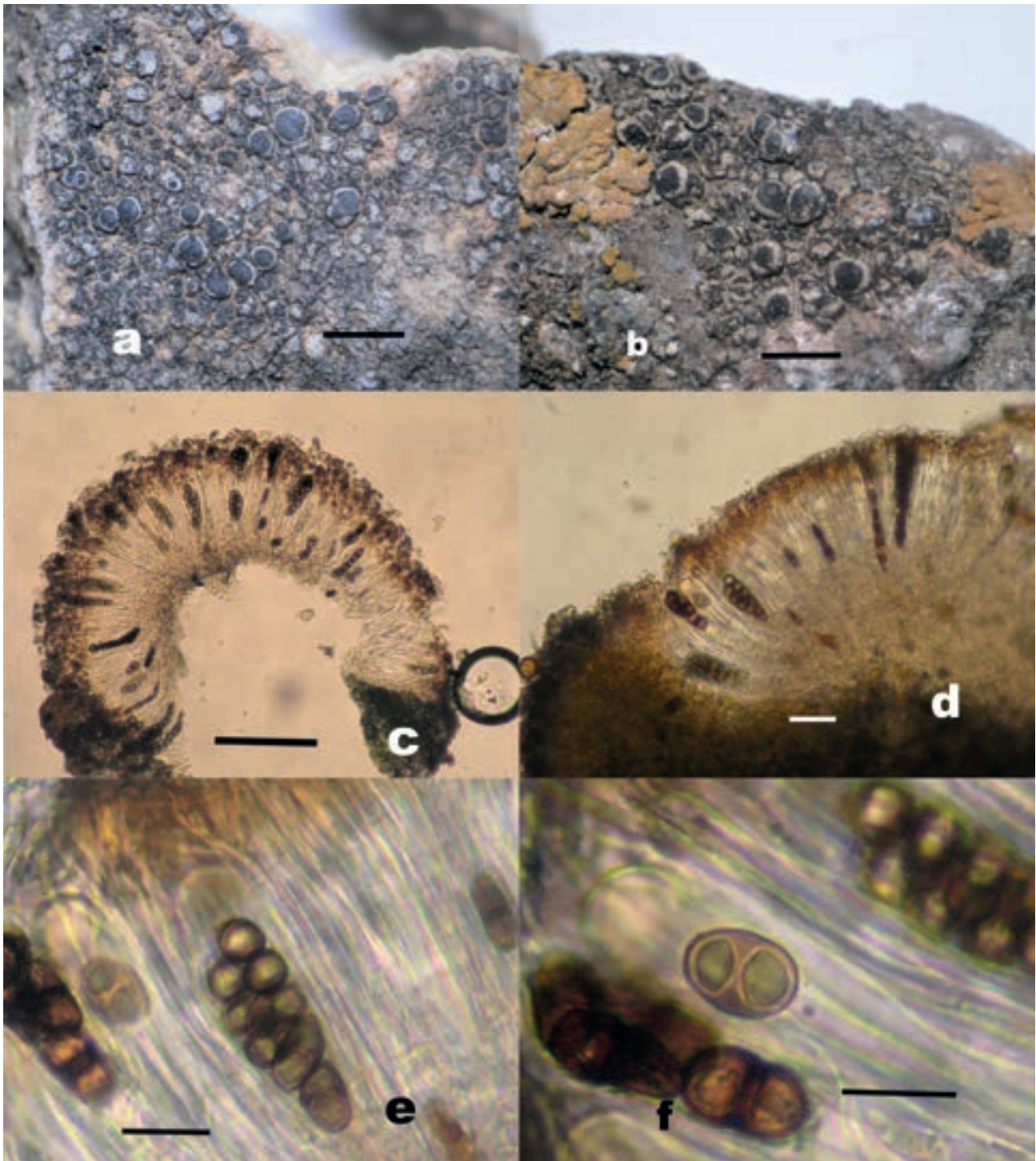


**Fig. 40.** *Rinodina sicula*. a–b. Thallus with apothecia. c. Apothecium in water, with hymenium, ascus, and ascospores. d. Apothecium in water, with epihymenium, hymenium, ascus, ascospores. e. Ascus and ascospores in water. f. Ascospores in water. Scale bars a–b 2 mm, c 100  $\mu\text{m}$ , d 50  $\mu\text{m}$ , e–f 20  $\mu\text{m}$ .

light brown at the bottom on PDA, 90 mm diam. within seven d. after inoculation with abundant production of pycnidia at bottom of Petri dish. –

Hyphae hyaline, thin, septate, 6.8–15.7  $\mu\text{m}$  (av. 10.3  $\mu\text{m}$ ) wide. – Pycnidia 460.3–582.7  $\mu\text{m}$  in diam., numerous, ostiolate [ostiole diam. 4.62–7.23

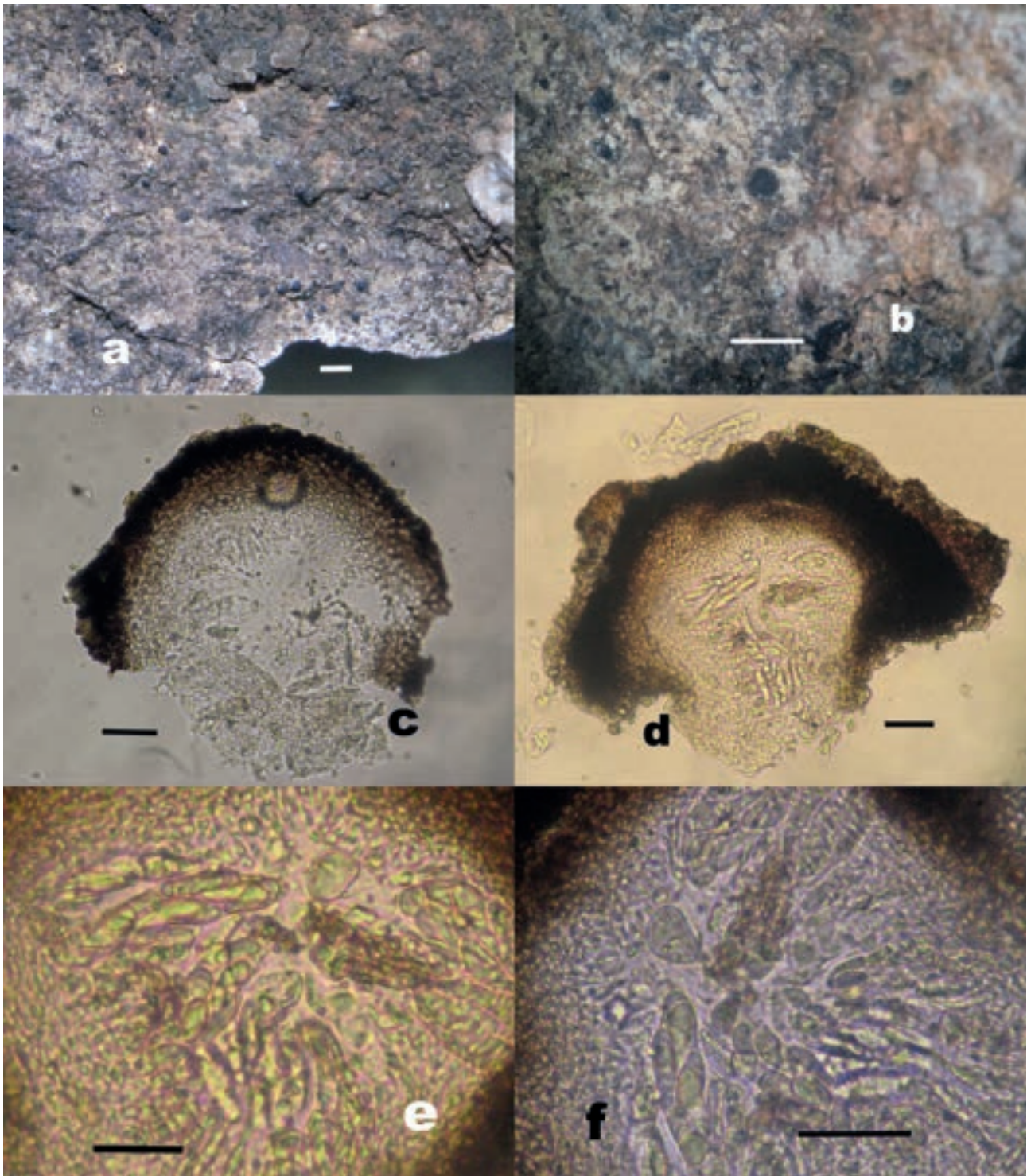


**Fig. 41.** *Verrucaria murina*. **a-b.** Thallus with perithecia. **c.** Perithecium in water, with involucrum, ascus, ascospores. **d-f.** Perithecium in water, with ascus and ascospores. Scale bars a-b 1 mm, c 50  $\mu\text{m}$ , d-f 210  $\mu\text{m}$ .

$\mu\text{m}$  (av. 6.81  $\mu\text{m}$ ), semi-immersed, solitary or confluent, glabrous, globose, papillate, brown to black with pseudoparenchymatous wall. – Conidia

double-layered, hyaline and unicellular when young (Fig. 42F) but light to dark brown and equally 2-celled when mature (Fig. 42G), oblong, bilamel-



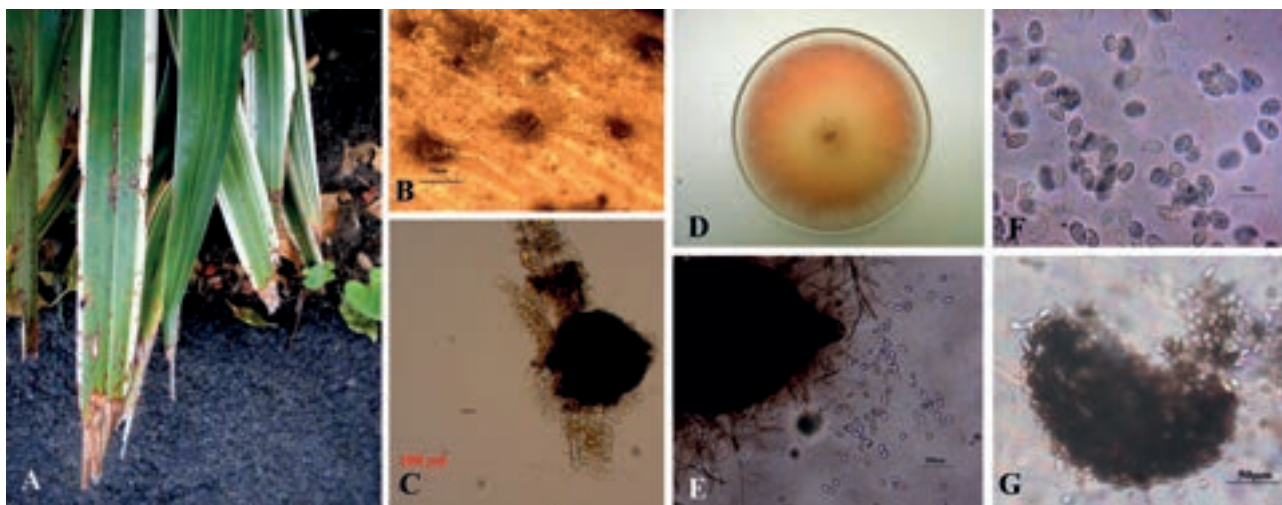


**Fig. 42.** *Lasiodiplodia theobromae* on *Dianella tasmanica* 'variegata'. **A.** Tip blight disease symptoms. **B, C.** Pycnidia on leaf surface. **D.** culture isolated from *Dianella tasmanica* 'variegata' on peptone salt agar (PSA). **E.** Pycnidium and conidia produced on PSA. **F.** Conidia after discharge from pycnidia. **G.** conidia after four weeks. Scale bars B 10  $\mu\text{m}$ ; C, E 100  $\mu\text{m}$ ; F–G 50  $\mu\text{m}$ .

late with longitudinally arranged striations,  $26.9\text{--}33.2 \times 11.9\text{--}20.1 \mu\text{m}$  (av.  $29.9 \times 15.9 \mu\text{m}$ ) with wall thickness around  $0.8\text{--}1.5 \mu\text{m}$  (av.  $1.1 \mu\text{m}$ ).

**Notes.** – In the recent past, *Dianella tasmanica* 'variegata' was found to be heavily attacked by the tip blight disease in West Bengal, India. This disease causes gradual and severe blighting of leaves followed by leaf drying and complete death of foliage (Banerjee 2016). The disease appears first as round to spindle-shaped lesions with ashy center, surrounded by a dark brown margin and distributed irregularly on one or both margins of leaves towards the leaf tip. Lesions coalesce to form a broad patch, progressing basipetally and becoming brown to grey or straw-colored (Fig. 42A). Numerous black dots like erumpent pycnidia, measuring  $224.6\text{--}255.1 \mu\text{m}$  (av.  $238.2 \mu\text{m}$ ), are formed subepidermally on the straw-colored dead tissues of the leaf tips (Figs. 42B, C). In severe condition, total leaves dry up and detach easily from the tip portion. Severity and sporulation of the pathogen were noticed from April to May.

The ITS sequence was 100 % similar to *Lasiodiplodia theobromae* (isolate ADB7, GenBank accession number MF671945). Also our SSU sequence was 100 % similar to *L. theobromae* (A1, KC442314). *Dianella* spp. are attacked by five fungal diseases. These are *Cladosporium* leaf spot by *Cladosporium dianellicola* (He & Zhang 2001), rust disease by *Puccinia dianellae* (McKenzie 1998), anthracnose by *Colletotrichum gloeosporioides* (Takeuchi et al. 2008), sheath blight by *Rhizoctonia solani* (Ono & Hoshi 2009), and *Mycosphaerella* leaf spots by *My-*

*cosphaerella queenslandica* (Sivanesan & Shivas 2002)]. Chaudhuri et al. (2017) described the cultural and morphological aspects of *L. theobromae* of *Dianella* in various carbon and nitrogen containing media, but this was not a disease report. To the best of our knowledge, this is the first molecular evidence of *L. theobromae* causing tip blight of *Dianella tasmanica* 'variegata' (variegated flax lily) from India.

**Authors:** A. Banerjee, B. Panja, J. Saha, A. Mookherjee & M.K. Maiti

### Basidiomycota, Agaricomycetes, Agaricales, Omphalotaceae

*Marasmiellus subpruinus* (Murrill) J.S. Oliveira, Mycol. Progress 18: 735 (2019). – Figs. 43–44

**Basionym.** – *Marasmius subpruinus* Murrill, N. Amer. Fl. 9(4): 266 (1915).

**Synonyms.** – *Collybia subpruinosa* (Murrill) Dennis, Trans. Br. mycol. Soc. 34(4): 449 (1951). *Gymnopus subpruinus* (Murrill) Desjardin, Halling & Hemmes, Mycologia 91(1): 171 (1999).

**Material examined.** – *Marasmiellus subpruinus*: PORTUGAL. Madeira, Ribeiro Frio to Portella, Levada do Furado,  $32^{\circ}43'53''\text{N}$ ,  $16^{\circ}52'58''\text{E}$ , decaying wood and broad-leaved twigs, 23 September 2015, leg. V. Antonín, H. Ševčíková & J. Borovička (BRNM 781138); *Ibid.*, decaying wood and litter of broadleaved trees, 23 September 2015, leg. J. Borovička (BRNM 781141). – *Marasmiellus luxurians* (Peck) J.S. Oliveira: AUSTRIA. Graz, Botanical garden, 30 April 1998, leg. H. Pidlich-Aigner (BRNM 652791). – BENIN. Borgou province, Wari-Maró, 22 August 1997, leg. V. Antonín (BRNM 648405). – CZECH REPUBLIC. České Budějovice, park, 3 August 1998, leg. V. Bicha (BRNM 695300); Prague, Botanical garden, greenhouse, February 1976, leg. M. Svrček 623/76 (PRM 820173, as

*Collybia dryophila* forma *pileo pallide*); *Ibid.*, 13 April 1983, leg. A. Vágner (PRM); Liberec, Stráž n. Nisou, greenhouse, 13 April 1983, leg. Z. Pelda (PRM); *Ibid.*, 13 & 20 April and 3 May 1983, leg. Z. Pelda (PRM); Olomouc, University campus, 30 August 2013, leg. M. Kříž (BRNM 761876); Přerov, city park, 8 July 2012, leg. J. Polčák (BRNM 766613); Janovice near Frýdek-Místek, garden, 14 June 2018, leg. E.M. Caklirpaloglu (BRNM 807659); Valašské Meziříčí, city park, 24 July 2018, leg. H. Ševčíková (BRNM 808899). – GERMANY. Speyer, north of Hanhofen, 21 July 1997, leg. W. Winterhoff 9765 (BRNM 695313). – NETHERLANDS. Limburg province, Venlo, 20 August 1991, leg. G.M. Gatzen (L 99341); Noord Brabant province, Eindhoven, P. de Jong Park, 20 & 28 September 1989, leg. H. Huijser (L 99338); Overijssel province, Nijverdal, 1 August 1994, leg. W. Ligterink (L 99335); Overijssel province, Rijssen, 1 August 1994, leg. W. Ligterink (L 99336). – REPUBLIC OF KOREA. Hongcheon County, Nae-myong, Jaun-ri, 26 July 2007, leg. V. Antonín & H.D. Shin (BRNM 714992). – USA. New York, Bronx County, Bronx, N.Y. Botanical Garden, 26 September 1989, leg. R.E. Halling 6317 (L 99340); Massachusetts, Hampshire County, Amherst, Village park, 27 July 1979, leg. R.E. Halling 2876 (L 99339). – *Gymnopus moseri* Antonín & Noordel.: SWEDEN. Småland, Femsjö, Erstaviken, Södra Färngen, 25 September 1976, leg. M. Moser 76/355 (IB, holotype); Västergötland, Trollhättan, near Hästvägen, 18 October 1983, leg. L. & A. Stridvall 83.166 (L, Herb. Stridvall).

**Description.** – Pileus 10–40 mm broad, convex to low-convex or appanate, obtuse or with low umbo at centre, involute, then straight at margin, hygrophanous, up to center translucently striate, distinctly striate-sulcate, especially when old, ± glabrous, watery brown when moist, pallescent to (dirty) ochraceous from centre towards margin when drying-out. – Lamellae distant, L = 14–18, l = 2–3, emarginate and with small tooth, intervenose when old, (greyish) brownish, with concolorous edge. – Stipe 15–50 × 1.5–2.5 mm, cylindrical or laterally compressed, tomentose-pubescent, especially at apex, dirty whitish to brownish above, brown (± concolorous with pileus centre or darker) towards base, basal tomentum whitish. Context without any special smell. – Basidiospores 8.0–9.5(10) × 4.25–5.0 µm, average 8.83 × 4.67 µm, E = 1.78–2.11, Q = 1.87–1.90, fusoid, fusoid-ellipsoid, rarely subovoid, thin-walled, non-dextrinoid. Basidia 22–29(35) × 6.5–8.0 µm, 4-spored, clavate. – Cheilocystidia 23–45 (60) × 5.0–15 µm, variable in shape, clavate, (sub)cylindrical, (sub)fusoid,



**Fig. 43.** *Marasmiellus subpruinus* BRNM 781138. Photo V. Antonín.

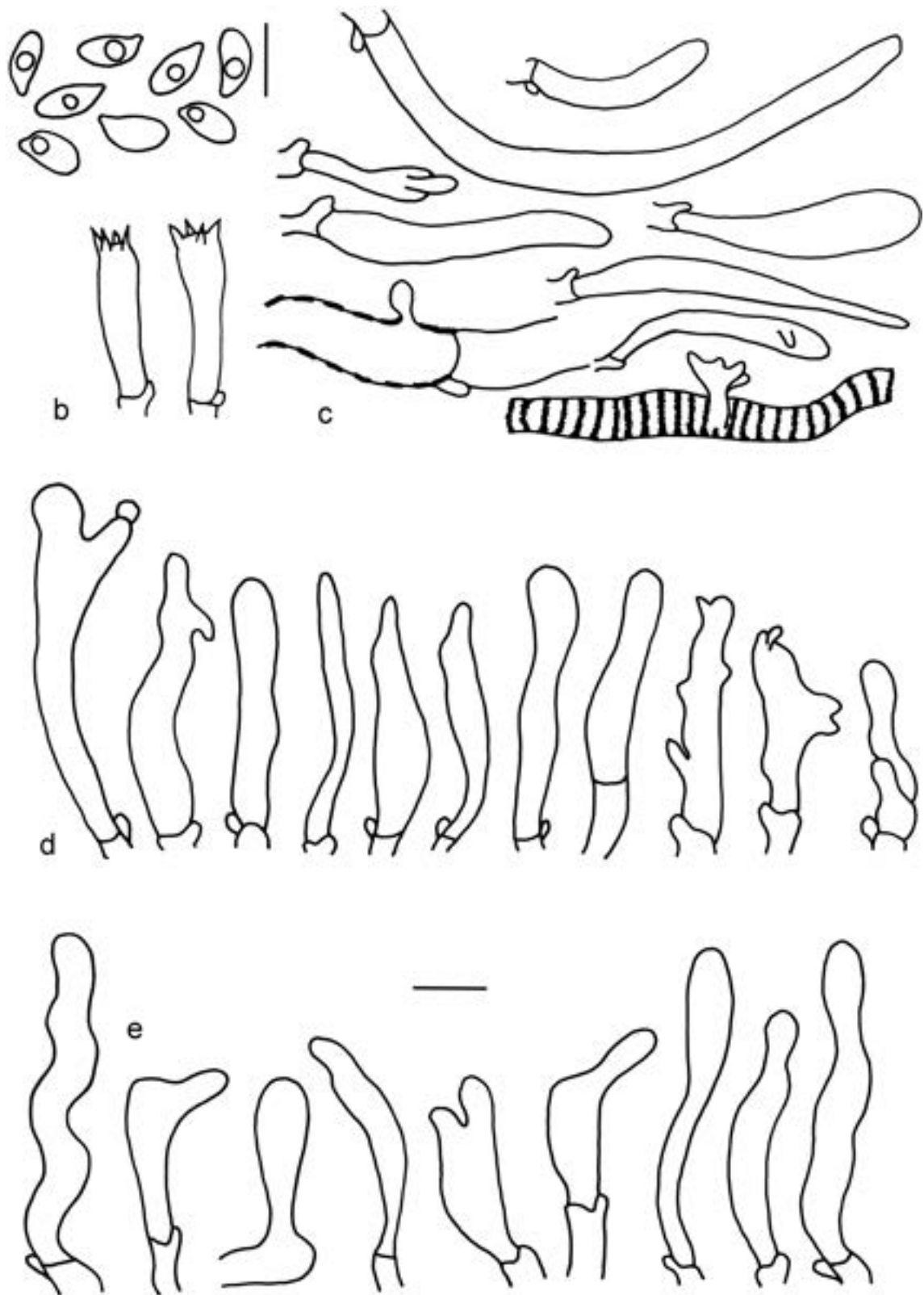


**Fig. 44.** *Marasmiellus subpruinusus* BRNM 781138. a. Basidiospores. b. Basidia. c. Pileipellis elements. d. Cheilocystidia. e. Caulocystidia. Scale bar 10  $\mu$ m, *del.* H. Ševčíková.

utriform, mostly irregular or branched, often with projection(s) or rostrate, thin-walled. – Pleurocystidia absent. – Pileipellis a cutis, composed of  $\pm$  cylindrical, thin- to slightly thick-walled, often incrustated (zebroid), 3.0–10  $\mu\text{m}$  wide hyphae with rare diverticula and digitate, lateral or terminal, often branched, 12–80  $\times$  5.0–9.0  $\mu\text{m}$  long projections. – Stipitipellis a cutis of cylindrical, slightly thick-walled, smooth or minutely incrustated, non-dextrinoid, 2.0–6.0  $\mu\text{m}$  wide hyphae. – Caulocystidia 24–75  $\times$  5.5–10  $\mu\text{m}$ , variable in shape, cylindrical, fusoid, narrowly clavate, (sub)utriform, irregular, (sub)moniliform, rarely with projection(s), subcapitate or subrostrate, thin- to slightly thick-walled. – Clamp connections present in all tissues.

**Ecology.** – In Madeira, this species was found on decaying wood, twigs, and litter of broadleaved trees in an evergreen humid laurel forest. This forest is unique by ancient relict endemics with a great affinity with Tertiary flora and fauna (Condé et al. 2002). The island of Madeira belongs to the Macaronesian Biogeographic Region, which is a part of the Holarctic with mostly Mediterranean climate heavily influenced by the ocean. This island is one of the hotspots for biodiversity, especially for plants (Condé et al. 2002), but the expanding agricultural industry and tourism had a major impact on original biodiversity. In other continents, *M. subpruinus* has been collected scattered to clustered on humus-rich soils, woody debris, and logs, on partially buried wood debris, on wood debris and twigs, scattered on wood debris and mulch (Desjardin et al. 1999, Mata & Ovrebo 2009), and on *Cyathea*, *Nothofagus truncata*, *Pinus pinaster*, *Pinus* sp., and *Podocarpus totara* in forests and parks (Anonymous 2012–2018); fruiting occurs in late summer in watered areas and after fall rains ([http://www.mykoweb.com/CAF/species/Gymnopus\\_subpruinus.html](http://www.mykoweb.com/CAF/species/Gymnopus_subpruinus.html)).

**Distribution.** – *Marasmiellus subpruinus* is known from the western part of the USA (including Puerto Rico and Hawaii; Baroni 1998, Desjardin et al. 1999, Barron 2012), Central America (Costa Rica, Jamaica, Panama; Pennington 1915, Ovrebo 1996, Mata & Ovrebo 2009), South America (Brazil, Ecuador; Rosa & Capelari 2009, Anonymous 2017), and New Zealand (Anonymous 2012–2018).

**Notes.** – *Marasmiellus subpruinus* is characterized by a hygrophanous, up to center translucently striate, distinctly striate-sulcate, watery brown pileus, pallescent to (dirty) ochraceous from center; (greyish) brownish lamellae; a tomentose-pubescent stipe, dirty whitish to brownish above,

brown towards base, basal tomentum whitish; moderately large [8.0–9.5(10)  $\times$  4.25–5.0  $\mu\text{m}$ ], fusoid, fusoid-ellipsoid, rarely subovoid basidiospores; variable, clavate, (sub)cylindrical, (sub)fusoid, utriform cheilocystidia, mostly irregular to branched, with projection(s) or rostrate; the absence of pleurocystidia; and mostly cylindrical, fusoid, narrowly clavate, (sub)utriform, irregular, (sub)moniliform caulocystidia. Desjardin et al. (1999) mentioned this species from the Hawaiian Islands; their description differs from the Madeira basidiomata by larger cheilocystidia (25–80  $\times$  5–16  $\mu\text{m}$ ) and caulocystidia (60–120  $\times$  2.5–10  $\mu\text{m}$ ). However, the shapes of all above-mentioned structures agree with the Madeira collections; Desjardin et al. (1999) called pileipellis terminal cells as pileocystidia. The sequence of the *Marasmiellus subpruinus* BRNM 781138 (as *Gymnopus subpruinus*) is well supported phylogenetically (Fig. 45). According these characters, this species belongs to sect. *Vestipedes* (Fr.) Antonín, Halling & Noordel. (Antonín & Noordeloos 2010). Oliveira et al. (2019) published a detailed paper dealing with the phylogeny of *Omphalotaceae* and transferred studied taxa of sect. *Vestipedes* to the genus *Marasmiellus*.

*Gymnopus rodhallii* Desjardin & B.A. Perry, described from São Tomé, Africa, has a paler pileus, pale brownish grey to cream centre, or beige to cream overall, close lamellae, smaller basidiospores (6.4–7.0  $\times$  3.0–3.5  $\mu\text{m}$ ), and a pileipellis with undifferentiated terminal cells (Desjardin & Perry 2017).

The phylogenetically similar *Marasmiellus polygrammus* (Mont.) J.S. Oliveira is known from South America (e.g., Costa Rica, Guyana, Puerto Rico; Baroni 1998, Mata & Petersen 2003, Mata & Ovrebo 2009), the Republic of Korea (Lee et al. 2014, Jang et al. 2016), and India (Dutta et al. 2015). This species macroscopically differs from *M. subpruinus* by close to subdistant lamellae and a dark brown to black stipe (Mata & Petersen 2003); however, concerning microscopic characters, these authors observed only basidiospores due to the poor condition of the type specimen. In comparison with *M. subpruinus*, Dutta et al. (2015) mentioned a distinctly larger pileus (5–11.5 (14) cm), a larger stipe, 40–68  $\times$  3–5 mm, with an upper part creamy white to light brownish cream, lower part creamy brown to creamy vinaceous brown, smaller basidiospores, (7.2)7.5–7.9(8.6)  $\times$  (3.5)3.9–4.3(5.4)  $\mu\text{m}$ , and narrower cheilocystidia, 35–54(72)  $\times$  5–7.5  $\mu\text{m}$ , in the Indian collection. Moreover, the authors have not mentioned the presence of distinct and long pileipellis terminal cells. The Korean authors (Jang et al. 2016) also described a smaller pileus (1.5–2 cm) and smaller ba-

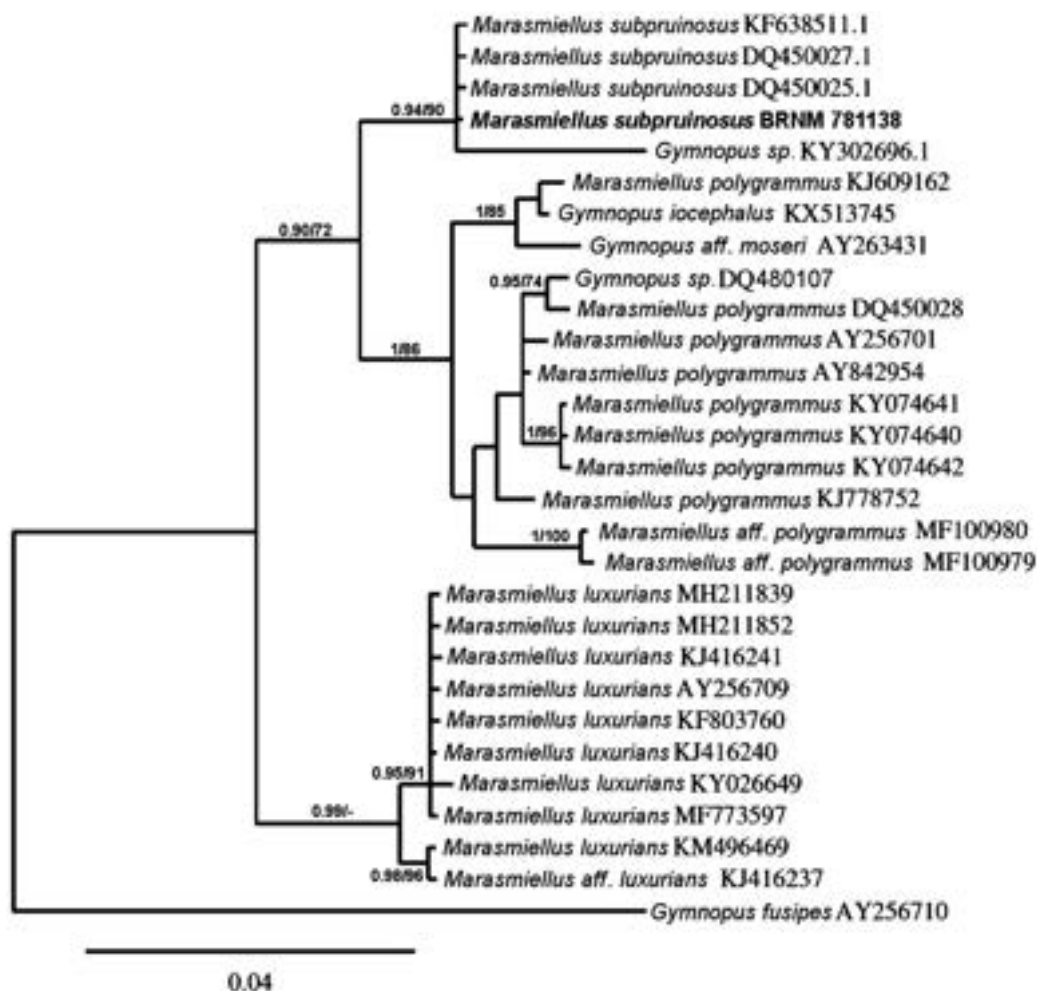


**Fig. 45.** Phylogenetic placement of *Marasmiellus subpruinusus* among closely related species inferred from ITS rDNA sequences. Support values are given above the branches ( $\geq 0.90$  for BI,  $\geq 70$  for ML).

sidiospores, (5)  $5.2\text{--}7.4 \times 2.6\text{--}3.5 \mu\text{m}$ , however, they mentioned the absence of cheilocystidia. Moreover, the sequence of their single Korean collection forms a small sister clade to the other *M. polygrammus* sequences. Therefore, the identity of this collection is not fully certain.

Macroscopically similar to *M. subpruinusus* is the Korean collection named *Gymnopus iocephalus* (Berk. & M.A. Curtis) Halling, but it differs by the absence of cheilocystidia (Jang et al. 2016); the authors of this paper described the pileus colour as yellowish brown to very pale brown when fresh, becoming very pale brown when dry. However, Berkeley & Curtis (1853) mentioned the pileus as violaceous in his original description. Halling (1983, 2013) in concordance with the original description mentioned its pileus as coloured in shades of purple at first, soon fading to purplish lilac as is typical for

*G. iocephalus*. Moreover, the sequence of this single Korean collection forms a small sister clade to the American ones and the identity of Korean *G. iocephalus* is not fully proven now. Halling (1983), in his description of *G. iocephalus*, also measured smaller basidiospores  $6.5\text{--}8.6 \times 3.2\text{--}4.4 \mu\text{m}$  in comparison with *M. subpruinusus*. Further, *G. iocephalus* has a pungent and unpleasant smell, and phylogenetically belongs to *Gymnopus* sect. *Impudicae* (Antonín & Noordel.) Antonín & Noordel. (Ryoo et al. 2016).

*Gymnopus moseri* Antonín & Noordel., known from Europe and North America, differs by larger basidiospores,  $8.5\text{--}11 \times 4.0\text{--}5.0 \mu\text{m}$  (Antonín & Noordel. 2010, our studies), and also phylogenetically.

The other phylogenetically closely related species *Marasmiellus luxurians* (Peck) Murrill, differs

from *M. subpruinus* by larger basidiomata (pileus 30–110 mm broad, stipe 50–100 × 5–10 mm), a frequently radially fibrillose pileus, very close ( $L > 200$ ), white to sordid pink lamellae, a strongly fibrillose-striate stipe, longer basidiospores, 7.0–11.5 (13) × 3.5–6.0 μm, slightly shorter cheilocystidia, shorter pileipellis terminal cells, and it grows mostly on places influenced by men (compost heaps, mulch, ruderal places) (Antonín & Herink 1999, Antonín & Noordeloos 2010, our studies). Moreover, Antonín & Herink (1999) described a unique character of *G. luxurians*, which has never been observed in other *Gymnopus* species: lamellae are divided in two edges and connected to each other when young, later the connection line cracks and both lamella edges start to diverge (lamellae with double edge), finally both edges of the lamellae are attached to each other and may be coalesced (lamellae with one edge).

The collections from Madeira given here represent the first records not only for Madeira and Macaronesia, but for Africa. Madeiran collections were found far away from other distribution localities of *Marasmiellus subpruinus* with distance from the Hawaiian Islands approx. 12,600 km, from the USA ca. 5,300 km, Brazil ca. 5,000 km, and New Zealand ca. 18,000 km. *Marasmiellus subpruinus* grows in the laurisilva forest containing endemic tree species as e.g., *Oxydendrum arboretum* (Condé et al. 2002), therefore, it may be native there. On the other hand, agricultural industry and tourism have an impact on a large part of the island, and this species may be introduced. During our field research, e.g., Australian species *Clathrus archeri* was found. Our studies (unpublished) show a mix of European, North American, Australian, and some unique species of macromycetes.

*Authors:* H. Ševčíková & V. Antonín

### Basidiomycota, Agaricomycetes, Agaricales, Mycenaceae

*Mycena albidolilacea* Kühner & Maire, Encyclop. Mycol. 10: 419 (1938). – Figs. 46, 49f–g

*Material examined.* – RUSSIA. Novgorod Oblast, near village Krasnofarfonyi, an oak forest of the flood-plain, on decaying leaves of *Populus tremula*, 22 July 2017, leg. L. Kalinina, det. A. Aronsen (LE 321756); Novgorodskaya Oblast, near village Savino, protected area “Savinskie dubravy”, on decaying leaves of *Quercus robur*, 16 August 2018, leg. L. Kalinina, det. A. Aronsen (LE 321757).

*Description.* – Basidiomata solitary or two together. – Pileus convex, 5–10 mm in diam., very pale pink with slightly darker centre, glabrous, somewhat sulcate. – Stipe cylindrical,

hollow, 30–40 × 1 mm, white with pale pink tinge, slightly pubescent (lens!), covered with white fibrils near the base. – Lamellae ventricose,  $L < 20$ , adnexed, white, with very slightly pinkish edge visible only under lens after drying. – Odor indistinctive, possibly somewhat farinaceous. – Basidiospores (7.0)7.6–10.5 × 3.8–5.2 μm,  $Q = 1.6–2.4$ ,  $Q_{av} = \sim 1.9$  ( $n=29$  from two specimens), amyloid, pip-shaped, smooth. – Basidia 17.6–30.1 × 6.6–7.9 μm. – Cheilocystidia 24.2–33.2 × 8.9–10.4 × 2.8–3.1 μm, forming sterile band, clavate, obpyriform, smooth, furcate or with 1–3 irregular curved excrescences 7.1–14.7 × 2.5–3.1 μm long. – Pleurocystidia absent. – Pileipellis hyphae up to 3 μm wide, diverticulate with numerous excrescences 2.0–11.4 × 1.0–1.8 μm. – Stipitipellis hyphae 3–4 μm wide, with numerous excrescences 1.0–4.0 × 1–2 μm, terminal cells up to 7.5 μm wide, covered with short excrescences. – Clamp connections present.

*Habitat and distribution.* – On decaying leaves of *Quercus robur* and *Populus tremula* in Austria, Denmark, France, Germany, Hungary, Italy, the Netherlands, Sweden, UK, and Russia.

*Notes.* – The genus *Mycena* (Pers.) Roussel was shown to be polyphyletic by Moncalvo et al. (2002) and Matheny et al. (2006). Since then, several papers on European species have been published introducing new taxa (e.g., Robich et al. 2005, Aronsen & Gulden 2007, Robich & Hausknecht 2008, Aronsen & Perry 2012), presenting rare and interesting records (e.g., Ronikier et al. 2006, Ludwig & Ryberg 2009, Holec & Kolařík 2017, Ševčíková 2017), and considering the phylogeny of section *Calodontes* (Harder et al. 2010, 2013). Three thorough monographs on European species were published in recent years (Robich 2003, 2016; Aronsen & Læssøe 2016), which follow the traditional approach treating *Mycena* in wide sense. These monographs are very valuable for species identification because of their high-quality photographs, descriptions, and drawings of microstructures.

According to Maas Geesteranus (1992a), whose description closely follows the protologue, basidiomata are described as “scattered to gregarious,” but our specimens are represented by a single basidioma found on a fallen aspen leaf (LE 321756) and two basidiomata found on fallen oak leaves (LE 321757). Basidiospore sizes match wide ranges given in Robich (2016) and Aronsen (2019); they are shorter compared to Maas Geesteranus (1992a) and Kühner (1938) but their width matches the one given in the latter reference. Cheilocystidia are somewhat narrower, excrescences shorter and wider

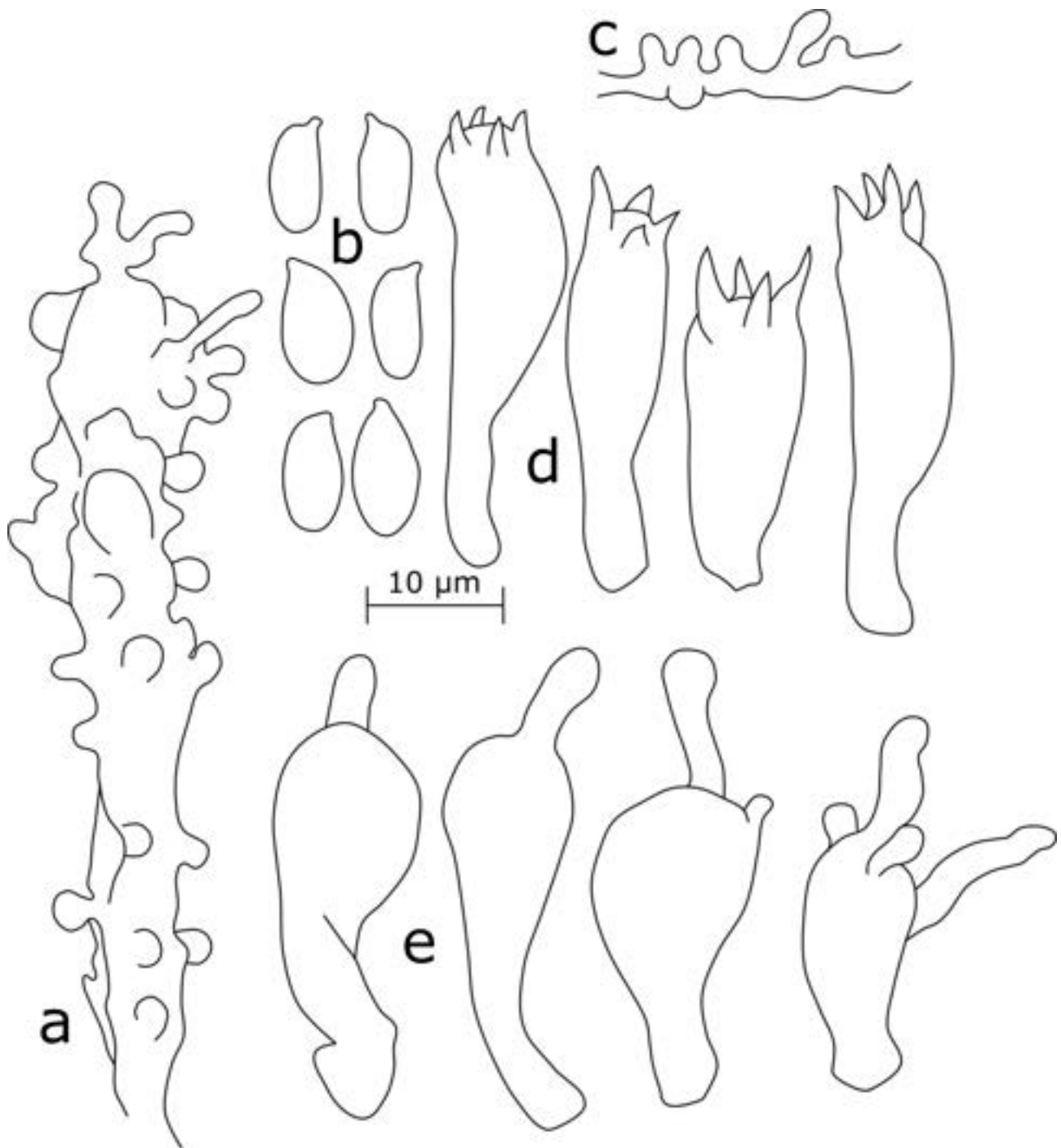


**Fig. 46.** Microstructures of *Mycena albidolilacea*. **a.** Caulocystidia. **b.** Basidiospores. **c.** Pileipellis hypha. **d.** Basidia. **e.** Cheilocystidia.

than those described earlier (Tab. 6). A French collection studied by Aronsen (2019) had a basidiospore size matching those described by Kühner (1938), and excrescences of cheilocystidia also were much shorter than in the description given by Maas

Geesteranus (1992a). So these differences should be considered within the variability of the species.

This species is similar to *M. mitis*, another slightly pinkish *Mycena* growing on fallen oak leaves. *Mycena mitis* is distinguished by lamellae decur-

**Tab. 6.** Comparison of micromorphological characters in *Mycena albidolilacea* basidiomata according to existing descriptions.

Character	Kühner (1938)	Maas Geesteranus (1992)	Robich (2016)	Aronsen (2019)	Present study
Basidia	30–38 × 6.5–8	25–30 × 7	24–26(33) × 7–7.5	21–40 × 7–9	17.6–25.9 × 7.3–7.9
Basidiospores	9.2–12.2 × 4.5–5.2	9.2–11.6 × 5.6–6.7	8–10 × 5–6	7.8–12 × 4.2–6	(7.0)7.6–10.5 × 3.8–5.2
Cheilocystidia	11–12 in diam.	22.5–60 × 5.5–14.5 × 1.8–7	13–50 × 6–16	17–45 × 5–17	24.2–33.2 × 8.9–10.4 × 2.8–3.1
Excrecences	No data	22.5 × 1.8–2.7	22 × 1.5–2.5	20 × 2	7.1–14.7 × 2.5–3.1

rent with a tooth, and stipitipellis and pileipellis with rather long (up to 25 µm) excrecences embedded in gelatinous matter (Maas Geesteranus 1992b, Ludwig & Ryberg 2009, Aronsen & Læssøe 2016).

*Author:* L.B. Kalinina

### Basidiomycota, Agaricomycetes, Agaricales, Mycenaceae

*Mycena tenuispinosa* J. Favre, Bull. Soc. Neuchat. Sci. Nat. 80: 96 (1957). – Figs. 47, 49a–e

**Material examined.** – RUSSIA. Leningrad Oblast, near village Orzhitsy, old abandoned park, on bark of deciduous trees (cf. *Ulmus*), 23 June 2018, *leg. & det.* L. Kalinina (LE 321754); Leningrad Oblast, near village Orzhitsy, old abandoned park, on bark of deciduous trees (cf. *Ulmus*), 30 June 2018, *leg. & det.* L. Kalinina (LE 321755).

**Description.** – Basidiomata tiny, solitary or scattered, young basidiomata have distinct bluish tinge both on stipe and pileus and nitrous smell. – Pileus ovoid when young, then convex, up to 3 mm in diam., greyish white with somewhat darker centre, with separable gelatinous pellicle and thin white hairs (“spinules”) visible under hand lens (×10). – Stipe cylindrical, 10–30 × 0.2–0.5 mm, greyish-white, darker towards the base, finely pubescent, with basal disc. – Lamellae 9–13 reaching the stipe, white, forming a pseudocollarium. – Basidiospores 7.8–10.5 × 4.2–5.2 µm, Q = 1.6–2.1, Q<sub>av</sub> = ~ 1.9 (n=30), amyloid, broadly pip-shaped. – Basidia 15.5–18.2 × 8.2–10.0 µm, 4-spored, broadly clavate to obpyriform, hardly seen, with sterigmata up to 2–3 µm long. – Cheilocystidia 10.6–22.5 × 6.0–11.0 µm, clavate with

cylindrical excrecences 2.0–4.4 × 0.8–1.1 µm, forming a sterile band. – Pleurocystidia absent. – Pileipellis hyphae 2.6–9.1 µm wide, hairs (“spinules”) up to 50 µm long, consisting of diverticulate hyphae covered with numerous excrecences up to 3.5 µm. – Stipitipellis hyphae smooth, 3.5–4.8 µm wide, with hair-like caulocystidia with clamp connections. – Clamp connections present.

**Habitat and distribution.** – On bark of deciduous trees. Described from Switzerland, also present in Denmark, Germany, Italy, Slovakia, the Netherlands, Poland and Russia.

**Notes.** – *Mycena tenuispinosa* was described in 1957 by Favre and until 1985 it was known only from type locality. Maas Geesteranus (1983) compiled a description that closely followed the original one, there was only one addition concerning the absence of clamp connections revealed by O.H. Monthoux in the type material. In 1985, two very similar collections were reported from Germany, but those possessed clamp connections. After re-examination of the type material, clamp connections were found (Maas Geesteranus 1991). This species is characterized by the presence of basal disc and pileal hairs (“spinules”) consisting of agglutinated diverticulate hyphae. All our specimens have been found in an abandoned park with *Quercus*, *Ulmus*, *Tilia*, *Corylus*, and a lot of dead wood. Specimen LE 321755 was collected on a fallen trunk covered with moss. It consisted of two very young basidiomata that in the field seemed to be different due to a bluish tinge, in addition to six

**Tab. 7.** Comparison of micromorphological characters in *Mycena tenuispinosa* basidiomata according to existing descriptions.

Character	Robich (2003)	Roniker et al. (2006)	Aronsen (2019)	Present study
Basidia	22–28 × 8.5–11	17–21 × 7–8	17–27 × 7–8	15.5–18.2 × 8.2–10.0
Basidiospores	8–9.5(12) × 5–6(6.5)	8.5–9 × 4.5–5.5	8–10 × 4–6	7.8–10.5 × 4.2–5.2
Q	No data	No data	Q 1.6–2.4, Q <sub>av</sub> ~2, 0	Q 1.6–2.1, Q <sub>av</sub> ~1.9
Cheilocystidia	18–24 × 9–16	12–19 × 6–10	10–23 × 6–15	10.6–22.5 × 6–11
Excrecences	1–7(9) × 0.1–1	4–8 × 1	2–8 × 0.5–1	2.0–4.4 × 0.8–1.1



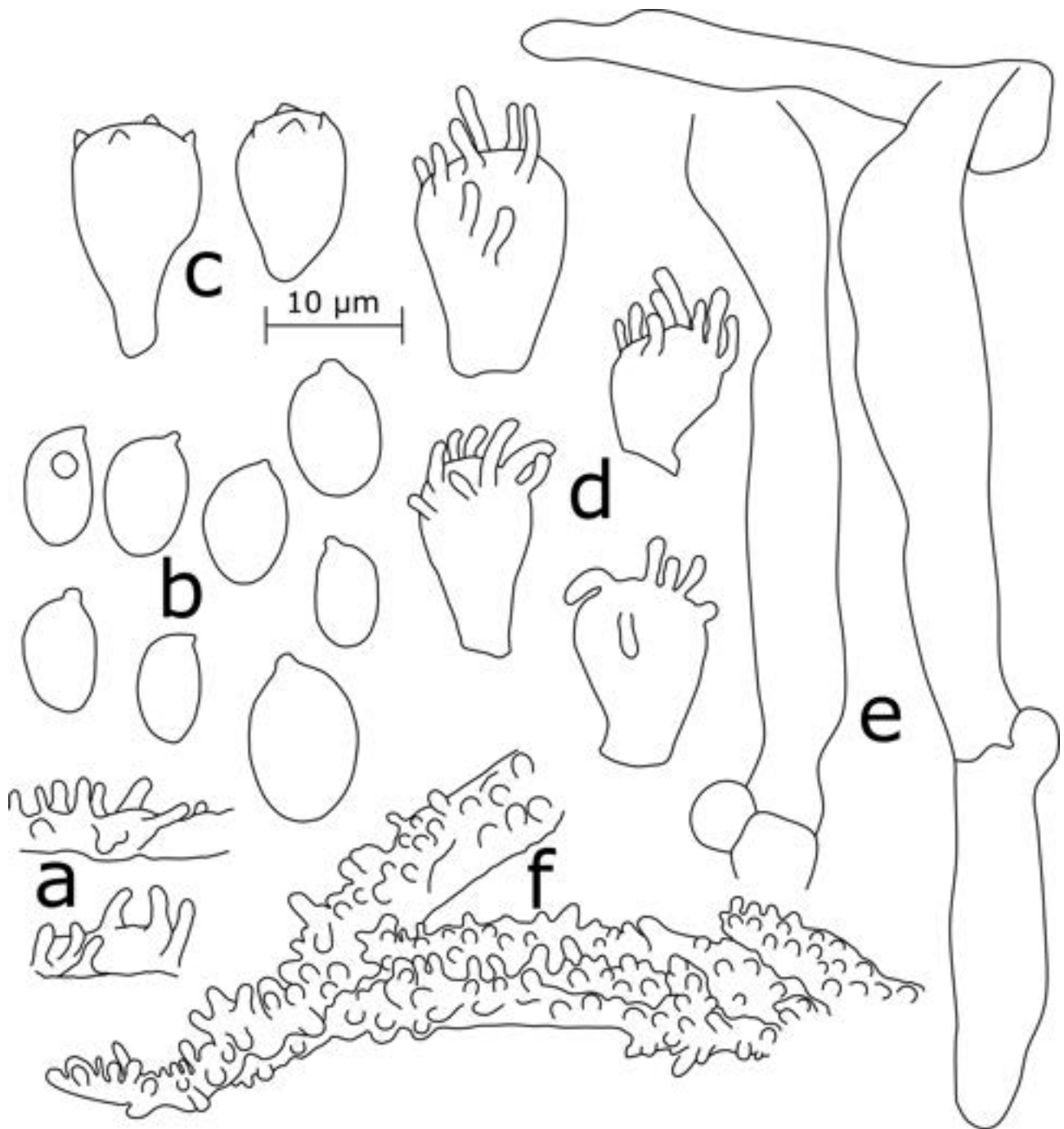


**Fig. 47.** Microstructures of *Mycena tenuispinosa*. **a.** Pileipellis hyphae. **b.** Basidiospores. **c.** Basidia. **d.** Cheilocystidia. **e.** Caulocystidia. **f.** Apex of pileal "spinula".

mature basidiomata that were white. All of them have a clearly visible basal disc, lamellae attached to a pseudocollarium, and pileal hairs seen under the hand lens. Microscopy revealed that spinules are built up of diverticulate hyphae in both samples. Caulocystidia are better seen in young basidi-

omata. Basidia size and form slightly differ from those of the previously described specimens and the observed spores are somewhat narrower; cheilocystidia match better with Polish (Ronikier et al. 2006) and Danish (Aronsen 2019) specimens (Tab. 7). Specimen LE 321755 was found on the same fallen

trunk one week later and consisted of three immature basidiomata; neither basidiospores nor mature basidia were observed, but cheilocystidia, caulocystidia, and pileal spinules match the original description.

The bluish tinge that we observed in young basidiomata was not mentioned in previous descriptions. This was observed only once under wet weather conditions (collection LE 321755). Another small bluish species, *M. occulta* Harmaja, is described from Finland. It differs from *M. tenuispinosa* by the absence of pileal spinules; ascending, narrowly adnate lamellae not forming a pseudocollarium; cheilocystidia with shorter excrescences (up to 1–1.5 µm long); heterogeneous lamellar edge; globose, clavate or subcylindrical terminal cells of pileipellis hyphae; and absence of clamp connections (Maas Geesteranus 1991).

There are two tropical species with similar pileal structures reported from Thailand: *M. pseudoseta* Desjardin, Boonprat. & Hywel-Jones and *M. mimicoseta* Desjardin, Boonprat. & Hywel-Jones (Desjardin et al. 2003). *Mycena pseudoseta* has ascending, narrowly to adnexed to subfree lamellae not forming a pseudocollarium, it lacks a separable gelatinous pellicle and caulocystidia, its cheilocystidia excrescences are longer (up to 7 µm long), and it grows on leaves of an undetermined dicotyledonous tree. *Mycena mimicoseta* has smaller basidiomata (pileus up to 1 mm in diam.), lacks cheilocystidia and caulocystidia, and has a pileipellis with acanthocysts forming the hymeniform layer.

*Author:* L.B. Kalinina

#### Basidiomycota, Agaricomycetes, Agaricales, Mycenaceae

*Mycena xantholeuca* Kühner, Encyclop. Mycol. 10: 314 (1938). – Figs. 48, 49h–i

*Material examined.* – RUSSIA. Leningrad Oblast, near village Vil’povitsy, on decaying leaves, 23 September 2018, *leg. & det.* L. Kalinina (LE 321752, LE 321753, LE 321758).

*Description.* – Basidiomata in small fascicles (up to 6) or solitary. – Pileus campanulate, 8–16 mm in diam., 10–12 mm in height, very pale yellowish with darker papilla and somewhat greenish tinge, dry. – Stipe cylindrical, 35–100 × 1–3 mm, pale whitish–yellowish darkening towards the base to pale grey with a somewhat brownish–olivaceous tinge, glabrous, hollow, covered with dense white fibrils near the base. – Lamellae segmentiform, pale yellowish, adnate. – Odor indistinct, somewhat farinaceous. – Basidio-

spores 6.4–9.7 × 3.5–5.0(5.5) µm, Q = 1.2–2.7, Q<sub>av</sub> = ~1.8 (n=85 from three specimens), amyloid, pip-shaped, ellipsoid. – Basidia 21.5–27.4 × 6.1–8.7 µm. – Cheilocystidia 13.3–24.8 × 5.9–15.9 µm, clavate, obpyriform, sessile or stipitate, with few thick excrescences (1.2)1.7–2.1(4.4) × (1.1)1.4–2.1(2.4) µm, often distinctly capitate. – Pleurocystidia absent. – Pileipellis hyphae 1.2–2.3 µm wide, diverticulate, forming coral-like mass. – Stipitipellis hyphae 1.1–2.9 µm wide, diverticulate, with numerous simple up to 4 µm long excrescences. – Clamp connections present.

*Habitat and distribution.* – On decaying wood and leaves of deciduous trees. Described from France, also known from Austria, Belgium, Germany, the Netherlands, Norway, Poland, and Russia.

*Notes.* – According to the protologue, the stipe is “hyaline blanc” and cheilocystidia are “claviformes ou piriformes, a partie superieure arrondie (9–12.5 µm diam., en brosse)” (Kühner 1938), and excrescences were not described. Later, Maas Geesteranus (1992a) compiled a new description based on the original one and noted apically swollen excrescences of cheilocystidia, as shown in the original table. Robich (2003) provided a description of this species based on examination of 30 specimens and noted not only swollen excrescences of cheilocystidia, but also a variable colour of the stipe from white to brown. According to Aronsen (2019) the stipe is watery white to grey, darker towards the base and emphasis is made on swollen excrescences as on one of the diagnostic features. The odor of the species was reported as iodoform when drying (Kühner 1938, Maas Geesteranus 1992a), as iodoform in mature basidiomata and when drying (Robich 2003), or without iodoform smell in both fresh and dried specimens (Aronsen 2019).

Our specimens were found on wood and fallen leaves in one locality – a limestone slope with *Ulmus*, *Acer*, *Corylus*, and *Fraxinus* (area of Baltic-Ladoga Klint near village Vil’povitsy). The basidiomata were quite similar and only pileus colour of LE 321753 was slightly paler than in other collections. The odor was faint and indistinct, at least more farinaceous than iodoform. Microscopical study revealed that all specimens lacked pleurocystidia and had sessile or stipitate cheilocystidia with apically swollen excrescences. Size of spores and cheilocystidia is somewhat smaller than in existing descriptions (see Tab. 8).

The p-distance between our ITS sequences of *M. xantholeuca* is 0.33 %. According to existing papers

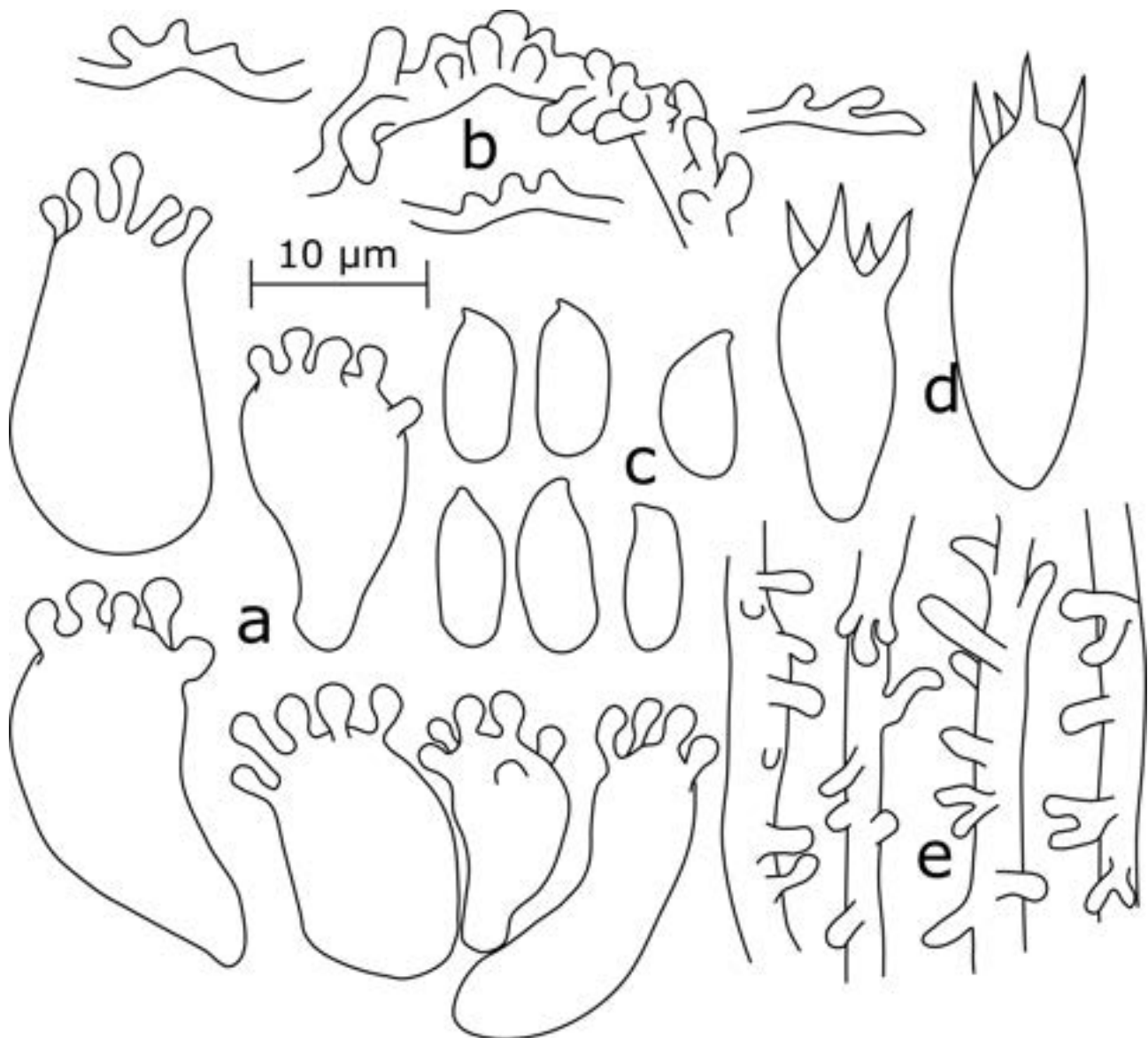


**Fig. 48.** Microstructures of *Mycena xantholeuca*. **a.** Cheilocystidia. **b.** Pileipellis hyphae. **c.** Basidiospores. **d.** Basidia. **e.** Stipitipellis hyphae.

(Petersen et al. 2008, Hughes et al. 2009), pairwise distances less than 3 % allow to consider that specimens belong to the same species. BLASTn searches revealed that our specimens are closer to *M. cicog-*

*nanii* (GenBank accession number JF908486, 97 % similarity) and *M. rhamnicola* (JF908372, 97 %) than to *M. xantholeuca* (JF908446, 93 %). Our specimens show morphological (yellowish white bell-

**Tab. 8.** Comparison of micromorphological characters in *Mycena xantholeuca* according to existing descriptions.

Character	Kühner (1938)	Robich (2003)	Aronsen (2019)	Present study
Basidia	27–28 × 6.5	26–33 × 7.5–9	25–29 × 6–8	21.5–27.4 × 6.1–8.7
Basidiospores	8–9 × 4.2–5	7.5–9.5 × 5–6	8–10(11) × 4.5–6(7)	6.4–9.7 × 3.5–5(5.5)
Cheilocystidia	9–12.5 in diam.	15–45 × 10–25	15–35(45) × 7–19.5	13.3–24.8 × 5.9–15.9
Excrescences size	No data	2–8	1–6(18) × 1–1.5	1.2–4.4 × 1.1–2.4



**Fig. 49.** Basidiomata of studied *Mycena* species. **a–d.** *Mycena tenuispinosa* (LE 321754). **e.** Pileal “hair” of *M. tenuispinosa* at 400× (LE 321754). **f–g.** *Mycena albidoloacea* (f: LE 321756, g: LE 321757). **h–i.** *Mycena xantholeuca* (h: LE 321753, i: LE 321752).

shaped cap, cheilocystidia with often distinctly capitate excrescences, absence of pleurocystidia) and ecological (decaying wood and leaves of deciduous trees) features that are typical for *M. xantholeuca*; pointing to misidentifications in submitted sequence data.

*Author:* L.B. Kalinina

#### Ascomycota, Sordariomycetes, Hypocreales, Neoneectriaceae

*Neoneectria neomacrospora* (C. Booth & Samuels) Mantiri & Samuels, in Mantiri et al., Can. J. Bot. 79(3): 339 (2001). – Fig. 50

*Material examined.* – *Madhuca longifolia* (Sapotaceae), commonly known as mahua, is an Indian tropical tree found largely in central and north Indian plains and forests. It is cultivated for its oleaginous seeds, flowers, and wood. It has been used in traditional medicine since long and is also used to prepare food products, alcohol, cosmetics, and oil-cake as bio-fertilizer. In September 2018, severe outbreaks of leaf spot occurred in *M. longifolia* plantations at the Kalyani District Seed Farm, 22°35'31.9200"N, 88°15'13.6800"E (Bidhan Chandra Krishi Viswavidyalaya, West Bengal State, India). The disease began as small brown spots (Fig. 50A), surrounded by irregular dark margins with characteristic yellow halos and reddish pigments that gradually increased from 0.5 to 0.8 cm in diam. (Figs. 50D, E), changing from circular to irregular lesions mostly confined on the upper surface of leaves (Fig. 50B). In severe cases, marginal necroses of leaves were noticed (Fig. 50C).

*Culture characteristics.* – In the laboratory, the margin of necrotic tissues and spotted areas of leaves were used for fungal isolation. The samples were surface sterilized for three minutes in a 4 % sodium hypochlorite solution for 30 s after which they were dipped in ddH<sub>2</sub>O and air-dried for ten minutes. Samples were placed on potato dextrose agar (PDA) and incubated at 22 °C in 12 h dark/12 h light cycle. Within a few days, white mycelium emerged from the samples and rapidly colonized the agar surface (Fig. 50F). One culture was deposited at NFCCI (Agharkar Research Institute, Pune, India).

*Notes.* – Ovoid to ellipsoid microconidia with an average size of 4–12 × 2–5 µm and straight one to three-septate round-ended macroconidia (12–60 × 4–6 µm) were observed in culture (Fig. 50G). DNA was extracted from mycelium and ITS amplification was done with primers ITS1 and ITS4 (White et al. 1990). The generated sequence was submitted to GenBank under accession number MK193872. Based on morphology (Ouellette 1972, Booth 1979) and the ITS sequence, the fungus was identified as *Neoneectria neomacrospora*. Pathogenicity tests were conducted by spraying conidial suspension on

attached healthy surface-sterilized green leaves with 20 µl of a suspension of 10<sup>5</sup> conidiospores/ml, prepared from 15 d-old PDA culture. Control leaves were sprayed only sterile water. After seven d, spots with extended necroses had developed on all inoculated leaves whereas control leaves remained healthy. The pathogen was re-isolated from infected leaves showing typical symptoms, thus fulfilling Koch postulates.

*Neoneectria neomacrospora* is mentioned on the EPPO *Alert List*. Recent incidence of this pathogen has been reported in several European countries from *Abies* species and other conifer hosts (Pettersson et al. 2016, Schmitz et al. 2017). Review of the literature revealed that our Indian report is the first one of leaf spot and necrosis on *Madhuca longifolia* caused by *N. neomacrospora* in the world.

*Authors:* A. Banerjee, S. Chatterjee, B. Panja & P. S. Nath

#### Ascomycota, Sordariomycetes, Magnaporthales, Magnaporthaceae

*Plagiosphaera immersa* (Trail) Petr., Sydowia 14(1–6): 351 (1960). – Fig. 51

*Basionym.* – *Ophiobolus immersus* Trail, Trans. Bot. Soc. Edinb. 17: 492 (1889).

*Synonyms.* – *Ophiobolus brachysporus* Fautrey & Roum., Revue Mycol. Toulouse 14(55): 109 (1892). *Ophiobolus moravicus* Petr., Ann. Mycol. 19(1/2): 80 (1921). *Plagiosphaera moravica* (Petr.) Petr., Ann. Mycol. 39(4/6): 289 (1941).

*Material examined.* – AUSTRIA. Niederösterreich, Sierndorf, Marchauen near Hufeisen, on dead stems of *Urtica dioica*, 22 August 2015, leg. H. Voglmayr (WU 40035, culture D98); Niederösterreich, Ebenfurth, Haschendorf, Fische-Ursprung, on dead stems of *U. dioica*, 2 September 2017, leg. H. Voglmayr (WU 40036, culture D266); Oberösterreich, St. Wilibald, Aicht, on dead stems of *U. dioica*, 15 August 2015, leg. H. Voglmayr (WU 40037, culture D148); *Ibid.*, 16 September 2017, leg. H. Voglmayr (WU 40038, culture D270); Wien, Ottakring, Wilhelminenberg, between Kreuzeichenwiese and Schottenhof, on dead stems of *Sambucus ebulus*, 24 July 2016, leg. H. Voglmayr (specimen lost).

*Description.* – Ascomata perithecial, immersed in and translucent through the dead host tissue, 200–350 µm diam., 100–180 µm high, black, scattered singly to gregarious, distinctly flattened, commonly horizontally oriented in parallel to the host tissue fibres with an apparently lateral (but in fact apical), upwardly bent ostiolar papilla; occasionally vertically oriented with a more or less centrally emerging ostiolar papilla. – *Ostiolar papilla* slightly excentric to distinctly lateral, cylindrical, ca. 100–150 µm long, 50–100 µm wide, black, not to slightly protruding above the substrate. – *Peridium* continuous, dark brown, 10–20 µm thick, of a *textura angularis* composed of thin-

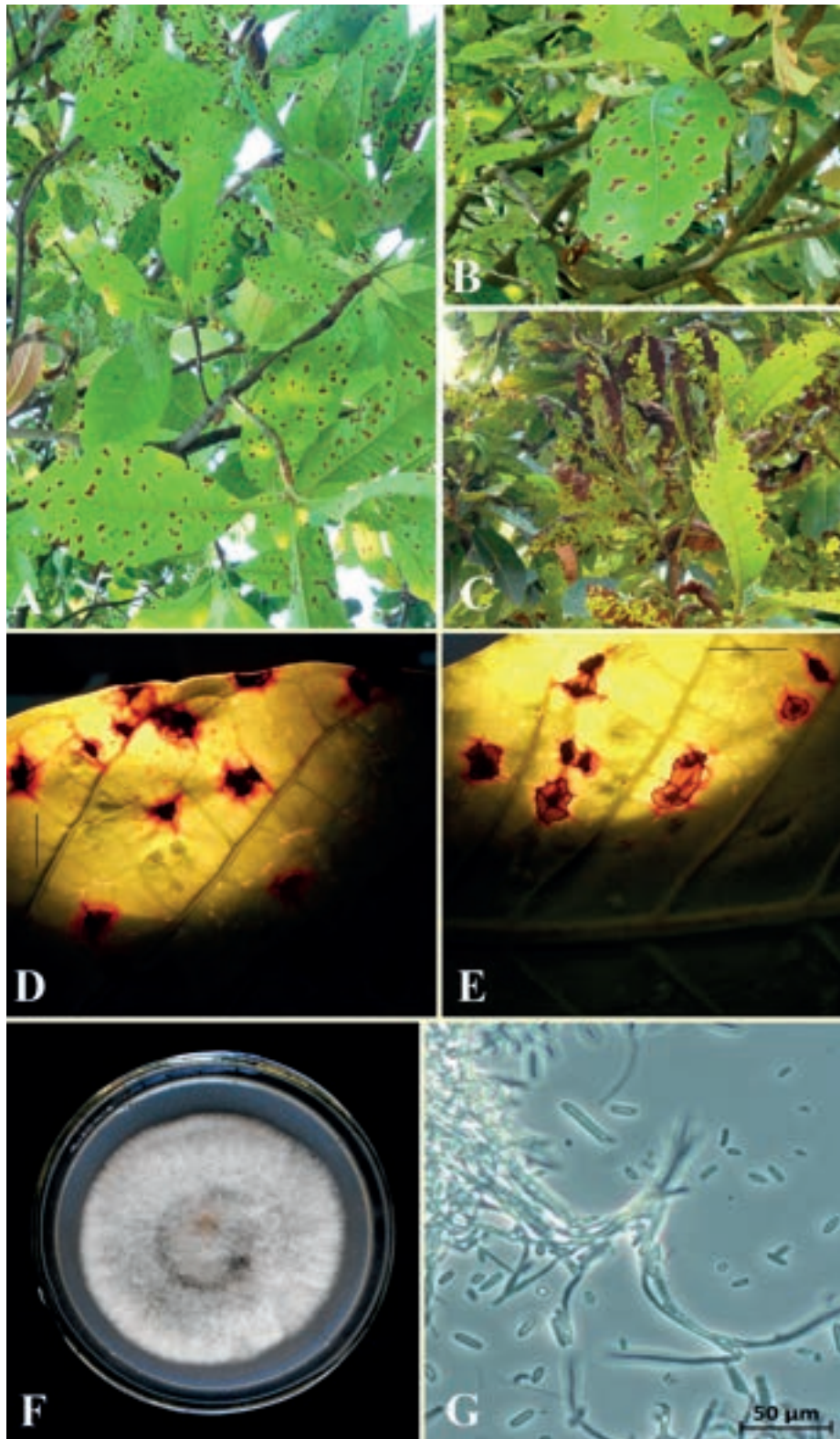


**Fig. 50.** *Neovectria neomacrospora*. **A.** Initial small brown leaf spots on *Madhuca longifolia*. **B.** Characteristic yellow halos and reddish-brown zonation surrounding leaf spots. **C.** Marginal necroses of leaves. **D.** Surface view of leaf spots on *M. longifolia* leaf. **E.** Bottom view of leaf spots. **F.** Colony on PDA. **G.** Micro- and macroconidia. Scale bars D, E 1 cm; G 50 µm.

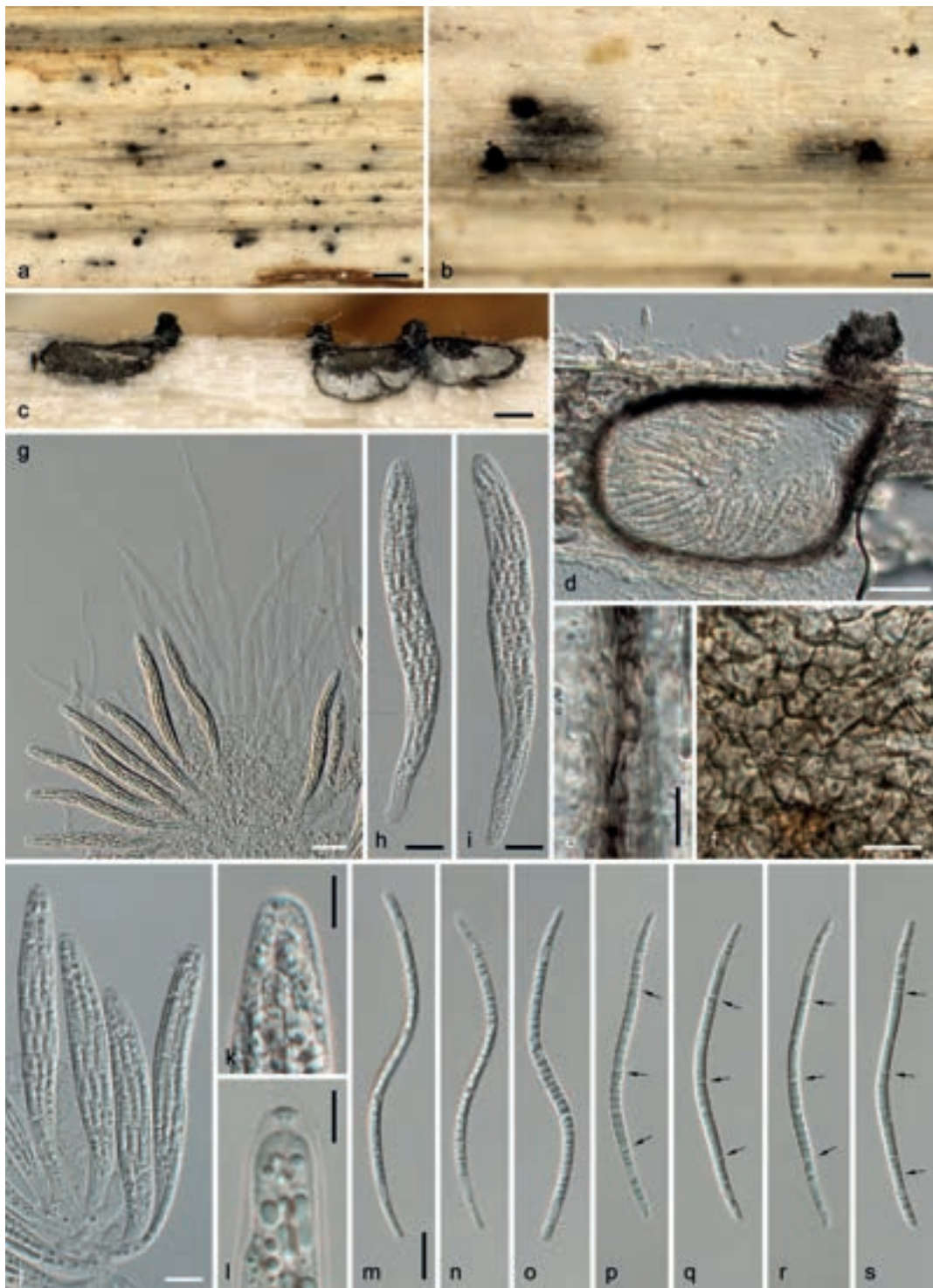


**Fig. 51.** *Plagiosphaera immersa* (WU 40035). **a, b.** Translucent perithecia with laterally emerging ostioles immersed in dead stems of *Urtica dioica*. **c, d.** Vertical section of immersed perithecia showing the horizontally oriented perithecia with asci emerging from the lower half of the perithecial wall (**d**) and the apparently lateral (but in fact apical) ostioles bent upwards in more or less a right angle. **e, f.** Perithecial wall in section (**e**) and in face view (**f**). **g.** Hymenium with vital asci and paraphyses. **h-i.** Asci in vital state, detached from hymenium. **j.** Asci in dead state. **k, l.** Ascus apices with refractive apical ring. **m-s.** Vital (**m-o**) and dead (**p-s**) ascospores with 3 septa (indicated by arrows). All in water, except **j, l, p-s** in 3% KOH. Scale bars **a** 500  $\mu\text{m}$ ; **b, c** 100  $\mu\text{m}$ ; **d** 50  $\mu\text{m}$ ; **e, f, h-j, m-s** 10  $\mu\text{m}$ ; **g** 20  $\mu\text{m}$ ; **k, l** 5  $\mu\text{m}$ .

walled, isodiametric to elongated cells 3.5–12  $\mu\text{m}$  diam with dark brown walls. – *H a m a t h e c i u m* composed of hyaline, smooth, thin-walled, septate paraphyses (100)120–163(180)  $\mu\text{m}$  long, 5–9  $\mu\text{m}$  wide at the base, apically gradually tapering to 1.5–3.5  $\mu\text{m}$  ( $n=17$ ); periphyses not observed. – *A s c i* numerous, arising from the lower half of the perithecial wall, (fresh) in water (90)94–114(138)  $\times$  (8.5)9–11(12.8)  $\mu\text{m}$  ( $n=51$ ); from herbarium specimens in 3 % KOH (65)73–86(93)  $\times$  (9.5)10.0–11.5(12.7)  $\mu\text{m}$ , pars sporifer (56)61–75(85)  $\mu\text{m}$ , stipe (6)8.7–14.0(15.5)  $\mu\text{m}$  long ( $n=32$ ), unitunicate, fusoid to cylindrical, curved to slightly sinuous, thin-walled, containing 8 ascospores arranged in a single contorted fascicle, with a distinct, refractive, inamyloid apical ring 1.5–2  $\mu\text{m}$  wide, at maturity becoming detached from the perithecial wall and free-floating. – *A s c o s p o r e s* (51)59–71(78)  $\times$  (1.8)2.3–2.8(3)  $\mu\text{m}$ , l/w = (21)23–29(34) ( $n=40$ ), substraight, slightly curved to sinuous, indistinctly 0–5 septate (only visible in 3 % KOH or after staining), hyaline, thin-walled, smooth, with rounded ends, densely multi-guttulate when vital. – *A s e x u a l m o r p h* not observed.

*H a b i t a t a n d d i s t r i b u t i o n.* – Common on dead overwintered stems of *Urtica dioica*; also reported from dead stems of other herbaceous hosts, e.g., *Aconitum napellus*, *Campanula latifolia* (type host), *Sambucus ebulus*. Widely distributed in Europe, known from Austria, Bulgaria, Czech Republic, France, Germany, Netherlands, Norway, Poland, Spain, UK.

*N o t e s.* – The genus *Plagiosphaera* was established by Petrak (1941) based on *Plagiosphaera moravica*, which he initially described as *Ophiobolus moravicus* (Petrak 1921) from dead stems of *Urtica dioica* collected in Mährisch-Weißkirchen (now Hranice na Moravě, Czech Republic). Later, he considered *P. moravica* to be synonymous with the earlier *Ophiobolus immersus*, which was described from Norway on dead stems of *Campanula latifolia* (type host) but also recorded from *U. dioica* (Trail 1889), and he proposed the new combination *Plagiosphaera immersa* (Petrak 1960). Petrak (1941) provided a detailed German description of the type species, in which he correctly interpreted the perithecia as horizontally oriented in parallel to the stem axis, due to which the apical, upwardly bent ostiolar papilla appears to be laterally inserted (see Fig. 51d). However, perithecia may also be vertically immersed, then having a more or less centrally emerging ostiolar papilla (Dennis 1975, Walker 1980, personal observations). After investigating the type, Dennis (1975) added another synonym,

*Ophiobolus brachysporus*, described from France on *U. dioica*.

Since the establishment of the genus, *Plagiosphaera* has commonly been considered to be closely related to genera now classified within Diaporthales. Petrak (1941) proposed close affinities to *Ophiognomonia*, and it has subsequently been classified within Diaporthaceae (e.g., Kobayashi 1970, Dennis 1975) or Gnomoniaceae (e.g., Barr 1978, Monod 1983). When establishing the genus *Gaeumannomyces*, Arx & Olivier (1952) supposed a close relationship to *Linospora*, *Ophiognomonia*, and *Plagiosphaera*, and Walker (1980) also hypothesized that *Gaeumannomyces* and *Plagiosphaera* were closely related. However, at that time, *Gaeumannomyces* was also classified within Gnomoniaceae. In light of variability of distinguishing features like lateral orientation of the ostioles, Walker (1980) considered the parasitic (*Gaeumannomyces*) versus saprobic (*Plagiosphaera*) habit as main diagnostic character for separating both genera. On the other hand, Barr (1990) did not agree with a close relationship between *Gaeumannomyces* and *Plagiosphaera*, retaining the former within Gnomoniaceae while classifying the latter within Lasiosphaeriaceae. Huhndorf et al. (2004) removed *Plagiosphaera* from Lasiosphaeriaceae and classified it as *Sordariomyces incertae sedis*, which was also followed in the last *Dictionary of the Fungi* (Kirk et al. 2008) and in *Index Fungorum* (2019).

Our phylogenetic analyses of the concatenated ITS–LSU–*rpb1*–*tef1* matrix (Fig. 52) revealed a well to highly supported placement of *P. immersa* as the most basal lineage of the Magnaporthaceae family (Magnaporthales). Therefore, close phylogenetic affinities with the morphologically similar genus *Gaeumannomyces* are confirmed (see also Walker et al. 2012), while disproving affinities with Gnomoniaceae (Diaporthales). Interestingly, our sequence data also revealed problems within *Plagiosphaera immersa* that currently cannot be satisfactorily resolved. Although all four accessions sequenced originated from the same host (*U. dioica*), and two (D148, D270) even from the same locality (but different years), a remarkable sequence variation was observed between the four accessions in all markers sequenced (sequence similarities ranging in the ITS from 89–99 % (4–57 substitutions, including gaps), in the LSU from 99–100 % (0–7 substitutions), in *tef1* from 91–99 % (3–119 substitutions, including gaps), and 95 % (72 substitutions, including gaps) in the *rpb1*; only two accessions sequenced in the latter). Although these marked differences indicate the presence of three genetically distinct lineages (D98,



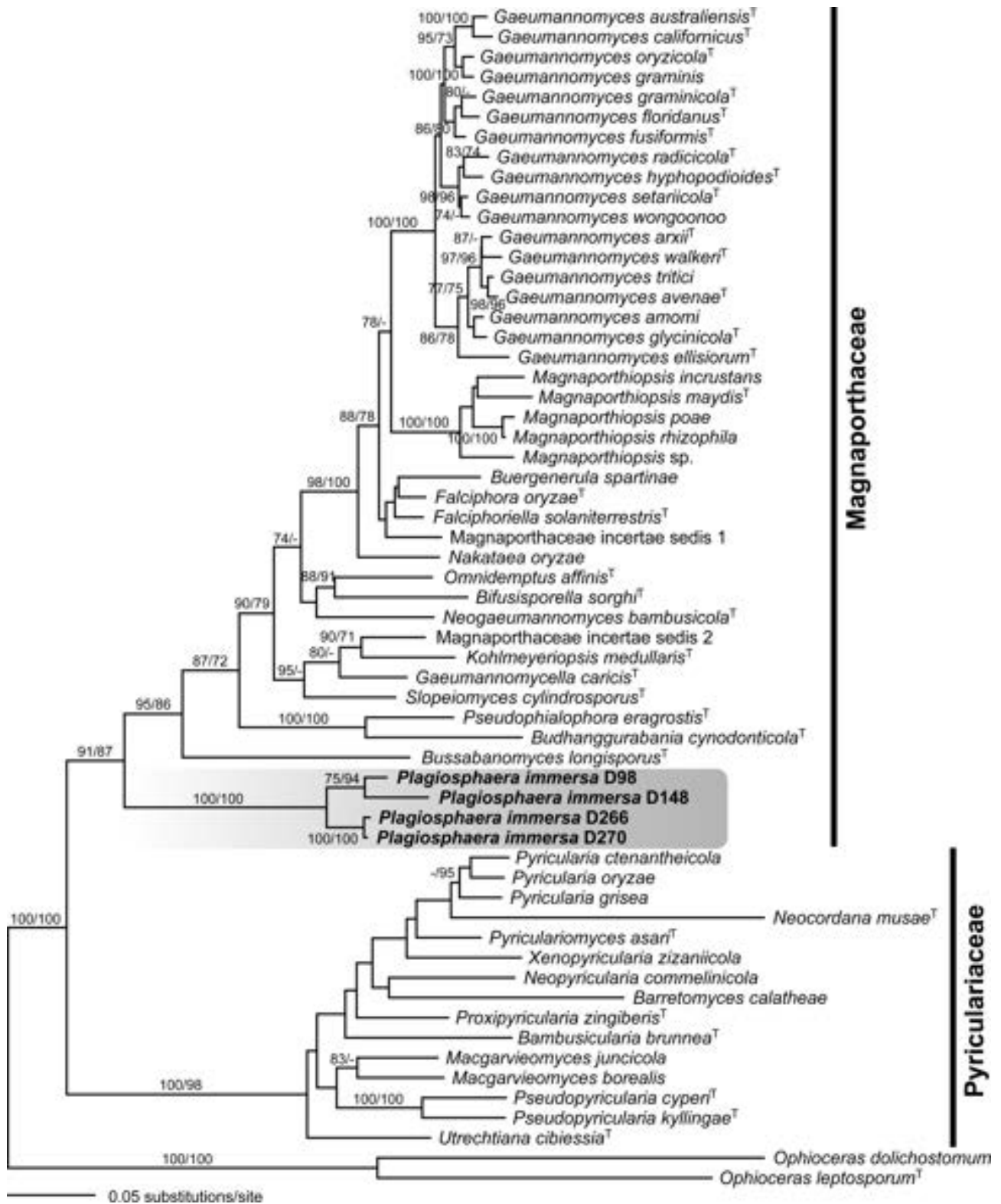


**Fig. 52.** ML phylogeny (-lnL = 28226.205) of selected Magnaporthales, reconstructed from the concatenated ITS–LSU–*rpb1*–*tef1* dataset, showing the phylogenetic position of *Plagiosphaera immersa* (in bold). ML/MP bootstrap support  $\geq 70$  are presented above or below the branches. Superscript <sup>T</sup> following taxon names indicates ex- epi-, holo-, or neotype isolates.

D148, D266+D270; see Fig. 52), no morphological differences were observed – pointing at another case of cryptic diversity. Additional extensive collecting, sequencing, and morphological investigations are required before these genetic differences can be evaluated; meanwhile it seems appropriate to classify them within a single genetically variable species, *Plagiosphaera immersa*.

Like in Diaporthales, the asci of *P. immersa* become free-floating when mature. In fresh vital material, asci mounted in water are distinctly longer than in herbarium specimens mounted in KOH; measurements are therefore given separately in the descriptions. The small, apical ascus ring is more obvious in material mounted in KOH, where it becomes slightly larger and distinctly refractive (Figs. 51k, l). Ascospore septation is indistinct and invisible in fresh material due to the numerous guttules and can only be seen in dead spores mounted in KOH or after staining; this may be the reason why e.g. Dennis (1975) described the spores as aseptate.

According to personal observations, *P. immersa* is common on old overwintered stems of *U. dioica* in moist habitats such as riverine and swamp forests. It was found in all investigated larger populations of its host. However, it can be easily overlooked and requires specific thorough searches. For these reasons, it has only rarely been recorded. Illustrations of a fresh Spanish collection from *U. dioica* are available at <https://www.asturnatura.com/fotografia/setas-hongos/plagiosphaera-immersa-trail-petr-/29364.html>.

Author: H. Voglmayr

## Ascomycota, Pezizomycetes, Pezizales, Pyrenomataceae

*Sphaerosporium lignatile* Schwein., Trans. Am. Phil. Soc., New Series 4(2): 303 (1832) [1834]. – Fig. 53

Synonym: *Coccospora lignatilis* (Schwein.) Höhn., Sber. Akad. Wiss. Wien, Math.-naturw. Kl., Abt. 1 120: 404 (1911).

Material examined. USA. Wisconsin, Sauk County, 334 m a.s.l., 43°25'10.56" N, 89°38'29.76" W, 10 November 2017, leg. A.C. Dirks, det. D.S. Newman, confirm. A.C. Dirks, ACD0062, D. Haelew. F-1614 (MICH 254984), <https://mushroomobserver.org/299262>. Sequences: MN756649 (SSU), MN749372–MN749373 (ITS), MN749494–MN749495 (LSU).

Description. – Fruiting body pulverulent masses of conidia, orbicular to effused, ochreous to honey-colored, up to 2 mm in diam. when discrete, extending for 1 cm or more when effused. – Hyphal system hyaline, branched, septate, smooth, swollen in the midsection and pinched at

the septa resulting in a torulose appearance, length (20.3)21.3–32.7(35.0) × (10.7)12.6–16.0(17.1) μm (n=10). – Conidiophores densely packed with basipetal, blastic conidiogenesis and schizolytic secession. – Conidia chlamydospore-like, unicellular, globose to ellipsoid, often with prominent lipid bodies; when globose to subglobose, (28.0)34.0–45.7(48.8) × (27.0)31.7–42.7(47.0) μm, Q (1.0)1.0–1.1(1.2) (n=44); when ellipsoid, (24.6)32.5–52.9(64.8) × (19.5)24.0–34.5(36.8) μm, Q (1.1)1.2–1.7(1.9) (n=16); pale yellow when mature with a hyaline, refractive spore wall up to 6 μm thick, truncate at points of secession.

Habitat and distribution. – On well-decayed hardwood logs of *Carya*, *Fraxinus*, *Quercus*, and possibly other tree species in eastern North America, extending into Central America (Panama) and northern South America (Colombia and Venezuela).

Notes. – *Sphaerosporium lignatile*, the type species of *Sphaerosporium* Schwein., was described in 1832 based on collections from Pennsylvania, USA. Since then, *S. lignatile* has been documented across eastern North America – from Ontario to Florida – and its range may extend as far south as Venezuela (Shear 1939, Sumstine 1949, Emmons et al. 1960, Martin 1960, Dennis 1965, Cooke 1975, Partridge & Morgan-Jones 2002). *Sphaerosporium lignatile* grows on dead, typically well-rotted hardwood logs, often in low lying wet areas, indicating a saprotrophic lifestyle. However, this fungus is difficult to grow on media (R. Healy, personal communication). We observed close association between *S. lignatile* and moss. Together, these observations hint at a symbiotic relationship between *S. lignatile* and bryophytes, challenging axenic culturing.

The phylogenetic placement of the genus *Sphaerosporium* has eluded mycologists for almost two centuries. First dumped into Hyphomycetes within the Fungi Imperfecti, throughout the years researchers have conjectured a phylogenetic affinity with *Coccospora* spp. in Myxomycota, *Chaetomium piluliferum* J. Daniels in Ascomycota (Sordariomycetes), and *Haplotrichum* spp. in Basidiomycota (Agaricomycetes) (Partridge & Morgan-Jones 2002). Most recently, Partridge and Morgan-Jones (2002) studied *S. lignatile* for its similarity to *Acladium* Link [as *Haplotrichum* Link], the anamorph of corticioid Botrybasidiaceae (Basidiomycota, Agaricomycetes, Cantharellales). The authors noted, however, that “basidiomyceteous affinity remains a matter for speculation.”

*Sphaerosporium equinum* (Desm.) J.L. Crane & Schokn., one of only two other species in the genus (Index Fungorum 2019), was recently the subject of

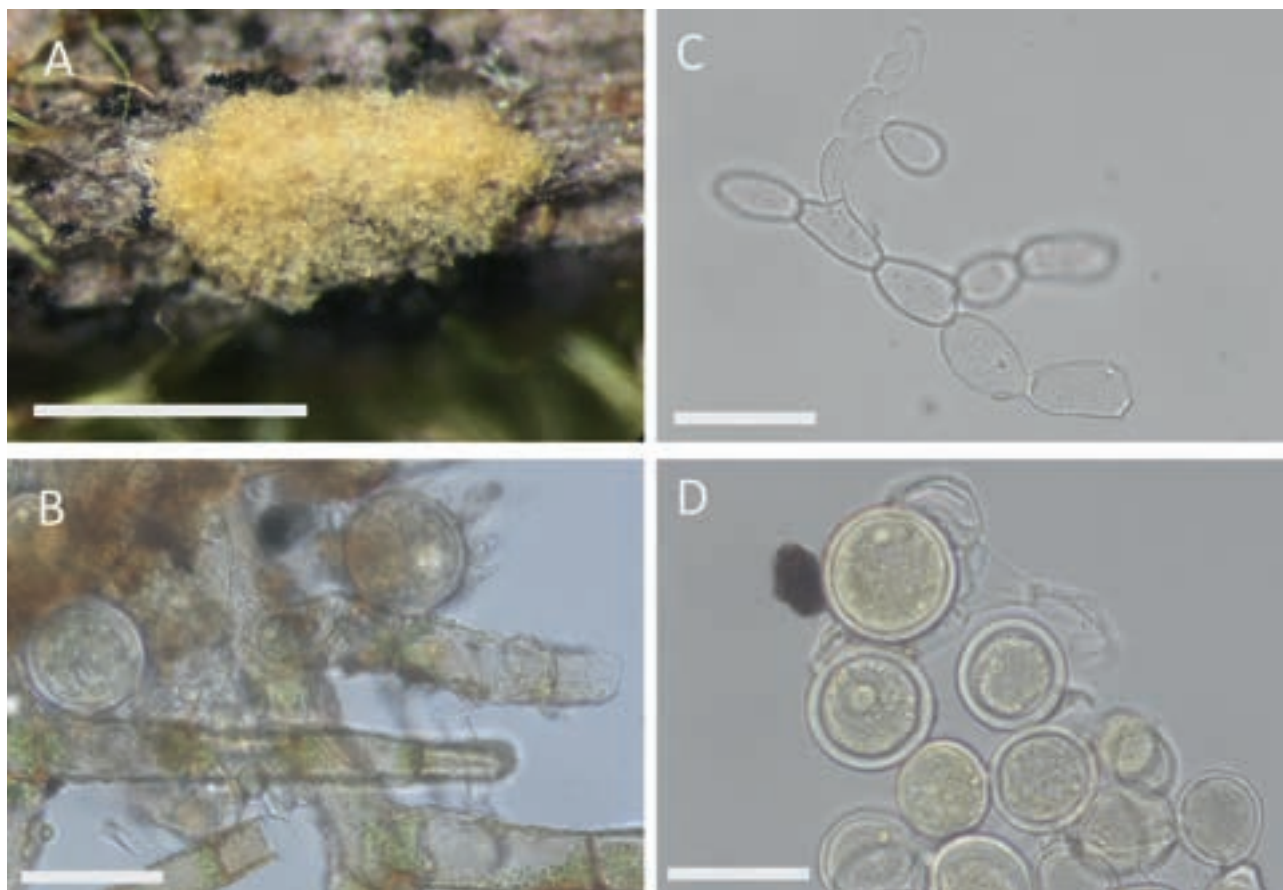


**Fig. 53.** Macroscopic and microscopic morphology of *Sphaerosporium lignatile* (MICH 254984). **A.** Fruiting bodies are small, cushion-shaped masses of ochreous to honey-colored spores. **B–D.** Squash mounts in deionized water. **B.** We observed close associations between *S. lignatile* and bryophyte rhizoids. **C.** Hyphae are torulose, branched, and generate monoblastic conidia. **D.** Chlamydospore-like conidia, surrounded by a thick, hyaline, refractive cell wall. Scale bars A 1 mm, B–D 50 µm.

a study on filamentous fungi inhabiting cheese (Ropars et al. 2012). Five *S. equinum* cultures isolated from French cheese were sequenced and resolved in Eurotiomycetes (Ascomycota, Pezizomycotina). Considering that *S. equinum* was originally described from old, humid horse hooves (hence the specific epithet), we believe the cultures from the above study were misidentified (Partridge & Morgan-Jones 2002). This is not surprising given the centuries-long debates surrounding *Sphaerosporium* and other simple anamorphic genera like *Coccospora*, *Oospora*, and *Torula*, which evade easy taxonomic classification (Damon & Downing 1954).

Based on initial BLAST searches, it was clear that *S. lignatile* was ascomycetous; all three loci (SSU, ITS, LSU) pointed at a relationship within Pezizomycetes. Our multi-locus molecular phylogenetic analysis including newly generated SSU and LSU sequence data (Fig. 54) placed *Sphaerosporium* among members of Pyronemataceae (Pezizomy-

cotina, Pezizomycetes, Pezizales) with maximum support. The closest relative in the analysis was *Scutellinia scutellata* (L.) Lambotte (MLBS = 100). Pyronemataceae is the largest, most heterogeneous, and least studied family in Pezizales. In their LSU-based phylogenetic study of the family, Perry et al. (2007) found that morphological characters traditionally used for subfamilial classification were not phylogenetically informative above the genus level. Given that *Pyronemataceae* is characterized by a lack of unifying morphological characteristics, it is fitting that *S. lignatile* with its enigmatic morphology would belong to this group.

Nonetheless, one commonality stands out: despite their diverse morphologies, species in the *Scutellinia* subclade are characterized by brightly pigmented taxa, which is true for *S. lignatile* as well. Whereas some genera in *Pyronemataceae* have been shown to be parasites of bryophytes – lending some credibility to our hypothesis of a non-sapro-

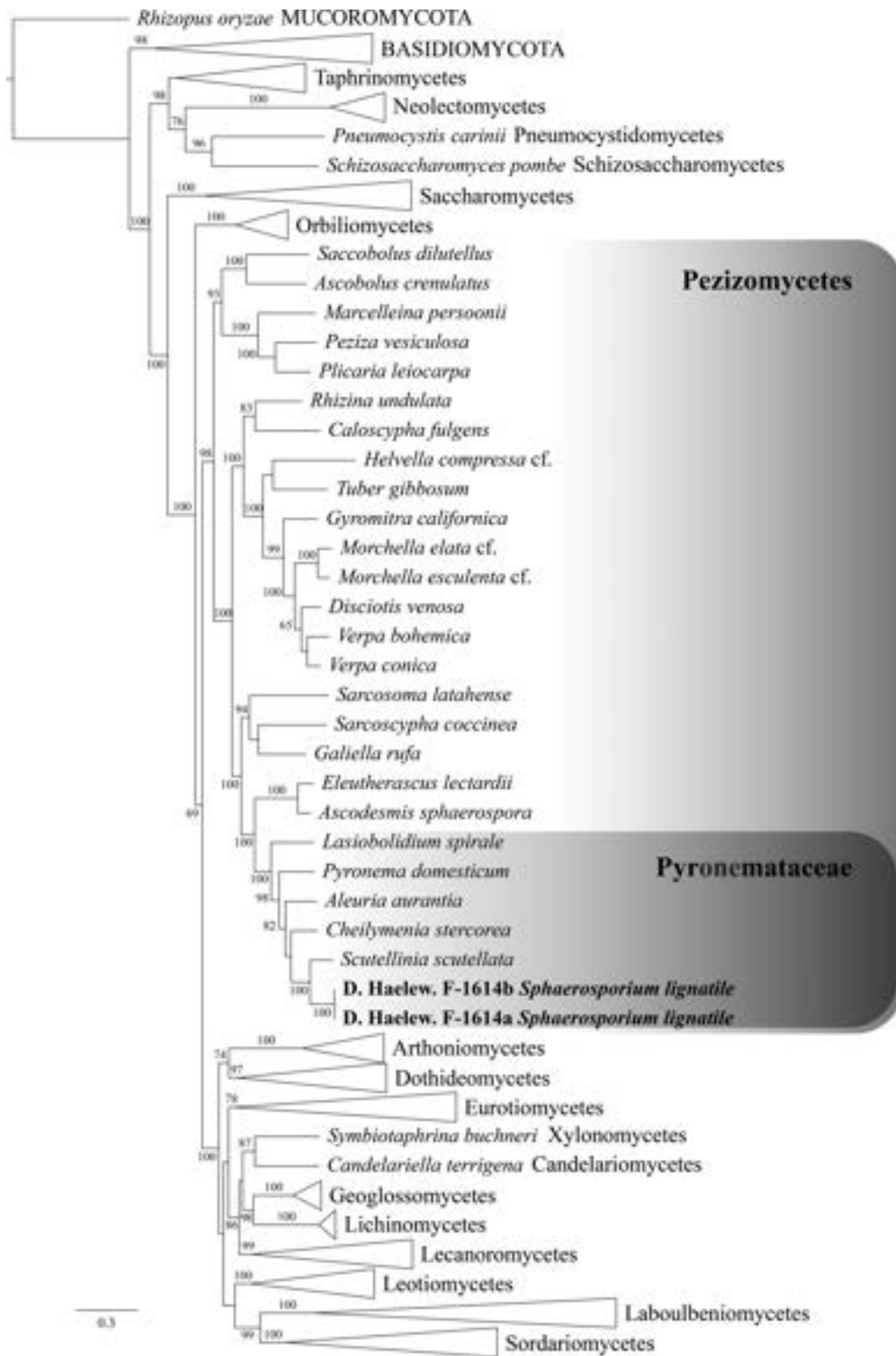


**Fig. 54.** Ascomycota-wide phylogeny reconstructed from a six-locus data matrix (SSU, LSU, *rpb1*, *rpb2*, *tef1*, mitSSU). The topology is the result of ML inference performed with RAxML with all lineages collapsed to class level except for Pezizomycetes. For each node, MLBS  $\geq 65$  is presented above or below the branch leading to that node. Class Pezizomycetes and family Pyronemataceae highlighted by gray shading.

trophic habit for *S. lignatile* – these bryophilous taxa are restricted to a single, well-resolved lineage distantly related to the *Scutellinia* subclade. More studies are needed to understand both the ecology of *S. lignatile* and the taxonomy of related species, the generic status of which remains to be proven. Our positioning of *S. lignatile* among Pyronemataceae adds greater intrigue to an already diverse and fascinating group of fungi.

*Authors:* D. Haelewaters, J. Liu & A.C. Dirks

### Acknowledgements

The *Russula* authors are grateful to Dr. Hai-Jiao Li for providing samples, and to Miss Xu-Meng Jiang and Mr. Yang-Kun Li (China) for the collection of specimens. The *Russula* project was funded by Science and Technology Project of Guangdong Province (2017B020205002) and the National Natural Science Foundation of China (nos. 31570544 and 31770657). *Cortinari* authors A. Razaq, S. Ilyas, and A.N. Khalid are thankful to Hira Bashir (Fungal Systematics Lab, Department of Botany, University of the Punjab, Lahore, Pakistan) for helping in the preparation of line drawings. K.C. Semwal and V.K. Bhatt are grateful to the Uttarakhand State Council for Science and Technology (UCoST), India for the financial support under project no. UCSandT/RandD/LS-1/12-13/4912. The *Curvularia* work was financially supported by grants from the Research Council of Shahid Chamran University of Ahvaz. The *Gloeocantharellus* authors are grateful to anonymous reviewers for constructive comments and suggestions on the manuscript. Xiang-Rong Zhong and Xiang-Nv Chen (Guangdong Institute of Microbiology) are acknowledged for help during fieldwork. The *Gloeocantharellus* study was supported by the National Natural Science Foundation of China (nos. 31700021, 31670018), the GDAS Project of Science and Technology Development (2019GDASYL-0104009), and the Science and Technology Project of Guangdong Province (2017A030303050). The *Laboulbenia* authors are grateful to Dr. Annette Aiello (Smithsonian Tropical Research Institute, Panama) to allow D. Haelewaters and Sarah J.C. Verhaeghen to screen the local insect collection at Tupper Center in 2015; Drs. Pilar Andrés and Sergi Santamaría (Universitat Autònoma de Barcelona, Spain) for sharing Nicaraguan material of *L. bernaliana*, collected under the project “Evaluación social multicriterios para la gestión sostenible y la conservación del Paisaje Protegido Miraflores-Moropotente” (2006–2010) funded by the Agencia Catalana para la Cooperación al Desarrollo (ACCD) and the Fundació Autònoma Solidaria (FAS) of the Universidad Autònoma de Barcelona; Michał Gorczak (University of Warsaw, Poland) for assistance during the description of *L. oiovellicola*; and Higor Rodrigues (Museu de Zoologia da Universidade de Sao Paulo, Brazil) for sending infected insect specimens. A. De Kesel acknowledges ASBL MIKEMBO (Lubumbashi, DR Congo) and Biodiversité au Katanga (DR Congo) for financial and logistical support of fieldwork in Katanga (2012–2018). D. Haelewaters acknowledges support of fieldwork in Panama in 2015 from the Torrey Botanical Society (2015 Graduate Student Research Fellowship), Georgia Entomological society (2015 PhD Scholarship), and Harvard University David Rockefeller Center for Latin American Studies (2015 Summer Research Travel Grant). D. Haelewaters received funding from a SYNTHESYS+ grant (no.

BE-TAF-151), financed by the Horizon 2020 Research Infrastructures Programme of the European Commission. The *Rhizoglossum* authors thank all the members of the Laboratorio de Biología y Genética Molecular for collaborating in the publication of this article and the farmers of the town Palmiche (Lamas) for providing the facilities for the collection of soil samples. The *Rhizoglossum* study was supported by the Programa Nacional de Innovación Agraria (PNIA) and the Universidad Nacional de San Martín-Tarapoto (UNSM-T) through the contract no. 037-2015-INIA-PNIA-IE; through the loan agreement no. 8331-PE, signed between the government of Peru and the International Bank for Reconstruction and Development–BIRF; by the Consejo Nacional de Ciencia y Tecnología, CIENCIACTIVA (CONCYTEC, Peru), within the framework of the project with SUBVENTION AGREEMENT no. 187-2015-FONDECYT. G.A. da Silva thanks Conselho Nacional de Desenvolvimento Científico e Tecnológico (CNPq) for Fellowship Proc. 312186/2016-9. The *Strobilomyces* authors are grateful to the Kunming Institute of Botany (KIB), Chinese Academy of Sciences. They also thank Z.J. Gu (KIB) and J.W. Liu (KIB) for help with scanning basidiospores. This work was supported by the Key Laboratory of Yunnan Province Universities of the Diversity and Ecological Adaptive Evolution for Animals and plants on Yun-Gui Plateau and the National Nature Science Foundation of China (nos. 31860005, 31800016 and 31860057). C. Liu thanks the Yunnan Local Colleges Applied Basic Research Projects (2017FH001-034). L.Z. Tang acknowledges the Yunnan Applied Basic Research Projects (2018FB050). The lichen study was supported by TUBITAK (project 117Z976). The *Marasmiellus* authors thank Jan Borovička (Prague, Czech Republic) for collaboration in the field and M. Sochor for molecular work. The studies of the authors were enabled by support provided to the Moravian Museum by the Ministry of Culture of the Czech Republic as part of its long-term conceptual development programme for research institutions (DKRVO, ref. MK000094862). The *Mycena* author is very grateful to Olga V. Morozova for help with molecular work and to Arne Aronsen for the identification of *M. albidolilacea* and valuable discussions. The *Mycena* research was carried out within the framework of the institutional research project of the Komarov Botanical Institute (AAAA-A19-119020890079-6) using the equipment of the Core Facility Center “Cell and Molecular Technologies in Plant Science” at the Komarov Botanical Institute RAS (Saint Petersburg, Russia). The *Plagiosphaera* author gratefully acknowledges financial support by the Austrian Science Fund (project P27645-B16).

### References

- Abbasi A.M., Khan M.A., Ahmad M., Zafar M. (2011) *Medicinal plant biodiversity of lesser Himalayas-Pakistan*. Springer Science & Business Media, Berlin.
- Accioly T., Sousa J.O., Moreau P.-A., Lécure C., Silva B.D.B., Roy M., Gardes M., Baseia I.G., Martín M.P. (2019) Hidden fungal diversity from the Neotropics: *Geastrum hirsutum*, *G. schweinitzii* (Basidiomycota, Geastrales) and their allies. *Plos One* **14**: e0211388.
- Afshan N., Ishaq A., Niazi A.R., Khalid A.N. (2015) Geographical distribution and host range of genus *Uromyces* (Pucciniaceae, Uredinales) in Pakistan. International Conference on Chemical, Agricultural and Biological Sciences (CABS-2015) Istanbul (Turkey), 48–54.

- Afshan N.S., Khalid A.N., Niazi A.R., Iqbal S.H. (2011) New records of Uredinales from Fairy Meadows, Pakistan. *Mycotaxon* **115**: 203–213.
- Ahmadpour S.A., Mehrabi-Koushki M., Farokhinejad R. (2017) *Neodidymelliopsis farokhinejadii*, a new fungal species from dead branches of trees in Iran. *Sydowia* **69**: 171–182.
- Aime M.C. (2004) Intercompatibility tests and phylogenetic analysis in the *Crepidotus Sphaerula* group complex: concordance between ICGs and nuclear rDNA sequences highlight phenotypic plasticity within Appalachian species. In: *Fungi in forest ecosystems: systematics, diversity, and ecology* (ed. Cripps C.L.), New York Botanical Gardens, New York: 71–80.
- Aime M.C. (2006) Toward resolving family-level relationships in rust fungi (Uredinales). *Mycoscience* **47**: 112–122.
- Aime M.C., McTaggart A.R., Mondo S.J., Duplessis S. (2017) Phylogenetics and phylogenomics of rust fungi. *Advances in Genetics* **100**: 267–307.
- Alcorn J.L. (1982) New *Cochliobolus* and *Bipolaris* species. *Mycotaxon* **15**: 1–19.
- Ali B., Sohail Y., Mumtaz A.S. (2016a) First record of *Pileolaria terebinthi* (Pucciniales) in Pakistan. *Mycotaxon* **131**: 403–405.
- Ali B., Sohail Y., Toome-Heller M., Mumtaz A.S. (2016b) *Melampsora pakistanica* sp. nov., a new rust fungus on *Euphorbia helioscopia* (Sun spurge) from Pakistan. *Mycological Progress* **15**: 1285–1292.
- Ali B., Sohail Y., Mumtaz A.S. (2017a) *Puccinia aizazii*, a new rust fungus on *Jasminum humile* from foothills of Himalayan ranges. *Sydowia* **69**: 131–134.
- Ali B., Sohail Y., Mumtaz A.S. (2017b) Distribution of rust fungi (*Puccinia* and *Phragmidium*) and host plants in Pakistan. *Journal on New Biological Reports* **6**: 27–32.
- Anonymous (2012–2018) *Ngā Harore o Aotearoa – New Zealand Fungi*. <https://nzfungi2.landcareresearch.co.nz/default.aspx?selected=NameDetails&NameId=94B72815-7284-4937-8837-E8C1A3D60461&StateId=&Sort=&TabNum=3> (accessed 4 June 2018).
- Anonymous (2017) *Galería de imágenes. Pontificia Universidad Católica del Ecuador*. <https://bioweb.bio/galeria/FotosEspecimenes/Gymnopus%20subpruinosis/1> (accessed 5 June 2018).
- Antonín V., Herink J. (1999) Notes on the variability of *Gymnopus luxurians* (Tricholomataceae). *Czech Mycology* **52**: 41–49.
- Antonín V., Noordeloos M.E. (2010) *A monograph of marasmioid and collybioid fungi in Europe*. IHW-Verlag, Eching.
- Antonín V., Sedláč P., Tomšovský M. (2013) Taxonomy and phylogeny of European *Gymnopus* subsection *Levipedes* (Basidiomycota, *Omphalotaceae*). *Persoonia* **31**: 179–187.
- Antonín V., Vizzini A., Ercole E., Leonardi M. (2015) *Strobilomyces pteroreticulosporus* (Boletales), a new species of the *S. strobilaceus* complex from the Republic of Korea and remarks on the variability of *S. confusus*. *Phytotaxa* **219**: 78–86.
- Araújo J.P.M., Evans H.C., Geiser D.M., Mackay W.P., Hughes D.P. (2015) Unravelling the diversity behind the *Ophiocordyceps unilateralis* (Ophiocordycipitaceae) complex: Three new species of zombie-ant fungi from the Brazilian Amazon. *Phytotaxa* **220**(3): 224–238.
- Aronsen A. (2019) *The Mycenas of Northern Europe*. <https://mycena.no/sections.htm> (accessed 24 November 2019).
- Aronsen A., Gulden G. (2007) Two new species of *Mycena* from alpine sites in Norway. *Mycological Progress* **61**: 1–6.
- Aronsen A., Læssøe T. (2016) The genus *Mycena* s.l. Fungi of Northern Europe 5. Narayana Press, Gylling.
- Aronsen A., Perry B.A. (2012) *Mycena guldeniana* – a new alpine species from Norway. *Mycotaxon* **118**(1): 187–195.
- Arx J.A., Olivier D.L. (1952) The taxonomy of *Ophiobolus graminis* Sacc. *Mycological Research* **35**: 29–33.
- Aveskamp M.M., Verkley G.J.M., de Gruyter J., Murace M.A., Perello A., Woudenberg J.H.C., Groenewald J.Z., Crous P.W. (2009). DNA phylogeny reveals polyphyly of *Phoma* section *Peyronellaea* and multiple taxonomic novelties. *Mycologia* **101**: 363–382.
- Aveskamp M.M., de Gruyter J., Woudenberg J.H.C., Verkley G.J.M., Crous P.W. (2010) Highlights of the Didymellaceae: a polyphasic approach to characterise *Phoma* and related pleosporalean genera. *Studies in Mycology* **65**: 1–60.
- Babaahmadi G., Mehrabi-Koushki M., Hayati J. (2018) *Allophoma hayatii* sp. nov., an undescribed pathogenic fungus causing dieback of *Lantana camara* in Iran. *Mycological Progress* **17**: 365–379.
- Ballarà J., Mahiques R., Garrido-Benavent I. (2016) Study of Cortinariaceae of the Cadi-Moixero Natural Park (III) *Moixero* **8**: 20–52.
- Banerjee A. (2016) Studies on pycnidia producing fungi of some ornamental plants grown under protected condition. M.Sc. thesis, Bidhan Chandra Krishi Viswavidyalaya.
- Baroni T.J. (1998) *Collybia subpruinosa* (Murr.) Dennis. <http://www.cortland.edu/nsf/8499coll.html> (accessed 5 June 2018).
- Barr M.E. (1978) The Diaporthales of North America. *Mycologia Memoir* **7**: 1–232.
- Barr M.E. (1990) Prodrum to nonlichenized, pyrenomycetous members of class Hymenoascomycetes. *Mycotaxon* **39**: 43–184.
- Barron G. (2012) *Gymnopus subpruinosis*. *Fungi image collection, University of Guelph*. <https://atrium.lib.uoguelph.ca/xmlui/handle/10214/4443> (accessed 5 June 2018).
- Benjamin R.K. (1967) Laboulbeniales on semi-aquatic Hemiptera. *Laboulbenia*. *Aliso* **6**(3): 111–136.
- Benjamin R.K. (1971) Introduction and supplement to Roland Thaxter's contribution towards a monograph of the Laboulbeniaceae. *Bibliotheca Mycologica* **30**: 1–155.
- Bentivenga S.P., Hetrick B.A.D. (1991) *Glomus mortonii* sp. nov., a previously undescribed species in the Glomaceae isolated from the tallgrass prairie in Kansas. *Mycotaxon* **42**: 9–15.
- Berbee M., Pirseyedi M., Hubbard S. (1999) Cochliobolus phylogenetics and the origin of known, highly virulent pathogens, inferred from ITS and glyceraldehyde-3-phosphate dehydrogenase gene sequences. *Mycologia* **91**: 964–977.
- Berkeley M.J. (1851) Decades of fungi. XXXVI. Sikkim-Himalayan fungi collected by Dr. Hooker. *Hooker's Journal of Botany and Kew Garden Miscellany* **3**: 77–84.
- Berkeley M.J., Curtis M.A. (1853) Centuries of North American fungi. *Annals and Magazine of Natural History* **12**: 417–435.
- Błaszowski J. (2012) *Glomeromycota*. W. Szafer Institute of Botany, Polish Academy of Sciences, Kraków.
- Błaszowski J., Chwat G., Kozłowska A., Goto B.T. (2014) *Rhizophagus natalensis*, a new species in the Glomeromycota. *Mycotaxon* **129**: 97–108.
- Błaszowski J., Kozłowska A., Niezgoda P., Goto B.T., Dalpé Y. (2018) A new genus, *Oehlia* with *Oehlia diaphana* comb. nov. and an emended description of *Rhizoglomerus vesiculiferum* comb. nov. in the Glomeromycotina. *Nova Hedwigia* **107**: 501–518.

- Boedijn K.B. (1933) Ueber einige phragmosporen Dematiaceen. *Bulletin du Jardin botanique de Buitenzorg* **13**: 120–134.
- Boerema G.H. (1993) Contributions towards a monograph of *Phoma* (Coelomycetes) – II. Section *Peyronellaea*. *Persoonia* **15**: 197–221.
- Boerema G.H., de Gruyer J., Noordeloos M.E., Hamers M.E.C. (2004). *Phoma identification manual*. Differentiation of specific and infra-specific taxa in culture. CABI, London, UK.
- Booth C. (1979) *Nectria macrospora*. *CMI Descriptions of Pathogenic Fungi and Bacteria* **623**: 1–2.
- Borchsenius F. (2009) *FastGap 1.2*. [http://www.aubot.dk/Fast-Gap\\_home.htm](http://www.aubot.dk/Fast-Gap_home.htm), Department of Biosciences, Aarhus University, Denmark.
- Brandrud T.E., Bendiksen E., Dima B. (2015) Some new and little known telamonioid *Cortinari* species from Norway. *Agarica* **36**: 11–42.
- Brandrud T.E., Dima B., Liimatainen K., Niskanen T. (2017) Telamonioid *Cortinari* species of the *C. puellaris* group from calcareous *Tilia* forests. *Sydowia* **69**: 37–45.
- Brundrett M., Melville L., Peterson L. (1994) *Practical Methods in Mycorrhizal Research*. Mycologue Publications, University of Guelph, Guelph.
- Buchli H.R. (1966) Notes sur les parasites fongiques des Isoptères. *Revue d'Ecologie et de Biologie du Sol* **3**: 589–610.
- Bulajic A., Filajdic N., Babovic M., Sutton T.B. (1996) First report of *Alternaria mali* on apples in Yugoslavia. *Plant Disease* **80**: 709.
- Burgaz AN. (2006) Check-list of lichenized and lichenicolous fungi of Madrid Community (Spain). *Fl. Medit.* **16**: 57–110.
- Buyck B. (1989) Utilité taxonomique du bleu de crésyl dans le genre *Russula* Persoon. *Bulletin de la Société Mycologique France* **95**: 1–6.
- Buyck B., Zoller S., Hofstetter V. (2018) Walking the thin line... ten years later: the dilemma of above versus below-ground features to support phylogenies in the Russulaceae (Basidiomycota). *Fungal Diversity* **89**: 267–292.
- Capella-Gutiérrez S., Silla-Martínez J.M., Gabaldón T. (2009) TrimAl: a tool for automated alignment trimming in large-scale phylogenetic analyses. *Bioinformatics* **25**: 1972–1973.
- Carbone I., Kohn L.M. (1999) A method for designing primer sets for speciation studies in filamentous ascomycetes. *Mycologia* **91**: 553–556.
- Castresana J. (2000) Selection of conserved blocks from multiple alignments for their use in phylogenetic analysis. *Molecular Biology and Evolution* **17**: 540–552.
- Cenis J.L. (1992) Rapid extraction of fungal DNA for PCR amplification. *Nucleic Acids Research* **20**(9): 2380.
- Chaudhuri T., Panja B.N., Saha J. (2017) Cultural and morphological characteristics of *Lasiodiplodia theobromae* of *Dianella* in various carbon and nitrogen containing media. *Journal of Pharmacognosy and Phytochemistry* **6**(6): 160–164.
- Chen Q., Hou L.W., Duan W.J., Crous P.W., Cai L. (2017) Didymellaceae revisited. *Studies in Mycology* **87**: 105–159.
- Chen Q., Jiang J.R., Zhang G.Z., Cai L., Crous P.W. (2015) Resolving the *Phoma* enigma. *Studies in Mycology* **82**: 137–217.
- Chiu W.F. (1948) The boletes of Yunnan. *Mycologia* **40**: 199–231.
- Chung W.H., Kakishima M., Tsukiboshi T., Ono Y. (2004) Morphological and phylogenetic analyses of *Uromyces appendiculatus* and *U. vignae* on legumes in Japan. *Mycoscience* **45**: 233–244.
- Çobanoğlu G., Doğan A. (2010) Lichen records from Tunceli Munzur Valley National Park (Turkey). *Journal of Botany and Plant Biology* **5**(2): 38–41.
- Çobanoğlu G., Yavuz M. (2007) Lichen records from South-East Anatolia (Bingöl and Şırnak). *Oltenia* **23**: 23–26.
- Cohn F. (1876) *Kryptogamen-Flora von Schlesien* 1. J.U. Kern (M. Müller).
- Coimbra V.R., Pinheiro F.G., Wartchow F., Gibertoni T.B. (2015) Studies on *Gymnopus* sect. *Impudicae* (Omphalotaceae, Agaricales) from Northern Brazil: two new species and notes on *G. montagnei*. *Mycological Progress* **14**(11): 110.
- Condé S., Richard D., Liamine N., Leclère A.-S., Sotolargo B., Pinborg U. (2002) *Biogeographical regions in Europe. The Macaronesian region – volcanic islands in the ocean. – Europe's biodiversity – biogeographical regions and seas*. <https://www.eea.europa.eu/.../biogeographical-regions-in-europe/MacaronesiaReg.pdf> (accessed 5 June 2018).
- Cooke W.B. (1975) The 1970 Indiana foray. *Mycologia* **67**(5): 1065–1071.
- Coppins B., Kondratyuk S.Y., Khodosovtsev A.Y., Wolseley P., Zelenko S.D. (2001) New for Crimea and Ukraine species of the lichens. *Ukrayins'kyi Botanichnyi Zhurnal* **58**(6): 716–722.
- Corazon-Guivin M.A., Mendoza A.C., Guerrero-Abad J.C., Vallejos-Tapullima A., Carballar-Hernández S., Silva G.A., Oehl F. (2019a) *Funneliglomus*, gen. nov., and *Funneliglomus sanmartinensis*, a new arbuscular mycorrhizal fungus from the Amazonia region in Peru. *Sydowia* **71**: 17–24.
- Corazon-Guivin M.A., Mendoza A.C., Guerrero-Abad J.C., Vallejos-Tapullima A., Carballar-Hernández S., Silva G.A., Oehl F. (2019b) *Microkamienskia* gen. nov. and *Microkamienskia peruviana*, a new arbuscular mycorrhizal fungus from Western Amazonia. *Nova Hedwigia* **109**(3–4): 355–368.
- Corner E.J.H. (1969) Notes on cantharelloid fungi. *Nova Hedwigia* **18**: 783–818.
- Corner E.J.H. (1972) *Boletus in Malaysia*. Singapore Botanic Gardens Press, Singapore.
- Cota B.B., Rosa L.H., Caligiorne R.B., Rabello A.L.T., Almeida Alves T.M., Rosa C.A., Zani C.L. (2008) Altenusin, a biphenyl isolated from the endophytic fungus *Alternaria* sp., inhibits trypanothione reductase from *Trypanosoma cruzi*. *FEMS Microbiology Letters* **285**: 177–182.
- Crous P.W., Carnegie A.J., Wingfield M.J., Sharma R., Mughini G., Noordeloos M.E., et al. (2019) Fungal planet description sheets: 868–950. *Persoonia* **42**: 291–473.
- Crous P.W., Schumacher R.K., Wingfield M.J., Lombard L., Giraldo A., Christensen M., Gardinnet A., Nakashima C., Pereira O., Smith A.J., Groenewald J.Z. (2015) Fungal systematics and evolution: FUSE 1. *Sydowia* **67**: 81–118.
- Cummins G.B., Hiratsuka Y. (2003) *Illustrated genera of rust fungi, 3rd edn*. American Phytopathological Society, St. Paul, MN.
- da Cunha K.C., Sutton D.A., Fothergill A.W., Gené J., Cano J., Madrid H., de Hoog S., Crous P.W., Guarro J. (2013) In vitro antifungal susceptibility and molecular identity of 99 clinical isolates of the opportunistic fungal genus *Curvularia*. *Diagnostic Microbiology and Infectious Disease* **76**: 168–174.
- Damon S.C., Downing M.H. (1954) Taxonomic studies in the genus *Coccospora*. *Mycologia* **46**(2): 209–221.
- de Gruyer J., Aveskamp M.M., Woudenberg J.H.C., Verkley G.J.M., Groenewald J.Z., Crous P.W. (2009) Molecular phylogeny of *Phoma* and allied anamorph genera: towards a

- reclassification of the *Phoma* complex. *Mycological Research* **113**: 508–519.
- De Hoog G.S., Gerrits van den Ende A.H.G. (1998) Molecular diagnostics of clinical strains of filamentous basidiomycetes. *Mycoses* **41**: 183–189.
- Dehdari F., Mehrabi-Koushki M., Hayati J. (2018) *Curvularia shahidchamranensis* sp. nov., a crude oil-tolerant fungus. *Current Research in Environmental and Applied Mycology* **8**: 572–584.
- Deng C.Y., Li T.H. (2008) *Gloeocantharellus persicinus*, a new species from China. *Mycotaxon* **106**: 449–453.
- Dennis R.W.G. (1965) Fungi Venezuelani: VII. *Kew Bulletin* **19**(2): 231–273.
- Dennis R.W.G. (1975) New or interesting British microfungi, III. *Kew Bulletin* **30**: 345–365.
- Desjardin D.E., Boonpratuang T., Hywel-Jones N. (2003) New spinose species of *Mycena* in sections *Basipedes* and *Polyadelphia* from Thailand. *Fungal Diversity* **12**: 7–17.
- Desjardin D.E., Halling R.E., Hemmes D.E. (1999) Agaricales of the Hawaiian Islands. 5. The genera *Rhodocollybia* and *Gymnopus*. *Mycologia* **91**: 166–176.
- Desjardin D.E., Perry B.A. (2017) The gymnopoid fungi (Basidiomycota, Agaricales) from the Republic of São Tomé and Príncipe, West Africa. *Mycosphere* **8**: 1317–1391.
- Dietrich M. (2012) *Die Flechten im Naturlehrgebiet Buchwald in Ettiswil*. Umweltbüro für Flechten.
- Dima B., Liimatainen K., Niskanen T., Kytövuori I., Bojantchev D. (2014) Two new species of *Cortinarius*, subgenus *Telamonia*, sections *Colymbadini* and *Uracei*, from Europe. *Mycological Progress* **13**: 867–879.
- Doyle J.J., Doyle J.L. (1987) A rapid DNA isolation procedure for small quantities of fresh leaf material. *Phytochemical Bulletin* **19**: 11–15.
- Doyle, J. (1991) CTAB total DNA isolation. In: *Molecular techniques in taxonomy* (ed. Hewitt G.M., Jonston A.W.B., Young J.P.W.), Springer, Berlin: 283–285.
- Dunham S.M., Larsson K.H., Spatafora J.W. (2007) Species richness and community composition of mat-forming ectomycorrhizal fungi in old- and second-growth Douglas-fir forests of the HJ Andrews Experimental Forest, Oregon, USA. *Mycorrhiza* **17**(8): 633–645.
- Dutta A.K., Wilson A.W., Antonín V., Acharya K. (2015) Taxonomic and phylogenetic study on gymnopoid fungi from Eastern India. I. *Mycological Progress* **14**: 79.
- Ebrahimi L., Fotouhifar K.-B. (2016) First report of *Cyphelophora fusarioides* (Chaetothyriales) on a plant host. *Sydowia* **68**: 131–137.
- Edgar R.C. (2004) MUSCLE: multiple sequence alignment with high accuracy and high throughput. *Nucleic Acids Research* **32**: 1792–1797.
- Ellis M.B. (1971) *Dematiaceous Hyphomycetes*. Kew Surrey, UK: Commonwealth Mycological Institute.
- Emmons C.W., Cummins G.B., Cooke B.W. (1960) The 1958 foray of the Mycological Society of America. *Mycologia* **52**(5): 808–817.
- Engler A. (1904) Botanische Jahrbücher für Systematik, Pflanzengeschichte und Pflanzengeographie **33**. Engelmann, Leipzig.
- Esmailzadeh M., Soleimani M.J. (2008) Occurrence of apple leaf blotch disease caused by *Alternaria mali* in Iran. *Proceedings of the 18th Iranian Plant Protection Congress II*: 121.
- Etebarian H.R., Sholberg P.L., Eastwell K.C., Sayler R.J. (2005) Biological control of apple blue mold with *Pseudomonas fluorescens*. *Canadian Journal of Microbiology* **51**: 591–598.
- Farr, D.F., Rossman, A.Y. (2019) *Fungal Databases*, U.S. National Fungus Collections, ARS, USDA. <https://nt.ars-grin.gov/fungaldb/databases/> (accessed 21 November 2019).
- Ferisin G., Dovana F., Justo A. (2019) *Pluteus bizioi* (Agaricales, Pluteaceae), a new species from Italy. *Phytotaxa* **408**(2): 99–108.
- Filajdic N., Sutton T.B. (1991) Identification and distribution of *Alternaria mali* on apples in North Carolina and susceptibility of different varieties of apples to *alternaria* blotch. *Plant Disease* **75**: 1045–1048.
- Fiorentina J. (2002) An appraisal of scientific names used in the 1915 list of lichens of the Maltese Islands by Stefano Sommier and Alfredo Caruana Gatto. *Central Mediterranean Naturalist* **3**(4): 189–196.
- Galun M., Mukhtar A. (1996) Checklist of the lichens of Israel. *Bocconea* **6**: 149–171.
- Gardes M., Bruns T.D. (1993) ITS primers with enhanced specificity for basidiomycetes — application to the identification of mycorrhizae and rusts. *Molecular Ecology* **2**(2): 113–118.
- Garnica S., Weiß M., Oertel B., Oberwinkler F. (2005) A framework for a phylogenetic classification in the genus *Cortinarius* (Basidiomycota, Agaricales) derived from morphological and molecular data. *Canadian Journal of Botany* **83**: 1457–1477.
- Gautam A.K., Kant M., Thakur Y. (2013) Isolation of endophytic fungi from *Cannabis sativa* and study their antifungal potential. *Archives in Phytopathology and Plant Protection* **46**: 627–635.
- Gelardi M., Vizzini A., Ercole E., Voyron S., Wu G., Liu X.Z. (2013) *Strobilomyces echinocephalus* sp. nov. (Boletales) from south-western China, and a key to the genus *Strobilomyces* worldwide. *Mycological Progress* **12**: 575–588.
- Gerdemann J.W., Trappe J.M. (1974) The Endogonaceae in the Pacific North West. *Mycologia Memoirs* **5**: 1–76.
- Giachini A.J. (2004) Systematics, phylogeny, and ecology of *Gomphus* sensu lato. Doctoral Thesis, Oregon State University, Corvallis.
- Giachini A.J., Castellano M.A. (2011) A new taxonomic classification for species in *Gomphus* sensu lato. *Mycotaxon* **115**: 183–201.
- Giachini A.J., Hosaka K., Nohura E., Spatafora J., Trappe J.M. (2010) Phylogenetic relationships of the Gomphales based on nuc-25S-rDNA, mit-12S-rDNA, and mit-atp6-DNA combined sequences. *Fungal Biology* **114**: 224–234.
- Giralt M., Llimona X. (1997) The saxicolous species of the genus *Rinodina* and *Rinodinella* lacking spot test reactions in the Iberian Peninsula. *Mycotaxon* **62**: 175–224.
- Goldmann L., Weir A., Rossi W. (2013) Molecular analysis reveals two new dimorphic species of *Hesperomyces* (Ascomycota, Laboulbeniomycetes) parasitic on the ladybird *Coleomegilla maculata* (Coleoptera, Coccinellidae). *Fungal Biology* **117**(11–12): 807–813.
- Gorny A.M., Kikkert J.R., Shivas R.G., Pethybridge S.J. (2016) First report of *Didymella americana* on baby lima bean (*Phaseolus lunatus*). *Canadian Journal of Plant Pathology* **38**: 389–394.
- Granata G., Refatti E. (1981) Decline and death of young grapevines by infection of *Phoma glomerata* on the rootstock. *Vitis* **20**: 341–346.
- Grünig C.R., Duo A., Sieber T.N., Holdenrieder O. (2008) Assignment of species rank to six reproductively isolated cryptic species of the *Phialocephala fortinii* s.l.-*Acephala applanata* species complex. *Mycologia* **100**(1): 47–67.



- Guindon S., Gascuel O. (2003) A simple, fast, and accurate algorithm to estimate large phylogenies by maximum likelihood. *System Biology* **52**: 696–704.
- Haelewaters D., De Kesel A., Gorczak M., Bao K., Gort G., Zhao S.Y., Pfister D.H. (2019a) Laboulbeniales (Ascomycota) of the Boston Harbor Islands II (and other localities): species parasitizing Carabidae, and the *Laboulbenia flagellata* species complex. *Northeastern Naturalist* **25**(Special Issue 9): 110–149.
- Haelewaters D., De Kesel A., Pfister D.H. (2018) Integrative taxonomy reveals hidden species within a common fungal parasite of ladybirds. *Scientific Reports* **8**(1): 15966.
- Haelewaters D., Gorczak M., Pfiogler W.P., Tartally A., Tischer M., Wrzosek M., Pfister D.H. (2015) Bringing Laboulbeniales to the 21st century: enhanced techniques for extraction and PCR amplification of DNA from minute ectoparasitic fungi. *IMA Fungus* **6**(2): 363–372.
- Haelewaters D., Pfister D.H. (2019) Morphological species of *Gloeandromyces* (Ascomycota, Laboulbeniales) evaluated using single-locus species delimitation methods. *Fungal Systematics and Evolution* **3**: 19–33.
- Haelewaters D., Pfiogler W.P., Gorczak M., Pfister D.H. (2019b) Birth of an order: Comprehensive molecular phylogenetic study excludes *Herpomycetes* (Fungi, Laboulbeniomycetes) from Laboulbeniales. *Molecular Phylogenetics and Evolution* **133**: 286–301.
- Haelewaters D., Verhaeghen S.J.C., Ríos González T.A., Bernal-Vega J.A., Villarreal Saucedo R.V. (2017) New and interesting Laboulbeniales (Fungi, Ascomycota) from Panama and neighboring areas. *Nova Hedwigia* **105**(3–4): 267–299.
- Hall T.A. (1999) BioEdit: a user-friendly biological sequence alignment editor and analysis program for windows 95/98/NT. *Nucleic Acids Symposium Series* **41**: 95–98.
- Halling R.E. (1983) The genus *Collybia* (Agaricales) in the northeastern United States and adjacent Canada. *Mycologia Memoir* **8**: 1–148.
- Halling R.E. (2013) A revision of *Collybia* s.l. in the northeastern United States & adjacent Canada. <https://www.nybg.org/bsci/res/col/> (accessed 13 January 2019).
- Han L.H., Buyck B., Yorou N.S., Halling R.E., Yang Z.L. (2017) *Afroboletus sequestratus* (Boletales), the first species with sequestrate basidioma in the genus. *Phytotaxa* **305**: 11–20.
- Han L.H., Feng B., Wu G., Halling R.E., Buyck B., Yorou N.S., Ebika S.T.N., Yang Z.L. (2018a) African origin and global distribution patterns: Evidence inferred from phylogenetic and biogeographical analyses of ectomycorrhizal fungal genus *Strobilomyces*. *Journal of Biogeography* **45**: 201–212.
- Han L.H., Hao Y.J., Liu C., Dai D.Q., Zhao K., Tang Z.L. (2018b) *Strobilomyces rubrobrunneus* (Boletaceae), a new species with reddish brown scales from eastern China. *Phytotaxa* **376**: 167–176.
- Harder C.B., Læssøe T., Frøslev T.G., Ekelund F., Rosendahl S., Kjoller R. (2013) A three-gene phylogeny of the *Mycena pura* complex reveals 11 phylogenetic species and shows ITS to be unreliable for species identification. *Fungal Biology* **117**: 764–775.
- Harder C.B., Læssøe T., Kjoller R., Frøslev T.G. (2010) A comparison between ITS phylogenetic relationships and morphological species recognition within *Mycena* sect. *Calodontes* in Northern Europe. *Mycological Progress* **9**(3): 395–405.
- Harrower E., Ammirati J.F., Cappuccino A.A., Ceska O., Kranabetter J.M., Kroeger P., Lim S., Taylor T., Berbee M.L. (2011) *Cortinarius* species diversity in British Columbia and molecular phylogenetic comparison with European specimen sequences. *Botany* **89**: 799–810.
- Harteveld D.O.C., Akinsanmi O.A., Drenth A. (2013) Multiple *Alternaria* species groups are associated with leaf blotch and fruit spot diseases of apple in Australia. *Plant Pathology* **62**: 289–297.
- Hawksworth D. L., Crous P.W., Redhead S. A., Reynolds D. R., Samson R. A., Seifert K. A., Taylor J. W., Wingfield M. J. [& 69 signatories] (2011) The Amsterdam Declaration on Fungal Nomenclature. *IMA Fungus* **2**: 105–112.
- He Y.H., Zhang Z.Y. (2001) Taxonomy of Cladosporium in China XXVI. *Mycosystema* **20**(4): 469–470.
- Heidari K., Mehrabi-Koushki M., Farokhinejad R. (2018) *Curvularia mosaddeghii* sp. nov., a novel species from the family Pleosporaceae. *Mycosphere* **9**: 635–646.
- Hernández-Restrepo M., Groenewald J.Z., Elliott M.L., Canning G., McMillan V.E., Crous P.W. (2016) Take-all or nothing. *Studies in Mycology* **83**: 19–48.
- Hernández-Restrepo M., Schumacher R.K., Wingfield M.J., Ahmad I., Cai L., Duong T.A., Edwards J., Gené J., Groenewald J.Z., Jabeen S., Khalid A.N., Lombard L., Madrid H., Marin-Felix Y., Marincowitz S., Miller A.N., Rajeshkumar K.C., Rashid A., Sarwar S., Stehlig A.M., Taylor P.W.J., Zhou N., Crous P.W. (2016) Fungal systematics and evolution: FUSE 2. *Sydowia* **68**: 193–230.
- Hewitt E.J. (1966) *Sand and water culture methods used in the study of plant nutrition*. Farnham Royal, Commonwealth Agricultural Bureau, Farnham, England.
- Hofstetter V., Buyck B., Croll D., Viret O., Couloux A., Gindro K. (2012) What if esca disease of grapevine were not a fungal disease? *Fungal Diversity* **54**: 51–67.
- Hofstetter V., Miadlikowska J., Kauff F., Lutzoni F. (2007) Phylogenetic comparison of protein-coding versus ribosomal RNA-coding sequence data: A case study of the Lecanoromycetes (Ascomycota). *Molecular Phylogenetics and Evolution* **44**: 412–426.
- Holec J., Kolařík M. (2017) First report of *Mycena clavata* (Fungi, Agaricales) in the Czech Republic including notes on its taxonomy, phylogenetic position and ecology. *Czech Mycology* **69**(1):1–14.
- Hongo T. (1982) Materials for the fungus flora of Japan (32). *Transactions of the Mycological Society of Japan* **23**: 195–200.
- Hughes K.W., Petersen R.H., Lickey E.B. (2009) Using heterozygosity to estimate a percentage DNA sequence similarity for environmental species delimitation across basidiomycete fungi. *New Phytologist* **182**: 795–798.
- Huhndorf S.M., Miller A.N., Fernández F.A. (2004) Molecular systematics of the Sordariales: the order and the family Lasiosphaeriaceae redefined. *Mycologia* **96**: 368–387.
- Index Fungorum (2019) <http://www.indexfungorum.org/names/Names.asp> (accessed 22 November 2019).
- Inman R.E. (1970) Observations on the biology of *Rumex rust Uromyces rumicis* (Schum.) Wint. *Botanical Gazette* **131**: 234–241.
- IPNI (2019) The International Plant Names Index. <http://www.ipni.org/index.html> (accessed 1 December 2019).
- Ivoilov A.V., Bolshakov S.Yu., Silaeva T.B. (2017) *The study of species diversity of macromycetes: a manual* [in Russian]. Publisher of the Mordovia State University, Saransk.
- Jaklitsch W.M. (2009) European species of *Hypocrea* – Part I. The green-spored species. *Studies in Mycology* **63**: 1–91.
- Jaklitsch W.M., Komon M., Kubicek C.P., Druzhinina I.S. (2005) *Hypocrea voglmayrii* sp. nov. from the Austrian

- Alps represents a new phylogenetic clade in *Hypocrea/Trichoderma*. *Mycologia* **97**: 1365–1378.
- Jaklitsch W.M., Stadler M., Voglmayr H. (2012) Blue pigment in *Hypocrea caerulescens* sp. nov. and two additional new species in sect. *Trichoderma*. *Mycologia* **104**: 925–941.
- Jang S., Jang Y., Lim Y.W., Kim C., Ahn B.J., Lee S.-S., Kim J.-J. (2016) Phylogenetic identification of Korean *Gymnopus* spp. and the first report of 3 species: *G. iocephalus*, *G. polygrammus*, and *G. subnudus*. *Mycobiology* **44**: 131–136.
- Jayawardena R.S., Purahong W., Zhang W., Wubet T., Li X.H., Liu M., Zhao W., Hyde K.D., Liu J.H., Yan J. (2018) Biodiversity of fungi on *Vitis vinifera* L. revealed by traditional and high-resolution culture-independent approaches. *Fungal Diversity* **90**: 1–84.
- Jena S.K., Tayung K. (2013) Endophytic fungal communities associated with two ethno-medicinal plants of Similipal Biosphere Reserve, India and their antimicrobial prospective. *Journal of Applied Pharmaceutical Science* **3**: 7.
- Jiang X.M., Li Y.K., Liang J.F., Wu J.R. (2018) *Russula brunneovinacea* sp. nov., from northeastern China. *Mycotaxon* **132**: 789–797.
- Jobim K., Vista X.M., Goto B.T. (2018) Updates on the knowledge of Arbuscular Mycorrhizal Fungi (Glomeromycotina) in the Atlantic Forest biome – an example of very high species richness in the Brazilian landscape. *Mycotaxon* **133**: 209.
- John V., Türk A. (2017) Türkiye Likenleri Listesi. [A Checklist of the Lichens of Turkey] Nezahat Gökyiğit Botanik Bahçesi Yayın, İstanbul.
- Jumbam B., Haelewaters D., Koch R.A., Dentinger B.T., Henkel T.W., Aime M.C. (2019) A new and unusual species of *Hericium* (Basidiomycota: Russulales, Hericiaceae) from the Dja Biosphere Reserve, Cameroon. *Mycological Progress* **18**(10): 1253–1262.
- Justo A., Battistin E., Angelini C. (2012) Two new species of *Pluteus* section *Celluloderma* from the Dominican Republic. *Mycotaxon* **120**: 11–21.
- Justo A., Caballero A., Muñoz G., Minnis A.M., Malysheva E. (2011c) Taxonomy of *Pluteus euagraptus* and morphologically similar taxa. *Mycologia* **103**: 646–655.
- Justo A., Minnis A.M., Ghignone S., Menolli Jr.N., Capelari M., Rodríguez O., Malysheva E., Contu M., Vizzini A. (2011b) Species recognition in *Pluteus* and *Volvopluteus* (Pluteaceae, Agaricales): morphology, geography and phylogeny. *Mycological Progress* **10**: 453–479.
- Justo A., Vizzini A., Minnis A.M., Menolli Jr. N., Capelari M., Rodríguez O., Malysheva E., Contu M., Ghignone S., Hibbett D.S. (2011a) Phylogeny of Pluteaceae (Agaricales, Basidiomycota): taxonomy and character evolution. *Fungal Biology* **115**: 1–20.
- Katoh K., Kuma K.I., Toh H., Miyata T. (2005) MAFFT version 5: improvement in accuracy of multiple sequence alignment. *Nucleic Acids Research* **33**: 511–518.
- Katoh K., Standley D.M. (2013) MAFFT multiple sequence alignment software version 7: Improvements in performance and usability. *Molecular Biology and Evolution* **30**: 772–780.
- Katoh K., Toh H. (2008) Recent developments in the MAFFT multiple sequence alignment program. *Briefings in Bioinformatics* **9**: 286–298.
- Katoh K., Standley D.M. (2013) MAFFT multiple sequence alignment software version 7: improvements in performance and usability. *Molecular Biology and Evolution* **30**: 772–780.
- Kearse M., Moir R., Wilson A., Stones-Havas S., Cheung M., Sturrock S., Buxton S., Cooper A., Markowitz S., Duran C., Thierer T., Ashton B., Meintjes P., Drummond A. (2012) Geneious Basic: an integrated and extendable desktop software platform for the organization and analysis of sequence data. *Bioinformatics* **28**: 1647–1649.
- Khodosovtsev A., Kondratyuk S., Kärnefelt I. (2004) *Candelariella boikoi*, a new lichen species from Eurasia. *Graphis Scripta* **16**: 11–15.
- Kirk P.M., Cannon P.F., Minter D.W., Stalpers J. (2008) *Ainsworth & Bisby's dictionary of the fungi*. 10th edn. CABI, Wallingford.
- Kobayashi T. (1970) Taxonomic studies of Japanese Diaporthaceae with special reference to their life-histories. *Bulletin of the Government Forest Experimental Station Meguro* **226**: 1–242.
- Kornerup A., Wanscher J.H. (1967) *Methuen handbook of colour*. Methuen & Co. Ltd, London.
- Kornerup A., Wanscher J.H. (1981) *Taschenlexikon der Farben*. Muster-Schmidt Verlag, Göttingen.
- Koske R.E. (1985) *Glomus aggregatum* emended: a distinct taxon in the *Glomus fasciculatum* complex. *Mycologia* **77**: 619–630.
- Koske R.E., Tessier B. (1983) A convenient, permanent slide mounting medium. *Mycological Society of America Newsletter* **34**: 59.
- Krisai-Greilhuber I., Chen Y., Sana Jabeen S., Madrid H., Marincowitz S., Razaq A., Ševčíková H., Voglmayr H., Yazici K., Aptroot A., Aslan A., Boekhout T., Borovička J., Crous P.W., Ilyas S., Jami F., Jiang Y.-L., Khalid A.N., Kolecka A., Konvalinková T., Norphanphoun C., Shaheen S., Wang Y., Wingfield M.J., Wu S.-P., Wu Y.-M., Yu J.-Y. (2017) Fungal systematics and evolution: FUSE 3. *Sydowia* **69**: 229–264.
- Kropp B.R. (2016) Russulaceae in American Samoa: new species and further support for an Australasian origin for Samoan ectomycorrhizal fungi. *Mycologia* **108**: 405–413.
- Krüger M., Stockinger H., Krüger C., Schüßler A. (2009) DNA-based species level detection of Glomeromycota: one PCR primer set for all arbuscular mycorrhizal fungi. *New Phytologist* **183**: 212–223.
- Krzewicka B. (2009) Some new records of *Verrucaria* from Beskid Niski Mts. *Acta Mycologica* **44**: 265–273.
- Kühner R. (1938) *Le Genre Mycena*. Paul Lechevalier, Paris.
- Kumar S., Stecher G., Li M., Knyaz C., Tamura K. (2018) MEGA X: Molecular evolutionary genetics analysis across computing platforms. *Molecular Biology and Evolution* **35**: 1547–1549.
- Kumar S., Stecher G., Tamura K. (2016) MEGA7: molecular evolutionary genetics analysis version 7.0 for bigger datasets. *Molecular Biology and Evolution* **33**(7): 1870–1874.
- Kuo M. (2011) *Cortinarius distans*. Retrieved from the MushroomExpert.Com: [http://www.mushroomexpert.com/cortinarius\\_distans.html](http://www.mushroomexpert.com/cortinarius_distans.html).
- Kusaba M., Tsuge T. (1994) Nuclear ribosomal DNA variation and pathogenic specialization in *Alternaria* fungi known to produce host specific toxins. *Applied and Environmental Microbiology* **60**: 3055–62.
- Lal M., Kumar S., Ali M., Khan A., Singh V., Murti S. (2013) Host range, susceptibility period of *Curvularia lunata* causing leaf spot of black gram and germplasm screening. *Agrivays* **1**: 142–146.
- Lanfear R., Frandsen P.B., Wright A.M., Senfeld T., Calcott B. (2017) PartitionFinder 2: new methods for selecting partitioned models of evolution for molecular and morphologi-

- cal phylogenetic analyses. *Molecular Biology and Evolution* **34**:772–773.
- Larkin M.A., Blackshields G., Brown N.P., Chenna R., McGettigan P.A. et al. (2007) Clustal W and Clustal X version 2.0. *Bioinformatics* **23**: 2947–2948.
- Lee W.D., Lee H., Fong J.J., Oh S.-Y., Park M.S., Quan Y., Jung P.E., Lim Y.W. (2014) A checklist of the basidiomycetous macrofungi and a record of five new species from Mt. Oseo in Korea. *Mycobiology* **42**: 132–139.
- Li F., Deng L.Q. (2018) Three new species of *Russula* from South China. *Mycological Progress* **17**: 1305–1321.
- Li G.J., Hyde K.D., Zhao R.L. et al. (2016) Fungal diversity notes 253–366: taxonomic and phylogenetic contributions to fungal taxa. *Fungal Diversity* **78**: 1–237.
- Li Y.M., Shivas R.G., Cai L. (2017) Cryptic diversity in *Tranzscheliella* spp. (Ustilaginales) is driven by host switches. *Scientific Reports* **7**: 43549.
- Li L.F., Li T., Zhang Y., Zhao Z.W. (2010) Molecular diversity of arbuscular mycorrhizal fungi and their distribution patterns related to host-plants and habitats in a hot and arid ecosystem, southwest China. *FEMS Microbiology Ecology* **71**: 418–427.
- Liang Y., Ran S.F., Bhat J., Hyde K.D., Wang Y., Zhao D.-G. (2018) *Curvularia microspora* sp. nov. associated with leaf diseases of *Hippeastrum striatum* in China. *MycoKeys* **29**: 49–61.
- Liang J.F., Xu J., Yang Z.L. (2009) Divergence, dispersal and recombination in *Lepiota cristata* from China. *Fungal Diversity* **38**: 105–124.
- Liimatainen K. (2017) Nomenclatural novelties. *Index Fungorum* **344**: 1–5.
- Lindström H., Bendiksen H., Bendiksen K., Larsson E. (2008) Studies of the *Cortinarius saniosus* (Fr.: Fr.) Fr. complex and a new closely related species, *C. aureovelatus* (Basidiomycota, Agaricales). *Sommerfeltia* **31**: 139–159. doi: 10.2478/v10208-011-0008-2
- Linhares F.T.F., Reck M.A., Daniëls P.P., Neves M.A. (2016) *Gloeocantharellus aculeatus* (Gomphaceae), a new neotropical species in the gomphoid-phalloid clade. *Phytotaxa* **268**: 193–202.
- Liu M., McCabe E., Chapados J.T., Carey J., Wilson S. K., Tropiano R., Scott A., Redhead C., Lévesque A., Hambleton S. (2015) Detection and identification of selected cereal rust pathogens by TaqMan® real-time PCR. *Canadian Journal of Plant Pathology* **37**: 92–105.
- Liu L.-N., Razaq A., Atri N.S., Bau T., Belbahri L., Bouket A.C., Chen L.-P., Deng C., Ilyas S., Khalid A.N., Kitaura M.J., Kobayashi T., Li Y., Lorenz A.P., Ma Y.-H., Malysheva E., Malysheva V., Nuytinck J., Qiao M., Saini M.K., Scur M.C., Sharma S., Shu L.-L., Spirin V., Tanaka Y., Tojo M., Uzuhashi S., Valério-Júnior C., Verbeken A., Verma B., Wu R.-H., Xu J.-P., Yu Z.-F., Zeng H., Zhang B., Banerjee A., Beddiar A., Bordallo J.-J., Dafri A., Dima B., Krisai-Greilhuber I., Lorenzini M., Mandal R., Morte A., Nath P.S., Papp V., Pavlík J., Rodríguez A., Ševčíková H., Urban A., Voglmayr H., Giacomo Zapparoli G. (2018) Fungal systematics and evolution: FUSE 4. *Sydowia* **70**: 211–286.
- Liu Y.J., Whelen S., Hall B.D. (1999) Phylogenetic relationships among ascomycetes: evidence from an RNA polymerase II subunit. *Molecular Biology and Evolution* **16**: 1799–1808.
- Liu M., Zhang W., Manawasinghe I.S., Zhou Y., Xing Q.K., Li X.H., Yan J.Y., Wang, S. (2018) First report of *Nothophoma quercina* causing trunk canker on crabapple (*Malus micromalus*) in China. *Plant Disease* **102**: 1462.
- López Ferrer G.J. (2004) *Collybia sensu lato* of the central and western regions of Puerto Rico: biotechnological capabilities, characterization and identification using traditional and molecular techniques. M.Sc. thesis, University of Puerto Rico.
- Lorenzini M., Cappello M.S., Logrieco A., Zapparoli G. (2016) Polymorphism and phylogenetic species delimitation in filamentous fungi from predominant mycobiota in withered grapes. *International Journal of Food Microbiology* **238**: 56–62.
- Lorenzini M., Zapparoli G. (2014) Characterization and pathogenicity of *Alternaria* spp. strains associated with grape bunch rot during post-harvest withering. *International Journal of Food Microbiology* **186**: 1–5.
- Lorenzini M., Zapparoli G. (2015) Occurrence and infection of *Cladosporium*, *Fusarium*, *Epicoccum* and *Aureobasidium* in withered rotten grapes during post-harvest dehydration. *Antonie Van Leeuwenhoek* **108**: 1171–1180.
- Ludwig E., Ryberg A. (2009) *Mycena mitis* ny för Sverige. *Svensk Mykologisk Tidskrift* **30**(3): 33–34.
- Maas Geesteranus R.A. (1983) Conspectus of the Mycenas of the Northern Hemisphere 1. Sections Sacchariferae, Basipedes, Bulbosae, Clavulares, Exiguuae, and Longisetae. *Proceedings of the Koninklijke Nederlandse Akademie van Wetenschappen* **86**(3): 401–421.
- Maas Geesteranus R.A. (1991) Studies in Mycenas. Additions and corrections, part 2. *Proceedings of the Koninklijke Nederlandse Akademie van Wetenschappen* **94**(4): 545–571.
- Maas Geesteranus R.A. (1992a) Mycenas of the Northern Hemisphere. II. Conspectus of the Mycenas of the Northern Hemisphere. North-Holland, Amsterdam.
- Maas Geesteranus R.A. (1992b) Two new Mycenas of section *Insignes* from the Netherlands. *Proceedings of the Koninklijke Nederlandse Akademie van Wetenschappen* **95**(4): 469–472.
- Machowicz-Stefaniak Z., Krol E. (2007) Characterization of *Phoma negriana* Thum., a new species from grapevine canes. *Acta Mycologica* **42**: 113–117.
- Madrid H., da Cunha K.C., Gene J., Dijksterhuis J., Cano J., Sutton D.A., Guarro J., Crous P.W. (2014) Novel *Curvularia* species from clinical specimens. *Persoonia* **33**: 48–60.
- Maier W., Wingfield B.D., Mennicken M., Wingfield M.J. (2007) Polyphyly and two emerging lineages in the rust genera *Puccinia* and *Uromyces*. *Mycological Research* **111**: 176–185.
- Maire R. (1917) Champignons Nord-Africains nouveaux ou peu connus. *Bulletin de la Société d'histoire naturelle de l'Afrique du Nord* **8**(7): 134–200.
- Malysheva E.F., Malysheva V.F., Justo A. (2016) Observation on *Pluteus* (Pluteaceae) diversity in South Siberia, Russia: morphological and molecular data. *Mycological Progress* **15**: 861–882.
- Manamgoda D.S., Cai L., Bahkali A.H., Chukeatirote E., Hyde K.D. (2011) *Cochliobolus*: an overview and current status of species. *Fungal Diversity* **51**: 3–42.
- Manamgoda D.S., Cai L., McKenzie E.H.C., Chukeatirote E., Hyde K.D. (2012a) Two new *Curvularia* species from northern Thailand. *Sydowia* **64**: 255–266.
- Manamgoda D.S., Cai L., McKenzie E.H.C., Crous P.W., Madrid H., Chukeatirote E., Shivas R.G., Tan Y.-P., Hyde K.D. (2012b) A phylogenetic and taxonomic re-evaluation of the *Bipolaris-Cochliobolus-Curvularia* complex. *Fungal Diversity* **56**: 131–44.

- Manamgoda D.S., Rossman A.Y., Castlebury L.A., Crous P.W., Madrid H., Chukeatirote E., Hyde K.D. (2014) The genus *Bipolaris*. *Studies in Mycology* **79**: 221–288.
- Manamgoda D.S., Rossman A.Y., Castlebury L.A., Chukeatirote E., Hyde K.D. (2015) taxonomic and phylogenetic reappraisal of the genus *Curvularia* (Pleosporaceae): human and plant pathogens. *Phytotaxa* **212**: 175–198.
- Marin-Felix Y., Groenewald J.Z., Cai L., Chen Q., Barnes I., Bensch K., Braun U., Camporesi E., Damm U., de Beer Z.W., Dissanayake A., Edwards J., Giraldo A., Hernández-Restrepo M., Hyde K.D., Jayawardena R.S., Lombard L., Luangsa-ard J., McTaggart A.R., Rossman A.Y., Sandoval-Denis M., Shen M., Shivas R.G., Tan Y.P., van der Linde E.J., Wingfield M.J., Wood A.R., Zhang J.Q., Zhang Y., Crous P.W. (2017a) Genera of phytopathogenic fungi: GOPHY 1. *Studies in Mycology* **86**: 99–216.
- Marin-Felix Y., Senwana C., Cheewangkoon R., Crous P.W. (2017b) New species and records of *Bipolaris* and *Curvularia* from Thailand. *Mycosphere* **8**: 1556–1574.
- Marinho F., da Silva I.R., Oehl F., Maia L.C. (2018) Checklist of arbuscular mycorrhizal fungi in tropical forests. *Sydowia* **70**: 107–127.
- Martin G.W. (1960) Notes on Iowa fungi. XIV. *Proceedings of the Iowa Academy of Science* **67**: 139–144.
- Mata J.L., Hughes K.W., Petersen R.H. (2004) Phylogenetic placement of *Marasmiellus juniperinus*. *Mycoscience* **45**: 214–221.
- Mata J.L., Hughes K.W., Petersen R.H. (2007) An investigation of Omphalotaceae (Fungi: Euagarics) with emphasis on the genus *Gymnopus*. *Sydowia* **58**: 191–289.
- Mata J.L., Ovrebo C.L. (2009) New reports and illustrations of *Gymnopus* for Costa Rica and Panama. *Fungal Diversity* **38**: 125–131.
- Mata J.L., Petersen R.H. (2003) Type studies of neotropical *Collybia* species. *Mycotaxon* **86**: 303–316.
- Matheny P.B., Curtis J.M., Hofstetter V., Aime M.C., Moncalvo J.-M., Ge Z.-W., Yang Z.-L., Slot J.S., Ammirati J.F., Baroni T.J., Bougher N.L., Hughes K.W., Lodge D.J., Kerrigan R.W., Seidl M.T., Aanen D.K., DeNittis M., Daniele G.M., Desjardin D.E., Kropp B.R., Norvell L.L., Parker A., Vellinga E.C., Vilgalys R., Hibbett D.S. (2006) Major clades of Agaricales: a multilocus phylogenetic overview. *Mycologia* **98**(6): 982–995.
- Mayrhofer H., Poelt J. (1979) Die saxicolen Arten der Flechtengattung *Rinodina* in Europa. *Bibliotheca Lichenologica* **12**: 1–186.
- Mayrhofer H., Sheard J.W. (2007) *Rinodina archaea* (Physciaceae, lichenized Ascomycetes) and related species. *Bibliotheca Lichenologica* **96**: 229–246.
- McAlpine D. (1906) *The rusts of Australia: their structure, nature, and classification*. Robt. S. Brain, Melbourne.
- McKenzie E.H.C. (1998) Rust fungi of New Zealand—An introduction, and list of recorded species. *New Zealand Journal of Botany* **36**(2): 233–271.
- Mehrabi-Koushki M., Pooladi P., Eisvand P., Babaahmadi G. (2018) *Curvularia ahvazensis* and *C. rouhaniai* spp. nov. from Iran. *Mycosphere* **9**: 1173–1186.
- Menolli Jr.N., Asai T., Capelari M. (2010) Records and new species of *Pluteus* from Brazil based on morphological and molecular data. *Mycology* **1**: 130–153.
- Menolli Jr.N., Justo A., Capelari M. (2015) Phylogeny of *Pluteus* section *Celluloderma* including eight new species from Brazil. *Mycologia* **107**(6): 1205–1220.
- Miadlikowska J., Lutzoni F. (2000) Phylogenetic revision of the genus *Peltigera* (lichen-forming Ascomycota) based on morphological, chemical, and large subunit nuclear ribosomal DNA data. *International Journal of Plant Sciences* **161**(6): 925–958.
- Milne I., Wright F., Rowe G., Marshal D.F., Husmeier D., et al. (2004) TOPALi: Software for automatic identification of recombinant sequences within DNA multiple alignments. *Bioinformatics* **20**: 1806–1807.
- Minnis A.M., Sundberg W.J. (2010) *Pluteus* section *Celluloderma* in the USA. *North American Fungi* **5**(1): 1–107.
- Moebius-Clune D.J., Anderson Z.U., Pawlowska T.E. (2013) Arbuscular mycorrhizal fungi associated with a single agronomic plant host across the landscape: the structure of an assemblage. *Soil Biology & Biochemistry* **64**: 181–190.
- Moncalvo J.-M., Vilgalys R., Redhead S.A., Johnson J.E., James T.Y., Aime M.C., Hofstetter V., Verduin S.J.W., Larsson E., Baroni T.J., Thorn R.G., Jacobsson S., Clemençon H., Miller Jr. O.K. (2002) One hundred and seventeen clades of euagarics. *Molecular Phylogenetics and Evolution* **23**: 357–400.
- Monod M. (1983) Monographie taxonomique des Gnomoniaceae (Ascomycètes de l'ordre des Diaporthales). *Beihefte zur Sydowia* **9**: 1–315.
- Moral J., Agusti-Brisach C., Perez-Rodriguez M., Xavier C., Raya M.C., Rhouma A., Trapero A. (2017) Identification of fungal species associated with branch dieback of olive and resistance of table cultivars to *Neofusicoccum mediterraneum* and *Botryosphaeria dothidea*. *Plant Disease* **101**: 306–316.
- Morehouse E.A., James T.Y., Ganley A.R.D., Vilgalys R., Berger L., Murphy P.J., Longcore J.E. (2003) Multilocus sequence typing suggests that the chytrid pathogen of amphibians is a recently emerged clone. *Molecular Ecology* **12**: 395–403.
- Morgan-Jones G., White J.F. (1983) Studies on the genus *Phoma*. III. *Paraphoma*, a new genus to accommodate *Phoma radicina*. *Mycotaxon* **18**: 57–65.
- Mosse B. (1962) Establishment of vesicular-arbuscular mycorrhiza under aseptic conditions. *Journal of Genetic Microbiology* **27**: 509–520.
- Myers N., Mittermeier R. A., Mittermeier C.G., Fonseca G.A.B da, Kent J. (2000) Biodiversity hotspots for conservation priorities. *Nature* **403**: 853–858.
- Nagy L.G., Kocsubé S., Csanádi Z., Kovács G.M., Petkovits T., Vágvolgyi Cs., Papp T. (2012) Re-mind the gap! Insertion-deletion data reveal neglected phylogenetic potential of the nuclear ribosomal internal transcribed spacer (ITS) of fungi. *Plos One* **7**(11): e49794.
- Nei M., Kumar S. (2000) *Molecular evolution and phylogenetics*. Oxford University Press.
- Nelson R.R. (1964) The perfect stage of *Curvularia geniculata*. *Mycologia* **56**: 777–779.
- Nilsson R.H., Tedersoo L., Abarenkov K., Ryberg M., Kristiansson E., Hartmann M., et al. (2012) Five simple guidelines for establishing basic authenticity and reliability of newly generated fungal ITS sequences. *Myckeys* **4**: 37–63.
- Nirenberg H. (1977) *Alternaria calendulae* spec. nov., ein parasitischer Pilz auf *Calendula officinalis* L. *Phytopathologische Zeitschrift* **88**: 106–113.
- Niskanen T., Kytövuori I., Liimatainen K. (2009) *Cortinari* sect. *Brunnei* (Basidiomycota, Agaricales) in North Europe. *Mycological Research* **113**: 182–206.
- Niskanen T., Kytövuori I. (2012) Key N: subgenus *Telamonia* sects *Hinnulei* and *Safranopedes*. In: *Funga Nordica, 2nd rev. edn. Agaricoid, boletoid, clavarioid, cyphelloid and*

- gastroid genera.* (eds. Knudsen H., Vesterholt J.) Nordsvamp, Denmark: 871–873.
- Niskanen T., Liimatainen K., Kytövuori I. (2006) Taxonomy, ecology and distribution of *Cortinarius rubroviroleipes* and *C. hinnuleoarmillatus* (Basidiomycota, Agaricales) in Fennoscandia. *Karstenia* **46**: 1–12.
- Norin I., Rumpunen K. (2003) Pathogens on Japanese Quince (*Chaenomeles japonica*) Plants. In: Japanese quince – potential fruit crop for northern Europe (ed. Rumpunen K.). Swedish University of Agricultural Sciences, Department of Crop Science, Uppsala: 37–58.
- Nuhn M.E., Binder M., Taylor A.F., Halling R.E., Hibbett D.S. (2013) Phylogenetic overview of the Boletineae. *Fungal Biology* **117**: 479–511.
- Nylander J.A.A. (2004) MrModeltest v2. Program distributed by the author. Evolutionary Biology Centre, Uppsala University, Sweden.
- Oehl F., Sánchez-Castro I., Sousa N.M.F., Silva G.A., Palenzuela J. (2015) *Dominikia bernensis*, a new arbuscular mycorrhizal fungus from a Swiss no-till farming site, and *D. aurea*, *D. compressa*, and *D. indica*, three new combinations in *Dominikia*. *Nova Hedwigia* **101**: 65–76.
- Oliveira J.J.S., Vargas-Isla R., Cabral T.S., Rodrigues D.P., Ishikawa N.K. (2019) Progress on the phylogeny of the Omphalotaceae: *Gymnopus* s. str., *Marasmiellus* s. str., *Paragymnopus* gen. nov. and *Pusillomyces* gen. nov. *Mycological Progress* **18**: 713–739.
- Ondřej M. (1996) Seven little known species of the genus *Alternaria*. *Czech Mycology* **49**(2): 119–127.
- Ono T., Hoshi H. (2009) Occurrence of sheath blight of umbrella dracaena (*Dianella ensifolia*) and leaf and stem blight of Madagascar periwinkle caused by *Rhizoctonia solani*. *Annual Report of the Kanto Tosan Plant Protection Society* **56**: 75–78.
- Ortiz R., Párraga M., Navarrete J., Carrasco I., de la Vega E., Ortiz M., Herrera P., Jurgens J.A., Held B.W., Blanchette R.A. (2014) Investigations of biodeterioration by fungi in historic wooden churches of Chiloé, Chile. *Microbial Ecology* **67**: 568–575.
- Ouellette G.B. (1972) *Nectria macrospora* (Wr.) Ouellette sp. nov. (= *N. fuckeliana* var. *macrospora*): strains, physiology and pathogenicity, and comparison with *N. fuckeliana* var. *fuckeliana*. *European Journal of Forest Pathology* **2**: 172–181.
- Ovrebo C.L. (1996) The Agaric flora (Agaricales) of La Selva Biological Station. *Revista de Biología Tropical* **44**: 39–57.
- Palenzuela J., Azcón-Aguilar C., Barea J.M., Silva G.A., Oehl F. (2013) *Acaulospora pustulata* and *Acaulospora tortuosa*, two new species in the Glomeromycota associated with endangered plants in Sierra Nevada (southern Spain). *Nova Hedwigia* **97**: 305–319.
- Partridge E.C., Morgan-Jones G. (2002) Notes on Hyphomycetes. LXXXIX. Concerning the genus *Sphaerosporium*. *Mycotaxon* **84**: 69–77.
- Peck C.H. (1881) New species of fungi. *Botanical Gazette* **6**(10): 274–279.
- Peintner U., Moser M., Thomas K.A., Manimohan P. (2003) First records of ectomycorrhizal *Cortinarius* species (Agaricales, Basidiomycetes) from tropical India and their phylogenetic position based on rDNA ITS sequences. *Mycological Research* **107**: 485–494.
- Pennington L. (1915) *Marasmius*. *North American Flora* **9**(4): 250–286.
- Perry B.A., Hansen K., Pfister D.H. (2007) A phylogenetic overview of the family Pyronemataceae (Ascomycota, Pezizales). *Mycological Research* **111**(5): 549–571.
- Petersen R.H., Hughes K.W. (2014) New North American species of *Gymnopus*. *North American Fungi* **9**(3): 1–22.
- Petersen R.H., Hughes K.W. (2016) *Micromphale* sect. *Perforantia* (Agaricales, Basidiomycetes); Expansion and phylogenetic placement. *MycKeys* **18**: 1–122.
- Petersen R.H., Hughes K.W., Lickey E.B., Kovalenko A.E., Morozova O.V., Psurtseva N.V. (2008) A new genus, *Cruentomyцена*, with *Mycena viscidocruenta* as type species. *Mycotaxon* **105**: 119–136.
- Petrak F. (1921) Mykologische Notizen. II. *Annales Mycologici* **19**: 17–128.
- Petrak F. (1941) Mykologische Notizen. XIV. *Annales Mycologici* **39**: 251–349.
- Petrak F. (1960) Ergebnisse einer Revision der Grundtypen verschiedener Gattungen der Askomyzeten und Fungi imperfecti. *Sydowia* **14**: 347–348.
- Pettersson M., Frampton J., Rönnerberg J., Talgo V. (2016) *Neonectria* canker found on spruce and fir in Swedish Christmas tree plantations. *Plant Health Progress* **17**: 202–205.
- Pfunder M., Schürch S. (2001) Sequence variation and geographic distribution of pseudoflower-forming rust fungi (*Uromyces pisi* s. lat.) on *Euphorbia cyparissias*. *Mycological Research* **105**: 57–66.
- Poisson R. (1954) Sur une Laboulbéniale ectoparasite de *Velia osborniana* Kirkaldy (Hemipt. Veliidae) *Laboulbenia* (s. g. *Veliomyces* nov.) *titschacki* n. sp. In: Beiträge zur Fauna Perus, vol. 4 (ed. Titschack E.), Gustav Fischer, Jena, Germany: 81–82.
- Posada D., Crandall K.A. (1998) Modeltest: testing the model of DNA substitution. *Bioinformatics* **14**: 817–818.
- Pradeep C.K., Justo A., Vrinda K.B., Shibu V.P. (2012) Two new species of *Pluteus* (Pluteaceae, Agaricales) from India and additional observations on *Pluteus chrysaegis*. *Mycological Progress* **11**: 869–878.
- Pringle A., Baker D.M., Platt J.L., Wares J.P., Latge J.P., Taylor J.W. (2005) Cryptic speciation in the cosmopolitan and clonal human pathogenic fungus *Aspergillus fumigatus*. *Evolution* **59**(9): 1886–1899.
- Raeder U., Broda P. (1985) Rapid preparation of DNA from filamentous fungi. *Letters in Applied Microbiology* **1**: 17–20.
- Rehner S.A., Buckley E. (2005) A *Beauveria* phylogeny inferred from nuclear ITS and EF1- $\alpha$  sequences: evidence for cryptic diversification and links to *Cordyceps* teleomorphs. *Mycologia* **97**: 84–98.
- Rehner S.A., Samuels G.J. (1994) Taxonomy and phylogeny of *Gliocladium* analysed from nuclear large subunit ribosomal DNA sequences. *Mycological Research* **98**: 625–634.
- Revankar S.G., Sutton S.A. (2010) Melanized fungi in human disease. *Clinical Microbiology Reviews* **23**: 884–928.
- Riddle O.C., Briggs F.N. (1950) Inheritance of resistance to scald in barley. *Hilgardia* **20**: 19–27.
- Robich G. (2003) *Mycena d'Europa*. Associazione Micologica Bresadola, Trento.
- Robich G. (2016) *Mycena d'Europa 2*. Associazione Micologica Bresadola, Trento.
- Robich G., Hausknecht A. (2008) *Mycena dobraensis*, a new species of section *Filipedes* (Agaricales, Tricholomataceae) from Eastern Austria. *Österreichische Zeitschrift für Pilzkunde* **17**: 41–46.
- Robich G., Miersch J., Karasch P. (2005) *Mycena haushoferi*, a new species of section *Intermediae* from Germany. *Mycological Progress* **4**(3): 257–264.
- Rondon Y. (1965) Une espece nouvelle de lichens: *Candelariella oleaginescens* nov. spec. *Revue Bryologique et Lichénologique* **34**: 831–832.

- Ronikier A., Chachula P., Kujawa A. (2006) *Mycena tenuispinosa* (Fungi, Agaricales), a species new to Poland. *Polish Botanical Journal* **51**(2): 217–220.
- Ronquist F., Huelsenbeck J.P. (2003) MrBayes 3: Bayesian phylogenetic inference under mixed models. *Bioinformatics* **19**: 1572–1574.
- Ronquist F., Teslenko M., van der Mark P., Ayres D.L., Darling A., Höhna S., Larget B., Liu L., Suchard M.A., Huelsenbeck J.P. (2012) MrBayes 3.2: efficient Bayesian phylogenetic inference and model choice across a large model space. *Systematic Biology* **61**: 539–542.
- Ropars J., Cruaud C., Lacoste S., Dupont J. (2012) A taxonomic and ecological overview of cheese fungi. *International Journal of Food Microbiology* **155**(3): 199–210.
- Rosa L.H., Capelari M. (2009) Agaricales fungi from atlantic rain forest fragments in Minas Gerais, Brazil. *Brazilian Journal of Microbiology* **40**: 846–851.
- Rossi W. (1974) Una nuova specie di *Laboulbenia* (Ascomycetes. Laboulbeniales) parassita di termiti. *Doriana* **5**(215): 1–5.
- Rossi W., Bernardi M., Torres J.A. (2016) New species of *Laboulbenia* parasitic on leaf beetles. *Mycological Progress* **15**: 4.
- Rossi W., Blackwell M. (1986) New species of *Laboulbenia* from termite hosts in Africa. *Mycologia* **78**: 142–145.
- Rossi W., Vávra, J.C., Barták, M. (2019) New species and new records of Laboulbeniales (Ascomycota) from the Czech Republic and Slovakia. *Nova Hedwigia* **109**(1–2): 149–159.
- Rossi W., Leonardi M. (2018) New species and new records of Laboulbeniales (Ascomycota) from Sierra Leone. *Phytotaxa* **358**(2): 91–116.
- Rossi W., Torres J.A., Bernardi M. (2015) New Laboulbeniales parasitic on weevils from the Amazon rainforest. *Phytotaxa* **231**(2): 187–192.
- Rossi W., Santamaría S. (2006) *Laboulbenia casnoniae* (Ascomycota, Laboulbeniales) and allied species. *Nova Hedwigia* **82**(1–2): 189–204.
- Roux C. (2012) Liste des lichens et champignons lichénicoles de France. Liste de la likenoj kaj nelikenigintaj fungoj de Francio. *Bulletin de la Société Linnéenne de Provence* **1**:1–220.
- Ryoo R., Antonín V., Ka K.-H., Tomšovský M. (2016) Marasmioid and gymnopoid fungi of the Republic of Korea. 8. *Gymnopus* sect. *Impudicae*. *Phytotaxa* **268**: 75–88.
- Saba M., Jabeen S., Khalid A.N., Dima B. (2017): *Cortinarius longistipitatus* sp. nov. (Agaricales), a new species in *Cortinarius*, subgenus *Telamonia* from Pakistan. *Phytotaxa* **328**(3): 257–266.
- Saccardo P.A. (1888) *Sylloge Fungorum omnium hucusque cognitorum* 7. Italy, Padua.
- Saccardo P.A. (1905) *Sylloge Fungorum omnium hucusque cognitorum* 17. Italy, Padua.
- Santamaría S. (2008) Laboulbeniales on semiaquatic Heteroptera. A new species of *Triceromyces* (Ascomycota, Laboulbeniales) on *Microvelia* (Heteroptera, Veliidae) from Spain. *Aliso* **26**: 15–21.
- Santamaría S., Faille A. (2009) New species of *Laboulbenia* and *Rhachomyces* (Laboulbeniales, Ascomycota), some of them polymorphic, parasitic on termiticolous ground beetles from tropical Africa. *Nova Hedwigia* **89**(1–2): 97–120.
- Sarnari M. (1998) *Monographia illustrate del genere Russula in Europe*. Associazione Micologica Bresadola, Trento.
- Sato H., Hattori T., Lee S.S., Murakami N. (2011) Two species of *Strobilomyces* (Boletaceae, Boletales), *S. seminudus* and *S. hongoi* sp. nov. from Japan. *Mycologia* **103**: 598–609.
- Sato H., Murakami N. (2009) *Strobilomyces verruculosus* sp. nov. from Japan. *Mycoscience* **50**: 173–178.
- Sato H., Tanabe A.S., Toju H. (2017) Host shifts enhance diversification of ectomycorrhizal fungi: diversification rate analysis of the ectomycorrhizal fungal genera *Strobilomyces* and *Afroboletus* with an 80-gene phylogeny. *New Phytologist* **214**: 443–454.
- Sato H., Yumoto T., Murakami N. (2007) Cryptic species and host specificity in the ectomycorrhizal genus *Strobilomyces* (Strobilomycetaceae). *American Journal of Botany* **94**: 1630–1641.
- Sawamura K. (1962) Studies on spotted disease of apple 1. Causal agent of *alternaria* blotch. *Bulletin of the Tohoku National Agricultural Experiment Station* **23**: 163–75.
- Schenck N.C., Smith G.S. (1982) Additional new and unreported species of mycorrhizal fungi (Endogonaceae) from Florida. *Mycologia* **74**: 566–574.
- Schenck N.C., Spain J.L., Sieverding E., Howeler R.H. (1984) Several new and unreported vesicular-arbuscular mycorrhizal fungi (Endogonaceae) from Colombia. *Mycologia* **76**: 685–689.
- Schmitz S., Charlier A., Chandelier A. (2017) First report of *Neonectria neomacrospora* on *Abies grandis* in Belgium. *New Disease Reports* **36**: 17.
- Schoch C.L., Sung G.H., López-Giráldez F., Townsend J.P., Miadlikowska J., Hofstetter V., et al. (2009) The Ascomycota tree of life: a phylum-wide phylogeny clarifies the origin and evolution of fundamental reproductive and ecological traits. *Systematic Biology* **58**(2): 224–239.
- Schubert K., Groenewald J.Z., Braun U., Dijksterhuis J., Starink M., Hill C.F., Zalar P., De Hoog G.S., Crous P.W. (2007) Biodiversity in the *Cladosporium herbarum* complex (Davidiellaceae, Capnodiales), with standardisation of methods for *Cladosporium* taxonomy and diagnostics. *Studies in Mycology* **58**: 105–156.
- Scott E.M., Carter R.T. (2014) Canine keratomycosis in 11 dogs: A case series (2000–2011). *Journal of the American Animal Hospital Association* **50**: 112–118.
- Semwal K.C., Bhatt V.K., Stephenson S.L. (2018) A survey of macrofungal diversity in the Bharsar region, Uttarakhand Himalaya, India. *Journal of Asia-Pacific Biodiversity* **11**: 560–565.
- Sesli E., Liimatainen K. 2018. *Cortinarius conicoumbonatus* (*Cortinarius* subgen. *Telamonia* sect. *Hinnulei*): a new species from spruce-beech forests of the East Black Sea Region of Turkey. *Turkish Journal of Botany* **42**: 327–334.
- Ševčíková H. (2017) *Mycena crocata* var. *vogesiana*, vzácná a málo známá varieta helmovky šafránové [*Mycena crocata* var. *vogesiana*, a rare and less known variety]. *Mykologické Listy* **137**: 11–19.
- Shear C.L. (1939) Mycological notes. III. *Mycologia* **31**(3): 322–336.
- Sheard J.W., Ezhkin A.K., Galanina I.A., Himelbrant D., Kuznetsova E., Shimizu A., Stepanchikova I., Thor G., Tønsberg T., Yakovchenko L.S., Spribille T. (2017) The lichen genus *Rinodina*, (Physciaceae, Caliciales) in north-eastern Asia. *Lichenologist* **49**(6): 617–672.
- Shivas R.G. (1987) *Rumex* rust (*Uromyces rumicis*) in Western Australia. *Australasian Plant Pathology* **16**: 40–41.
- Sieverding E. (1991) *Vesicular-arbuscular mycorrhiza management in tropical agroecosystems*. Deutsche Gesellschaft für Technische Zusammenarbeit No. 224. Hartmut Bremer Verlag, Friedland, Germany.

- Sieverding E., Silva G.A., Berndt R., Oehl F. (2014) *Rhizoglo-mus*, a new genus in the Glomeraceae. *Mycotaxon* **129**: 373–386.
- Silva R.M.F., Oliveira R.J.V., Bezerra J.D.P., Bezerra J.L., Souza-Motta C.M., Silva G.A. (2019) *Bifusisporella sorghi* gen. et sp. nov. (Magnaporthaceae) to accommodate an endophytic fungus from Brazil. *Mycological Progress* **18**: 847–854.
- Silvestro D., Michalak I. (2012) raxmlGUI: a graphical front-end for RAxML. *Organisms Diversity and Evolution* **12**: 335–337.
- Simmons E.G. (2007) *Alternaria*: an identification manual. CBS-KNAW Fungal Biodiversity Centre, the Netherlands.
- Simmons M.P., Ochoterena H., Carr T.G. (2001) Incorporation, relative homoplasy, and effect of gap characters in sequence-based phylogenetic analysis. *Systematic Biology* **50**(3): 454–462.
- Singer R. (1945) New genera of fungi. *Lloydia* **8**: 139–144.
- Singer R. (1986) *The Agaricales in modern taxonomy*. 4<sup>th</sup> edn. Koeltz Scientific Books, Koenigstein.
- Singh G., Dal Grande F., Divakar P.K., Otte J., Leavitt S.D., Szczepanska K., Crespo A., Rico V.J., Aptroot A., da Silva Cáceres M.E., Lumbsch H.T., Schmitt I. (2015) Coalescent-based species delimitation approach uncovers high cryptic diversity in the cosmopolitan lichen-forming fungal genus *Protoparmelia* (Lecanorales, Ascomycota). *Plos One* **10**: e0124625.
- Sivanesan A., Shivas R.G. (2002) Studies on *Mycosphaerella* species in Queensland, Australia. *Mycological Research* **106**(3): 355–364.
- Skrede I., Carlsen T., Schumacher T. (2017) A synopsis of the saddle fungi (*Helvella*: Ascomycota) in Europe – species delimitation, taxonomy and typification. *Persoonia* **39**: 201–253.
- Smith C.W., Aptroot A., Coppins B.J., Fletcher A., Gilbert O.L., James P.W., Wolseley P.A., Orange A. (2009) *The Lichens of Great Britain and Ireland*. The British Lichen Society, London.
- Smith S. A., Dunn C. W. (2008) Phyutility: a phyloinformatics tool for trees, alignments and molecular data. *Bioinformatics* **24**: 715–716.
- Sochorová Z., Döbbeler P., Sochor M., van Rooy J. (2019) *Octospora conidiophora* (Pyrrenomataceae)–a new species from South Africa and the first report of anamorph in bryophilous Pezizales. *Mycoskeys* **54**: 49–76.
- Song Y., Buyck B., Li J.W., Yuan F., Zhang Z.W., Qiu L.H. (2018) Two novel and a forgotten *Russula* species in sect. *Ingratae* (Russulales) from Dinghushan Biosphere Reserve in southern China. *Cryptogamie Mycologie* **39**: 341–357.
- Sousa J.O., Suz L.M., García M.A., Alfredo D.S., Conrado L.M., Marinho P., Ainsworth A.M., Baseia I.G., Martín M.P. (2017) More than one fungus in the pepper pot: Integrative taxonomy unmasks hidden species within *Myriostoma coliforme* (Geastraceae, Basidiomycota). *Plos One* **12**(6): e0177873.
- Spain J.L. (1990) Arguments for diagnoses based on unaltered wall structures. *Mycotaxon* **38**: 71–76.
- Spatafora J.W., Chang Y., Benny G.L., Lazarus K., Smith M.E., Berbee M.L., Bonito G., Corradi N., Grigoriev I., Gryganskiy A., James T.Y. (2016) A phylum-level phylogenetic classification of zygomycete fungi based on genome-scale data. *Mycologia* **108**(5): 1028–1046.
- Stamatakis A. (2006) RAxML-VI-HPC: maximum likelihood-based phylogenetic analyses with thousands of taxa and mixed models. *Bioinformatics* **22**: 2688–2690.
- Stamatakis A. (2014) RAxML version 8: a tool phylogenetic analysis and post-analysis of large phylogenies. *Bioinformatics* **30**: 1312–1313.
- Stefani F.O., Jones R.H., May T.W. (2014) Concordance of seven gene genealogies compared to phenotypic data reveals multiple cryptic species in Australian dermocyboid *Cortinari* (Agaricales). *Molecular Phylogenetics and Evolution* **71**: 249–260.
- Stewart R. (1982) *Flora of Pakistan*: history and exploration of plants in Pakistan and adjoining areas (NO. 581.95491 S851). PanGraphics.
- Stiller J.W., Hall B.D. (1997) The origin of red algae: implications for plastid evolution. *Proceedings of the National Academy of Sciences of the USA* **94**: 4520–4525.
- Suleiman M.K., Dixon K., Commander L., Nevill P., Quoreshi A.M., Bhat N.R., Manuvel A.J., Sivadasan M.T. (2019) Assessment of the diversity of fungal community composition associated with *Vachellia pachyceras* and its rhizosphere soil from Kuwait desert. *Frontiers in Microbiology* **10**: 63.
- Sumstine D.R. (1949) The Albert Commons Collection of Fungi in the Herbarium of the Academy of Natural Sciences in Philadelphia. *Mycologia* **41**(1): 11–23.
- Sung G.H., Sung J.M., Hywel-Jones N.L., Spatafora J.W. (2007) A multi-gene phylogeny of Clavicipitaceae (Ascomycota, Fungi): Identification of localized incongruence using a combinational bootstrap approach. *Molecular Phylogenetics and Evolution* **44**: 1204–1223.
- Swofford D.L. (2002) *PAUP\* 4.0b10: phylogenetic analysis using parsimony (\*and other methods)*. Sinauer Associates, Sunderland, Massachusetts.
- Symanczik S., Błaszczkowski J., Chwat G., Boller T., Wiemken A., Al-Yahya'ei M. (2014) Three new species of arbuscular mycorrhizal fungi discovered at one location in a desert of Oman: *Diversispora omaniana*, *Septoglo-mus nakheelum* and *Rhizophagus arabicus*. *Mycologia* **106**: 243–259.
- Tadych M., Bergen M., Johnson J.C., Polashock J., Vorsa N. (2012) Endophytic and pathogenic fungi of developing cranberry ovaries from flower to mature fruit: diversity and succession. *Fungal Diversity* **54**: 101–116.
- Taheriyan V., Khodaparast S.A., Hashemi A. (2014) New records for anamorphic fungi of Guilan province, Iran. *Mycologia Iranica* **1**(1): 7–11.
- Takehashi S., Kasuya T. (2009) *Pluteus magnus* and *Pluteus podospileus* f. *podospileus*, two agaric species new to Japan. *Mycoscience* **50**: 74–77.
- Takeuchi J., Kagiwada S., Namba S., Horie H. (2008) First report of anthracnose of *Reineckea* caused by *Colletotrichum dematium* and blue flax lily by *C. gloeosporioides* occurring in Japan. *Annual Report of the Kanto Tosan Plant Protection Society* **55**: 93–96.
- Tamura K., Stecher G., Peterson D., Filipowski A., Kumar S. (2013) MEGA6: molecular evolutionary genetics analysis version 6.0. *Molecular Biology and Evolution* **30**: 2725–2729.
- Tan Y.P., Madrid H., Crous P.W., Shivas R.G. (2014) *Johncornia* gen. et. comb. nov., and nine new combinations in *Curvularia* based on molecular phylogenetic analysis. *Australasian Plant Pathology* **43**: 589–603.
- Tan Y.P., Crous P.W., Shivas R.G. (2018) Cryptic species of *Curvularia* in the culture collection of the Queensland Plant Pathology Herbarium. *Mycoskeys* **35**: 1–25.
- Tedersoo L., Kõljalg U., Hallenberg N., Larsson K.-H. (2003) Fine scale distribution of ectomycorrhizal fungi and roots

- across substrate layers including coarse woody debris in a mixed forest. *New Phytologist* **159**(1): 153–165.
- Terashima Y., Takahashi H., Taneyama Y. (2016) *The fungal flora in southwestern Japan: Agarics and boletes*. Tokai University Press, Tokyo.
- Thaxter R. (1895) Notes on Laboulbeniaceae, with descriptions of new species. *Proceedings of the American Academy of Arts and Sciences* **30**: 467–481.
- Thaxter R. (1896) Contribution towards a monograph of the Laboulbeniaceae. *Memoirs of the American Academy of Arts and Sciences* **12**(3): 187–429.
- Thaxter R. (1912) New or critical Laboulbeniales from the Argentine. *Proceedings of the American Academy of Arts and Sciences* **48**: 155–223.
- Thomma B.P.H.J. (2003) *Alternaria* spp.: from general saprophyte to specific parasite. *Plant Pathology* **4**: 225–236.
- Thompson J.D., Higgins D.G., Gibson T.J. (1994) CLUSTAL W: improving the sensitivity of progressive multiple sequence alignment through sequence weighting, position specific gap penalties and weight matrix choice. *Nucleic Acids Research* **22**(22): 4673–80.
- Thor G., Wirth V. (1990) *Candelariella viae-lacteeae*, a new lichen species from Europe. *Stuttgarter Beiträge zur Naturkunde, Serie A* **445**: 1–4.
- Tibpromma S., Hyde K.D., Jeewon R., Maharachchikumbura S.S.N., Liu J.K., Bhat D.J., et al. (2017) Fungal diversity notes 491–602: taxonomic and phylogenetic contributions to fungal taxa. *Fungal Diversity* **83**: 1–261.
- Tiedeseura S. (1861) *Bidrag till kännedom af Finlands natur och folk*. Helsingfors, Finska Litteratur-sällskapet 4.
- Tomaso-Peterson M., Jo Y.K., Vines P.L., Hoffmann F.G. (2016) *Curvularia malina* sp. nov. incites a new disease of warm-season turfgrasses in the southeastern United States. *Mycologia* **108**: 915–924.
- Toome-Heller M. (2016) Latest development in the research of rust fungi and their allies (Pucciniomycotina). In: *Biology of microfungi* (ed. D.W. Li), Springer International Publishing: 147–168.
- Trail J.W.H. (1889) Enumeration of fungi collected in Hardanger in 1887. *Transactions of the Botanical Society of Edinburgh* **17**: 487–495.
- Turland N.J., Wiersema J.H., Barrie F.R., Greuter W., Hawksworth D.L., Herendeen P.S., Knapp S., Kusber W.-H., Li D.-Z., Marhold K., May T.W., McNeill J., Monro A.M., Prado J., Price M.J., G.F. Smith. (2018) International Code of Nomenclature for algae, fungi, and plants (Shenzhen Code) adopted by the Nineteenth International Botanical Congress Shenzhen, China, July 2017. *Regnum Vegetabile* **159**. Koeltz Botanical Books, Oberreifenberg, Germany.
- Turrini A., Saran M., Giovannetti M., Oehl F. (2018) *Rhizoglyphus venetianum*, a new arbuscular mycorrhizal fungal species from a heavy metal contaminated site, downtown Venice in Italy. *Mycological Progress* **17**: 1213–1224.
- Valadbeigi T. (2014) Lichen flora of the Ilam province, South West Iran. *Mycotaxon* **128**: 248–255.
- Valenzuela-Lopez N., Cano-Lira J.F., Guarro J., Sutton D.A., Wiederhold N., Crous P.W., Stchigel A.M. (2018) Coelomycetous Dothideomycetes with emphasis on the families Cucurbitariaceae and Didymellaceae. *Studies in Mycology* **90**: 1–69.
- Van der Merwe M., Ericson L., Walker J., Thrall P.H., Burdon J.J. (2007) Evolutionary relationships among species of *Puccinia* and *Uromyces* (Pucciniaceae, Uredinales) inferred from partial protein coding gene phylogenies. *Mycological Research* **111**: 163–175.
- Vellinga E.C. (1988) Glossary. In *Flora Agaricina Neerlandica* (eds. Bas C., Kuyper T.H.W., Noordeloos M.E., Vellinga E.C.), A.A. Balkema, Rotterdam: 54–64.
- Vellinga E.C. (1990) *Pluteus*. In: *Flora Agaricina Neerlandica* 2 (eds. Bas C., Kuyper Th.W., Noordeloos M.E., Vellinga E.C.), A.A. Balkema, Rotterdam: 31–55.
- Vierheilig H., Coughlan A.P., Wyss U., Piché Y. (1998) Ink and vinegar, a simple staining technique for arbuscular-mycorrhizal fungi. *Applied and Environmental Microbiology* **4**: 5004–5007.
- Vilgalys R., Hester M. (1990) Rapid genetic identification and mapping of enzymatically amplified ribosomal DNA from several *Cryptococcus* species. *Journal of Bacteriology* **172**: 4238–4246.
- Voglmayr H., Jaklitsch W.M. (2008) *Prosthecium* species with *Stegonsporium* anamorphs on *Acer*. *Mycological Research* **112**: 885–905.
- Voglmayr H., Jaklitsch W.M. (2011) Molecular data reveal high host specificity in the phylogenetically isolated genus *Massaria* (Ascomycota, Massariaceae). *Fungal Diversity* **46**: 133–170.
- Voglmayr H., Rossman A.Y., Castlebury L.A., Jaklitsch W.M. (2012) Multigene phylogeny and taxonomy of the genus *Melanconiella* (Diaporthales). *Fungal Diversity* **57**: 1–44.
- Vondrák J., Halıcı M.G., Güllü M., Demirel R. (2016) Taxonomy of the genus *Athallia* and its diversity in Turkey. *Turkish Journal of Botany* **40**(3): 319–328.
- Walker J. (1980) *Gaeumannomyces*, *Linocarpon*, *Ophiobolus* and several other genera of scolecospored Ascomycetes and *Phialophora* conidial states, with a note on hyphopodia. *Mycotaxon* **11**: 1–129.
- Walker D.M., Castlebury L.A., Rossman A.Y., Mejía L.C., White J.F. (2012) Phylogeny and taxonomy of *Ophiognomonia* (Gnomoniaceae, Diaporthales), including twenty-five new species in this highly diverse genus. *Fungal Diversity* **57**(1): 85–147.
- Wang J., Li M., Qiao Z. (1997) Experiment on suitable timing of applying special germicide for control of apple leaf spot disease. *China Fruits* **1**: 29–30.
- Wartchow F., Sá M.C.A., Coimbra V.R.M. (2017) A new species of *Gloeocantharellus* from the Atlantic Forest of Paraíba, Brazil. *Current Research in Environmental & Applied Mycology* **7**: 183–186.
- Weir A., Beakes G.W. (1996) Biology and identification of species of *Laboulbenia* Mont. & C.P. Robin (Fungi, Ascomycetes) parasitic on alticine Chrysomelidae. In: *Chrysomelidae biology*. Vol. 2: ecological studies (eds. Jolivet P.H.A., Cox M.L.), SPB Academic Publishing, Amsterdam: 117–134.
- Wen H.A., Ying J.Z. (2001) Supplementary notes on the genus *Strobilomyces* from China II. *Mycosystema* **20**: 297–300.
- Werle E., Schneider C., Renner M., Völker M., Fiehn W. (1994) Convenient single-step, one tube purification of PCR products for direct sequencing. *Nucleic Acids Research* **22**: 4354–4355.
- White T.J., Bruns T., Lee S., Taylor J. (1990) Amplification and direct sequencing of fungal ribosomal RNA genes for phylogenetics. In: *PCR protocols: a guide to methods and applications* (eds. Innis M.A., Gelfand D.H., Sninsky J.J., White T.J.), Academic Press, New York: 315–322.
- Wijayawardene N.N., Hyde K.D., Rajeshkumar K.C., Hawksworth D.L., Madrid H., Kirk P.M., et al. (2017) Notes for genera: Ascomycota. *Fungal Diversity* **86**(1): 1–594.
- Wilson A.W., Desjardin D.E., Horak E. (2004) Agaricales of Indonesia. 5. The genus *Gymnopus* from Java and Bali. *Sydowia* **56**: 137–210.



- Wingfield M.J., De Beer Z.W., Slippers B., Wingfield B.D., Groenewald J.Z., Lombard L., Crous P.W. (2012) One fungus, one name promotes progressive plant pathology. *Molecular Plant Pathology* **13**(6): 604–613.
- Woudenberg J.H.C., Aveskamp M.M., de Gruyter J., Spiers A.G., Crous P.W. (2009) Multiple *Didymella* teleomorphs are linked to the *Phoma clematidina* morphotype. *Persoonia* **22**: 56–62.
- Wu G., Feng B., Xu J., Zhu X.T., Li Y.C., Zeng N.K., Hosen M.I., Yang Z.L. (2014) Molecular phylogenetic analyses redefine seven major clades and reveal 22 new generic lineages in the fungal family Boletaceae. *Fungal Diversity* **69**: 93–115.
- Ying J.Z., Ma Q.M. (1985) New taxa and records of the genus *Strobilomyces* in China. *Acta Mycologica Sinica* **4**: 95–102.
- Ying J. Z. (1986) Supplement notes on genus *Strobilomyces* from China. *Acta Mycologica Sinica Suppl. I*: 305–308.
- Yu S.H. (2001) Korean species of *Alternaria* and *Stemphylium*. National Institute of Agricultural Science and Technology, Suwon, Korea.
- Zakii Z., Ershad D. (1986) Storage fungal diseases of apple. *Proceedings of 8th Iranian Plant Protection Congress*: 61.
- Zeng H., Tan F., Shu Y., Zhang Y., Feng Y., Wang J. (2015) The Cry1Ab protein has minor effects on the arbuscular mycorrhizal fungal communities after five seasons of continuous Bt maize cultivation. *PLoS ONE* **10**: e0146041.
- Zhang J.B., Li J.W., Li F., Qiu L.H. (2017) *Russula dinghuensis* sp. nov. and *R. subpallidirosea* sp. nov., two new species from southern China supported by morphological and molecular evidence. *Cryptogamie Mycologie* **38**: 191–203.
- Zhao Q., Li Y.K., Zhu X.T., Zhao Y.C., Liang J.F. (2015) *Russula nigrovirens* sp. nov. (Russulaceae) from southwestern China. *Phytotaxa* **236**: 249–256.
- Zhiguang H., Xin S., Mengsha L. (2016) Effects of forest age on soil fungal community in a Northern temperate ecosystem. *Indian Journal of Microbiology* **56**(3): 328–334.

(Manuscript accepted 11 November 2019; Corresponding Editors: D. Haelewaters & I. Krisai-Greilhuber)

